

# Cosmology with vector dark energy

by

**Jose Beltrán Jiménez**

under the supervision of

Dr. Antonio López Maroto



Thesis submitted for the Degree of Doctor in Physics in the  
Universidad Complutense de Madrid

· November 2009 ·



# Contents

---

<b>Acknowledgments</b>	<b>v</b>
<b>Publications</b>	<b>vii</b>
<b>Preface</b>	<b>ix</b>
<b>1 The Standard Model of Cosmology</b>	<b>1</b>
1.1 Introduction . . . . .	1
1.2 Theoretical Framework . . . . .	2
1.3 Basics of FLRW universe . . . . .	5
1.4 The Standard Model . . . . .	8
1.5 Dark Energy . . . . .	11
1.5.1 Observational evidences . . . . .	12
1.5.2 Dark Energy models . . . . .	17
1.6 Final remarks . . . . .	26
<b>2 Moving dark energy</b>	<b>29</b>
2.1 Introduction . . . . .	29
2.2 Large-scale dark flows . . . . .	32
2.3 Slow-moving fluids: second order equations . . . . .	35

---

2.4	Sachs-Wolfe effect with moving fluids . . . . .	39
2.5	CMB dipole from moving dark energy . . . . .	42
2.6	Contribution to the CMB quadrupole . . . . .	45
2.7	Fast-moving fluids: exact equations . . . . .	51
2.8	Model examples . . . . .	54
2.8.1	Constant equation of state . . . . .	54
2.8.2	Scaling models . . . . .	55
2.8.3	Tracking models . . . . .	61
2.8.4	Null dark energy . . . . .	62
2.9	Conclusions and discussion . . . . .	66
<b>3</b>	<b>Cosmology in vector-tensor theories of gravity</b>	<b>69</b>
3.1	Introduction . . . . .	69
3.2	Generalities . . . . .	73
3.3	Evolution in an isotropic universe . . . . .	77
3.3.1	Inflationary (de Sitter) epoch . . . . .	78
3.3.2	Barotropic fluid domination . . . . .	80
3.4	Vector dominance . . . . .	86
3.4.1	Accelerating solutions . . . . .	95
3.5	Late-time accelerated solutions with matter . . . . .	98
3.6	Conclusions and discussion . . . . .	107
<b>4</b>	<b>Viability of vector-tensor theories of gravity</b>	<b>109</b>
4.1	Introduction . . . . .	109
4.2	Local gravity constraints . . . . .	111
4.3	Classical and quantum stability . . . . .	114
4.3.1	Gauge non-invariant models . . . . .	116

---

4.3.2	Gauge invariant models . . . . .	121
4.4	Gravitational Waves . . . . .	123
4.5	Conclusions and discussion . . . . .	125
<b>5</b>	<b>Cosmic Vector for dark energy</b>	<b>127</b>
5.1	Introduction . . . . .	127
5.2	Vector Dark energy . . . . .	129
5.3	Phase Map . . . . .	135
5.4	Anisotropic evolution . . . . .	137
5.5	Stability and consistency . . . . .	139
5.6	Constraints from SN, CMB and BAO . . . . .	143
5.6.1	Likelihood calculations . . . . .	146
5.6.2	Results . . . . .	150
5.7	Conclusions and discussion . . . . .	152
<b>6</b>	<b>Electromagnetic dark energy</b>	<b>155</b>
6.1	Introduction . . . . .	155
6.2	Quantization in Minkowski spacetime . . . . .	158
6.3	Quantization in an expanding universe . . . . .	160
6.4	Quantization without the Lorenz condition . . . . .	163
6.5	Quantum fluctuations during inflation . . . . .	167
6.6	Cosmological evolution . . . . .	169
6.7	Perturbations . . . . .	172
6.7.1	Evolution during radiation and matter dominated eras . . . . .	177
6.7.2	Evolution of the perturbations . . . . .	180
6.8	Conclusions and discussion . . . . .	186

**Final conclusions and prospects**

**189**

**Bibliography**

**205**

# Acknowledgments

---

Comenzaré este espacio mostrando mi más profundo agradecimiento a mi director de Tesis, Antonio López Maroto, por la impecable labor que ha realizado. Debo decir que me siento extremadamente afortunado por haber tenido un director tan activo y tan comprometido. Aprecio especialmente el esfuerzo que ha hecho en todo momento para que las cosas se hicieran de forma apropiada y para que mi formación fuese la adecuada. Sinceramente, no se me ocurre nada que pudiera haber hecho mejor.

En segundo lugar, querría expresar mi gratitud a los compañeros que he tenido a lo largo de estos años de doctorado. Quizás especialmente a aquellos con quienes he compartido despacho: a Álvaro por haber sido mi compañero de viajes, a Alejandro por sus enseñanzas estilísticas y cofundar *el círculo*, a Javi por esas luchas épicas, a Juan por ese momento carajillo, a Lourdes por haberme obligado a integrarme, a Carlos por ser una bellísima persona y a Héctor por su incomprensible confianza en mí. No puedo olvidar sin embargo, a aquellos con quienes no he compartido despacho, pero sí otras muchas cosas: a Bea, a Dani, a David, a Diego, a Jacobo, a Jeny y a Willy. Tampoco quiero olvidarme aquí de Ángel, que me acompañó durante toda la carrera, ni de Irene y Paco, con quienes tan buenos momentos pasé. Quizás este sea el párrafo más apropiado para incluir también a Domingo, que tan presente ha estado con sus *quedadas*, y a Jose Alberto, con quien tuve la suerte de poder discutir nuestro trabajo y que tanto me recuerda a “El Almendro”.

Esta Tesis se ha elaborado en el Departamento de Física Teórica I de la Universidad Complutense de Madrid, al que agradezco todas las facilidades que me ha proporcionado, y bajo la financiación del proyecto de investigación *Aplicaciones de las teorías efectivas en Física de Partículas* FPA2008-00592 cuyo investigador principal es Antonio Dobado y gracias al cual he podido asistir a un gran número de congresos y visitar

otros centros. En estos viajes he conocido a personas que también merecen una mención aquí. Seguiré un orden cronológico y comenzaré por Fernando, cuyas preguntas y comentarios me ayudaron a afianzar mis conocimientos e incluso motivaron una parte de la Tesis, y Ruth, con quien he tenido la suerte de colaborar y de quien pude obtener unos conocimientos valiosísimos durante mi visita a Bilbao.

Al Departamento de Física Teórica de la Universidad de Heidelberg, querría agradecerle la hospitalidad que me brindó durante mi estancia allí. De esta visita, me gustaría hacer mención especial a dos personas. En primer lugar, a Tomi, que no sólo es un excelente científico, gracias al cual amplié mis conocimientos teóricos y aprendí a utilizar una herramienta fundamental en la Cosmología moderna, sino que también es una gran persona y me dispensó un trato exquisito. En segundo lugar, quiero agradecer a Javi el haberme hecho disfrutar, tanto de una estancia llena de buenos momentos en Heidelberg, como de un cierto viaje semionírico por la selva negra que dio lugar a unos proceedings magníficos.

A David, quisiera agradecerle las oportunidades que me ha dado (que han sido muchas) y el que sea una persona tan afable. También quisiera mostrar mi gratitud hacia él por haberme ofrecido su apoyo y obligarme a visitar Sognsvaten, que resultó ser un lugar precioso. A todas las personas del departamento de Astrofísica Teórica de la Universidad de Oslo, con una mención especial para Nicolaas, les agradezco el haber hecho posible una estancia tan agradable.

A mi madre, a mi padre y a mi hermana debo agradecerles todo el amor que me ofrecen y que siempre me hayan apoyado en mi decisión de dedicarme a esto, que tan lejos queda de lo suyo, e incluso me hayan animado a seguir en los peores momentos. A Marisa, por los mismos motivos y por compartir una gran afición conmigo. También aquí me gustaría agradecerle a Ana todo lo que me ha aportado y sin la cual, muy posiblemente, esta Tesis nunca hubiera tenido lugar.

Concluiré estos agradecimientos con un recuerdo muy especial a mi abuela, a quien tendría tanto que agradecer que sólo puedo decir: gracias por haber existido.

# Publications

---

The research activity performed in this thesis has produced the following list of publications in regular journals:

1. *Perturbations in electromagnetic dark energy*. Jose Beltrán Jiménez, Tomi S. Koivisto, Antonio L. Maroto and David F. Mota. *JCAP* **0910**:029 (2009).
2. *Cosmological evolution in vector-tensor theories of gravity*. Jose Beltrán Jiménez and Antonio L. Maroto. *Physical Review* **D80**, 063512 (2009).
3. *Cosmic vector for dark energy: constraints from SN , CMB and BAO*. Jose Beltrán Jiménez, Ruth Lazkoz and Antonio L. Maroto. *Physical Review* **D80**, 023004 (2009).
4. *Large-scale cosmic flows and moving dark energy*. Jose Beltrán Jiménez and Antonio L. Maroto. *JCAP* **0903**:015 (2009).
5. *Viability of vector-tensor theories of gravity*. Jose Beltrán Jiménez and Antonio L. Maroto. *JCAP* **0902**:025 (2009).
6. *Cosmological electromagnetic fields and dark energy*. Jose Beltrán Jiménez and Antonio L. Maroto. *JCAP* **0903**:016 (2009).
7. *Cosmic vector for dark energy*. Jose Beltrán Jiménez and Antonio L. Maroto. *Physical Review* **D78**, 063005 (2008).  
Editorial comment in *Nature Physics* **4**, 751 (Oct. 2008).
8. *Cosmology with moving dark energy and the CMB quadrupole*. Jose Beltrán Jiménez and Antonio L. Maroto. *Physical Review* **D76**, 023003 (2007).

The work developed in the thesis has been presented in a series of workshops with the following contributions to the corresponding Proceedings:

1. *Dark energy in vector-tensor theories of gravity*. Jose Beltrán Jiménez and Antonio L. Maroto. Proceedings of the Spanish Relativity Meeting ERE 2009, Journal of Physics: Conference Series (JPCS).
2. *Electromagnetic nature of dark energy*. Jose Beltrán Jiménez and Antonio L. Maroto. To be published in the proceedings of *The Invisible Universe*, June 29th -July 3rd 2009, UNESCO, Paris.
3. *On the dark energy rest frame and the CMB*. Jose Beltrán Jiménez and Antonio L. Maroto. AIP Conf. Proc. 1122: 193-196 (2009).
4. *Avoiding the dark energy coincidence problem with a cosmic vector*. Jose Beltrán Jiménez and Antonio L. Maroto. AIP Conf. Proc. 1122: 107-114 (2009).
5. *Vector models for dark energy*. Jose Beltrán Jiménez and Antonio L. Maroto. Proceedings of 43th Recontres de Moriond: Cosmology, La Thuile, Italy 15-22 March 2008, Cosmology, eds. J. Dumarchez, Y. Giraus-Heraud, J. Tran Thanh Van, The Gioi Publishers, pag. 291-294 (2008).

Some of the results obtained in the thesis have been used to write the following Essay:

- *Dark energy: the absolute electric potential of the universe*. Jose Beltrán Jiménez and Antonio L. Maroto. Accepted for publication in *Int. J. Mod. Phys. D* (2009)

which was selected for "Honorable Mention" in the 2009 Awards for Essays on Gravitation (Gravity Research Foundation).

Finally, the following e-print is being refereed for publication:

- *The electromagnetic dark sector*. Jose Beltrán Jiménez and Antonio L. Maroto. arXiv:0903.4672 [astro-ph.CO].

# Preface

---

We are probably witnessing a golden age of Cosmology. The reason is that, for the very first time, we have the sufficiently developed technology to design and perform experiments that allow us to observe the Universe on large scales with great precision. Moreover, the accurate measurements provided by these observations enable us to test our theoretical models about the composition, structure and evolution of the Universe so that we can advance in our understanding of the Cosmos. Nonetheless, the advances that Cosmology has undergone in recent years are not exclusively due to the technological progress, that has allowed high precision observations, but dramatic improvements have also been made in theoretical Cosmology in order to incorporate the enormous amount of observations that we have available nowadays. It is remarkable the case of the cosmological perturbations theory that includes many different physical processes and that successfully accounts for the observed power spectrum of the Cosmic Microwave Background (CMB) radiation and the hierarchy of structures present in the matter distribution, providing us with a large amount of very valuable cosmological information.

In spite of all the advances in the cosmological observations and the corresponding refinements of our theoretical models, we still have to deal with some mysterious features of the Universe on large scales. Apart from the dark matter problem, the most intriguing one appeared when distant supernovae measurements revealed that the expansion of the Universe is currently speeding up, rather than being decelerating as it would correspond to a universe filled with matter and in which gravity would be described by General Relativity. Such a discovery seemed to indicate the presence of some sort of antigravity on large scales that would tend to push the matter apart. Surprisingly, the simplest explanation to this problem turned out to be the introduction of a cosmological constant like the one discarded by Einstein when the expansion of the Universe

was discovered. However, the cosmological constant happened to be uncomfortable from a theoretical point of view because, in order to fit the observations, it should have an extremely tiny value as compared to the Planck mass, which is the scale already present in the gravitational action. Thus, if the cosmological constant was a true constant of nature, the gravitational theory would contain two dimensional constants differing by many orders of magnitude. For that reason, cosmologists started considering the possibility that the cosmic acceleration was not caused by the presence of a cosmological constant, but it was an effect due to the existence of a new component which would dominate the Universe content on large scales and that could evolve in time. This new component was generally called *dark energy* and will play a central role in this thesis. In order to explain this dark component, many different theoretical models have been proposed to date, although none of them seems to offer a satisfactory alternative. The most popular ones are those based on the introduction of a new scalar field on cosmological scales in the presence of a certain potential. The problem with these models is that they require either the introduction of an unnatural scale in the potential or to fine tune the initial conditions in order to give rise to accelerated expansion today. Moreover, not only models based on the introduction of a new field have been considered to explain the cosmic acceleration, but also modifications of General Relativity on large scales have been proposed.

The Standard Model of Cosmology, in which dark energy is assumed to be a pure cosmological constant, is based on the assumption, supported by matter distribution and CMB observations, that the Universe is homogeneous and isotropic on large scales. However, recent cosmological observations have suggested that such an assumption could be inappropriate. Thus, the CMB temperature fluctuations present a certain alignment for the lowest multipoles with a high significance that might be signaling the presence of a preferred spatial direction in the Universe. Also the observations of large scale matter bulk flows whose amplitude could conflict with the predictions of the Standard Model of Cosmology could be indicating the existence of a privileged direction which would spoil the isotropy assumption. These measurements might indicate that any of the components present in the Universe could exhibit some vector properties. In this thesis we shall explore the possibility that such a vector character could be attributed to the dark energy component. Moreover, also from a pure theoretical point of view, considering a vector nature for dark energy is well-motivated because vector fields are already present in the description of fundamental interactions in nature as carriers of the

gauge interactions, so that one could expect the presence of vector fields over cosmological scales that could play an important role for the evolution of the Universe.

The thesis will be organized in the following way. In the first Chapter, we shall introduce the basic concepts of Modern Cosmology and present the main features of the Standard Model of Cosmology. We shall pay especial attention to the cosmic acceleration problem to show how it has become firmly established by means of a variety of cosmological observations. Moreover, we shall summarize the main theoretical proposals for dark energy that have been considered in the literature.

After having shown why the existence of a current phase of accelerated expansion is broadly accepted according to the observations, we shall move on to explore potential vector properties of dark energy. Since the actual reason why the expansion is speeding up remains unknown, we shall assume that, as the rest of components, dark energy can be effectively described by a perfect fluid. However, we shall provide it with a vector property by allowing for a relative motion with respect to matter and radiation. We shall adopt this description in the second Chapter of this thesis and we shall study the potential effects on the CMB temperature fluctuations because of having different rest frames for dark energy and for the rest of components.

Once we have considered that dark energy could be moving with respect to matter and radiation, we shall explore the possibility of describing the cosmic expansion within the context of a particular class of gravitational theories, called vector-tensor theories, in which, in addition to the usual metric field, we have a vector field non-minimally coupled to the metric. Chapter 3 will be devoted to the study of the cosmological evolution in a general vector-tensor theory. The interest of these theories is that, as we shall show, they have solutions with accelerated expansion so that the vector field might actually play the role of dark energy. In fact, we shall identify those theories in which isotropic accelerated expansion can be realized.

In Chapter 4 we shall investigate the viability conditions for general vector-tensor theories attending to their compatibility with local gravity tests and the absence of instabilities. The procedure will be to identify those models which are indistinguishable from General Relativity by means of Solar Systems experiments and, then, check whether they have instabilities, both at the classical and quantum level.

In the last two Chapters of the thesis we shall present two specific dark energy models based on vector fields which allow to avoid the naturalness or fine-tuning problems that plague most of the dark energy models. In the first of them we can avoid these problems thanks to a scaling behavior of the vector field in the early Universe. For the second model, we shall resort to a modification of electromagnetism to explain the cosmic acceleration in which naturalness problems can also be evaded. We shall show that the usual covariant quantization method of the electromagnetic field is difficult to realize in an expanding universe. We shall propose a new consistent quantization method that avoids those difficulties and that introduces an extra electromagnetic degree of freedom. This new mode can be excited during an inflationary era and gives rise to an effective cosmological constant on large scales.

Finally, we shall summarize the main contributions made in this thesis. In particular, we shall compare our results with the already existing proposals and comment on some prospects concerning future potential investigations.

Madrid, November 2009

---

## Chapter 1

# The Standard Model of Cosmology

---

## 1.1 Introduction

Before proceeding with the central topic of the thesis, it seems quite convenient, in addition to be a good starting point, to present the state-of-art in Modern Cosmology, so that the research activity performed throughout the thesis is appropriately contextualized. To that end, we shall start by explaining the two basic pillars that support the Standard Model of Cosmology, namely the Cosmological Principle and General Relativity, and show how they give rise to the Hot Big Bang model describing the evolution of our Universe since the Planck era up to now. We shall go through its different phases, paying special attention to the most relevant events that have led to the current composition of the Universe that we can observe today.

After having presented a brief review of the Universe composition and evolution in the Standard Model, a major part of the Chapter will be devoted to the main topic of this thesis, namely the dark energy component. We shall explain why dark energy is so fundamental in order to understand the supernovae measurements and what other sorts of cosmological observations performed to date support the idea of a current phase of accelerated expansion. We shall see how several data sets coming from different observations converge towards a model in which the Universe is about one quarter of matter and three quarters of dark energy.

Since the discovery of the cosmic acceleration, an enormous amount of different models has been proposed trying to explain it. The appear-

ance of so many models is essentially motivated by two reasons. The first one is that, even though a simple cosmological constant has the ability of explaining almost all the cosmological observations, it suffers from some problems from the theoretical point of view so that it is necessary to explore alternative explanations. The second reason is that, in the Standard Model, we already had an era of accelerated expansion during inflation so that we can adapt the existing inflationary models in order to explain the present cosmic acceleration. Once again, since we shall be investigating on dark energy throughout this thesis, we shall explain some of the most popular models that will enable us to show how the results of the thesis can help to have a better understanding of such an unknown components and why the models proposed here introduce improvements with respect to other already existing models in the literature.

Finally, this Chapter will also be useful in order to set most of the notation and conventions used in the rest of the thesis. This is especially necessary in cosmology because of the existence of several conventions which may appear as overall minus (or plus) signs as well as some global numerical factors in the final results that might cause some confusion.

## 1.2 Theoretical Framework

The Standard Model of Cosmology gives a simple and accurate understanding of the whole (observable) Universe as we see it today. The starting point is the Cosmological Principle, which establishes the symmetries of the Universe on very large scales to be isotropy and homogeneity. Physically, it means that there are neither privileged places nor preferred directions in the Universe so that it will appear the same to any observer. Although it was initially postulated (probably for philosophical reasons) as a principle of modesty in the sense that it implies that the Earth does not occupy a privileged place in the Universe, nowadays it has been extensively confirmed by numerous cosmological observations. The lack of privileged directions can be seen in the Cosmic Microwave Background (CMB) radiation where departures from pure isotropy can only be found at the level of one part in one hundred thousand. However, this is only true once the dipole contribution is removed, which is justified in Standard Cosmology because it is usually ascribed to our relative motion with

respect to CMB photons<sup>1</sup>. On the other hand, the current galaxy surveys comprising more than 250.000 galaxies like the 2 Degree Field Galaxy Redshift Survey (2DFGRS) or around one million galaxies like the Sloan Digital Sky Survey (SDSS) show the high homogeneity of the galaxies distribution in the Universe on scales beyond  $\sim 1$  Gpc (see Fig. 1.1).

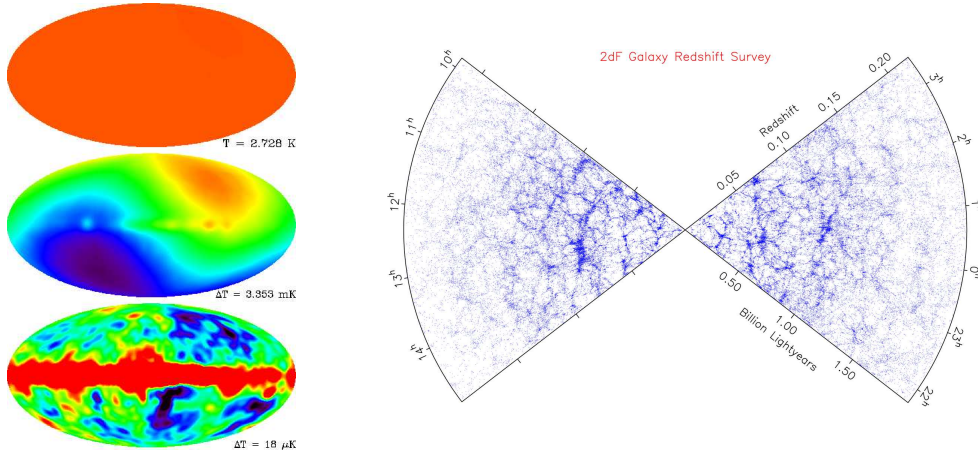


Figure 1.1: In these figures we can see the observational support of the Cosmological Principle. In the left figure it is shown the CMB temperature anisotropies as first discovered by the COBE satellite. In the upper panel we see the highly isotropy present in the temperature distribution of the CMB, in the middle panel we see the  $10^{-3}$  anisotropy corresponding to the dipole and that is usually attributed to a kinematical effect which, once it is removed, leads to the characteristic  $10^{-5}$  anisotropies of the CMB shown in the lower panel. In the right figure, we show the 2dFGRS galaxy survey supporting the large scale homogeneity of the Universe.

The other key ingredient present in the Standard Model is the use of General Relativity (GR) as the theory describing the gravitational interaction, which is the most relevant force when dealing with problems on cosmological scales. Such a theory describes gravitation as a curvature effect of the spacetime where the physical processes take place in such a way that its energy content determines the curvature of the spacetime whereas the curvature of the spacetime determines the trajectories of the particles<sup>2</sup>. Following the modern approach of building a physical theory by establishing the fields content and a set of symmetries, GR can be seen as the theory describing a spin two field (the graviton) and which is invariant under diffeomorphisms and local Lorentz transformations, i.e.,

<sup>1</sup>In Chapter 2, we shall show how such a dipole contribution might actually have a cosmological origin.

<sup>2</sup>John Wheeler said at this respect: *Matter tells spacetime how to bend and spacetime returns the complement by telling matter how to move.*

physics does not depend on the way that we use to describe it. Actually, GR is only the simplest theory of a wide class of theories with such fields content and symmetries. However, if we require the gravitational theory to describe a pure spin two particle, then GR is the theory we are looking for. In some sense, GR is the analogous for a spin two particle to Maxwell electromagnetism for a spin one particle.

We should note that General Relativity gives a twofold description of gravity. Firstly, it states that the physical processes take place in a dynamical 4-dimensional manifold and that the physical laws must be expressed in terms of tensors defined on such a manifold. And secondly, it relates the dynamics of the manifold metric to its energy content by means of Einstein equations<sup>3</sup>:

$$G_{\mu\nu} \equiv R_{\mu\nu} - \frac{1}{2}Rg_{\mu\nu} = 8\pi GT_{\mu\nu} \quad (1.1)$$

where  $G$  is the Newton constant,  $G_{\mu\nu}$  is the Einstein tensor,  $R_{\mu\nu}$  the Ricci tensor,  $R = g^{\mu\nu}R_{\mu\nu}$  the scalar curvature and  $T_{\mu\nu}$  is the energy-momentum tensor of the fields contained in the spacetime. Formally, these equations can be obtained from the Einstein-Hilbert action:

$$S = - \int d^4x \sqrt{-g} \frac{R}{16\pi G} + S_m \quad (1.2)$$

where  $S_m$  is the action corresponding to the fields present in the spacetime so that  $T_{\mu\nu} \equiv \frac{2}{\sqrt{-g}} \frac{\delta S_m}{\delta g^{\mu\nu}}$ . In the equations (1.1) we have the anticipated interplay between the geometry of the spacetime and its material content.

In the gravitational sector, it is possible to introduce a constant term so that the total action becomes:

$$S = - \int d^4x \sqrt{-g} \left( \frac{R}{16\pi G} + 2\Lambda \right) + S_m \quad (1.3)$$

where  $\Lambda$  is the so-called cosmological constant. Then, Einstein equations become:

$$R_{\mu\nu} - \frac{1}{2}Rg_{\mu\nu} = 8\pi G(T_{\mu\nu} + \Lambda g_{\mu\nu}) \quad (1.4)$$

and we can interpret the cosmological constant as a component whose energy-momentum tensor is proportional to the metric tensor.

---

<sup>3</sup>We set the speed of light  $c = 1$ .

## 1.3 Basics of FLRW universe

The geometry of the Universe can be established from the symmetries imposed by the Cosmological Principle. According to it, the metric of the Universe must belong to the class:

$$ds^2 = dt^2 - a(t)^2 \left[ \frac{dr^2}{1 - kr^2} + r^2 (d\theta^2 + \sin^2 \theta d\phi^2) \right], \quad (1.5)$$

known as Friedmann-Lemaître-Robertson-Walker (FLRW) metric. In this expression,  $a(t)$  is called the scale factor and  $k$  determines the curvature of the spatial sections, which can be open ( $k < 0$ ), flat ( $k = 0$ ) or closed ( $k > 0$ ).

It is usual to describe the content of the Universe on very large scales by means of an ideal perfect fluid as the source of the energy-momentum tensor so that:

$$T_{\mu\nu} = (\rho + p)u_\mu u_\nu - pg_{\mu\nu}, \quad (1.6)$$

with  $\rho$  the energy density as measured by a comoving observer,  $p$  the pressure and  $u^\mu$  the 4-velocity of the observer. We can see that, for a fluid with  $\rho + p = 0$ , the energy-momentum tensor is proportional to the metric tensor so that the latter expression also comprises the case of a cosmological constant.

Einstein equations for the FLRW metric in the presence of the latter energy-momentum tensor give rise to the following set of equations:

$$H^2 = \frac{8\pi G}{3}\rho - \frac{k}{a^2}, \quad (1.7)$$

$$\dot{H} = -4\pi G(p + \rho) + \frac{k}{a^2}, \quad (1.8)$$

where  $H = \dot{a}/a$  is the so-called Hubble expansion rate and a dot stands for derivatives with respect to cosmic time  $t$ . The first equation is known as Friedmann equation and gives the expansion rate in terms of the total energy density and curvature of the Universe. If we eliminate the curvature term from the two previous equations we obtain:

$$\frac{\ddot{a}}{a} = -\frac{4\pi G}{3}(\rho + 3p), \quad (1.9)$$

which shows that the expansion of the Universe only accelerates whenever  $\rho + 3p < 0$  holds. In particular, a cosmological constant having

$p_\Lambda = -\rho_\Lambda$  satisfies this condition. Moreover, the content of the Universe also determines its geometry to be flat, open or closed. This is easily seen from Friedmann equation evaluated at present time, which can be written in the form:

$$\Omega + \Omega_k = 1 \quad (1.10)$$

known as the cosmic sum rule. In this expression we have introduced the density parameters  $\Omega = \rho/\rho_{cr}$  and  $\Omega_k = k/(aH_0)^2$  with the critical density defined as  $\rho_{cr} = 3H_0^2/(8\pi G)$ , being  $H_0$  the Hubble parameter today. Hence, we have that depending on whether the energy density is larger, equal or smaller than the critical density, the geometry of the Universe is spatially closed, flat or open respectively.

The conservation of the energy-momentum tensor for the perfect fluid yields the continuity equation:

$$\dot{\rho} + 3H(\rho + p) = 0. \quad (1.11)$$

This equation is not independent of Einstein equations, but a consequence of Bianchi identities. If the fluid happens to satisfy a barotropic equation of state of the form  $p = w\rho$  with  $w$  constant, the continuity equation can be easily integrated to give:

$$\rho = \rho_0 a^{-3(1+w)}. \quad (1.12)$$

According to these solutions, we have that the energy density of a radiation fluid ( $w = 1/3$ ) decays as  $a^{-4}$ , whereas that of a pressureless component ( $w = 0$ ) evolves as  $a^{-3}$ . Moreover, a fluid with equation of state  $w = -1$  (like that of a cosmological constant) has constant energy density. These solutions for the evolution of the energy densities allow to write the Friedmann equation corresponding to a universe filled with matter and radiation and in the presence of a cosmological constant as follows:

$$\frac{H^2}{H_0^2} = \Omega_R a^{-4} + \Omega_M a^{-3} + \Omega_k a^{-2} + \Omega_\Lambda \quad (1.13)$$

where we have used the definition of the density parameters given above.

If the Universe is dominated by one single component with equation of state  $w$  and we neglect the contribution from the spatial curvature, we can integrate the Friedmann equation to obtain the scale factor:

$$a = a_0 t^{\frac{2}{3(1+w)}}, \quad (1.14)$$

and, therefore, the Hubble parameter is given by:

$$H = \frac{2}{3(1+w)t}. \quad (1.15)$$

Thus, in the presence of a radiation fluid we have that  $a \propto t^{1/2}$  and  $H = \frac{1}{2t}$  whereas for a matter component we have  $a \propto t^{2/3}$  and  $H = \frac{2}{3t}$ .

In the following, we shall show how to calculate distances in a FLRW universe. To that end, it is convenient to introduce a new radial coordinate  $\chi$  defined by the equation

$$d\chi^2 = \frac{dr^2}{1 - kr^2} \quad (1.16)$$

in terms of which the line element reads:

$$ds^2 = dt^2 - a^2(t) \left[ d\chi^2 + S_k^2(\chi) \left( d\theta^2 + \sin^2 \theta d\phi^2 \right) \right] \quad (1.17)$$

with  $S_k(\chi) = r(\chi)$ . According to (1.16), this function is given by

$$S_k(\chi) = \frac{1}{\sqrt{k}} \sin \left( \sqrt{k} \chi \right) \quad (1.18)$$

which happens to be  $S_k(\chi) = \sin \chi$ ,  $\chi$ ,  $\sinh \chi$  for  $k > 0$ ,  $k = 0$  and  $k < 0$  respectively. The null geodesics of this metric along the  $\chi$  direction are obtained from the condition  $ds^2 = dt^2 - a^2(t)d\chi^2 = 0$  and, for a geodesic starting from the origin, we obtain:

$$\chi = \int_{t_0}^t \frac{d\hat{t}}{a(\hat{t})} = \int_{a_0}^a \frac{d\hat{a}}{\hat{a}^2 H^2(\hat{a})} \quad (1.19)$$

where we have used that  $\dot{a} = aH$ . Thus, the comoving distance  $r = S_k(\chi)$  is given by:

$$r(a) = \frac{1}{\sqrt{k}} \sin \left( \sqrt{k} \int_{a_0}^a \frac{d\hat{a}}{\hat{a}^2 H^2(\hat{a})} \right). \quad (1.20)$$

This expression can be related to the content of the Universe by means of Friedmann equation so that the measurement of known sizes at different epochs will give clues about the actual composition of the Universe. This is helpful because if we know the size of some physical scale in the Universe at some particular time, we can measure that same scale at other epochs and, from those measurements, infer the expansion history of the Universe. Finally, another useful quantity is the so-called luminosity distance, which is given by:

$$d_L(a) = \frac{1}{a} r(a) = \frac{1}{a\sqrt{k}} \sin \left( \sqrt{k} \int_{a_0}^a \frac{d\hat{a}}{\hat{a}^2 H^2(\hat{a})} \right). \quad (1.21)$$

## 1.4 The Standard Model

The most accepted idea in Cosmology about the composition of the Universe today is that it is made of about 4% of baryons, 23% of dark matter and 73% of dark energy, being the contribution of radiation negligible  $\sim 0.001\%$  and the spatial geometry of the Universe very approximately flat. Such a cosmic inventory is obtained from observations of different sources (that we shall discuss later on) within the context of the  $\Lambda$ CDM model in which the Universe is currently dominated by a cosmological constant term and a cold dark matter component. However, because the different components evolve according to (1.12), as we go back in time we find an intermediate period of matter domination and that the early Universe was dominated by radiation. This fact leads to the idea of the Hot Big Bang theory, which states that the Universe started in an extremely hot and dense state. From that initial state on, the Universe began to expand and cool down and, at some point, it underwent a period of accelerated expansion known as inflation. The precise physical mechanism driving the inflationary era is not very clear yet, although the important feature of such a phase is that it smooths out the Universe and connect causally regions of the Universe which otherwise would be disconnected. This period in the early Universe is needed in order to explain some of the observations of our Universe. First of all, it explains why the Universe appears so homogeneous and isotropic given that some regions would have never been causally connected in the absence of inflation. Second of all, it gives an origin for the near flatness of our Universe, which otherwise would require an enormous fine-tuning in the initial conditions, since the flat solution of Einstein equations happens to be unstable. Finally, it provides a mechanism for the generation of the density fluctuations leading to the structures that we observe today.

After inflation, we end up with a Universe which is essentially empty and very cold, with all the available energy stored in the inflaton field. This energy is transferred into heat in a process called reheating in such a way that the Universe becomes hot again and filled with the particles of the Standard Model of Elementary Particles (leptons, quarks, photons, gluons, Z's and W's) and, perhaps, some other unknown particles. When the Universe becomes cool enough, quarks are no longer free and they confine forming hadrons. Meanwhile, the Universe continues expanding and getting colder and, when the temperature is  $10^9$  K, the lightest

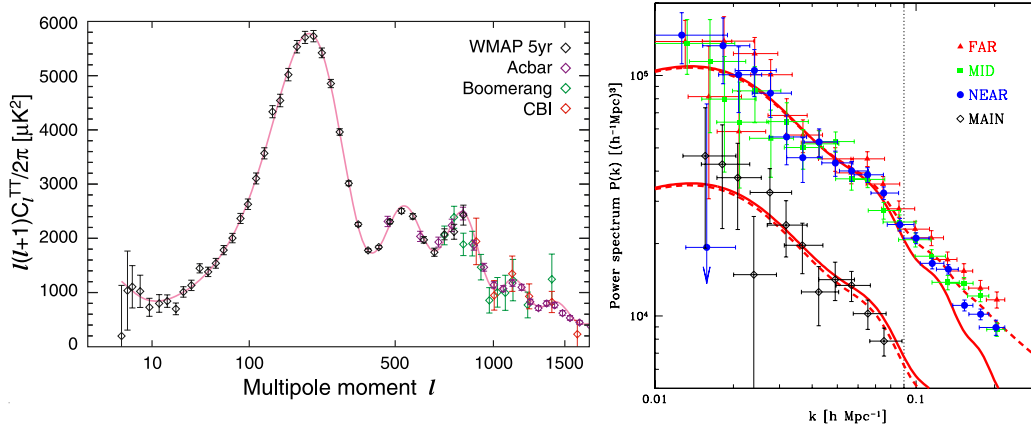


Figure 1.2: In this figure we show the CMB temperature power spectrum (left panel [1]) and the matter distribution power spectrum (right panel from SDSS [2]) for the  $\Lambda$ CDM model as well as the results obtained from several experiments. We see how both spectra are in good agreement with the observations, supporting our current vision of the Universe.

nuclei<sup>4</sup> can form. This process is known as primordial Big Bag Nucleosynthesis (BBN) and is the responsible for the relative abundance of light elements in the Universe. When the Universe is  $\sim 300.000$  years old, matter starts driving the expansion and, after 380.000 years since the Big Bang, the light nuclei can bound the electrons so that photons can propagate freely, i.e., the Universe becomes transparent. This moment is called the decoupling time and it forms the last scattering surface as seen from our position today because it is the time when photons were scattered by electrons for the last time. Moreover, these are the photons that we can see today in the CMB radiation. After the decoupling time, stars, galaxies and all the structures that we see today in the Universe can start forming because of the gravitational collapse of the small inhomogeneities existing in the matter distribution. However, the gravitational collapse of the baryons fluid by itself is not strong enough for such structures to have been able to form since decoupling time until today. For that reason, we need to assume that a dark matter component became decoupled from photons before baryons did so that its gravitational collapse started earlier and, thus, it can enhance the subsequent formation of structures for the baryons. Moreover, the dark matter component must be cold for its gravitational collapse to be able to take place.

<sup>4</sup>Others than  $^1\text{H}$  which, obviously already existed since the confinement of the

## Cosmological parameters from WMAP5

$10^2\Omega_b h^2$	$2.273 \pm 0.062$	$1 - n_s$	$0.037^{+0.015}_{-0.014}$
$1 - n_s$	$0.0081 < 1 - n_s < 0.0647$ (95% CL)	$A_{\text{BAO}}(z = 0.35)$	$0.457 \pm 0.022$
$C_{220}$	$5756 \pm 42$	$d_A(z_{\text{eq}})$	$14279^{+186}_{-189}$ Mpc
$d_A(z_*)$	$14115^{+188}_{-191}$ Mpc	$\Delta_{\mathcal{R}}^2$	$(2.41 \pm 0.11) \times 10^{-9}$
$h$	$0.719^{+0.026}_{-0.027}$	$H_0$	$71.9^{+2.6}_{-2.7}$ km/s/Mpc
$k_{\text{eq}}$	$0.00968 \pm 0.00046$	$\ell_{\text{eq}}$	$136.6 \pm 4.8$
$\ell_*$	$302.08^{+0.83}_{-0.84}$	$n_s$	$0.963^{+0.014}_{-0.015}$
$\Omega_b$	$0.0441 \pm 0.0030$	$\Omega_b h^2$	$0.02273 \pm 0.00062$
$\Omega_c$	$0.214 \pm 0.027$	$\Omega_c h^2$	$0.1099 \pm 0.0062$
$\Omega_\Lambda$	$0.742 \pm 0.030$	$\Omega_m$	$0.258 \pm 0.030$
$\Omega_m h^2$	$0.1326 \pm 0.0063$	$r_{\text{hor}}(z_{\text{dec}})$	$286.0 \pm 3.4$ Mpc
$r_s(z_d)$	$153.3 \pm 2.0$ Mpc	$r_s(z_d)/D_V(z = 0.2)$	$0.1946 \pm 0.0079$
$r_s(z_d)/D_V(z = 0.35)$	$0.1165 \pm 0.0042$	$r_s(z_*)$	$146.8 \pm 1.8$ Mpc
$R$	$1.713 \pm 0.020$	$\sigma_8$	$0.796 \pm 0.036$
$A_{\text{SZ}}$	$1.04^{+0.96}_{-0.69}$	$t_0$	$13.69 \pm 0.13$ Gyr
$\tau$	$0.087 \pm 0.017$	$\theta_*$	$0.010400 \pm 0.000029$
$\theta_*$	$0.5959 \pm 0.0017^\circ$	$t_*$	$380081^{+5843}_{-5841}$ yr
$z_{\text{dec}}$	$1087.9 \pm 1.2$	$z_d$	$1020.5 \pm 1.6$
$z_{\text{eq}}$	$3176^{+151}_{-150}$	$z_{\text{reion}}$	$11.0 \pm 1.4$
$z_*$	$1090.51 \pm 0.95$		

Figure 1.3: Cosmological parameters obtained by the WMAP5 team for a  $\Lambda$ CDM model. This table has been taken from the website <http://lambda.gsfc.nasa.gov/>, where the cosmological parameters corresponding to the combination of different datasets and for different theoretical models can be found.

Finally, at recent epochs, the Universe has entered into a phase dominated by some kind of exotic energy that leads to an accelerated expansion analogous to that experimented in the inflationary era. In the Standard Model, the current accelerated expansion is attributed to the presence of a cosmological constant whose energy density is constant throughout the expansion history of the Universe. This sort of contribution can be effectively interpreted as a perfect fluid having equation of state  $p = -\rho$ . However, one should be aware that such an equivalence only holds for the homogeneous regime, since, unlike a pure cosmological constant, a perfect fluid will typically give rise to inhomogeneous perturbations. The drawback of the cosmological constant, even though it is in agreement with most of the cosmological observations (for this

---

quarks.

reason it is usually called the concordance model), it suffers from some theoretical problems. The first of them has to do with the smallness of the cosmological constant whose scale is given by  $\Lambda \sim (10^{-3} \text{ eV})^4$ , that should be compared to the Planck mass scale  $M_P \sim 10^{19} \text{ GeV}$ . This is also called the naturalness problem because a theory containing two dimensional constants which differ in so many orders of magnitude does not seem to be very *natural*. Another problem with the cosmological constant is that it seems somehow surprising that its energy density is comparable to that stored in matter form precisely today, when they have evolved very differently in the past. Thus, although this could be just a *coincidence*, there could also be some hidden physical reason behind it.

## 1.5 Dark Energy

Since this thesis will be devoted to the study of different aspects and models for dark energy, it is appropriate to discuss here the current observational status of such an unknown component as well as to present a brief review of the most popular models proposed to so far account for it. It is worth indicating that, even though the first signals pointing out that our Universe is undergoing an accelerated expansion came about from supernovae measurements, there are other independent indicators of this phenomenon (as we shall show) so that it would be somehow surprising if all of them were affected by some kind of systematics which would make us believe that our Universe (at least our local patch) is accelerating when actually it is not. Therefore, even though we still do not know the true mechanism behind the cosmic acceleration, it is broadly accepted in Cosmology that the expansion of our Universe is truly speeding up and, indeed, this poses one of the greatest mysteries in fundamental physics.

Despite the enormous effort made to date, it is not very clear yet whether the accelerated expansion of the Universe is due to the presence of some unknown field or it is actually signaling the breakdown of GR on cosmological scales. An additional difficulty for such a distinction arises because one cannot discard any of them just by means of geometrical tests measuring uniquely the expansion history of the Universe. To clarify this issue, let us imagine that the true culprit responsible for the accelerated expansion is a new gravitational theory that modifies GR on large scales. This new theory will yield a new term on the LHS of Friedmann equation that can be moved to the RHS and be interpreted as the energy density

of a new field. For that reason, the study of the perturbations of the dark energy fluid is a crucial piece to understand the cosmic acceleration since it can help to discriminate between the two approaches. However, the effect is typically small because dark energy has become dominant only very recently so that we need cosmological observations of great accuracy. Indeed, this is one of the goals of the next generation of satellites and ground based observations as well as the use of alternative probes, like the weak lensing that will be more sensitive to the presence of dark energy perturbations.

### 1.5.1 Observational evidences

The first clue of the accelerated expansion of the Universe came about from observations of distant Type Ia supernovae (SNIa) in 1998 by two independent groups, leaded by Riess [3] and Perlmutter [4] respectively. The unexpected finding was that those supernovae seemed to be fainter than expected. Some authors suggested that this could be due to the extinction produced by the presence of some grey dust or the evolution in time of the supernovae rather than being signaling a true cosmic acceleration [5, 6], although subsequent SNIa surveys extended up to  $z \simeq 1.8$  favored the idea of the accelerated expansion over the alternative explanations [7]. Since then, the presence of a dark energy component in the Universe has been widely supported by more accurate SNIa observations and also by other independent cosmological sources of information like CMB or Large Scale Structures (LSS) that, providing transverse constraints, allow to break the degeneracy of the cosmological parameters obtained when considering SNIa measurements uniquely. In this Section, we shall discuss how the different observations support the idea of dark energy.

#### Type Ia supernovae

These standard candles represent the most direct evidence for the existence of a transition from a period of decelerated expansion to a late-time phase of accelerated expansion. Although they are not exactly standard candles, their luminosity curves can be described with a few parameters so that they can be standardized and, thus, are excellent tools to measure cosmological distances. The procedure consists of comparing the measured apparent magnitude of the SNIa (once it has been standardized) with

the theoretically expected one, which is given in terms of the luminosity-distance relation by:

$$m = 5 \log_{10} d_L(z; \Omega_M, \Omega_{DE}, w(z)) + \mathcal{M}(M, H_0) \quad (1.22)$$

where  $d_L = (1+z)r(z; \Omega_M, \Omega_{DE}, w(z))$  is the luminosity-distance already defined in (1.21) and  $\mathcal{M} \equiv M - 5 \log_{10}(H_0 \text{ Mpc}) + 25$  is the parameter to be constrained by nearby SNIa, i.e., it is determined by the calibration of the supernovae. Here  $M$  represents the absolute magnitude of the supernovae, defined as its apparent magnitude as seen from 10 Mpc. Thus, we can obtain a direct determination of the cosmological parameters by comparing the theoretical apparent magnitude with the observed one. However, since the comoving distance exhibits some degeneracy, in the sense that different values of the cosmological parameters can lead to the same luminosity-distance value, the SNIa cannot determine the precise values of the cosmological parameters by themselves, being necessary to resort to some complementary measurements. Fortunately, we have other sources of cosmological information which break the degeneracy.

## CMB

One might think that, since the CMB is a snapshot of the Universe at a time when dark energy was negligible, little knowledge concerning dark energy can be gained from it. However, the positions and amplitudes of the acoustic peaks in the CMB power spectrum provides us with an extremely useful information about the cosmological parameters. In particular, if we assume a dark energy model with  $w$  close to  $-1$ , then the position of the first acoustic peak constrains the spatial curvature of the Universe to be very nearly flat<sup>5</sup>. In any case, the CMB provides information on the allowed values of  $\Omega_M$  and  $\Omega_k$  in such a way that constraints on the combination  $\Omega_M + \Omega_{DE}$  can be obtained. It is worth mentioning that the CMB alone is not able to constrain the total amount of matter  $\Omega_M$ , but in combination with independent measurements of  $H_0$  or it indicates that matter can only account for about one quarter of the total energy density of the Universe so that a missing component is needed to accomplish the flatness suggested by the position of the first acoustic peak.

---

<sup>5</sup>It is usually said that the position of the first peak is given by  $\ell \simeq 200\Omega_0^{-1/2}$ . However, this formula is only approximately valid when  $\Omega_{DE} = 0$ , which is far from the realistic case. We can find an analytical expression for the dependence of the first peak position on the background density parameters in [9].

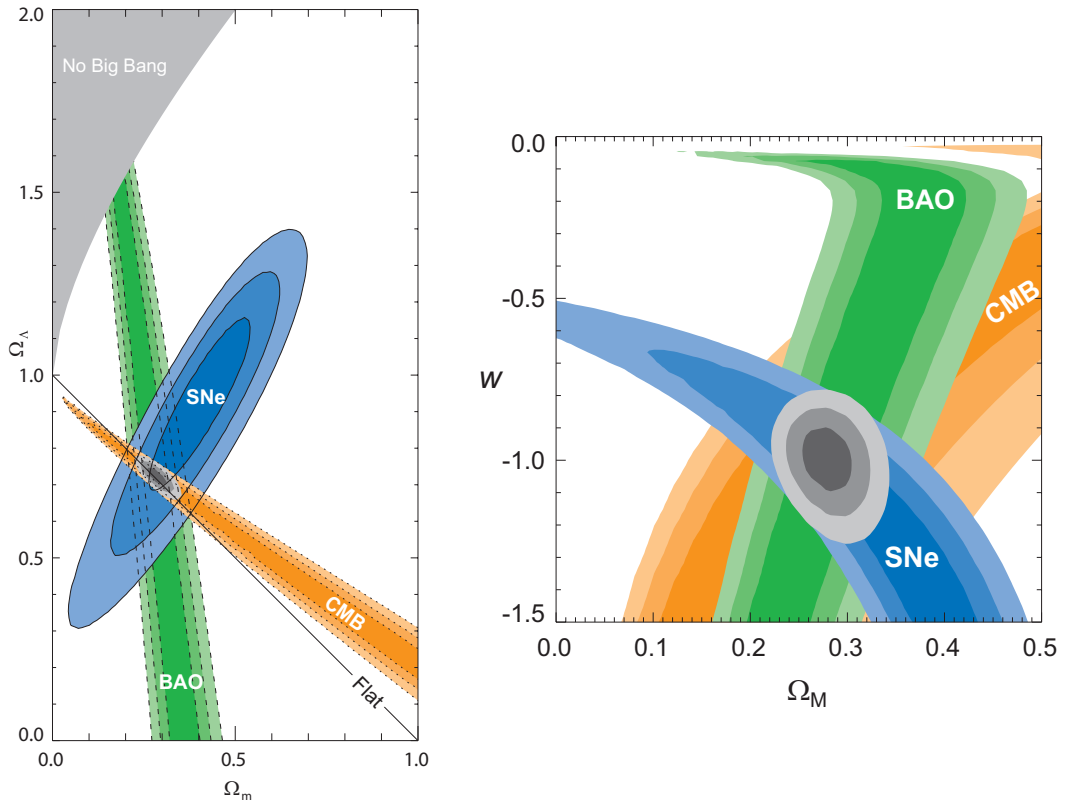


Figure 1.4: In this plot we show the constraints obtained in [8] from different data sets (SNIa, BAO and CMB) for a  $\Lambda$ CDM model (left panel) and for a model with dark energy having constant equation of state  $w$  (right panel).

## LSS

The growth of matter perturbations is affected by dark energy through the expansion rate of the Universe. When the Universe becomes neutral at recombination and baryons can start collapsing towards the overdense regions, we have two competing mechanisms. On one hand, the baryons tend to form structures as a consequence of the gravitational collapse and, on the other hand, the expansion of the Universe tends to break the collapse, effectively acting as a damping agent. The relative importance of the two effects depends on the ratio of the timescale for the perturbations to grow and the damping time, which will be driven by the Hubble expansion rate. The interesting feature is that, while in a pure matter dominated universe the perturbations of matter tend to grow proportionally to the scale factor, once the accelerated expansion starts the linear perturbations does not grow anymore. Therefore, by studying the distri-

bution of galaxies on large scales one can extract information about the expansion history of the Universe.

On the other hand, the distribution of galaxies provides us with a standard ruler, i.e., a physical scale whose comoving size is known at a specific time. This standard ruler has its origin in the sound waves propagating in the primordial plasma of the Universe before recombination. These waves are produced in the early Universe because of the presence of the attracting gravitational interaction and the repulsion produced by the pressure of the photons, which compete among them and give rise to the oscillations in the plasma that produce the waves. These oscillations are present as long as photons and baryons are coupled, but, once they decouple, the oscillations disappear. Therefore, it is expected to find a larger correlation of galaxies at scales corresponding to the last scattering surface in the matter distribution. Then, if we measure this scale at several redshifts we can obtain information about the evolution of the Hubble parameter. These Baryon Acoustic Oscillations (BAO) were detected by the Sloan Digital Sky Survey [10, 11] and they could measure them at two different redshifts  $z = 0.24$  and  $z = 0.35$ . These measurements again, favor a universe with a transition to an accelerated expansion at late times. The same result has been found in the papers [12, 13] by studying the baryon acoustic peak along the line-of-sight.

### Age of the Universe

There is another problem which, although does not directly point out towards the presence of a dark energy component, can be elegantly solved if we introduce it. Such a trouble arises when we compare the predicted age of the Universe with the oldest stellar objects that we know. From the age of the stars in globular clusters we can obtain a lower limit for the age of the Universe to be  $t_0 > 11 - 12$  Gyr [14, 15]. However, the age of the Universe can be calculated as:

$$t_0 = \int_0^{t_0} dt = \int_0^\infty \frac{dz}{H(1+z)} \quad (1.23)$$

where  $H$  is given by Friedmann equation (1.13). In order to calculate the age of the Universe we can neglect the radiation contribution because it is important only for  $z \gtrsim 1100$  and that region contributes negligibly to the

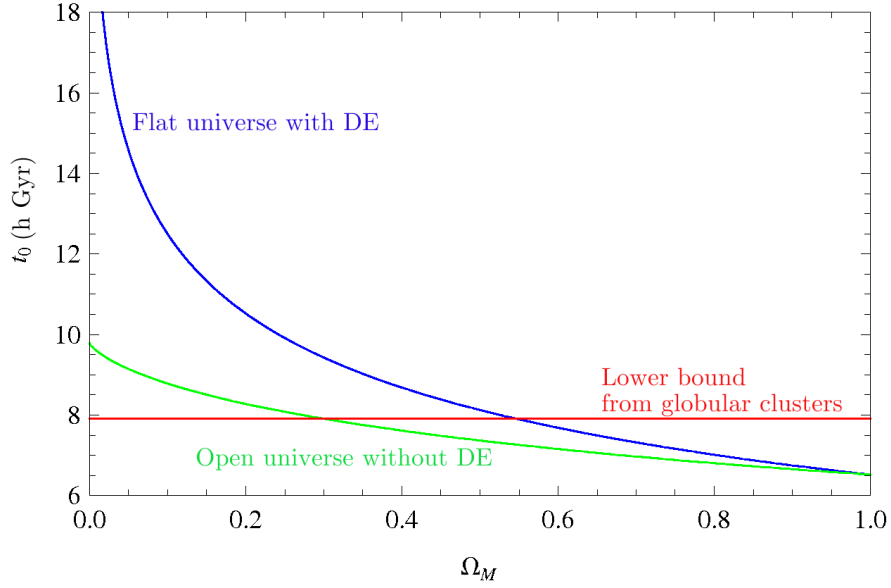


Figure 1.5: In this figure we show the age of the Universe as a function of  $\Omega_M$  for an open universe without dark energy (green line) and for a flat universe with dark energy in the form of a cosmological constant term. We also show the lower bound obtained from the oldest stellar objects in globular clusters (red line). We can see that the open case without dark energy only satisfies such a bound if  $\Omega_M \leq 0.3$  and this implies that  $\Omega_k \geq 0.7$  which conflicts with CMB observations. However, a flat universe with a cosmological constant easily evades those limits for  $\Omega_M \leq 0.5$  or, equivalently,  $\Omega_\Lambda \geq 0.5$ .

total integral. In a flat universe without cosmological constant we have:

$$t_0 = \frac{2}{3H_0}. \quad (1.24)$$

Then, if we take  $H_0^{-1} = 9.785h^{-1}$  Gyr with  $0.706 < h < 0.778$  obtained from the SHOES Team [16] we have that the age of the Universe is  $t_0 = 8.4 - 9.2$  Gyr which conflicts with the lower bound imposed by the oldest stellar objects. The situation does not get much better if we consider an open universe without dark energy. In that case, as shown in Fig 1.5, we need the curvature of the Universe to satisfy  $\Omega_k \geq 0.7$ , but this is in conflict with CMB observations which constrain the spatial curvature to be very small. However, when we consider a cosmological constant term, we can see in the Fig. 1.5 that the bounds from globular clusters can be satisfied with a  $\Omega_k = 0$  and  $\Omega_\Lambda \geq 0.5$ . Hence, also the age of the Universe strongly supports the idea of dark energy.

### 1.5.2 Dark Energy models

Even though we have an enormous lack of knowledge about the true nature of dark energy, the proliferation of theoretical models trying to account for it has provided a wide variety of possible explanations for the accelerated expansion by resorting to very different mechanisms, which can be broadly classified into two groups: on one hand, those models based on the introduction of new fields over cosmological scales and, on the other hand, those models that modify the gravitational theory either by adding new terms in the Einstein-Hilbert action or by assuming the existence of additional dimensions. Although all the proposed models are, in principle, plausible explanations for the current speed up of the cosmic expansion, most of them actually fail in the purpose for which they were introduced as alternatives to  $\Lambda$ , namely to avoid the naturalness problem. This is so because they usually require the introduction of either new dimensional constants differing by many orders of magnitude from the Planck scale, or initial conditions that must be very fine-tuned in order to get the desired effects.

At this point, we should notice that the majority of dark energy models assume that the cosmological constant is set to zero by some unknown mechanism. Although this might seem to be a very strong assumption, it is easier to imagine a zero cosmological constant (arising for instance from some symmetry principle) rather than one with the tiny observed value. In [17], alternative measures of integration in the action are considered in order to avoid a cosmological constant. For instance, if the usual measure  $\sqrt{-g}$  is changed by  $\nabla_\mu A^\mu \sqrt{-g} = \partial_\mu(\sqrt{-g} A^\mu)$ , the action remains invariant under the addition of a constant term to the lagrangian so that the potential presence of a cosmological constant becomes irrelevant. The same sort of symmetry principle is pursued in [18] by means of the so-called Normalized General Relativity, in which the usual Einstein-Hilbert action is normalized by a volume functional, in order to set the cosmological constant to zero.

Another flaw that many dark energy models have to face is the presence of instabilities (both at the classical and the quantum level) when the inhomogeneous perturbations are brought into the game, spoiling that way all the nice properties of the homogeneous solutions and thus the predictability of the model.

In the following, we shall present a brief summary of the most popular dark energy models proposed to date. It will not be exhaustive at all and,

for further details, I would refer to the excellent review [19] and the most recent ones [20] and [21].

### Scalar fields

One might be a bit suspicious about the use of scalar fields to explain dark energy because none of the known fields in the Standard Model of Elementary Particles has such a nature. However, the appearance of scalar fields is a very typical feature in high energy physics like string theories. Thus, it is well-motivated to consider the existence of cosmological scalar fields as well as their implications on the Universe evolution and, in particular, as possible candidates for dark energy. On the other hand, there exist objects that behave as scalar fields even though they are made of non-scalar fields like condensates. Moreover, this is a natural extension of the already developed models based on scalar fields for the early inflationary epoch.

Among all the possibilities, the simplest case that one can think of is that of a scalar field with a canonical kinetic term plus an effective potential term whose action is given by:

$$S = \int d^4x \sqrt{-g} \left[ \frac{1}{2} \partial_\mu \phi \partial^\mu \phi - V(\phi) \right]. \quad (1.25)$$

The models based on this action are usually referred to as quintessence models and can lead to late time accelerated expansion for suitable choices of the potential. Obviously, the arbitrariness on the choice of the potential enables us with a great freedom to achieve the desired evolution for the scalar field. The field equation derived from this action in a flat FLRW metric reads:

$$\ddot{\phi} + 3H\dot{\phi} + \frac{dV}{d\phi} = 0, \quad (1.26)$$

whereas the corresponding energy-momentum tensor is given by:

$$T_{\mu\nu} = \partial_\mu \phi \partial_\nu \phi - g_{\mu\nu} \left[ \frac{1}{2} \partial_\mu \phi \partial^\mu \phi - V(\phi) \right]. \quad (1.27)$$

This expression yields the following energy density and pressure for the scalar field in a FLRW metric:

$$\rho_\phi = \frac{1}{2} \dot{\phi}^2 + V(\phi), \quad (1.28)$$

$$p_\phi = \frac{1}{2} \dot{\phi}^2 - V(\phi), \quad (1.29)$$

where we have assumed that the scalar field is homogeneously distributed in space. Then, the effective equation of state is given by:

$$w_\phi = \frac{p_\phi}{\rho_\phi} = \frac{\frac{1}{2}\dot{\phi}^2 - V(\phi)}{\frac{1}{2}\dot{\phi}^2 + V(\phi)}. \quad (1.30)$$

This expression shows that quintessence models are constrained to have  $-1 \leq w_\phi \leq 1$ . The two limiting cases correspond to the domination of the kinetic energy over the potential with  $w_\phi \simeq 1$  (stiff matter) and the cases with a flat enough potential leading to a cosmological constant-like behavior with  $w_\phi \simeq -1$ .

A crucial difference between the quintessence fields and the inflaton fields is that the former are not required to lead to a finite period of accelerated expansion, but rather that they produce a late-time phase of accelerated expansion with the appropriate scale. Typical potentials that fulfill the mentioned requirement are the inverse power law potentials

$$V(\phi) = M^4 \left( \frac{M_P}{\phi} \right)^n \quad (1.31)$$

and the exponential potential

$$V(\phi) = M^4 e^{-\alpha \frac{\phi}{M_P}}. \quad (1.32)$$

In these potentials,  $M$  is some scale that must be fitted from data. The problem arising here is that, again, the obtained scale for  $M$  turns out to be very far away from the Planck scale so that these models do not offer a satisfactory solution to the naturalness problem. In some cases, the resulting value for the new scale  $M$  can be compatible with particle physics, but there are some other theoretical problems like how the given potential can be effectively obtained from particle physics or the need for fine-tunings in the initial conditions. In any case, one interesting property arising for some potentials is the possibility of having scaling solutions in which the energy density of the scalar field mimics the evolution of the dominant component and the fraction of energy density stored in the scalar field remains constant throughout the expansion of the Universe. Moreover, such solutions happen to be attractors so that one might alleviate the coincidence problem.

As we commented above, the quintessence models do not allow the crossing of the so-called phantom divide line. However, current observations allow (and some authors even claim that they favor) that dark

energy might have an equation of state smaller than  $-1$ , becoming that way a phantom component. One simple way to achieve this behavior with scalar fields is by changing the sign of the kinetic term in (1.25) so that:

$$S = \int d^4x \sqrt{-g} \left[ -\frac{1}{2} \partial_\mu \phi \partial^\mu \phi - V(\phi) \right]. \quad (1.33)$$

The models with this action are called phantom fields and were first proposed in [22]. The corresponding equation of state is given by:

$$w_\phi = \frac{p_\phi}{\rho_\phi} = \frac{\frac{1}{2} \dot{\phi}^2 + V(\phi)}{\frac{1}{2} \dot{\phi}^2 - V(\phi)}. \quad (1.34)$$

Unlike for the quintessence field, here we can have  $w_\phi < -1$ . A common feature of these models is that a universe dominated by a phantom fluid evolves towards a Big Rip singularity in which the curvature becomes infinity in a finite time. Nonetheless, this can be avoided in the presence of a potential with a local maximum so that the field oscillates around such a maximum and leads to a future de-Sitter universe with the field at rest at the top of the potential. Notice that, because of having the opposite sign for the kinetic term, the field climbs the potential rather than rolls down. In any case, these models have to face a more serious difficulty arising from the ultra-violet quantum instabilities related to the negativity of the kinetic terms. The problem is that the corresponding vacuum is unstable against the production of normal particles with positive energy in processes involving ghosts fields [23, 24].

A natural generalization of the latter phantom models that find a good motivation in string theories are the so-called K-essence theories first proposed to drive inflation [25] and later applied to the problem of dark energy [26, 27, 28]. These models describe a scalar field with an arbitrary kinetic term so that the corresponding action is given by:

$$S = \int d^4x \sqrt{-g} p(X, \phi) \quad (1.35)$$

with  $X = \frac{1}{2} \partial_\mu \phi \partial^\mu \phi$ . This action, of course, include both quintessence and phantom models. There is much freedom in the choice of the kinetic function  $p(X, \phi)$ , although a simplified form  $p(X, \phi) = f(\phi) \hat{p}(X)$  motivated by string theory is usually assumed [26, 27, 28]. An interesting property of these models is that they can lead to tracking solutions in which, for a wide range of initial conditions, the scalar field evolves in such a way that it tracks the energy density in matter so that it can solve the coincidence problem. However, we cannot get rid of some fine-tunings. Also,

it is possible to obtain phantom behavior, but again we have to face the presence of instabilities.

### Modified gravity

Another very popular approach to the dark energy problem adopted by cosmologists is the modification of Einstein gravity, so that the accelerated expansion would be the natural late-time evolution in a universe dominated by a matter component.

One class of modified theories which has received a huge amount of attention in the last years consists of assuming that the gravitational action is an arbitrary function of the Ricci scalar:

$$S = \int d^4x \sqrt{g} \left[ \frac{1}{16\pi G} R + f(R) \right]. \quad (1.36)$$

These type of models are usually referred to as  $f(R)$  models. Indeed, corrections to Einstein-Hilbert action proportional to  $R^2$  were already known to produce early accelerated solutions [29]. Since the scalar curvature drops as the Universe expands, the  $R^2$  term becomes negligible at late times as compared with the linear term so that it cannot give rise to late-time acceleration. However, if we add inverse powers of the scalar curvature, we will have the opposite situation, namely the new terms are negligible at early times, while they can be important at late times. In fact, this late-time modifications can give rise to accelerated solutions [30, 31, 32].

The modified Einstein equations of motion arising from this action can be written as:

$$(1 + f_R)R_{\mu\nu} - \frac{1}{2}g_{\mu\nu}(R + f) + (g_{\mu\nu}\square - \nabla_\mu\nabla_\nu)f_R = 8\pi GT_{\mu\nu} \quad (1.37)$$

where  $f_R \equiv \frac{df}{dR}$ . Since the gravitational action is no longer linear in the Ricci scalar, the modified Einstein equations are generally fourth order differential equations for the metric tensor and so it is much more difficult to find analytical solutions unless appropriately simple forms for the function  $f(R)$  are chosen. For a FLRW metric, the modified Einstein

equations give rise to:

$$H^2 + \frac{1}{6} - \frac{\ddot{a}}{a} f_R + H \dot{f}_R = \frac{8\pi G}{3} \rho \quad (1.38)$$

$$\frac{\ddot{a}}{a} - f_R H^2 + \frac{1}{6} f + \frac{1}{2} \ddot{f}_R = -\frac{4\pi G}{3} (\rho + 3p). \quad (1.39)$$

From these equations we see that, unlike in GR, accelerated expansion does not require  $\rho + 3p < 0$  anymore. In fact, one can interpret the effect of the  $f(R)$  term as an extra fluid with equation of state:

$$w_{eff} = -\frac{1}{3} - \frac{2}{3} \frac{6H^2 f_R - f - 6H \dot{f}_R - 3\ddot{f}_R}{-6H^2 f_R - f - 6H \dot{f}_R + \ddot{f}_R}. \quad (1.40)$$

One can see from this expression that any background evolution can be reproduced by means of a suitable choice of the  $f(R)$  function since, given  $w_{eff}$ , one can integrate the equation (1.40) to obtain the corresponding form of the function  $f(R)$  that reproduces such a cosmology. For instance, in [33] the function  $f(R)$  that mimics the behavior of a cosmological constant without cosmological constant (i.e., for  $f(R)$  different from a constant) has been obtained.

The fact that the modified action introduces non-linear terms of the Ricci scalar implies that the theory contains additional degrees of freedom which are not present in GR. These new degrees of freedom become apparent if we perform a conformal transformation of the form  $g_{\mu\nu}^{(E)} = e^{2\omega} g_{\mu\nu}$ . In the new (Einstein) frame, the action acquires the following form:

$$S_E = -\frac{1}{16\pi G} \int d^4x \sqrt{-g_E} R + \int d^4x \sqrt{-g_E} \left[ \frac{1}{2} (\nabla_E \phi)^2 + V(\phi) \right] \quad (1.41)$$

where  $\phi$  is a scalar field and  $V(\phi)$  and effective potential that depends on the function  $f(R)$ . Thus, we see that the  $f(R)$  theory in the old (Jordan) frame is equivalent to Einstein-Hilbert action plus a scalar field in the conformally transformed (Einstein) frame. However, there is a crucial difference between both frames, namely, while in the Jordan frame the test particles follow the geodesics of  $g$ , in the Einstein frame they do not fall along the geodesics of  $g_E$  since the scalar field  $\phi$  is coupled to all the fields. Thus, even though both approaches are mathematically equivalent, they describe different physical worlds.

A major problem that the pioneering proposals with  $f(R) \propto 1/R$  had to face is the presence of instabilities [34, 35] and some conflicts with Solar

System experiments [36], although one can get these problems around by introducing counterterms proportional to  $R^2$  [37].

So far, we have considered the theory in the so-called metric formalism in which the fundamental gravitational field is the metric tensor. However, there is another approach (already considered by Einstein) in which the fundamental fields are the metric tensor and the connection symbols, usually called the Palatini formalism (see for instance [38] for cosmological evolution and constraints within this formalism). In GR, both approaches lead to the same gravitational theory as long as the corresponding energy-momentum tensor does not depend on the connection, but in general  $f(R)$  theories they are no longer equivalent<sup>6</sup>. The main difference arises because, while the metric formalism gives rise to fourth order equations of motion for  $g_{\mu\nu}$ , the Palatini formalism leads to second order differential equations for both the metric tensor and the connection symbols. Indeed, this feature of the Palatini formalism can help avoiding the presence of instabilities (e.g. [39, 40]).

Once that one opens the possibility of adding higher order terms in the gravitational action, one can include more general curvature terms involving the Ricci and/or the Riemann tensors. Among all the possible choices, it is usual to consider the invariants  $P = R_{\mu\nu}R^{\mu\nu}$  and  $Q = R_{\alpha\beta\gamma\delta}R^{\alpha\beta\gamma\delta}$ . Obviously, the  $f(R)$  theories are contained into this broader class of theories and one could expect to have the same kind of problems with instabilities and small scales behavior.

Finally, a modified theory of gravity resorting to extra dimensions in order to explain the accelerated expansion of the Universe is the Dvali-Gabadadze-Porrati (DGP) model [41], that considers our Universe as a brane embedded in a 5-dimensional Minkowski bulk. In this model, gravity behaves as four dimensional at small distances, but as long as we consider larger distances it leaks into the bulk. The scale at which the higher dimensional effects become important is given by the crossover scale:

$$r_c = \frac{M_P^2}{2M_5^3} \quad (1.42)$$

where  $M_P$  is the usual 4-dimensional Planck mass and  $M_5$  is the 5-dimensional Planck scale. In a flat FLRW universe, the DGP model leads

---

<sup>6</sup>This is a reflect of the fact that GR is the theory describing a pure spin two particle, whereas the modified  $f(R)$  theories contain extra degrees of freedom.

to the following modified Friedmann equation:

$$\left(1 - \frac{\epsilon}{Hr_c}\right) H^2 = \frac{8\pi G}{3}\rho \quad (1.43)$$

with  $\epsilon = \pm 1$ . Hence, when the Hubble radius is much smaller than the crossover scale  $Hr_c \gg 1$  we recover the usual Friedmann equation, but when the Hubble radius is comparable to the crossover scale the higher dimensional effects becomes important. In a dust dominated universe with  $\rho \propto a^{-3}$  and in the branch with  $\epsilon = +1$  we see that the universe evolves towards a de-Sitter expansion with  $H \rightarrow r_c^{-1}$  in the presence of any component whose energy density dilutes as the universe expands. The problem with this model is that it contains ghost-like modes which make it unstable. Moreover, it provides a poor fit to SNeIa, BAO and CMB data, being  $\Lambda$ CDM much more favored.

Recently, a generalization of this model in six dimensions instead of the five dimensions already present in the original one has been proposed [42]. This generalization has been called *Cascading Gravity* because, since our 3-brane is embedded in a 4-brane, each of them with their respective induced gravity terms, and both embedded in a flat 6-dimensional bulk, the gravitational potential follows a cascading behavior in the form  $1/r$  for small scales,  $1/r^2$  when the fifth dimension starts being important and  $1/r^3$  when the sixth dimension becomes relevant. Indeed, this can realize the so-called degravitation of the vacuum energy that might shed some light into the cosmological constant problem because the gravitational force becomes weaker and weaker as we consider larger and larger scales. Finally, the main advantage of this generalization as compared to the original proposal is that it is free of ghosts-like instabilities, as long as the tension on the 3-brane is larger than a certain value.

### Other approaches to dark energy

In addition to the dark energy models based on either scalar fields or modifications of GR, there is a number of interesting, although not so popular, alternatives to explain the accelerated expansion.

One attempt of unifying dark matter and dark energy is realized by the so-called Chaplygin gas [43] whose equation of state is given by the particular law:

$$p = -\frac{A}{\rho}. \quad (1.44)$$

With this equation of state, the energy conservation equation yields the following evolution for its energy density:

$$\rho = \sqrt{A + B(1+z)^6}. \quad (1.45)$$

Hence, at high redshifts the fluid behaves as a matter component with  $\rho \simeq \sqrt{B}(1+z)^3$  whereas at low redshifts its energy density is nearly constant  $\rho \simeq \sqrt{A}$ . Moreover, these models can be obtained from a canonical scalar field with the following potential:

$$V(\phi) = \frac{\sqrt{A}}{2} \left[ \cosh(\sqrt{24\pi G}\phi) + \frac{1}{\cosh(\sqrt{24\pi G}\phi)} \right], \quad (1.46)$$

so that they can be considered as particular cases of the already discussed quintessence models.

These models were modified to include more general equations of state of the form

$$p = -\frac{A}{\rho^\alpha} \quad (1.47)$$

to alleviate some problems with CMB observations, but even in this case there are strong limits in the parameters of the model.

Another interesting class of models is that in which the cosmological constant is not a true constant, but it can run with the renormalization group equations [44, 45]. Modifications of this scenario in which a *cosmon* component is considered to describe dark energy in addition to the running cosmological constant have also been proposed [46], and they could solve the coincidence problem because the ratio  $\rho_{DE}/\rho_M$  remains bounded and of order 1.

So far we have seen that most of the attempts to explain the cosmic acceleration resort to some kind of unknown physics either by appealing to the existence of a new field or by modifying the gravitational theory. However, there are proposals in the literature which do not make use of new physics as well. One of these explanations consists of studying whether the backreaction of inhomogeneous cosmological perturbations [47, 48, 49] (both super and sub-horizon) could accelerate our local Hubble patch even though the whole Universe is not accelerating. However, this explanation cannot account for the whole observed acceleration. Another class of models which does not introduce new physics is that in

which it is assumed that we live very close to the center of a spherically symmetric underdense region (void) described by the Lemaître-Tolman-Bondi (LTB) metric [50]. That way, even though we measure a matter density parameter smaller than one inside the void, the actual value for it outside the void would match that corresponding to the critical density. However, these models require the same kind of fine-tuning to explain why we happen to be so close to the center of the void as  $\Lambda$ CDM to explain why the cosmological constant is so small. That is why it is usually said that these models shift the coincidence problem from *why now?* to *why here?* because we need to be placed very close to the center of the spherically symmetric void in order to explain the SN measurements without giving rise to a too large CMB dipole. The possibility of having an anisotropic rather than isotropic void has also been explored [51].

## 1.6 Final remarks

The discovery of the accelerated expansion of the Universe in 1998 put on the table the necessity of introducing an exotic component in the Universe inventory, dark energy, which should compose about three quarters of the total energy of the Universe. Although we have advanced in the understanding of the properties of dark energy, it is fair to say that we lack a satisfactory explanation of what the agent causing the cosmic acceleration is. We do not even know whether it is due to the presence of a new field or to the breakdown of GR at cosmological scales or to some other physical mechanism that we are overlooking. Then, even though we have advanced in the understanding of this phenomenon we still have a long way ahead before we can address it. The reason is that we need to compile more and more precise cosmological observations which will enable us to constrain the possible models and, eventually, find the true mechanism behind the cosmic acceleration. Among this new generation of observations we might cite here the future surveys comprising several thousands of SNIa, with the corresponding reduction of statistical uncertainties, the Gamma Ray Burst (GRB), that will allow to explore the deep Universe<sup>7</sup>, the weak gravitational lensing, that will probe dark energy by means of its effects in the growth of structures or BAO measurements at more redshifts (SDSS only reported measurements at two different redshifts). In [20], we can find an exhaustive list of the future projects to

<sup>7</sup>Recently, a GRB at redshift  $z \simeq 8.3$  has been reported in [52].

probe dark energy. Then, we will have to wait until the results of those experiments appear, although, meanwhile, we can continue advancing in our theoretical understanding of dark energy.



# Moving dark energy

---

## 2.1 Introduction

As we have extensively seen in the previous Chapter, still nowadays dark energy remains as the most intriguing component in the Universe and, probably for that reason, many different models to describe it have been proposed to date whose main motivation is caused by the theoretical problems related to the cosmological constant. Even though there exists a wide variety of models arising from very different approaches (quintessence, phantom fields, K-essence, modified gravities, etc.), in most of them one can finally reduce the model to be effectively described as a perfect fluid characterized by the value of its density parameter today and its equation of state, which, in some cases, can even evolve in time. Parameterizations for such evolving equations of state by means of some suitable analytical function depending on a few parameters have also been proposed. This phenomenological description of dark energy is very useful when confronting to observations because it allows to obtain model-independent constraints on the dark energy fluid. In other words, we can infer the energy-momentum tensor components (as well as its evolution) for the dark energy fluid directly from the observations without any a priori assumed fiducial consideration which might lead to biased findings. The motivation for this approach is that it can comprise many theoretical models at once so that one can deduce what region of the parameter space of a determined theoretical model will be more favored by data without having to perform the whole analysis. In order to obtain a full knowledge about the dark energy properties we should include all the components of its energy-momentum tensor, although the most widely used parameterizations for the dark energy

fluid assume vanishing off-diagonal components. We can give up this assumption in two different ways: by allowing anisotropic stresses<sup>1</sup> or a non-vanishing momentum density.

The highly isotropic CMB power spectrum that we observe today impose stringent limits in the possible presence of anisotropic stresses at the largest scales or, equivalently, in the low multipoles. However, these low multipoles are affected by large uncertainties due to the cosmic variance and they even present potential anomalies. It is worth mentioning that the possibility of having anisotropic stresses in the Universe was already considered before the discovery of the accelerated expansion. In fact, we can find a detailed study on the constraints obtained from the CMB to the late-time anisotropic stresses generated by matter sources like electric and magnetic fields or topological defects among others in [53]. Nonetheless, the interest on anisotropic effects grew after the discovery of the accelerated expansion because the presence of a new dark energy component in the Universe opened up the possibility of having a new source of anisotropic stresses with cosmological implications. This is not exclusive of dark energy models with a new field causing the acceleration, but also in modified gravities the existence of additional stresses is a typical feature. To mention some explicit examples, in [54] an anisotropic cosmological constant arising from an infrared non-commutativity of the spacetime is studied, the presence of magnetic fields at the decoupling time making the Universe ellipsoidal by that time was considered in [55] and, finally, in the series of papers [56], [57] and [58] a very exhaustive theoretical study of anisotropic stresses in dark energy models as well as confrontation with observations was performed.

In the previous paragraph we have focused on the possibility of having anisotropic contributions to the low CMB multipoles from dark energy models whose energy-momentum tensor has non-vanishing anisotropic stresses. Since the CMB anisotropies are of order  $10^{-5}$ , the corresponding constraints for the anisotropic stresses are expected to be at the same level (or lower). In the analysis leading to these limits, the contribution from the dipole, which is of order  $10^{-3}$ , is not taken into account because it is usually considered as a pure kinematical Doppler effect and so it can be removed when dealing with cosmological phenomena. How-

---

<sup>1</sup>By anisotropic stresses, usually labeled  $\Pi_j^i$ , we refer to the spatial non-isotropic piece of the energy-momentum tensor so that this can be decomposed as  $T_j^i = \frac{1}{3}T\delta_j^i + \Pi_j^i$  with  $T = T_j^j$ . This sort of contributions are not unusual and even massive neutrinos can produce them.

ever, some authors have also considered the possibility of a cosmological origin for the dipole from entropy gradients [59] or super-horizon preinflationary perturbations [60]. Hence, it seems worthwhile to pursue the possibility that dark energy could modify the usual interpretation of the dipole and provide it with a cosmological origin, violating that way the Cosmological Principle. This can be achieved by allowing for the existence of non-vanishing momentum density of dark energy, i.e.,  $T_{DE}^{0i} \neq 0$  [61, 62]. In terms of the effective fluid description, this can be interpreted as a relative motion between the standard components of the Universe (radiation, baryons and dark matter particles) and dark energy or, equivalently, that the dark energy rest frame does not coincide with that of the rest of components of the Universe on large scales. We should remind here that we know essentially nothing about the origin of dark energy (or more precisely, about the origin of the cosmic acceleration) so that a complete knowledge about its properties requires a study of *all* the components of its energy-momentum tensor. However, we do know some of the properties it should have in order not to spoil the Standard Cosmology predictions. In particular, it is usually considered as a highly homogeneous fluid because, in most of the models, the sound speed is very close to the speed of light so that one can prevent the formation of dark energy structures below the Hubble scale. Moreover, its interactions with the rest of components must be very weak and, indeed, in most of the cases dark energy is supposed to interact with the standard components only gravitationally so that it can be considered as a totally decoupled fluid. Hence, on the grounds of these assumptions about the dark energy component, it seems possible to consider different large scale rest frames for dark energy and for the primordial plasma in the early Universe and, thus, it makes sense to ask whether the dark energy rest frame coincides with the radiation or matter rest frames at large scales. On the other hand, the fact that a pure cosmological constant is invariant under change of frame implies that the potential effects associated to a non-vanishing relative motion will be exclusively present in dynamical dark energy models.

Leaving aside the actual origin of the dark energy flow, it seems clear that its existence is an expected feature when treating the dark energy component as a totally decoupled fluid. We shall investigate this possibility throughout this Chapter and show its potential effects on the CMB.

This Chapter contains the results corresponding to the following works:

- *Cosmology with moving dark energy and the CMB quadrupole.*  
Jose Beltrán Jiménez and Antonio L. Maroto.  
*Physical Review D* **76**, 023003 (2007).
- *Large-scale cosmic flows and moving dark energy.*  
Jose Beltrán Jiménez and Antonio L. Maroto.  
*JCAP* **0903**:015 (2009).

## 2.2 Large-scale dark flows

The Cosmological Principle states that the Universe is homogeneous and isotropic on large scales, i.e., on scales beyond  $\sim 1\text{Gpc}$ . However, when we go down to smaller scales, the Universe does not look homogeneous anymore and we can start distinguishing structures like super-clusters ( $\sim 100\text{Mpc}$ ), clusters ( $\sim 1 - 10\text{Mpc}$ ) or galaxies ( $\sim 1 - 100\text{kpc}$ ). These structures that we observe today in the matter distribution are thought to be formed by primordial quantum fluctuations originated during an inflationary era that, later on in the Universe evolution, would play the role of seeds around which the aforementioned hierarchy of structures would tend to grow. Moreover, these structures attract to each other gravitationally giving rise to the existence of relative motions due to the falling of the smaller structures into the larger ones. Hence, if we observe small enough volumes of matter, and once the Hubble flow has been subtracted, we would expect to see peculiar velocities of statistical origin for such volumes with respect to the large scale rest frame of the whole matter component. Indeed, the peculiar velocity of a galaxy placed at the position  $\vec{r}$  is given by [63]:

$$\vec{v}(\vec{r}) = \frac{\Omega_M^{0.55}}{4\pi} \int d^3\vec{r}' \delta_M(\vec{r}') \frac{\vec{r}' - \vec{r}}{|\vec{r}' - \vec{r}|^3} \quad (2.1)$$

where  $\delta_M$  is the density contrast of matter. From this expression we can see that for sufficiently large volumes of matter where the Universe becomes homogeneous, the peculiar velocities disappear. Whether the frame in which this effect decays as we consider large scales is the same as the CMB rest frame or not is not very clear from the observational point of view, as we shall see later, and, therefore, should be observationally tested.

In the standard  $\Lambda$ CDM model, matter and radiation share a common large scale rest frame because they were strongly coupled in the early Universe when forming the primordial photon-baryon plasma fluid. In this scenario, it is natural to expect the presence of relative motions for small volumes of matter with respect to the CMB frame, although such peculiar velocities (in the CMB rest frame) should vanish as we consider larger volumes because of the convergence of radiation and matter rest frames, as the Cosmological Principle dictates. In fact, this is nothing but a direct consequence of the momentum conservation before and after decoupling time. Since radiation and baryons had the same velocity before decoupling, if we use the center of mass frame (defined as the frame where the primordial plasma is at rest) the mentioned velocity vanishes identically. Then, since there are no additional momentum sources, the individual momentum conservation for each component makes them to remain at rest with respect to each other after decoupling. Nonetheless, the presence of the dark energy with non-vanishing relative velocities component may give rise to an additional source of momentum at that time so that the latter prediction in the standard  $\Lambda$ CDM model breaks down and baryons and photons are allowed to acquire relative velocities. This issue will become clearer in the subsequent Sections when going through the actual equations.

The formula given in (2.1) shows that the peculiar velocities of galaxies are sensitive to the matter power spectrum so that they provide a powerful tool in order to probe matter density fluctuations on large scales. For this reason, a big effort has been made to compile peculiar velocities of a large number of galaxies by using different tracers, namely individual galaxies [64, 65, 66, 67], clusters of galaxies [68, 69, 70] or type Ia supernovae [71]. Although surveys based on different distance indicators seem to agree with predictions of  $\Lambda$ CDM on small scales, on larger scales they have seemed to be in conflict among them and with  $\Lambda$ CDM for many years, yielding peculiar velocities in the wide range 0 – 1000 km/s. However, new data analysis performed in recent years like those in [72, 73, 74, 75, 76, 77] suggest that most of the surveys could also agree with each other on such large scales.

A completely new approach to obtain peculiar velocities of large volumes of matter which makes use of the Kinematic Sunyaev-Zeldovich effect on the CMB photons by the hot gas in clusters of galaxies was proposed in [78] and carried out in [79] and [80]. They find coherent bulk flows on scales of  $300h^{-1}$  Mpc towards  $l = 283^\circ \pm 14^\circ$ ,  $b = 11^\circ \pm 14^\circ$  (in

galactic coordinates). The reported amplitude for those peculiar velocities are in the range 600-1000 km/s, although the authors point out that, even though there is no doubt about the existence and direction of the flows, the obtained values for the amplitudes may have some systematic offset. In [79], they attribute these peculiar velocities to pre-inflationary super-Hubble perturbations (see [60]).

On the other hand, a calculation of peculiar velocities using some of the available measurements has been performed in [81], but with a new method which allows to reduce the sensitivity to small scale power and makes possible to compare the results obtained from different surveys. In that work, they find a consistent flow of matter on scales of  $100h^{-1}$  Mpc towards  $l = 287^\circ \pm 9^\circ$ ,  $b = 8^\circ \pm 6^\circ$  and with an amplitude of  $407 \pm 81$  km/s. The direction of the detected flow is in very good agreement with the results in [79], in spite of having used a very different method. The authors of this work claim that these peculiar velocities may be due to structures larger than the reached scale of  $100h^{-1}$  Mpc.

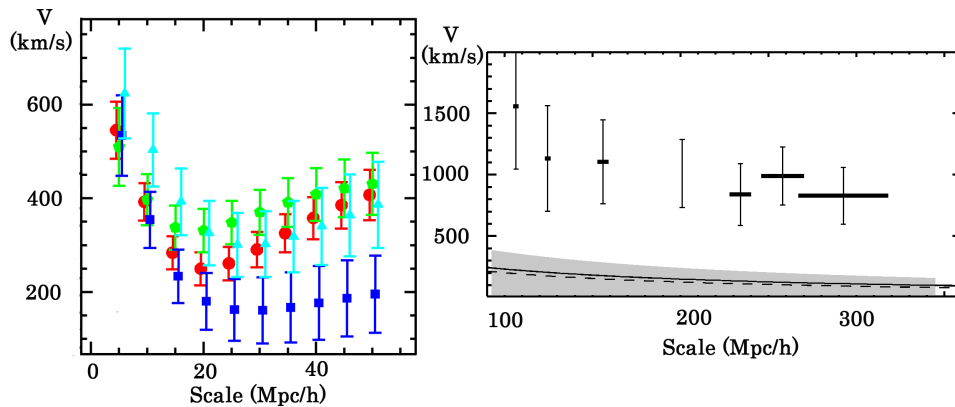


Figure 2.1: Left panel: bulk flows reported in [81] where we again see the consistent bulk flow on scales up to  $60h^{-1}$  Mpc. The different symbols represent different surveys. Right panel: peculiar velocities obtained in [80]. We can see that the amplitude of the peculiar velocities are above the prediction of the  $1\text{-}\sigma$  standard  $\Lambda$ CDM represented by the grey band for scales up to  $300h^{-1}$  Mpc.

In conclusion, these results suggest the existence of a coherent flow of matter with respect to the CMB rest frame on very large scales which could be signaling the breakdown of the Cosmological Principle. In both works, such a flow is explained resorting to very large-scale matter perturbations, i.e., the observed peculiar velocities would be caused by the

existence of some super-structure which must be further away than the Great Attractor, located at  $40 - 60h^{-1}$  Mpc from us [82, 83]. In any case, the presence of flows with such a large amplitude seems to be difficult to understand within the context of standard  $\Lambda$ CDM cosmology, which predicts much smaller velocities on the quoted scales.

However, the observed bulk flow could be indicating that matter is globally moving with respect to radiation, i.e., that matter and radiation do not share a common rest frame on very large scales rather than being due to some super-horizon perturbation. In other words, the velocity of a matter bulk of size  $R$  may have two independent components:  $\vec{V}_{R,bulk} = \vec{V}_{R,sta} + \vec{V}_{cosmic}$  where  $\vec{V}_{R,sta}$  is the statistical r.m.s. velocity fluctuation generated by density inhomogeneities and  $\vec{V}_{cosmic}$  is the cosmic velocity of matter with respect to the CMB because of having a different rest frame. Then, as we average over a large volume of matter, the first term becomes negligible whereas the second term remains constant and gives rise to a net cosmic flow. Indeed, as we discussed in the Introduction of this Chapter, this is the sort of phenomenon that one would expect in a scenario where dark energy rest frame differs from that of matter and radiation so that the detected large scale bulk flows could be naturally explained in the context of a moving dark energy model. We could see this the other way around, i.e., the detected large scale coherent motion of matter volumes with respect to the CMB might be signaling the presence of a dark moving component which could be identified with dark energy.

## 2.3 Slow-moving fluids: second order equations

The implications of having a moving dark energy component can be appropriately accounted for by considering the usual scenario of a Universe filled with four perfect fluids, namely: radiation, baryons, dark matter particles and dark energy and allowing for the presence of relative velocities among them. In this framework, the content of the Universe is well described by the following energy-momentum tensor:

$$T_{\mu\nu} = \sum_{\alpha} \left[ (\rho_{\alpha} + p_{\alpha}) u_{\mu}^{\alpha} u_{\nu}^{\alpha} - p_{\alpha} g_{\mu\nu} \right] \quad (2.2)$$

where  $\alpha$  stands for the components of the Universe  $\alpha = R, B, DM, DE$  and the 4-velocities of the fluids in an arbitrary frame are:

$$u_\alpha^\mu \equiv \frac{dx^\mu}{d\tau} = \gamma_\alpha (1, \vec{v}_\alpha) \quad (2.3)$$

with

$$\gamma_\alpha = \frac{1}{\sqrt{g_{00} + g_{ij}v_\alpha^i v_\alpha^j}}. \quad (2.4)$$

In order to simplify the problem and to obtain some analytical solutions we shall use cosmological perturbations theory, assuming that the fluids velocities are small<sup>2</sup>, i.e.  $\vec{v}_\alpha^2 \ll 1$ . To that end, we expand the different quantities of the four fluids up to second order as follows:

$$\begin{aligned} \rho_\alpha &= \rho_\alpha^{(0)} + \rho_\alpha^{(1)} + \rho_\alpha^{(2)} + \dots \\ \vec{v}_\alpha &= \vec{v}_\alpha^{(1)} + \vec{v}_\alpha^{(2)} + \dots \end{aligned} \quad (2.5)$$

where we have imposed the fluids to be at rest to zeroth order, i.e.,  $\vec{v}_\alpha^{(0)} = 0$ . That way, the most general form for the metric is given by the perturbed Friedmann-Robertson-Walker metric:

$$\begin{aligned} ds^2 &= a^2 \left[ \left[ 1 + 2 \left( \phi^{(1)} + \phi^{(2)} \right) \right] d\eta^2 + 2 \left[ S_i^{(1)} + S_i^{(2)} \right] dx^i d\eta \right. \\ &\quad \left. - \left[ \left( 1 - 2 \left( \psi^{(1)} + \psi^{(2)} \right) \right) \delta_{ij} + h_{ij} \right] dx^i dx^j \right]. \end{aligned} \quad (2.6)$$

We shall consider the homogeneous part (or zero-Fourier mode) of the energy-momentum tensor so that all the quantities in the problem will depend only on time. In the line element given above,  $\phi^{(1)}$  and  $\psi^{(1)}$  are scalar perturbations of first order and will be determined from  $\rho_\alpha^{(1)}$  in the first order equations of motion. However, the second order scalar perturbations  $\phi^{(2)}$  and  $\psi^{(2)}$  can depend, not only on  $\rho_\alpha^{(2)}$  and  $(\rho_\alpha^{(1)})^2$  terms, but also on  $(\vec{v}_\alpha^{(1)})^2$  which are also scalars. Analogously, the first order vector perturbations  $\vec{S}^{(1)}$  can only be related to the first order velocities  $\vec{v}_\alpha^{(1)}$  in the equations of motion, whereas to second order,  $\vec{S}^{(2)}$  will be determined by combinations of  $\vec{v}_\alpha^{(2)}$  and  $F^{(1)}\vec{v}_\alpha^{(1)}$  where  $F^{(1)}$  is a scalar function of the first order scalar perturbations. Finally,  $h_{ij}$  is a traceless tensor

<sup>2</sup>Note that, according to the reported amplitudes for the large scale bulk flows in [79] and [81], the velocities of the fluids are expected to be smaller than  $\mathcal{O}(10^{-2})$ .

perturbation which should be of second order and depend on the combinations  $v_{\alpha i}^{(1)} v_{\alpha j}^{(1)} - \frac{1}{3} (v_{\alpha}^{(1)})^2 \delta_{ij}$ . Note that, since we are considering only time-dependent perturbations on the energy-momentum tensor, all the perturbations on the metric will be uniquely functions of time and, therefore, the perturbed metric does not contain any terms involving spatial derivatives.

So far, we have not done any specific gauge choice, so we still have four gauge degrees of freedom which can be removed by making a choice of the coordinate system. Hence, we can simplify the problem if we choose our coordinates appropriately. In particular, we can fix the spatial coordinates in a way that the vector part of the metric vanishes  $\vec{S} = 0$ . The physical interpretation of this condition is apparent when solving the  $({}^0_i)$  Einstein equation of the exact problem, that allows to obtain the condition:

$$S_i = \frac{\sum_{\alpha} \gamma_{\alpha}^2 (\rho_{\alpha} + p_{\alpha}) g_{ij} v_{\alpha}^j}{\sum_{\alpha} \gamma_{\alpha}^2 (\rho_{\alpha} + p_{\alpha})}. \quad (2.7)$$

Hence,  $\vec{S}$  can be interpreted as the **relativistic cosmic center of mass velocity** (CCM velocity), since the combination  $\rho + p$  plays the role of inertial mass density for the corresponding fluid in General Relativity. We shall see later on that this velocity gives a cosmological contribution to the CMB dipole. Notice that, in general, an observer at rest with respect to cosmic center of mass could be moving with respect to radiation or matter. On the other hand, the temporal coordinate can be chosen so that  $\sum_{\alpha} (\rho_{\alpha} - \rho_{\alpha}^{(0)}) = 0$ , which means that the total density perturbations are identically zero. With this gauge choice, the  $({}^0_0)$  and  $({}^i_j)$  components of Einstein equations  $G^{\mu}_{\nu} = 8\pi G T^{\mu}_{\nu}$  up to second order adopt the form:

#### Zeroth order

$$\mathcal{H}^2 = \frac{8\pi G}{3} a^2 \sum_{\alpha} \rho_{\alpha}^{(0)} \quad (2.8)$$

$$2\mathcal{H}' + \mathcal{H}^2 = -8\pi G a^2 \sum_{\alpha} p_{\alpha}^{(0)} \quad (2.9)$$

#### First order

$$-\frac{6}{a^2} \mathcal{H} (\psi'^{(1)} + \mathcal{H} \phi^{(1)}) = 0 \quad (2.10)$$

$$\psi''^{(1)} + 2\mathcal{H}\psi'^{(1)} + \mathcal{H}\phi'^{(1)} + (\mathcal{H}^2 + 2\mathcal{H}')\phi^{(1)} = 0 \quad (2.11)$$

### Second order

$$\begin{aligned} & -\frac{2\mathcal{H}}{a} \left[ a \left( \psi^{(2)} + (\psi^{(1)})^2 \right)' - 2 \left( \phi^{(1)} \right)^2 \right] + \psi'^{(1)} \left( \psi'^{(1)} + 4\mathcal{H}\phi^{(1)} \right) \\ & = \frac{8\pi G}{3} a^2 \sum_{\alpha} \left( \rho_{\alpha}^{(0)} + p_{\alpha}^{(0)} \right) \left( v_{\alpha}^{(1)} \right)^2 \end{aligned} \quad (2.12)$$

$$\begin{aligned} & \frac{2}{a^2} \left[ \left( 2\mathcal{H}' + \mathcal{H}^2 \right) \phi^{(2)} + \mathcal{H}\phi'^{(2)} + \psi''^{(2)} + 2\mathcal{H}\psi'^{(2)} - 2 \left( \mathcal{H}^2 + 2\mathcal{H}' \right) \left( \phi^{(1)} \right)^2 \right. \\ & + \frac{1}{2} \psi'^{(1)} \left( \psi^{(1)} - 2\phi^{(1)} \right)' + 2\psi''^{(1)} \left( \psi^{(1)} - \phi^{(1)} \right) \\ & \left. + 2\mathcal{H} \left[ \left( (\psi^{(1)})^2 + (\phi^{(1)})^2 \right)' + 2\phi^{(1)}\psi'^{(1)} \right] \right] \delta_j^i \\ & + \frac{1}{2a^4} \left( a^2 h'^i_j \right)' = 8\pi G \sum_{\alpha} \left( \rho_{\alpha}^{(0)} + p_{\alpha}^{(0)} \right) v_{\alpha}^{(1)i} v_{\alpha j}^{(1)} \end{aligned} \quad (2.13)$$

with  $' \equiv \frac{d}{dt}$  and  $\mathcal{H} = a'/a$  is the Hubble parameter.

Nevertheless, the system is incomplete because there are more unknown variables than equations. In general, the problem with  $n$  fluids has ten independent Einstein equations, but the unknown quantities are the densities (assuming a given equation of state) and the three independent components of the four-velocity of each fluid (because of the constraint  $u^2 = 1$ ). Therefore, there are  $10 + 4n$  unknown functions, although, since there are four gauge degrees of freedom, we can fix four quantities and reduce the number of undetermined functions to  $6 + 4n$ . With this count, one needs  $4(n - 1)$  additional equations to complete the system. The simplest way to close the problem is by requiring the conservation of each energy-momentum tensor, assuming they are decoupled from each other:  $T_{\alpha}^{\mu\nu}{}_{;\nu} = 0$  with  $\alpha = 1 \dots n$ . Obviously, one can modify these relations by changing the right hand side in order to consider interactions between the fluids. This guarantees the completeness of the system since it provides the  $4(n - 1)$  required equations (there are  $4n$  extra equations, but the conservation of the total energy-momentum tensor makes one of those equations superfluous). For our case, these additional equations read for the energy and momentum conservation (notice that momentum conservation is trivial at zeroth order):

**Zeroth order**

$$\rho_\alpha'^{(0)} + 3\mathcal{H}(\rho_\alpha^{(0)} + p_\alpha^{(0)}) = 0 \quad (2.14)$$

**First order**

$$\rho_\alpha'^{(1)} + 3\mathcal{H}(\rho_\alpha^{(1)} + p_\alpha^{(1)}) = 3(\rho_\alpha^{(0)} + p_\alpha^{(0)})\psi'^{(1)} \quad (2.15)$$

$$\left[ a^4 (\rho_\alpha^{(0)} + p_\alpha^{(0)}) \vec{v}_\alpha^{(1)} \right]' = 0 \quad (2.16)$$

**Second order**

$$\begin{aligned} \rho_\alpha'^{(2)} + 3\mathcal{H}(\rho_\alpha^{(2)} + p_\alpha^{(2)}) = & \\ - \frac{1}{a^4} \left[ a^4 (\rho_\alpha^{(0)} + p_\alpha^{(0)}) \right]' (\vec{v}_\alpha^{(1)})^2 - (\rho_\alpha^{(0)} + p_\alpha^{(0)}) \left( (\vec{v}_\alpha^{(1)})^2 \right)' & \\ + 3 \left[ (\rho_\alpha^{(0)} + p_\alpha^{(0)}) \left( (\psi^{(1)})^2 + \psi^{(2)} \right)' + (\rho_\alpha^{(1)} + p_\alpha^{(1)}) \psi'^{(1)} \right] & \end{aligned} \quad (2.17)$$

$$\begin{aligned} \left[ a^4 \left( (\rho_\alpha^{(0)} + p_\alpha^{(0)}) (\vec{v}_\alpha^{(2)} - 2\phi^{(1)} \vec{v}_\alpha^{(1)}) + (\rho_\alpha^{(1)} + p_\alpha^{(1)}) \vec{v}_\alpha^{(1)} \right) \right]' & \\ = a^4 (\rho_\alpha^{(0)} + p_\alpha^{(0)}) (5\psi^{(1)} - \phi^{(1)})' \vec{v}_\alpha^{(1)} & \end{aligned} \quad (2.18)$$

where we have used the previous orders equations at each order.

## 2.4 Sachs-Wolfe effect with moving fluids

The homogeneous scalar perturbations can only affect the overall isotropic temperature of the CMB, i.e., the value of the monopole, being such a contribution expected to be much smaller than the mean CMB temperature so that we can safely neglect it. Concerning vector perturbations, we can absorb them in the definition of the frame in which we are performing the calculations, although we must be careful in appropriately interpreting the obtained final results. In particular, if we use the cosmic center of mass frame we can ignore the vector perturbations in the calculations and, then, introduce them back at the end by a proper interpretation of the velocities appearing in the final result. After considering all these

simplifications we conclude that, in order to calculate the new contributions produced by the motion of the fluids to the CMB temperature power spectrum, only the tensor perturbations are truly relevant so that the perturbed line element considered in the subsequent calculations will be:

$$ds^2 = a^2(d\eta^2 - (\delta_{ij} + h_{ij})dx^i dx^j). \quad (2.19)$$

In order to calculate all the contributions to the temperature anisotropies generated by the metric perturbations, we should solve the corresponding radiative transfer equations (see [84, 85]). This is the system of Einstein-Boltzmann equations for the set of fluids. However, since we only expect effects on large scales, leading to modifications in the dipole and the quadrupole (which are not affected by microphysics at the time of recombination), the only relevant contribution for such a large angle contribution will be given by the Sachs-Wolfe effect, which takes into account the variation in the energy of photons propagating from the last scattering surface [85] and is given by:

$$\frac{\delta T}{T} = \frac{a_0 \mathcal{E}_0 - a_{dec} \mathcal{E}_{dec}}{a_{dec} \mathcal{E}_{dec}}. \quad (2.20)$$

Here, the indices 0 and *dec* denote the present and decoupling times respectively and  $\mathcal{E}$  is the energy of the photon. For an observer with velocity  $u^\mu = \gamma(1, \vec{v})$  this energy is given by:

$$\mathcal{E} = g_{\mu\nu} u^\mu P^\nu, \quad (2.21)$$

with

$$P^\nu = E \frac{dx^\nu}{d\lambda}, \quad (2.22)$$

where  $E$  parameterizes the photon energy and  $\lambda$  is an affine parameter. By the invariance of the action of the geodesics of a massless particle under conformal transformations of the affine parameter, the geodesics of the metric  $g_{\mu\nu}$  given by (2.19) with affine parameter  $\lambda$  are the same as those of the metric  $\hat{g}_{\mu\nu} = a^{-2}g_{\mu\nu}$  with affine parameter  $\eta$  such that  $d\lambda = a^2 d\eta$ . The trajectory of the photon coming from the direction given by the Minkowski-null vector  $n^\mu = (1, \vec{n})$  with  $\vec{n}^2 = 1$  will be perturbed in such a way that we can write  $x^\mu(\eta) = n^\mu \eta + \delta x^\mu$ , where the second term corresponds to the contribution from  $h_{ij}$  which is of second order.

Then, assuming that the observer velocity is of first order, the momentum of the photon to second order is:

$$P^\nu = \frac{E}{a^2} \left( n^\nu + \frac{d\delta x^\nu}{d\eta} \right). \quad (2.23)$$

Inserting this expression in (2.21) we obtain:

$$\mathcal{E} = \frac{E}{a} \left( 1 + \frac{1}{2} \vec{v}^2 - \vec{v} \cdot \vec{n} + \frac{d\delta x^0}{d\eta} \right). \quad (2.24)$$

For the  $\hat{g}_{\mu\nu}$  metric, the second order of the zero component of the geodesic equations in terms of the metric perturbation reduces to:

$$\frac{d^2\delta x^0}{d\eta^2} + \frac{1}{2} \frac{dh_{ij}}{d\eta} n^i n^j = 0 \quad (2.25)$$

which can be easily integrated to get:

$$\frac{d\delta x^0}{d\eta} = -\frac{1}{2} h_{ij} n^i n^j. \quad (2.26)$$

Then, the energy of the photon results finally:

$$\mathcal{E} = \frac{E}{a} \left( 1 + \frac{1}{2} \vec{v}^2 - \vec{v} \cdot \vec{n} - \frac{1}{2} h_{ij} n^i n^j \right). \quad (2.27)$$

Thus, by using this formula for the energy of the photon in equation (2.20) and expanding up to second order we obtain the following expression for the temperature fluctuations:

$$\frac{\delta T}{T} \simeq \frac{1}{2} \vec{v}^2|_{dec}^0 - \vec{v} \cdot \vec{n}|_{dec}^0 - (\vec{v}_{dec} \cdot \vec{n})(\vec{v} \cdot \vec{n})|_{dec}^0 - \frac{1}{2} h_{ij} n^i n^j|_{dec}^0. \quad (2.28)$$

The first term in (2.28) only contributes to the monopole and can be neglected. The second term is the familiar Doppler effect, but with the novelty that, since the velocities appearing in  $\vec{v} \cdot \vec{n}|_{dec}^0$  are referred to the  $\vec{S} = 0$  frame, in the case of moving fluids the dipole must be interpreted as being caused by the motion of emitter and observer with respect to the cosmic center of mass and this frame, in general, will differ from that of CMB. Finally, the last two terms give new contributions to the quadrupole. These new contributions to both the dipole and the quadrupole will be studied in detailed in the following Sections.

## 2.5 CMB dipole from moving dark energy

Before proceeding with the analysis of the dipole contribution obtained in the preceding Section it will be convenient to get a deeper insight on the velocities evolution of the different components of the Universe. If we place ourselves in the CCM rest frame, defined by the condition  $\vec{S} = 0$ , we have that the condition (2.7) must hold which, for small velocities, reads<sup>3</sup>:

$$\sum_{\alpha} (\rho_{\alpha} + p_{\alpha}) \vec{v}_{\alpha} = 0. \quad (2.29)$$

Notice that this is the usual definition for the center of mass frame as long as the combination  $\rho_{\alpha} + p_{\alpha}$ , as commented before, is interpreted as the inertial mass of the corresponding fluid. In the early Universe, radiation dominates over the rest of components so it will drag baryons and dark matter particles in such a way that they all will share a common rest frame, as expected for interacting species in thermal equilibrium. Concerning dark energy, because it does not interact with photons, it can move in a different way. However, in the CCM rest frame, radiation (and matter) and dark energy velocities are related by means of (2.29) as follows:

$$\vec{v}_{DE}^{early} = -\frac{4}{3} \frac{\rho_R^{early}}{\rho_{DE}^{early} + p_{DE}^{early}} \vec{v}_R^{early} \quad (2.30)$$

where we have made use of the fact that matter and radiation velocities are the same and that matter energy density is negligible compared to that of radiation at that epoch. Notice that this relation provides a preferred axis in the Universe given by the fluids motion direction. In other words, the Universe will acquire an axial symmetry around the axis defined by the motion of the different components. This issue will be discussed in more detailed in next Sections.

In order to obtain the scaling of the different components velocities relative to the CCM rest frame we shall use the momentum conservation equation for each fluid expressed in (2.16), which, in the CCM rest frame, reads:

$$\frac{d}{dt} \left[ a^4 (\rho_{\alpha} + p_{\alpha}) (\vec{S} - \vec{v}_{\alpha}) \right] = 0. \quad (2.31)$$

---

<sup>3</sup>Hereafter we shall omit the indices denoting the perturbation order of the corresponding quantity to alleviate the notation. There will be no confusion since all the energy densities and pressures will be zeroth-order and all the velocities will be first-order.

This equation can be immediately integrated if we assume a constant equation of state  $w_\alpha = \frac{p_\alpha}{\rho_\alpha}$  to give:

$$\vec{S} - \vec{v}_\alpha = \vec{v}_\alpha^0 a^{3w_\alpha - 1} \quad (2.32)$$

with  $\vec{v}_\alpha^0$  the present value of the velocity. Thus, radiation ( $w_R = \frac{1}{3}$ ) moves with constant velocity with respect to the CCM, whereas matter ( $w = 0$ ) velocity decays as  $a^{-1}$ . The evolution of dark energy velocity depends on the particular model under consideration. Therefore, according to (2.32), matter and radiation have constant velocity before decoupling, but, after that, matter starts reducing its velocity as the Universe expands whereas radiation keeps moving with the same constant velocity. As a consequence, the presence of moving dark energy at the time of recombination makes possible that matter and radiation could acquire a relative velocity after decoupling. This effect can only take place if dark energy is not a cosmological constant, otherwise there would be no momentum contribution from dark energy to (2.29). Notice that, since dark matter particles should decouple before baryons do (in order to be able to form the structures we observe today) and they both have the same equation of state, we expect them to have a relative motion with constant velocity. Thus, the complete picture of the motions would be as follows: radiation moving with constant velocity, baryons and dark matter moving in the same direction with constant relative velocity and, both, slowing down with respect to radiation. Finally, dark energy would move along the opposite direction.

Now that we know how the different components of the Universe move throughout the Universe history we can move on to discuss the dipole contribution in these cosmologies. In the previous section we have shown that the CMB dipole must actually be reinterpreted when moving fluids are present in the Universe. Thus, rather than being a pure kinematical effect due to our motion with respect to the CMB photons, the dipole acquires an intrinsically cosmological contribution from the fluids motion. Such a motion spoils the Cosmological Principle by introducing a privileged frame in the Universe or, equivalently, a preferred direction given by the velocities of the fluids. According to the expression (2.28) obtained above, the dipole produced by the Sachs-Wolfe effect is nothing but a Doppler effect due to the motion with respect to the cosmic center of mass rest frame and not with respect to the CMB rest frame as it is usually stated. Although the dipole contribution appearing in (2.28) was derived in the CCM rest frame, we can obtain its expression in an arbi-

trary frame by performing the corresponding transformation to yield:

$$\frac{\delta T_{dipole}}{T_0} \simeq \vec{n} \cdot \left( \vec{S} - \vec{v} \right)_{dec}^0 \quad (2.33)$$

where, as in (2.28),  $\vec{n}$  is a unitary vector along the direction of observation,  $\vec{v}_0$  is the velocity of the observer today and  $\vec{v}_{dec}$  is the velocity of the emitter at decoupling time, although such velocities are not referred to any particular frame in this case. Notice that, according to (2.33), when several fluids with relative velocities are present, the CMB dipole is given by the velocities of emitter and observer with respect to the CCM frame. In the case in which all the fluids share a common rest frame, the velocities are referred to that frame which is nothing but the CMB frame. However, when the fluids velocities are different, the physically relevant frame for the dipole is the CCM which is different from the CMB frame. In this sense, if emission took place from a source at rest with respect to the CCM frame, that frame could be determined physically as the frame attached to an observer who measures a vanishing dipole.

If we assume that the intrinsic dipole fluctuation at the last scattering surface is negligible we can take  $\vec{v}_{dec} \simeq \vec{v}_R^{dec}$ . On the other hand, if the observer today is at rest with respect to matter we have  $\vec{v}_0 \simeq \vec{v}_M^0$ . Thus, if we now refer the velocities to the CCM frame, we finally get:

$$\frac{\delta T_{dipole}}{T_0} \simeq \vec{n} \cdot \left( \vec{v}_R^0 - \vec{v}_M^0 \right) \quad (2.34)$$

where we have used that the velocity of radiation with respect to the CCM is constant. Then, according to (2.34), we conclude that the contribution to the dipole temperature fluctuation of the CMB is due to the relative motion of matter with respect to radiation. This is precisely the kind of flow detected in [79, 80] and [81], so the direction reported in both papers gives directly the direction of motion of the fluids.

Notice that, although calculated in the CCM frame, (2.34) is valid for any frame since it is expressed as the difference of two velocities evaluated at the same time. According to (2.32), today the velocity of matter with respect to the CCM is expected to be much smaller than that of radiation and the dipole can also be written as:

$$\frac{\delta T_{dipole}}{T_0} \simeq \vec{n} \cdot \vec{v}_R^0 \quad (2.35)$$

so that the cosmological dipole could be alternatively interpreted as due to the relative motion of radiation with respect to the CCM.

Using again expression (2.29), it is possible to relate the amplitude of the dipole ( $v_R^0$ ) to the present value of the dark energy velocity with respect to the CCM frame:

$$v_{DE}^0 = \frac{v_R^0}{(1 + w_{DE}^0)\Omega_{DE}} \left( \frac{2}{3}\Omega_R + \frac{\Omega_B}{1 + z_{dec}} + \frac{\Omega_{DM}}{1 + z_*} \right) \quad (2.36)$$

where  $z_*$  is the decoupling redshift of dark matter and radiation and  $w_{DE}^0$  is the present value of the dark energy equation of state. We can estimate typical values of the present dark energy velocity. Thus, from the measured bulk flows we can take  $v_R^0 \sim 500$  km/s and assuming  $\Omega_{DE} \simeq 0.7$ ,  $z_* > 10^5$  and  $w_{DE}^0 \simeq -0.97$ , we get  $v_{DE}^0 \sim 1$  km/s, which agrees with our assumption of small velocities. Notice that the closer  $w_{DE}^0$  is to  $-1$  the larger the dark energy velocity is. Finally, an interesting feature which is worth mentioning and that can also be seen from (2.30) is that, for a phantom-like dark energy model with  $w_{DE} < -1$ , dark energy will move in the same direction as the other fluids in the CCM rest frame. This is so because for a phantom-like dark energy model the density of inertial mass  $\rho + p$  is negative so that it contributes to the CCM as a fluid of inertial mass  $-(\rho + p)$  moving in the opposite direction.

## 2.6 Contribution to the CMB quadrupole

The CMB quadrupole acquires two new contributions from the fluids motion as shown in the last two terms in (2.28). The first of them does not depend on the metric perturbation since it comes from the second order expansion of the denominator in (2.20)<sup>4</sup>. As we will show below, this term is expected to be smaller than the last one. Therefore, the dominant contribution to the quadrupole is given by the following expression:

$$\frac{\delta T_Q}{T} = -\frac{1}{2}(h_{ij}(a_0) - h_{ij}(a_{dec}))n^i n^j. \quad (2.37)$$

This formula shows that we only need to know  $h_{ij}$  in order to calculate the quadrupole contribution and, in addition, this term does not depend on the observer velocity as we can see in its corresponding equation (2.13). Moreover, this equation can be integrated to obtain the general solution

---

<sup>4</sup>In fact, this term is also present in the usual case without moving dark energy.

for  $h_{ij}$ :

$$h_{ij} = \int_{a_*}^a \frac{6}{\tilde{a}^4} \left[ \int_{a_*}^{\tilde{a}} \hat{a}^2 \sum_{\alpha} (\rho_{\alpha} + p_{\alpha}) \left( v_{\alpha i} v_{\alpha j} - \frac{1}{3} \vec{v}_{\alpha}^2 \delta_{ij} \right) \frac{d\hat{a}}{\sqrt{\sum_{\alpha} \rho_{\alpha}}} \right] \frac{d\tilde{a}}{\sqrt{\sum_{\alpha} \rho_{\alpha}}}, \quad (2.38)$$

where  $a_*$  is the value of the scale factor at the time at which we specify the initial conditions for  $h_{ij}$ . Notice that the quadrupole does not depend on  $h_{ij}(a_*)$ , but only on the initial value of the derivatives. For simplicity we will assume that the metric anisotropies are generated by the fluids motion and therefore we consider a purely isotropic Universe for  $a < a_*$ , i.e., we take  $h_{ij}(a_*) = h'_{ij}(a_*) = 0$ . The solution of the metric perturbation  $h_{ij}$  shows that the quadrupole depends on both the zeroth order energy densities of the fluids and their first order velocities with respect to the center of mass, whose solution was obtained in the previous section and, in the CCM rest frame, read:

$$\vec{v}_{\alpha} = \vec{v}_{\alpha}^0 a^{3w_{\alpha}-1}. \quad (2.39)$$

As we already said, the presence of the fluids motion induces axial symmetry around the axis defined by the velocities. That way, each energy-momentum tensor (and therefore the total one) will have an axial symmetry which will also be present in the metric. This means that the tensor perturbation  $h_{ij}$  adopts a diagonal form. In fact, if we choose the velocities lying along the  $z$ -axis, the tensor perturbation given by (2.38) will be proportional to  $diag(-1/3, -1/3, 2/3)$ , as deduced from its tensorial structure given by the combination  $\hat{v}_i \hat{v}_j - \frac{1}{3} \delta_{ij}$  with  $\hat{v}_i$  a unitary vector parallel to the velocities of the fluids. Taking into account the previous discussion, the final expression for the quadrupole results:

$$\frac{\delta T_Q}{T} = -\frac{1}{2} (h(a_0) - h(a_{dec})) \left( \cos^2 \theta - \frac{1}{3} \right) \quad (2.40)$$

where  $\theta$  is the angle formed by the observation direction and the velocities of the fluids, and  $h(a) = \sum_{\alpha} h_{\alpha}(a)$  with

$$h_{\alpha}(a) = 6 \int_{a_*}^a \frac{1}{\tilde{a}^4} \left[ \int_{a_*}^{\tilde{a}} \hat{a}^2 (\rho_{\alpha} + p_{\alpha}) v_{\alpha}^2 \frac{d\hat{a}}{\sqrt{\sum_{\alpha} \rho_{\alpha}}} \right] \frac{d\tilde{a}}{\sqrt{\sum_{\alpha} \rho_{\alpha}}}. \quad (2.41)$$

The function of  $\theta$  appearing in (2.40) is proportional to the spherical harmonic  $Y_{20}$  so we can express the quadrupole fluctuation as:

$$\frac{\delta T_Q}{T} = \frac{2}{3} \sqrt{\frac{\pi}{5}} (h_0 - h_{dec}) Y_{20}. \quad (2.42)$$

It is usual to introduce the power spectrum of the temperature fluctuations of the CMB as:

$$\frac{\delta T_\ell}{T} = \sqrt{\frac{1}{2\pi} \frac{\ell(\ell+1)}{2\ell+1} \sum_m |a_{\ell m}|^2} \quad (2.43)$$

where  $a_{\ell m}$  are the coefficients of the expansion in spherical harmonics. Moreover, the quadrupole is usually defined as:

$$Q \equiv \frac{\delta T_2}{T} = \sqrt{\frac{3}{5\pi} \sum_{m=-2}^2 |a_{2m}|^2} \quad (2.44)$$

which, in our case, reduces to:

$$Q_A = \frac{2}{5\sqrt{3}} |\Delta h|, \quad (2.45)$$

where we have defined  $\Delta h = h_0 - h_{dec}$ .

The quadrupole given by (2.45) is due to the anisotropy of the space-time background (that is why the index  $A$  is introduced), but we have to add the standard isotropic fluctuation produced during inflation. Then, if we assume that the anisotropies are small, the total effect will be the linear superposition of both contributions (see [86]):

$$\delta T_T = \delta T_A + \delta T_I \quad (2.46)$$

and, therefore:

$$a_{\ell m}^T = a_{\ell m}^A + a_{\ell m}^I. \quad (2.47)$$

Notice that, as discussed in [86], there is the possibility that the inflation-produced contribution could be strongly biased or anti-biased by the anisotropic background, mainly in the case in which anisotropies grew as we go back in time. However as discussed in that reference, this is unlikely in general since it would require a correlation between the quantum origin and subsequent classical evolution. Moreover, in our case, the background evolution during inflation is isotropic and we do not expect any interference effect.

Following [55], we can easily generalize our results to the case of an arbitrary orientation of our frame in which the velocities lie along the

direction given by  $(\hat{\theta}, \hat{\phi})$ . In that case, the coefficients of the expansion are:

$$\begin{aligned} a_{20}^A &= \frac{\sqrt{\pi}}{6\sqrt{5}} [1 + 3 \cos 2\hat{\theta}] |\Delta h|, \\ a_{21}^A &= -(a_{2-1}^A)^* = -\sqrt{\frac{\pi}{30}} e^{-i\hat{\phi}} \sin 2\hat{\theta} |\Delta h|, \\ a_{22}^A &= (a_{2-2}^A)^* = \sqrt{\frac{\pi}{30}} e^{-2i\hat{\phi}} \sin^2 \hat{\theta} |\Delta h|. \end{aligned} \quad (2.48)$$

It is easy to show that the anisotropy quadrupole according to (2.44) is still given by (2.45) since  $h$  is scalar under rotations. Now, assuming that the coefficients  $a_{2m}^I$  only differ one from each other in a phase factor we can write:

$$\begin{aligned} a_{20}^I &= \sqrt{\frac{\pi}{3}} e^{i\alpha_1} Q_I, \\ a_{21}^I &= -(a_{2-1}^I)^* = \sqrt{\frac{\pi}{3}} e^{i\alpha_2} Q_I, \\ a_{22}^I &= (a_{2-2}^I)^* = \sqrt{\frac{\pi}{3}} e^{i\alpha_3} Q_I. \end{aligned} \quad (2.49)$$

which is justified because the standard inflation fluctuations are statistically isotropic. Then, the total quadrupole can be expressed as:

$$Q_T^2 = Q_A^2 + Q_I^2 - 2f Q_A Q_I \quad (2.50)$$

where  $f$  is a function depending on the direction of the velocities  $(\hat{\theta}, \hat{\phi})$  and the phase factors  $\alpha_i$  of the coefficients  $a_{2m}^I$ , and whose expression is:

$$\begin{aligned} f &= \frac{1}{4\sqrt{5}} \left[ 2\sqrt{6} [-\sin \hat{\theta} \cos(2\hat{\phi} + \alpha_3) + 2 \cos \hat{\theta} \cos(\hat{\phi} + \alpha_2)] \sin \hat{\theta} \right. \\ &\quad \left. - (1 + 3 \cos(2\hat{\theta})) \cos \alpha_1 \right]. \end{aligned} \quad (2.51)$$

This function takes values such that:

$$|f| \leq \bar{f} = \frac{\sqrt{39 + 6\sqrt{6}} + \sqrt{6} - 1}{4\sqrt{5}}. \quad (2.52)$$

Since the values of the phases  $\alpha_i$  are random, the total quadrupole lies between  $Q_+^2$  and  $Q_-^2$ , being:

$$Q_{\pm}^2 = Q_A^2 + Q_I^2 \pm 2\bar{f} Q_A Q_I \quad (2.53)$$

with  $\bar{f}$  the maximum of  $f$ .

The observed quadrupole from WMAP [87, 88] is given by  $(\delta T)_{obs}^2 = 236_{-137}^{+560} \mu\text{K}^2$  at the 68% C.L. or  $(\delta T)_{obs}^2 = 236_{-182}^{+3591} \mu\text{K}^2$  at the 95% C.L. These results define the corresponding 68% C.L. or 95% C.L. intervals for the measured temperature fluctuations that we denote:  $((\delta T)_{min}^2, (\delta T)_{max}^2)$ . For the theoretical quadrupole temperature interval  $((\delta T)_-^2, (\delta T)_+^2)$ , obtained from (2.53), to be compatible with observations, we therefore require  $(\delta T)_{max}^2 \gtrsim (\delta T)_-^2$  and  $(\delta T)_{min}^2 \lesssim (\delta T)_+^2$ . Using (2.53) these two conditions impose limits on  $(\delta T_A)^2$  once the value of  $(\delta T)_I^2$  is fixed.

Let us first assume that inflation alone is able to account for the observed quadrupole, i.e.,  $(\delta T)_I^2 \simeq 236 \mu\text{K}^2$ , then the first condition  $(\delta T)_{max}^2 \gtrsim (\delta T)_-^2$  is automatically satisfied, because the minimum of  $(\delta T)_+^2$ , as a function of  $\delta T_A$ , is  $(\delta T)_I^2$  which is larger than  $(\delta T)_{min}^2$ . Therefore, we obtain bounds on  $\delta T_A$  just from the second condition above, which are given by:

$$\begin{aligned} 0 \mu\text{K}^2 &\lesssim (\delta T_A)^2 \lesssim 1861 \mu\text{K}^2 & 68\% \text{ C.L.} \\ 0 \mu\text{K}^2 &\lesssim (\delta T_A)^2 \lesssim 5909 \mu\text{K}^2 & 95\% \text{ C.L.} \end{aligned} \quad (2.54)$$

These constraints lead to the following limits in the growth of the degree of anisotropy:

$$\begin{aligned} 0 &\lesssim |\Delta h| \lesssim 6.92 \times 10^{-5} & 68\% \text{ C.L.} \\ 0 &\lesssim |\Delta h| \lesssim 1.23 \times 10^{-4} & 95\% \text{ C.L.} \end{aligned} \quad (2.55)$$

However, it is well-known that the predictions of standard inflation, calculated from an almost flat spectrum of density perturbations, is larger than the central value of the measured quadrupole, in particular [55]:  $(\delta T)_I^2 \simeq 1252 \mu\text{K}^2$ . In such a case the anisotropic contribution could help reducing the value of the quadrupole for certain values of the phases and fluid velocities. Once again the first condition is automatically satisfied, and the second condition yields:

$$\begin{aligned} 54 \mu\text{K}^2 &\lesssim (\delta T_A)^2 \lesssim 3857 \mu\text{K}^2 & 68\% \text{ C.L.} \\ 0 \mu\text{K}^2 &\lesssim (\delta T_A)^2 \lesssim 9256 \mu\text{K}^2 & 95\% \text{ C.L.} \end{aligned} \quad (2.56)$$

or, in terms of the degree of anisotropy growth:

$$\begin{aligned} 1.18 \times 10^{-5} &\lesssim |\Delta h| \lesssim 9.96 \times 10^{-5} & 68\% \text{ C.L.} \\ 0 &\lesssim |\Delta h| \lesssim 1.54 \times 10^{-4} & 95\% \text{ C.L.} \end{aligned} \quad (2.57)$$

Notice that the 95% confidence interval includes the standard prediction from inflation and for that reason the lower limit vanishes in that case in (2.56). According to these results, for certain orientations of the velocities and the values of the phase factors,  $Q_A$  could lower the value of the quadrupole and make it compatible with the observed one even at the  $1\sigma$  level. Now, since the initial conditions for the velocities directions  $(\hat{\theta}, \hat{\phi})$  and the phase factors  $\alpha_i$  are random, we can simulate different realizations for the total quadrupole and thus compute the likelihood of having a total quadrupole as low as the measured one with the anisotropic contribution in addition to the standard isotropic contribution generated during inflation as a function of the model-dependent parameter  $\Delta h$ . In Fig. 2.2 we show the resulting probability distribution which peaks at  $\Delta h \simeq 3.5 \times 10^{-5}$  with a probability of  $\simeq 7\%$ .

Finally, we would like to comment on the fact that the total quadrupole has a preferred axis which happens to coincide with the direction of the velocities and, as a consequence, with that of the dipole. Therefore, a moving dark energy model could also shed some light on the so-called axis of evil problem [89, 90]. Although this anomaly usually refers to the observed alignment of the  $\ell = 2 - 5$  multipoles, there are also evidence that the axis of such alignment is correlated with the dipole direction at more than 99% C.L. [91, 92]. Since moving dark energy gives a common physical mechanism for both the dipole and quadrupole contributions, it is expected to have correlations among them. The solution of the low quadrupole problem arises because the relative motion of the fluids generates a certain degree of anisotropy which is seen by the photons coming from the last scattering surface and acquire a quadrupolar anisotropy. In a frame with the  $z$ -axis pointing along the fluids motions, the power of the quadrupole given by the generated anisotropy is zonal, i.e., it is concentrated in the  $m = 0$  component so that it gives rise to a cylindrical contribution. However, we still have to add the standard isotropic fluctuation generated during inflation, whose components are all comparable. Then, if we add linearly both contributions in such a way that the resulting quadrupole is lower than the inflationary one, the suppression has to take place for the  $m = 0$  component and, therefore, the total quadrupole will be non-cylindrical.

In the following we shall compare the limits obtained above with the predictions from several dark energy models, but before that we need to extend our calculations beyond the perturbative regime.

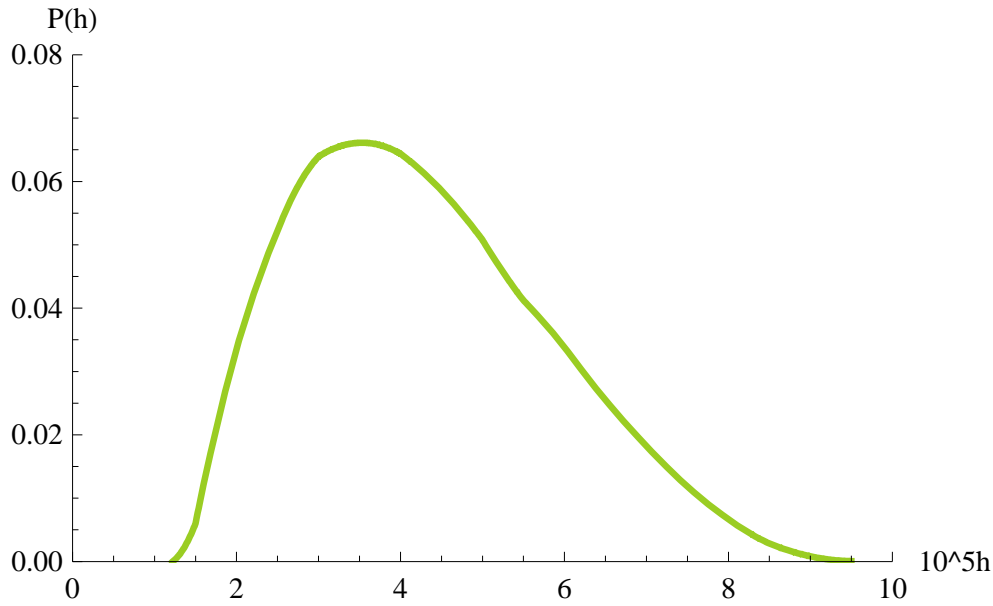


Figure 2.2: Likelihood of having a quadrupole within the  $1\sigma$  interval of the observed one as a function of the parameter  $\Delta h$ , which contains the information about the dark energy model.

## 2.7 Fast-moving fluids: exact equations

In the previous Section we have studied the problem of how the quadrupole is affected by the fact that dark energy does not share a common rest frame with matter and radiation. To that end, we have used cosmological perturbation theory to compute the metric perturbations by means of the simple formula (2.38), valid when the velocities are small. Such formula could also be reasonably useful for high initial velocities provided they decay in time and rapidly reach the perturbative regime. If we look at Eq. (2.39) we conclude that this condition is satisfied if  $w_\alpha < \frac{1}{3}$ . Moreover, if  $w_\alpha = \frac{1}{3}$ , as in the radiation case, the velocity is constant so we just need to have a small initial velocity. However, some models have been proposed in which the total energy density of the Universe could contain in certain epochs a non-negligible contribution of fluids with equation of state such that  $w_\alpha > \frac{1}{3}$ . This is for instance the case of stiff-fluid cosmologies or some tracking dark energy models. In those cases the velocities grow in time, perturbation theory will eventually break down at some point and it becomes necessary to solve the exact problem.

In order to simplify the equations in this case, we shall change the gauge used so far by one in which  $g_{00} = 1$  and keeping the condition  $g_{0i} = 0$ , i.e., we shall perform the calculations in the CCM rest frame. Moreover, we shall also assume that the fluids are moving along the  $z$ -axis with no rotation which means that axial symmetry still holds. The most general metric having that symmetry with the explained gauge choice can be written as follows:

$$ds^2 = dt^2 - a_{\perp}^2(dx^2 + dy^2) - a_{\parallel}^2 dz^2 \quad (2.58)$$

which corresponds to the axisymmetric Bianchi I metric. On the other hand, the energy-momentum tensor for each fluid reads:

$$\begin{aligned} T_{\alpha 0}^0 &= \gamma_{\alpha}^2 (\rho_{\alpha} + p_{\alpha}) - p_{\alpha}, \\ T_{\alpha 0}^i &= \gamma_{\alpha}^2 (\rho_{\alpha} + p_{\alpha}) v_{z\alpha} \delta^{iz}, \\ T_{\alpha i}^0 &= -\gamma_{\alpha}^2 (\rho_{\alpha} + p_{\alpha}) a_{\parallel}^2 v_{z\alpha} \delta_{iz}, \\ T_{\alpha j}^i &= -\gamma_{\alpha}^2 (\rho_{\alpha} + p_{\alpha}) a_{\parallel}^2 v_{z\alpha}^2 \delta^{iz} \delta_{jz} - p_{\alpha} \delta_j^i. \end{aligned} \quad (2.59)$$

Note that the velocities appearing in these expressions are no longer the same as those of the previous sections since, here, we have defined them as derivatives with respect to the time  $t$  not with respect to  $\eta$ . However, it is easy to translate these velocities into the others just by defining a mean scale factor  $a \equiv \sqrt[3]{a_{\perp}^2 a_{\parallel}}$  because  $dt \simeq a d\eta$  and, therefore,  $\frac{dx^i}{dt} \simeq a \frac{dx^i}{d\eta}$ , which is a good approximation in the perturbative regime. Moreover, we have to notice that for an appropriate definition of fluid velocity, we have to rescale  $V \equiv a_{\parallel} v$ , so that  $V^2 \leq 1$ .

Now, it is convenient to introduce the rapidity variables  $\theta_{\alpha}$  defined by  $\cosh \theta_{\alpha} = \gamma_{\alpha}$  so that the equations adopt a simpler structure. Velocities are related to  $\theta_{\alpha}$  by means of  $\tanh \theta_{\alpha} = a_{\parallel} v_{\alpha}$ . With these new variables, the Einstein equations from (2.58) and (2.59) take the form:

$$H_{\perp}^2 + 2H_{\perp}H_{\parallel} = 8\pi G \sum_{\alpha} \left( \cosh^2 \theta_{\alpha} + w_{\alpha} \sinh^2 \theta_{\alpha} \right) \rho_{\alpha}, \quad (2.60)$$

$$\dot{H}_{\perp} + \dot{H}_{\parallel} + H_{\perp}^2 + H_{\parallel}^2 + H_{\perp}H_{\parallel} = -8\pi G \sum_{\alpha} p_{\alpha}, \quad (2.61)$$

$$2\dot{H}_{\perp} + 3H_{\perp}^2 = -8\pi G \sum_{\alpha} \left( w_{\alpha} \cosh^2 \theta_{\alpha} + \sinh^2 \theta_{\alpha} \right) \rho_{\alpha}, \quad (2.62)$$

where  $\dot{\phantom{x}} \equiv \frac{d}{dt}$  and  $H_{\perp} \equiv \dot{a}_{\perp}/a_{\perp}$ ,  $H_{\parallel} \equiv \dot{a}_{\parallel}/a_{\parallel}$  are the transverse and longitudinal expansion rates respectively. These equations reduce to the Friedmann ones when  $a_{\perp} = a_{\parallel}$  and  $v_{z\alpha} = 0$ . Again, as in the perturbative case, we need some extra equations to close the problem which are those given by the independent energy-momentum tensor conservation. These equations can be written as follows:

$$\dot{v}_{z\alpha} = -\frac{\left((w_{\alpha} - 1) \cosh^2 \theta_{\alpha} - 1\right) H_{\parallel} + 2w_{\alpha} H_{\perp}}{(w_{\alpha} - 1) \cosh^2 \theta_{\alpha} - w_{\alpha}} v_{z\alpha}, \quad (2.63)$$

$$\dot{\rho}_{\alpha} = \frac{(1 + w_{\alpha}) \left(H_{\parallel} + 2H_{\perp} \cosh^2 \theta_{\alpha}\right)}{(w_{\alpha} - 1) \cosh^2 \theta_{\alpha} - w_{\alpha}} \rho_{\alpha}. \quad (2.64)$$

Besides, one can find the following equations for the evolution of  $\theta_{\alpha}$ :

$$\dot{\theta}_{\alpha} = -\frac{(w_{\alpha} - 1)H_{\parallel} + 2w_{\alpha}H_{\perp}}{(w_{\alpha} - 1) \cosh^2 \theta_{\alpha} - w_{\alpha}} \sinh \theta_{\alpha} \cosh \theta_{\alpha}. \quad (2.65)$$

The spatial geodesic equations for the metric considered are:

$$\begin{aligned} \frac{d^2x}{d\lambda^2} + 2H_{\perp} \frac{dt}{d\lambda} \frac{dx}{d\lambda} &= 0, \\ \frac{d^2y}{d\lambda^2} + 2H_{\perp} \frac{dt}{d\lambda} \frac{dy}{d\lambda} &= 0, \\ \frac{d^2z}{d\lambda^2} + 2H_{\parallel} \frac{dt}{d\lambda} \frac{dz}{d\lambda} &= 0, \end{aligned} \quad (2.66)$$

where  $\lambda$  is an affine parameter. The first integral for these equations is given by:

$$\frac{d\vec{r}}{d\lambda} = \left( \frac{n_x}{a_{\perp}^2}, \frac{n_y}{a_{\perp}^2}, \frac{n_z}{a_{\parallel}^2} \right) \quad (2.67)$$

being  $\vec{r} = (x, y, z)$  and the integration constants can be chosen for simplicity in such a way that  $\vec{n}^2 = 1$ . Moreover, from the condition of null geodesic we get:

$$\frac{dt}{d\lambda} = \sqrt{\frac{n_{\perp}^2}{a_{\perp}^2} + \frac{n_{\parallel}^2}{a_{\parallel}^2}} \quad (2.68)$$

with  $n_{\perp}^2 = n_x^2 + n_y^2$  and  $n_{\parallel}^2 = n_z^2$ . Then, for an observer with velocity  $u^\mu = \gamma(1, \vec{v})$  the energy of the photon is:

$$\mathcal{E} = \gamma E \left[ \sqrt{\frac{n_{\perp}^2}{a_{\perp}^2} + \frac{n_{\parallel}^2}{a_{\parallel}^2}} - \vec{n} \cdot \vec{v} \right] \quad (2.69)$$

and the corresponding temperature fluctuation reads:

$$\frac{\delta T}{T} = \frac{\gamma_0 a_0}{\gamma_{dec} a_{dec}} \frac{\sqrt{\frac{n_{\perp}^2}{a_{\perp 0}^2} + \frac{n_{\parallel}^2}{a_{\parallel 0}^2}} - \vec{n} \cdot \vec{v}_0}{\sqrt{\frac{n_{\perp}^2}{a_{\perp dec}^2} + \frac{n_{\parallel}^2}{a_{\parallel dec}^2}} - \vec{n} \cdot \vec{v}_{dec}} - 1 \quad (2.70)$$

where again the indices 0 and *dec* denote the present and decoupling times respectively.

## 2.8 Model examples

### 2.8.1 Constant equation of state

The simplest dark energy model we will consider is that corresponding to a fluid with constant equation of state  $w_{DE} \simeq -1$ . Note that in the case  $w_{DE} = -1$ , i.e. pure cosmological constant, dark energy does not contribute to the center of mass velocity (2.7) and, therefore, the center of mass frame agrees with the radiation frame. This means that all the fluids would share a common rest frame and no effects on the CMB would be possible. When  $w_{DE}$  is close to  $-1$ , the velocity of dark energy scales as  $\sim a^{-4}$  and its energy density is nearly constant (see Fig. 2.3). Since dark energy velocity decreases very fast, its contribution to the quadrupole is very small. Besides, the velocity of radiation (and therefore that of matter) is determined by the initial dark energy velocity and the gauge condition (2.29) as:

$$\vec{v}_R = \frac{1 + w_{DE}}{1 + w_R} \frac{\Omega_{DE}}{\Omega_R} a_*^4 \vec{v}_{DE}^* \quad (2.71)$$

where  $\vec{v}_{DE}^*$  is the initial dark energy velocity. Taking  $\Omega_{DE} = 0.73$ ,  $\Omega_R = 8.18 \times 10^{-5}$ ,  $w_{DE} = -0.97$  and  $a_* \sim 10^{-6}$ , we get  $\vec{v}_R \simeq 2 \times 10^{-22} \vec{v}_{DE}^*$ .

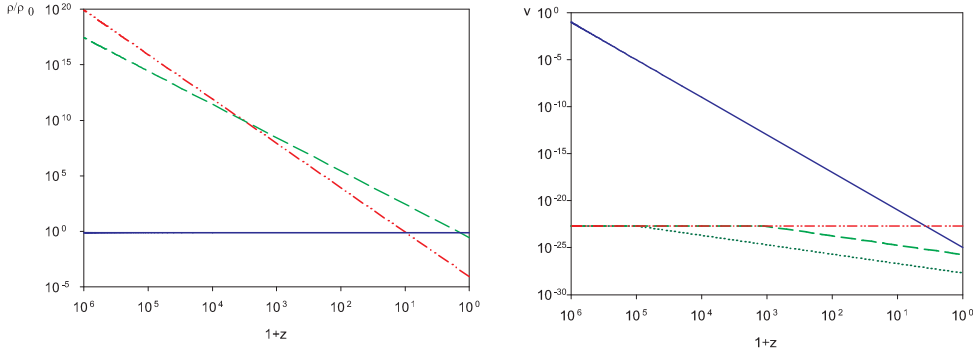


Figure 2.3: Evolution of densities and velocities in a model with constant equation of state as described in the text. Continuous line (blue) for dark energy, dashed-dotted (red) for radiation, dotted (cyan) for dark matter and dashed (green) for baryonic matter. On the left baryonic and dark matter are added together and plotted in dashed (green). Notice that in this plot dark matter is assumed to decouple at  $z \simeq 10^5$ .

The value of  $a_*$  taken corresponds to a favorable case since lower values would lead to much lower velocities of radiation and matter. Then, even for initial velocities of dark energy close to 1, the velocities of matter and radiation are extremely small, which means that the three fluids are very nearly at rest in the cosmic center of mass frame. That way, the quadrupole generated in this model is totally negligible.

## 2.8.2 Scaling models

As explained in the first Chapter, scaling models are those with an equation of state such that dark energy mimics the dominant component of the Universe throughout most of the expansion history. Thus, dark energy evolves as radiation before matter-radiation equality and as matter after that. However, in order to explain the accelerated expansion of the Universe, dark energy has to exit from that regime and join into one with  $w_{DE} < -1/3$  at some point. Then, the evolution of the dark energy den-

sity is given by:

$$\rho_{DE} = \begin{cases} \rho_{DE0} a_T^{-3w_{DE}} a_{eq} a^{-4} & a < a_{eq} \\ \rho_{DE0} a_T^{-3w_{DE}} a^{-3} & a_{eq} < a < a_T \\ \rho_{DE0} a^{-3(w_{DE}+1)} & a > a_T \end{cases} \quad (2.72)$$

where as commented before,  $a_T$  is the scale factor when dark energy leaves the scaling regime and  $\rho_{DE0}$  is the present value of the dark energy density.

In the evolution of dark energy velocity, we have to take into account the momentum conservation equation given (to first order) by (2.16). This equation implies that the dark energy velocity must be discontinuous at the transition points since the equation of state jumps at those times whereas the quantity  $a^4(1+w_{DE})\rho_{DE}\vec{v}_{DE}$  is constant, being  $\rho_{DE}$  continuous. With this in mind, we get the following evolution for dark energy velocity:

$$\vec{v}_{DE} = \begin{cases} \vec{v}_{DE}^* & a < a_{eq} \\ \frac{4}{3}a_{eq}a^{-1}\vec{v}_{DE}^* & a_{eq} < a < a_T \\ \frac{4a_{eq}a_T^{-3w_{DE}}}{3(1+w_{DE})}a^{3w_{DE}-1}\vec{v}_{DE}^* & a > a_T \end{cases} . \quad (2.73)$$

The discontinuities in the velocity arise because we are considering abrupt changes in the equation of state. If these changes were smooth, the results would be essentially unaffected since the final values of the velocities would remain those in (2.73). In Fig. 2.4, we show the evolution of the energy densities and velocities for a typical scaling model.

We can see from the previous expression that, in the second transition, the closer  $w_{DE}$  is to  $-1$ , the more the velocity grows after the transition. The case  $w_{DE} = -1$  is not divergent because, if that was the case, the conservation equation would become trivial and the velocity evolution got from (2.39) would not make sense anymore.

In these scaling models, the first transition can be set at the matter-radiation equality and the second one must be chosen such that we get

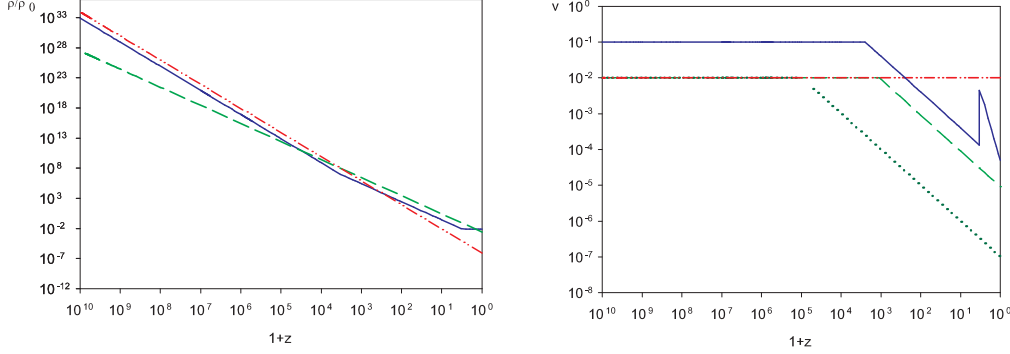


Figure 2.4: Densities and velocities evolution in a scaling model with  $v_{DE}^* = 0.1$  and  $\epsilon = 0.1$ . As in the previous figure, the continuous line (blue) is for dark energy, dashed-dotted (red) for radiation, dotted (cyan) for dark matter and dashed (green) for baryonic matter. On the left baryonic and dark matter are added together and plotted in dashed (green). Notice that in this plot dark matter is also assumed to decouple at  $z \simeq 10^5$  and  $a_* = 10^{-10}$ .

the observed dark energy density today. Moreover, the initial velocity of radiation, and therefore that of matter, is fixed by the initial velocity of dark energy via the gauge condition (2.29). Because matter is subdominant with respect to radiation before equality, the matter contribution in (2.29) can be neglected and we obtain that:

$$\vec{v}_R^* = -\epsilon \vec{v}_{DE}^* \quad (2.74)$$

where  $\epsilon \equiv \rho_{DE}(a_*)/\rho_R(a_*)$  is the initial dark energy density fraction (neglecting the matter contribution). Notice that this fraction does not depend on  $a_*$ , because dark energy scales as radiation in the radiation dominated era. Then, we can obtain a relation between  $a_T$  and  $\epsilon$  just by computing that quotient from the known expressions for the energy densities evolutions of each fluid. When doing that it results:

$$a_T = \left[ \frac{\Omega_{DE} a_{eq}}{\Omega_R \epsilon} \right]^{\frac{1}{3w_{DE}}}. \quad (2.75)$$

Since we need  $w_{DE}(z_T) < -1/3$  in order to have accelerated expansion, we see from the previous formula that  $a_T$  grows as  $\epsilon$  grows, more precisely if we take  $w_{DE}(z < z_T) = -0.97$ , then  $a_T \propto \epsilon^{0.34}$ . Since primordial nucleosynthesis imposes an upper limit on  $\epsilon$ , we can establish also an upper limit on  $a_T$  just by setting the maximum value of  $\epsilon$  on (2.75).

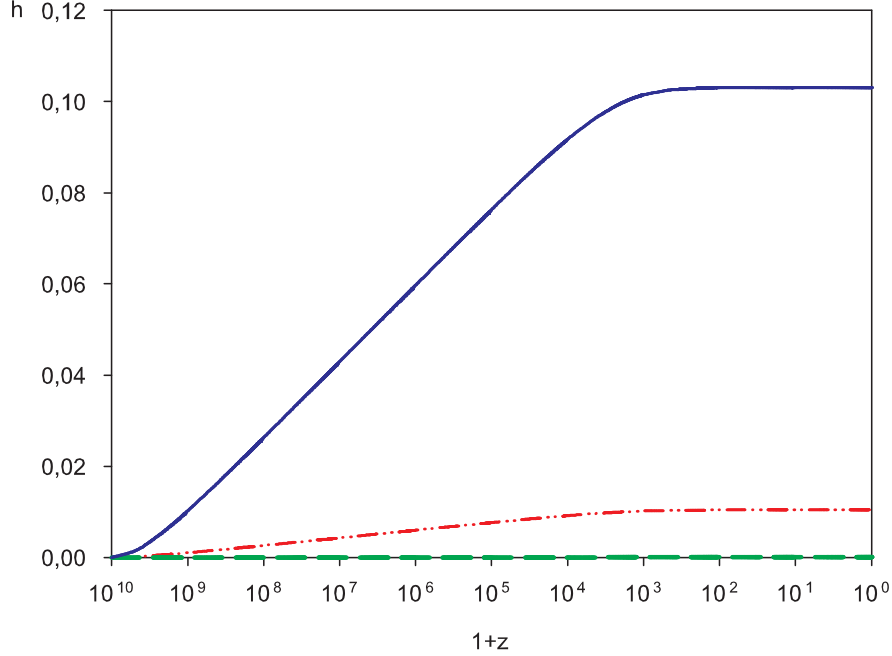


Figure 2.5: Evolution of metric perturbations due to each fluid in a scaling model with  $\epsilon = 0.1$  and  $v_* = 0.1$ . We can see that the largest contribution comes from dark energy (continuous blue line) and matter (dashed green) essentially does not contribute. Radiation is shown with a dashed-dotted (red) line.

This maximum value is  $\epsilon_{max} \simeq 0.2$ , (see for instance [93]) so we get the constraint  $a_T \lesssim 0.41$  for this kind of scaling models where we have taken  $\Omega_{DE} = 0.73$ ,  $\Omega_R = 8.18 \times 10^{-5}$  and  $a_{eq} = \frac{1}{3300}$ .

By inserting the corresponding values for the densities and velocities of the four fluids, as well as the equation of state considered into (2.41), we can compute the quadrupole produced by the relative motion of the fluids. For our calculations we shall take  $\Omega_B = 0.046$ ,  $\Omega_{DM} = 0.23$ ,  $a_{dec} = \frac{1}{1100}$  and  $w_{DE}(z < z_T) = -0.97$  and the values given above. Fig. 2.5 shows the evolution of the contribution of each fluid to the metric perturbation  $h_\alpha$ . We can see that the typical behavior is a rapid growth during the radiation era to reach finally a slightly growing regime in the matter era (notice that the dependence on  $a_*$  is only logarithmic). In spite of the fact that the perturbation is  $\mathcal{O}(v_{DE}^{*2})$ , the quadrupole is expected to be smaller because  $h$  barely grows in the epoch since decoupling to today

and, as we mentioned in Section 2.6, the quadrupole is essentially given by the growth of the perturbation during that epoch.

The quadrupole produced by scaling models is fixed by two parameters: the initial velocity  $v_{DE}^*$  and the initial energy ratio  $\epsilon$  of dark energy. It is easy to see from (2.41) that  $h_\alpha$  and, therefore the quadrupole, is proportional to  $v_{DE}^{*2}$ . Obviously, this dependence is valid just for small velocities since when we consider velocities close to the speed of light we have to take into account relativistic effects. The dependence of the quadrupole on  $\epsilon$  can be found to be linear for  $\epsilon \lesssim 0.07$  with a slope 0.44 so we can conclude that the quadrupole is very well approximated by the simple expression:

$$Q_A \simeq 0.44 \epsilon v_{DE}^{*2}. \quad (2.76)$$

As commented before, this expression is valid only for small velocities. According to the bounds on the quadrupole obtained in (2.54) and (2.56), there are allowed regions in the parameter space  $(\epsilon, v_{DE}^*)$ , which from (2.76) are limited by the curves  $\epsilon = k_\pm / v_*^2$  where the constants  $k_\pm$  correspond to the upper and lower limits on  $Q_A$ . In Fig. 2.6 we show these regions obtained numerically with the exact equations. As we said above, the second order calculation is a good approximation for velocities lower than 0.1. However, when the velocities are large (close to 1) values of  $\epsilon \lesssim \mathcal{O}(10^{-6})$  are necessary in order to explain the observed quadrupole. Notice once again that these regions have been obtained in the case in which the measured quadrupole has two contributions, one coming from inflation and a second contribution coming from the fluids motion. Since  $v_{DE}^*$  relates to radiation velocity through (2.74) as follows:  $v_R = \epsilon v_{DE}^*$  we can express the quadrupole as  $Q_A \simeq 0.44 v_R^2 \epsilon^{-1} \simeq 1.23 \times 10^{-6} \epsilon^{-1}$  or, equivalently, we have that  $\Delta h \simeq 5.32 \times 10^{-6} \epsilon^{-1}$ , where we have assumed that the total bulk flow is due to the motion of the fluids and we have taken the velocity of radiation to be  $v_R \simeq 500 \text{ km/s} = 1.67 \times 10^{-3} c$  in the CCM rest frame. Therefore, constraints (2.57) read:

$$\begin{aligned} 7.69 \times 10^{-2} &\lesssim \epsilon \lesssim 0.2 && 68\% \text{ C.L.} \\ 4.32 \times 10^{-2} &\lesssim \epsilon \lesssim 0.2 && 95\% \text{ C.L.} \end{aligned} \quad (2.77)$$

where the upper limit comes from primordial nucleosynthesis, as commented before. Therefore, in this kind of models it is possible to explain the presence of the matter bulk flow from the dark energy motion in a compatible way with the measurements of the CMB quadrupole.

To end this Section we shall show why we can neglect the third term in (2.28) with respect to that containing the metric perturbation  $h_{ij}$ . Let

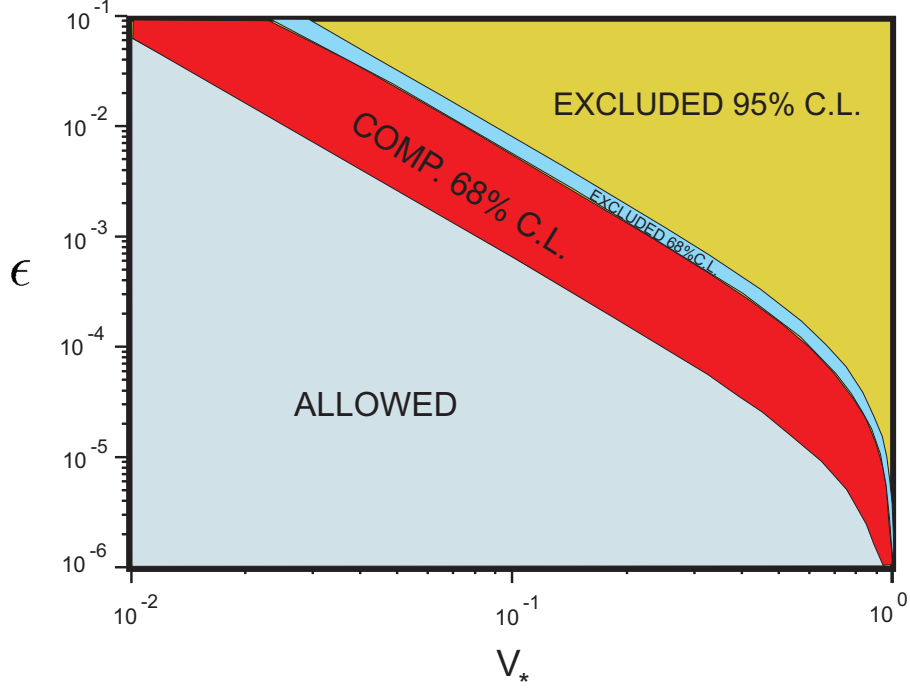


Figure 2.6: Exclusion plot in the parameter space  $(\epsilon, v_{DE}^*)$  for a scaling dark energy model. The allowed region corresponds to the limits given in (2.54). The dark (red) strip corresponds to the regions for which  $Q_A$  could explain the observed quadrupole at the 68% C.L. according to (2.56)

us recall that term:

$$(\vec{v} \cdot \vec{n})|_{dec}^0 (\vec{v}_{dec} \cdot \vec{n}). \quad (2.78)$$

The first factor in this expression is nothing but the dipole which is  $\sim 10^{-3}$ . The second factor contains the velocity of the observer at decoupling time which coincides with matter velocity (and therefore with that of radiation) at that moment. Then, if we recall the relation (2.74) between radiation and dark energy velocities, we find that this term is  $\sim 10^{-3} \epsilon v_{DE}^*$ . On the other hand, the last term in (2.28) is  $\sim \epsilon v_{DE}^{*2}$  as we have just seen above. Hence, if we call  $Q_v$  and  $Q_h$  to the last two terms in (2.28) respectively we have that  $Q_h \sim 10^3 v_{DE}^* Q_v$  and we see that  $Q_v$  will be larger than  $Q_h$  only for  $v_{DE}^* < 10^{-3}$ . However, in such a case the contribution to the quadrupole is  $\lesssim 10^{-6} \epsilon$  which is negligible.

### 2.8.3 Tracking models

In this Section we would like to comment on the difficulties which can appear in certain dark energy models when we consider perturbations in the fluids velocities. In general, any model with a stiff stage in which its equation of state satisfies  $w > \frac{1}{3}$ , would be unstable with respect to velocity perturbations according to (2.39). This could be the case of certain tracking models. These are models in which the energy density of dark energy follows a common evolutionary track for a wide range of initial conditions. This attractor behavior makes this kind of models an interesting alternative to a cosmological constant since they alleviate the so called coincidence problem. Unlike scaling models, in this case dark energy does not necessarily mimics the dominant component. In the model proposed in [94] the equation of state is initially close to 1, then it changes to  $-1$  and, finally, it oscillates around  $-0.2$ .

Fig. 2.7 shows a typical behavior when  $w > \frac{1}{3}$ : first the velocity perturbation (defined as  $V \equiv a_{\parallel} v$ ) grows according to (2.39) and asymptotically approaches 1. We can understand this from the exact conservation equations (2.63) by taking the ultrarelativistic limit  $\theta \gg 1$ . This yields the

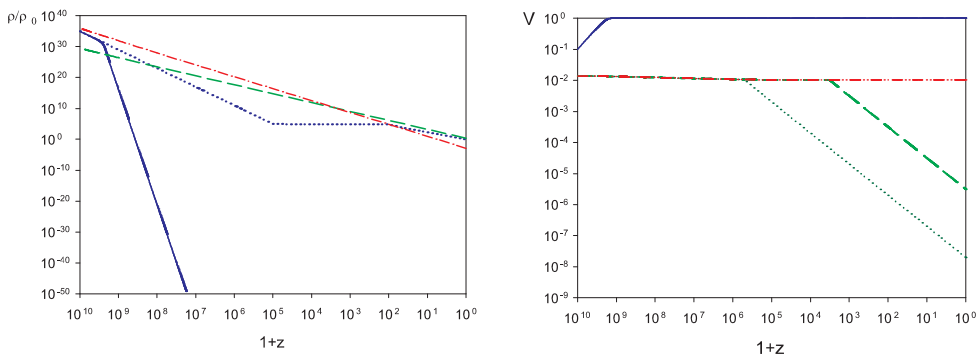


Figure 2.7: Densities and velocities evolution in a typical tracking model with an initial equation of state  $w_{DE} = 0.9$ , which changes to  $w_{DE} = -1$  and then to  $w_{DE} \sim -0.2$ . The continuous line (blue) is for dark energy in the model with moving dark energy, whereas the blue dotted line is for static dark energy, dashed-dotted (red) for radiation, dashed (green) for baryonic and dark matter. We see that when  $V_{DE}$  reaches 1, the corresponding density begins falling too fast to be able to recover the present value for  $\Omega_{DE}$ .

solutions:

$$\begin{aligned} v &= v_0 a_{\parallel}^{-1}, \\ \rho &= \rho_0 a_{\perp}^{-2 \frac{1+w}{1-w}}. \end{aligned} \quad (2.79)$$

This means that  $V \simeq 1$  is a solution of the equations. In addition, the energy density for  $w > 1/3$  falls very fast with the expansion when compared with the usual behavior  $\rho = \rho_0 a^{-3(1+w)}$ . In addition,  $\gamma^2 \rho$ , which is the quantity that contributes to the Hubble rate in (2.60), decays as  $(a_{\parallel} a_{\perp})^{-2}$ , once the fluid reaches the ultra-relativistic regime, regardless the value of  $w$ .

In the limiting case of stiff fluids with  $w = 1$ , it is possible to obtain exact solutions. Thus the velocity perturbation and the energy density are:

$$\begin{aligned} V &= V_0 a_{\perp}^2, \\ \rho &= \rho_0 \frac{e^{-4 \int H_{\perp} \cosh^2 \theta dt}}{a_{\parallel}^2}. \end{aligned} \quad (2.80)$$

Thus, the velocity of the fluid grows as  $a_{\perp}^2$  until it reaches the speed of light in a finite time and the density falls to zero at the same time because  $\theta$  becomes infinity at that moment. From that time on, the fluid will keep moving at the speed of light with vanishing energy density. Notice that  $\gamma$  becomes infinity in such a way that the momentum is conserved i.e. the matching between the two regimes must be taken so that  $\gamma^2 \rho$  is finite and continuous. In any case, we see that when the velocity is high enough the density falls to zero and, the closer is  $w$  to one, the faster is the fall of the density, so that we cannot recover the present value for the dark energy density. Notice that this general behavior is independent of the value of the initial velocity and, accordingly, even in models in which all the fluids are initially at rest, a small perturbation in the velocity could change dramatically the final values of the densities, unless fine tunings of the transition redshifts are introduced.

### 2.8.4 Null dark energy

In this Section we shall study the case in which dark energy behaves as a null fluid, whose energy-momentum tensor reads:

$$T_N^{\mu\nu} = (\rho_N + p_N) l^{\mu} l^{\nu} - p_N g^{\mu\nu} \quad (2.81)$$

with  $l^\mu$  a null vector given, in the Bianchi type I metric (2.58), by  $l^\mu = (1, 0, 0, a_{\parallel}^{-1})$ . For this kind of fluid, the conservation of energy and momentum can be expressed as follows:

$$0 = \dot{p}_N, \quad (2.82)$$

$$0 = (\dot{\rho}_N + \dot{p}_N) + 2(H_{\parallel} + H_{\perp})(\rho_N + p_N). \quad (2.83)$$

These equations imply that the pressure is constant and that the combination  $(\rho_N + p_N)$  scales as  $(a_{\parallel}a_{\perp})^{-2}$ , so that the energy density is given by  $\rho_N = \rho_{N0}(a_{\parallel}a_{\perp})^{-2} - p_{N0}$  where  $p_{N0}$  and  $\rho_{N0}$  are constants of integration. Since the anisotropy is expected to be small, the energy density of this fluid behaves as radiation during the early epoch and as a cosmological constant with energy density  $-p_{N0}$  at late times. Now, if we require  $\rho_N$  to be positive at all times, we conclude that the pressure must be negative, as corresponds to a cosmological constant. Notice that this is a general result for any null fluid whose energy-momentum tensor is given by (2.81). The transition between both regimes can be easily calculated and it is given by  $a_T \simeq (-\frac{\rho_{N0}}{p_{N0}})^{1/4}$ . Since  $p_{N0} = -0.73\rho_{c0}$ , where  $\rho_{c0}$  is the critical density today, we have that  $a_T = 0.1\epsilon^{1/4}$  where  $\epsilon \equiv \frac{\rho_{N0}}{\rho_{R0}}$  is the ratio of dark energy density with respect to radiation which is almost constant. Besides, this ratio is also the initial contribution of dark energy to the total energy density which has an upper limit imposed by primordial nucleosynthesis. Taking once again  $\epsilon_{max} \lesssim 0.2$ , we have an upper limit on the transition given by:  $a_T \lesssim 2 \times 10^{-2}$ .

The exact Einstein equations in this case are:

$$H_{\perp}^2 + 2H_{\perp}H_{\parallel} = 8\pi G \sum_{\alpha} \left( \cosh^2 \theta_{\alpha} + w_{\alpha} \sinh^2 \theta_{\alpha} \right) \rho_{\alpha} + 8\pi G \rho_N, \quad (2.84)$$

$$\dot{H}_{\perp} + \dot{H}_{\parallel} + H_{\perp}^2 + H_{\parallel}^2 + H_{\perp}H_{\parallel} = -8\pi G \sum_{\alpha} p_{\alpha} - 8\pi G p_N, \quad (2.85)$$

$$2\dot{H}_{\perp} + 3H_{\perp}^2 = -8\pi G \sum_{\alpha} \left( w_{\alpha} \cosh^2 \theta_{\alpha} + \sinh^2 \theta_{\alpha} \right) \rho_{\alpha} - 8\pi G (\rho_N + 2p_N), \quad (2.86)$$

where now  $\alpha = B, DM, R$ . Moreover, we still have the gauge condition  $\vec{S} = 0$  which yields the following constraint:

$$\sum_{\alpha} \gamma_{\alpha}^2 (\rho_{\alpha} + p_{\alpha}) v_{\alpha} + (\rho_N + p_N) = 0. \quad (2.87)$$

In the radiation-dominated era we can neglect the contribution of matter (dark matter and baryons) to the latter sum, so we get:

$$\gamma_R^2 v_R = -\frac{\rho_N + p_N}{\rho_R + p_R} \quad (2.88)$$

Since, in that epoch, dark energy must be subdominant with respect to radiation, the quotient on the RHS is small and, therefore, the velocity of radiation is also small. This allows us to consider the perturbative regimen in the velocities (except, obviously for the null fluid).

Therefore, if we assume that the anisotropy generated is small we can set the following form for  $a_{\parallel}$  and  $a_{\perp}$ :

$$\begin{aligned} a_{\perp} &= a(1 + \delta_{\perp}), \\ a_{\parallel} &= a(1 + \delta_{\parallel}). \end{aligned} \quad (2.89)$$

With this ansatz it is easy to see that  $h = 2(\delta_{\parallel} - \delta_{\perp})$ . Then, inserting (2.89) in (2.86) and expanding up to first order in  $\delta$ 's and  $v_{\alpha}$  we can get the following equation for  $h$ :

$$\frac{d}{dt} \left( a^3 \frac{dh}{dt} \right) = 2a^3 (\rho_N + p_N). \quad (2.90)$$

This equation can be easily solved by means of two direct integrations and its solution can be expressed as follows:

$$h = 6 \int_{a_*}^a \frac{1}{\tilde{a}^4} \left[ \int_{a_*}^{\hat{a}} \hat{a}^2 (\rho_N + p_N) \frac{d\hat{a}}{\sqrt{\sum_{\alpha} \rho_{\alpha}}} \right] \frac{d\tilde{a}}{\sqrt{\sum_{\alpha} \rho_{\alpha}}}. \quad (2.91)$$

In principle, the problem is not solved yet since  $\rho_N + p_N$  depends on  $\delta_{\parallel}$  and  $\delta_{\perp}$ . However, we can consider the lowest order in this quantity, i.e.,  $\rho_N + p_N = \rho_{N0} a^{-4}$  to obtain the dominant contribution to the quadrupole. This is justified because  $\frac{\rho_{N0}}{\rho_{R0}}$  is of the same order as  $v_R$  as we can see from (2.88). We have to note that, to this order, the quadrupole depends just on the null fluid because the first contribution to the anisotropy due to the rest of fluids is of second order in the velocities, whereas the null fluid contributes to first order. In Fig. 2.8 we plot the evolution of the fluids densities and  $h$  function for a null fluid with  $\epsilon = 5 \times 10^{-6}$ .

In this model we only have one free parameter:  $\rho_{N0}$  or, equivalently,  $\epsilon \equiv \frac{\rho_{N0}}{\rho_{R0}}$ , so we can get bounds on  $\epsilon$  just from (2.54) and (2.56). Besides, the quadrupole is linear in  $\epsilon$ , as we see looking at (2.91), more precisely

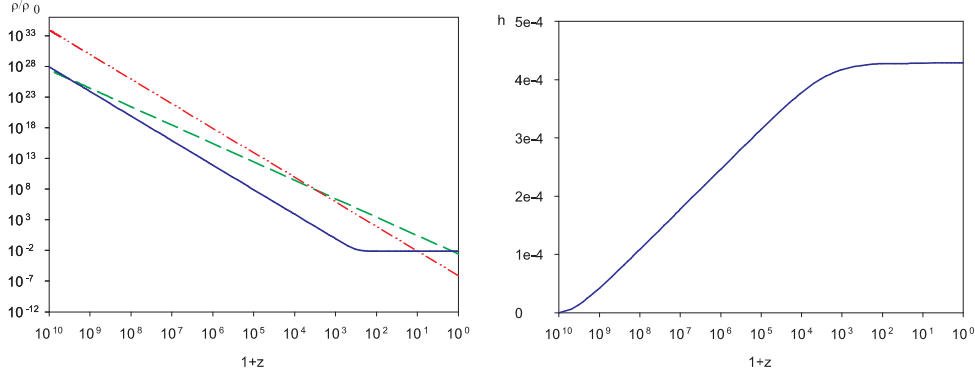


Figure 2.8: Left: densities evolution for a null fluid with  $\epsilon = 5 \times 10^{-6}$ . Matter is plotted with dashed (green) line, dotted-dashed (red) for radiation and continuous (blue) line for dark energy. We see that the null fluid behaves as in a scaling model except during the matter dominated epoch. Right: evolution of  $h$  showing that the anisotropy grows up to a maximum value where it remains nearly constant.

we have that the quadrupole is given by:  $Q_A \simeq 2.58 \epsilon$ . Now again the contribution from the term  $Q_v$  given by (2.78) is negligible compared with  $Q_A$  since  $Q_v \simeq 10^{-3} \epsilon$ .

This expression is nearly independent of  $a_*$  because the quadrupole depends on the difference  $h_0 - h_{dec}$  which is not very sensitive to the time at which we set the initial conditions. Comparing the expression obtained for the quadrupole with the previous bounds, we get that the allowed region in (2.54) corresponds to:

$$\begin{aligned} \epsilon &\lesssim 6.1 \times 10^{-6} \quad 68\% \text{ C.L.} \\ \epsilon &\lesssim 1.1 \times 10^{-5} \quad 95\% \text{ C.L.} \end{aligned} \quad (2.92)$$

whereas for:

$$\begin{aligned} 1 \times 10^{-6} &\lesssim \epsilon \lesssim 8.8 \times 10^{-6} \quad 68\% \text{ C.L.} \\ 0 &\lesssim \epsilon \lesssim 1.4 \times 10^{-5} \quad 95\% \text{ C.L.} \end{aligned} \quad (2.93)$$

the null fluid could make the predicted quadrupole to agree with observations, as shown in (2.56).

## 2.9 Conclusions and discussion

In this Chapter we have studied homogeneous models of dark energy in which the rest frame of the different fluids can differ from each other. Within this framework, the large scale bulk flows detected in [79] and [81] can be naturally explained because the presence of a dark component moving at the time when photons and baryons decouple allow them to acquire a global relative motion. We have considered the evolution of slow-moving and fast-moving fluids and shown that, starting from an initially isotropic Universe, the fluids motions can generate an anisotropic expansion in which the degree of anisotropy typically grows in time. Such anisotropies have been shown to contribute mainly to both the CMB dipole and quadrupole, being the contributions to higher multipoles negligible because the effect to the  $\ell$ th multipole scales as  $|\vec{v}|^\ell$  so the effect decreases very rapidly as we go to higher multipoles due to the smallness of the velocities. We apply those results to some dark energy models and find that in models with constant equation of state, even for initial velocities of dark energy close to the speed of light, throughout the matter era all the fluids would practically share a common rest frame so that they cannot account for the large scale peculiar velocities and no effects on the quadrupole are expected. However, in the case of scaling models it has been shown that the anisotropy grows during the radiation era and reaches a nearly constant value during matter domination. The effect on the CMB quadrupole can be relevant and bounds on the velocity and initial fraction of dark energy can be found. We have also found that for models with an initial stage in which the equation of state is stiffer than radiation, as for instance in some tracking models, the velocity approaches the speed of light whereas the energy density decays faster than in the case in which dark energy is at rest with respect to matter and radiation. This fact spoils the predictions of those models for the density parameters at late times. Finally we have considered also fluids moving at the speed of light and found that generically they behave as a cosmological constant at late time, provided their energy density is positive at all times, whereas they act as radiation at early times. The contribution to the quadrupole is also used to set limits on the relative contribution of dark energy in the radiation dominated era.

The scenario considered here with moving fluids leads to axisymmetric Bianchi I metrics as those arising in other contexts. For instance, in [55] the anisotropy arises from the presence of magnetic fields that produce

---

an ellipsoidal Universe at the decoupling time and, then, it isotropizes as the Universe expands. However, unlike that model with decaying anisotropies, the motion of dark energy supports the anisotropies which could have a non-negligible value today.

To summarize, we can say that the observed large scale bulk flows can be explained within the context of moving dark energy models and that the presence of relative motions between the different components of the Universe leads to interpret the CMB dipole as caused by the relative motion of the CMB photons and the cosmic center of mass rest frame. Finally, we have obtained the constraints imposed by the CMB anisotropies on the amplitude of these relative motions.



# Cosmology in vector-tensor theories of gravity

---

## 3.1 Introduction

In the previous Chapter we have studied the possibility of having a dark energy component with a relative motion with respect to the rest of components of the Universe. However, our study was made on the pure phenomenological basis of effectively describing the dark energy component as a perfect fluid. In other words, we have considered the potential effects of having dark energy carrying a non-vanishing homogeneous density of momentum, i.e.,  $T_{DE}^{0i} \neq 0$ . The following step in this research line would be to try to build a theoretical model realizing the fact of having moving dark energy. Obviously, this cannot be achieved on the grounds of scalar fields because there is no way of constructing a  $T^{0i}$  component with a homogeneous scalar field, being necessary the existence of gradients to have such kind of components.

A natural candidate giving rise to moving dark energy that one would immediately think of is a vector field because it would be possible, in principle, to have a homogeneous  $T^{0i}$  thanks to the presence of spatial components of the vector field that can pick up a determined direction without the need of any gradients. This was our first motivation to study the so-called vector-tensor theories of gravity in which the gravitational interaction is described by a vector field in addition to the metric tensor. Unfortunately, as we shall show, this is not the case in the context of pure vector-tensor theories because  $T^{0i}$  vanishes identically over the vector field equations of motion in the homogeneous case. Nonetheless, even

though this was our initial motivation to consider vector-tensor theories of gravity as dark energy candidates, it turns out that they offer a very rich variety of cosmologies and give rise to some interesting models that might help solving some of the fundamental problems arising in Modern Cosmology. At this respect we can mention the anomalies discovered in the CMB that may suggest the presence of a preferred direction in the Universe. Moreover, the presence of vector fields over cosmological scales could also help understanding the large scale bulk flows discussed in the precedent Chapter because they contain a support for vector perturbations which is absent in the standard  $\Lambda$ CDM as well as in the dark energy models based on scalar fields. Finally, vector fields also offer the possibility of alleviating the coincidence problem or even propose a satisfactory solution, as we shall show in the last Chapters of this thesis.

The study of vector-tensor theories to describe the gravitational interaction as alternatives to GR started long time ago with the works by Will, Nordtvedt and Hellings [95, 96, 97] in the early 70's as candidates to produce preferred frame effects. After these pioneering works, vector-tensor theories were abandoned because gravitational experiments seemed to rule out such preferred frame effects. Moreover, fluctuations of the vector field could be either timelike or spacelike so that those models were generally thought to be plagued by instabilities.

A special class of vector-tensor theories reemerged due to the increasing interest in models with Lorentz violation [98, 99, 100, 101, 102, 103] where the breaking of Lorentz invariance was achieved by the presence of a vector field with a non-vanishing vacuum expectation value. In this sort of models, the norm of the vector field was forced to be constant by means of a Lagrange multiplier so that the vector field is constrained to be either time-like or space-like depending on the sign of the norm. Moreover, some of these models are free of instabilities as it was shown in [104]. A detailed study on the stability of the ether models (as they are generally called) was done in [105] and it was shown that there is only one stable model, which was further studied in [106]. Another interesting result of this work is that the Lagrange multiplier cannot be considered as the limit of a given potential because, in that case, a ghost-like degree of freedom shows up and makes the theory unstable.

More recently, after the discovery of the accelerated expansion of the Universe, cosmological vector fields have received some attention as possible candidates for dark energy. In [107], an extension of Maxwell electrodynamics by including an inverse power of the field strength in the action

was considered and it was shown that such a model leads to accelerated expansion with  $w < -1$  and the Universe ending in a future Big Rip singularity. A time-like vector field with a non-standard kinetic term of the Maxwell type and with a potential was proposed in [108]. The problem of using the standard Maxwell kinetic term for the vector field lies in the fact that the temporal component of those models in a homogeneous background becomes trivial, so that they cannot give rise to homogeneous and isotropic accelerated solutions because only the spatial components are true dynamical degrees of freedom and they will produce a certain anisotropy in the case that the expansion of the Universe is governed by them. This difficulty was avoided in [109] by introducing three mutually orthogonal vector fields with standard kinetic terms and in the presence of some potential. This ensemble of vector fields, called *triad*, allows the total energy-momentum tensor corresponding to the triad to be isotropic, even though the energy-momentum tensor of each vector field is not. One may think that this is an extremely special configuration for a set of three vector fields. However, if we consider a set of  $N$  vector fields pointing along random spatial directions, we may expect to have a very approximate isotropic situation provided  $N$  is sufficiently large. In any case, one important result obtained in [110] shows that this model (among others in which one spatial component of the vector field acquires a non-vanishing vacuum expectation value) presents instabilities. A model based on a massive vector field with standard kinetic term and including couplings of the vector field to the curvature was proposed in [111]. The presence of couplings to the curvature prevents the temporal component to become trivial and, indeed, it can drive an accelerated expansion era. Several vector field models, including couplings to curvature through Gauss-Bonnet terms, are extensively studied in [112] as candidates to produce accelerated expansion for both the time-like and the space-like cases. Again, these models usually present instabilities and fine-tuning problems.

Finally, vector fields are not exclusive of dark energy models builders, but they have also received attention in other branches of Cosmology. Indeed, a vector field with the standard Maxwell action supplemented with a suitable potential was already used in [113] as an alternative to scalar fields for driving an inflationary epoch during the early Universe. In this sense we can say that some of the dark energy models based on vector fields could also be good candidates to produce an inflationary era [112] because they both try to explain a phase with accelerated expansion. Vector fields have also been used as dark matter candidates in the fully covariant generalization of the MOND models with an action containing

tensor, vector and scalar fields (TeV $\bar{S}$ ) [114, 115]. The generation of non-singular cosmologies has also been shown to be possible by resorting to vector fields [107]. The anomalies discovered in the CMB which seem to indicate preferred directions have inspired the use of vector fields on Cosmology as well.

As we have seen in the previous paragraphs, vector fields have been extensively used in Cosmology. However, in spite of all the partial studies on vector-tensor theories, there is not a systematic study of the cosmological evolution, stability or compatibility with local gravity tests for these models. In this Chapter and the following, we shall present such a detailed study. We shall perform a classification of the models attending to the evolution of the vector field during the different epochs of the Universe history, namely, inflation, radiation dominated era and matter dominated era. The case in which the vector field dominates the energy density is analyzed and the solutions with accelerated expansion are identified. Moreover, we shall consider a universe filled with a matter component in addition to the vector field and obtain the models giving rise to late-time accelerated expansion.

This Chapter is based on the results contained in the paper:

- *Cosmological evolution in vector-tensor theories of gravity*. Jose Beltrán Jiménez and Antonio L. Maroto. *Physical Review* **D80**, 063512 (2009).

## 3.2 Generalities

We shall start by writing the most general action for a vector-tensor theory without any other restriction apart from having second order linear equations of motion [116]:

$$S[g_{\mu\nu}, A_\mu] = \int d^4x \sqrt{-g} \left[ -\frac{1}{16\pi G} R + \omega R A_\mu A^\mu + \tilde{\sigma} R_{\mu\nu} A^\mu A^\nu + \tau \nabla_\mu A_\nu \nabla^\mu A^\nu + \epsilon F_{\mu\nu} F^{\mu\nu} \right], \quad (3.1)$$

with  $\omega$ ,  $\tilde{\sigma}$ ,  $\tau$ ,  $\epsilon$  dimensionless parameters and  $F_{\mu\nu} = \partial_\mu A_\nu - \partial_\nu A_\mu$ . In the so-called ther-Einstein models, the vector field norm is fixed by introducing a Lagrange multiplier in the action of the form  $\lambda_m (A_\mu A^\mu \pm m^2)$  so that  $A_\mu$  is constrained to be either timelike or spacelike. In other cases (as those mentioned in the Introduction of this Chapter, the vector field is supplied with a mass term or even more complicated potential terms. However, throughout the present study we shall focus on vector-tensor theories without Lagrange multipliers nor potential terms. The reason for this restriction is that we want to deal with a theory without other dimensional constants rather than the Newton constant. At this respect, notice that the terms given in (3.1) are the only possibilities without introducing new scales in the theory and that give rise to linear equations of motion for the vector field. If such an action is just a low energy limit of some underlying theory, one would expect to have corrections involving terms of dimension higher than 4 which would be suppressed by some high scale  $M$ .

For subsequent calculations we shall work with an alternative form of action (3.1) obtained via an integration by parts:

$$S[g_{\mu\nu}, A_\mu] = \int d^4x \sqrt{-g} \left[ -\frac{1}{16\pi G} R + \omega R A_\mu A^\mu + \sigma R_{\mu\nu} A^\mu A^\nu + \lambda (\nabla_\mu A^\mu)^2 + \epsilon F_{\mu\nu} F^{\mu\nu} \right] \quad (3.2)$$

where the new parameters relate to the old ones as follows:

$$\begin{aligned} \sigma &= \tilde{\sigma} - \tau \\ \lambda &= \tau \\ \epsilon &= \frac{2\epsilon + \tau}{2}. \end{aligned} \quad (3.3)$$

We prefer the new form of the action because it allows a more suggestive interpretation for each term, namely: the  $\epsilon$ -term is nothing but the  $U(1)$  gauge invariant kinetic term for the vector field, the  $\lambda$ -term is analogous to the gauge fixing term introduced in the electromagnetic quantization and, finally, both the  $\omega$  and  $\sigma$  terms are non-minimal couplings to gravity and play the role of effective mass terms for the vector field driven by gravity.

The gravitational equations obtained from action (3.2) by varying with respect to the metric tensor can be written in the following way:

$$G_{\mu\nu} = 8\pi G \left( \omega T_{\mu\nu}^{\omega} + \sigma T_{\mu\nu}^{\sigma} + \lambda T_{\mu\nu}^{\lambda} + \epsilon T_{\mu\nu}^{\epsilon} + T_{\mu\nu}^{NG} \right), \quad (3.4)$$

where  $T_{\mu\nu}^{NG}$  is the energy-momentum tensor corresponding to other fields rather than  $A_{\mu}$  (generally the inflaton, matter and radiation) and we have defined:

$$\begin{aligned} T_{\mu\nu}^{\omega} &= 2 \left[ \square A^2 g_{\mu\nu} + A^2 G_{\mu\nu} + R A_{\mu} A_{\nu} - \nabla_{\mu} \nabla_{\nu} A^2 \right], \\ T_{\mu\nu}^{\sigma} &= g_{\mu\nu} \left[ \nabla_{\alpha} \nabla_{\beta} \left( A^{\alpha} A^{\beta} \right) - R_{\alpha\beta} A^{\alpha} A^{\beta} \right] + \square \left( A_{\mu} A_{\nu} \right) - 2 \nabla_{\alpha} \nabla_{(\mu} \left( A_{\nu)} A^{\alpha} \right) \\ &\quad + 4 A^{\alpha} A_{(\mu} R_{\nu)\alpha}, \\ T_{\mu\nu}^{\lambda} &= g_{\mu\nu} \left[ \left( \nabla_{\alpha} A^{\alpha} \right)^2 + 2 A^{\alpha} \nabla_{\alpha} \left( \nabla_{\beta} A^{\beta} \right) \right] - 4 A_{(\mu} \nabla_{\nu)} \left( \nabla_{\alpha} A^{\alpha} \right), \\ T_{\mu\nu}^{\epsilon} &= 4 F_{\mu\alpha} F_{\nu}{}^{\alpha} - g_{\mu\nu} F_{\alpha\beta} F^{\alpha\beta}, \\ T_{\mu\nu}^{NG} &= \frac{2}{\sqrt{-g}} \frac{\delta S_{NG}}{\delta g^{\mu\nu}}, \end{aligned} \quad (3.5)$$

with  $\square = \nabla_{\mu} \nabla^{\mu}$ ,  $A^2 = A_{\mu} A^{\mu}$  and brackets in a pair of indices denoting symmetrization with respect to the corresponding indices.

Apart from the gravitational equations we can obtain a set of field equations for  $A_{\mu}$  by varying the action with respect to the vector field to give:

$$2\epsilon \nabla_{\nu} F^{\mu\nu} - \lambda \nabla^{\mu} \left( \nabla_{\nu} A^{\nu} \right) + \omega R A^{\mu} + \sigma R_{\nu}^{\mu} A^{\nu} = 0. \quad (3.6)$$

Since we are interested in the cosmological evolution of the vector field (especially as candidate for dark energy) we shall focus on the simplest case in which the field is homogeneous, i.e., we shall study the evolution of the Fourier zero mode of the vector field. Actually, this will correspond to all Fourier modes whose physical wavelengths are much larger than the Hubble radius (super-Hubble modes). In fact, this is the relevant part of the field for the cosmological expansion evolution, although the inhomogeneous part could also be very important for the CMB anisotropies or structure formation. Besides, we shall choose the spatial component of the field lying along the  $z$ -axis in such a way that we can write  $A_\mu = (A_0(t), 0, 0, A_z(t))$  and, therefore, we have axial symmetry around that axis<sup>1</sup>. Thus, the metric tensor will be appropriately described by that of the axisymmetric Bianchi type I space-time:

$$ds^2 = dt^2 - a_\perp(t)^2 (dx^2 + dy^2) - a_\parallel(t)^2 dz^2, \quad (3.7)$$

where  $a_\perp$  and  $a_\parallel$  are the transverse and longitudinal scale factors respectively. For this metric, the field equations read:

$$\lambda \left[ \ddot{A}_0 + (2H_\perp + H_\parallel) \dot{A}_0 \right] + m_{A_0}^2 A_0 = 0, \quad (3.8)$$

$$2\epsilon \left[ \ddot{A}_z + (2H_\perp - H_\parallel) \dot{A}_z \right] + m_{A_z}^2 A_z = 0, \quad (3.9)$$

with

$$\begin{aligned} m_{A_0}^2 &= (2\omega + \sigma)(2H_\perp^2 + H_\parallel^2) \\ &\quad + (2\omega + \sigma + \lambda)(2\dot{H}_\perp + \dot{H}_\parallel) + 2\omega(2H_\perp H_\parallel + H_\perp^2), \\ m_{A_z}^2 &= 2\omega(3H_\perp^2 + 2\dot{H}_\perp) + (2\omega + \sigma)(\dot{H}_\parallel + H_\parallel^2 + 2H_\perp H_\parallel), \end{aligned} \quad (3.10)$$

where a dot stands for derivative with respect to the cosmic time  $t$  and  $H_\parallel = \dot{a}_\parallel / a_\parallel$  and  $H_\perp = \dot{a}_\perp / a_\perp$  are the longitudinal and transverse expansion rates respectively. In these equations we see that the expansion of the universe provides an effective mass for each component of the vector field as well as a friction term. It is interesting to note that the dynamics of  $A_0$  and  $A_z$  are driven by the  $\lambda$  and  $\epsilon$  terms respectively, whereas the rest of parameters of the action,  $\omega$  and  $\sigma$ , only affect the effective mass of

---

<sup>1</sup>Notice that the situation is completely analogous to that described in chapter 2 when considering fluids moving along the  $z$ -direction.

the field. In fact, the presence of non-vanishing values for  $\lambda$  and  $\epsilon$  ensures the existence of evolving  $A_0$  and  $A_z$  respectively. On the contrary, if one of these parameters is zero, the corresponding component does not have dynamics and, in general, will vanish.

The highly isotropic CMB power spectrum that we observe today shows that the anisotropy at the last scattering surface was very small so that it is justified to consider small deviations from a pure isotropic universe with

$$\begin{aligned} a_{\perp}(t) &= a(t) \\ a_{\parallel}(t) &= a(t) \left( 1 + \frac{1}{2} h \right) \end{aligned} \quad (3.11)$$

with  $h \ll 1$  and  $a(t)$  the isotropic scale factor. Then, we can describe the anisotropy by means of the degree of anisotropy  $h$  in terms of which the metric can be written as a perturbed FLRW given by:

$$ds^2 = dt^2 - a(t)^2 (\delta_{ij} + h_{ij}) dx^i dx^j \quad (3.12)$$

with  $h_{ij} = h \delta_{iz} \delta_{jz}$  and  $a(t)$  the usual scale factor. Moreover, the degree of anisotropy can be related to the linearized Einstein tensor for the Bianchi type I metric as follows:

$$G_{\perp} - G_{\parallel} = \frac{1}{2a^3} \frac{d}{dt} (a^3 \dot{h}) + \mathcal{O}(h^2) \quad (3.13)$$

where  $G_{\perp} = G_x^x = G_y^y$  and  $G_{\parallel} = G_z^z$ . Then, from Einstein equations we can obtain the evolution for the degree of anisotropy which happens to be:

$$h = 16\pi G \int \frac{1}{a^3} \left[ \int a^3 \Delta p dt \right] dt \quad (3.14)$$

with  $\Delta p \equiv p_{\parallel} - p_{\perp}$ . In principle, the problem has not been solved yet because the expression inside the integral will depend on  $h$  as well. However, we can obtain an approximate solution by replacing such an integrand by its expression in the isotropic case. In fact, one could obtain more accurate solutions by an iterative process. Thus, if we now assume that the only source of anisotropy comes from the spatial component of the vector field we have that:

$$\begin{aligned} a^2 \Delta p &= \left[ (24\omega_{\epsilon} + 12\omega_{\epsilon}\sigma_{\epsilon} + 8\sigma_{\epsilon} + 3\sigma_{\epsilon}^2) H^2 \right. \\ &\quad \left. + (12\omega_{\epsilon} + 6\omega_{\epsilon}\sigma_{\epsilon} + 4\sigma_{\epsilon} + \sigma_{\epsilon}^2) \dot{H} \right] A_z^2 + 4\sigma_{\epsilon} H A_z \dot{A}_z - 2(2 + \sigma_{\epsilon}) \dot{A}_z^2 \end{aligned} \quad (3.15)$$

where  $H = \dot{a}/a$  the Hubble expansion rate and we have introduced the notation  $\omega_\epsilon = \omega/\epsilon$  and  $\sigma_\epsilon = \sigma/\epsilon$ . In the rest of this chapter we shall perform a detailed analysis of the isotropic evolution so that we could eventually use those results to evaluate (3.14) and, therefore, to discriminate those models in which the degree of anisotropy grows or decays as the universe expands, that is, what models would give rise to large scale anisotropies. For a detailed treatment on the anisotropy evolution in dark energy models see [58]. Moreover, the generated large-scale anisotropy would affect the photons coming from the last scattering surface so that it would give a new contribution to the low multipoles of the CMB. In fact, this can be used to rule out those models in which the new contribution is larger than the observed one.

To end this Section we would like to comment on a very interesting feature of these models. In Chapter 2 we have shown that a dark energy field carrying a non-vanishing density of momentum could modify the usual interpretation of the CMB dipole as well as the value of the quadrupole. The density of momentum of dark energy can be interpreted as a relative motion of this component with respect to the others. Therefore, since a vector field has spatial components one would expect it to carry density of momentum, essentially determined by  $A_i$ , and, as consequence, it would be a natural candidate for a moving dark energy model. However, once one uses the equations of motion it turns out that the density of momentum vanishes identically, i.e.,  $T^{0i} = 0$  over the field equations so that it cannot produce moving dark energy. Hence, although the vector field can provide large scale anisotropy supported by its spatial component, it does not modify the cosmic rest frame and no effects on the CMB dipole are expected.

### 3.3 Evolution in an isotropic universe

In this section we shall write down and solve the equations for the vector field in a universe dominated by an isotropic perfect fluid, with the energy density of the vector field being negligible. In such a case, both expansion factors become the same  $a_\perp = a_\parallel = a$  as well as the expansion rates  $H_\perp = H_\parallel = H$ . This is equivalent to neglect the effects of the small degree of anisotropy that may be present. In such a case, the field

equations read:

$$\begin{aligned} \ddot{A}_0 + 3H\dot{A}_0 + \left[3(4\omega_\lambda + \sigma_\lambda)H^2 + 3(1 + 2\omega_\lambda + \sigma_\lambda)\dot{H}\right] A_0 &= 0, \\ \ddot{A}_z + H\dot{A}_z + \frac{1}{2} \left[3(4\omega_\epsilon + \sigma_\epsilon)H^2 + (6\omega_\epsilon + \sigma_\epsilon)\dot{H}\right] A_z &= 0. \end{aligned} \quad (3.16)$$

On the other hand, the energy density associated to  $A_0$  and  $A_z$  in the isotropic case are:

$$\begin{aligned} \rho_{A_0} &= \lambda \left[3(3 + 2\omega_\lambda + 2\sigma_\lambda)H^2 A_0^2 + 6(1 + 2\omega_\lambda + \sigma_\lambda)HA_0\dot{A}_0 + \dot{A}_0^2\right], \\ \rho_{A_z} &= -\frac{2\epsilon}{a^2} \left[-(3\omega_\epsilon + \sigma_\epsilon)H^2 A_z^2 + (6\omega_\epsilon + \sigma_\epsilon)HA_z\dot{A}_0 + \dot{A}_z^2\right]. \end{aligned} \quad (3.17)$$

In these expressions we have introduced again the notation  $\omega_\lambda = \omega/\lambda$ ,  $\sigma_\lambda = \sigma/\lambda$ ,  $\omega_\epsilon = \omega/\epsilon$  and  $\sigma_\epsilon = \sigma/\epsilon$ , which only makes sense for  $\lambda \neq 0$  and  $\epsilon \neq 0$ . However, if that is not the case, the corresponding component does not have dynamics and, generally, vanishes so that it does not play any role, as we explained above.

Although we are restricting ourselves to the case of isotropic expansion, one should be aware of the fact that the presence of a small shear could modify the evolution of the spatial components of the vector field because, in the stability analysis around a FRW metric, there could be vanishing eigenvalues (as shown in [53, 117]) and, as a consequence, the evolution of  $A_z$  could be different from that determined by (3.16).

In next subsections we shall study the evolution of the vector field in the different epochs of the expansion history of the universe and carry out a classification of the models according to their behaviors.

### 3.3.1 Inflationary (de Sitter) epoch

During the inflationary era, the universe undergoes an exponential expansion so that the Hubble parameter  $H$  is constant, i.e.,  $a \propto e^{Ht}$ . In such a case, the solutions to (3.16) can be expressed as:

$$\begin{aligned} A_0 &= \left(A_0^+ e^{c_0 Ht} + A_0^- e^{-c_0 Ht}\right) e^{-3Ht/2} \\ A_z &= \left(A_z^+ e^{c_z Ht} + A_z^- e^{-c_z Ht}\right) e^{-Ht/2} \end{aligned} \quad (3.18)$$

where

$$c_0 = \frac{1}{2}\sqrt{9 - 48\omega_\lambda - 12\sigma_\lambda} \quad (3.19)$$

$$c_z = \frac{1}{2}\sqrt{1 - 24\omega_\epsilon - 6\sigma_\epsilon} \quad (3.20)$$

Then, the evolution of the temporal component depends on whether  $c_0$  is real or complex. That way, we find that it oscillates with frequency  $|c_0 H|$  and it is modulated by a damping factor of the form  $e^{-3Ht/2}$  for  $16\omega_\lambda + 4\sigma_\lambda > 3$  whereas it evolves as  $e^{(c_0-3/2)Ht}$  for  $16\omega_\lambda + 4\sigma_\lambda < 3$ . When  $16\omega_\lambda + 4\sigma_\lambda = 3$  we have that  $c_0 = 0$  and the vector field evolves as  $A_0 = (C_1^0 + C_2^0 t)e^{-3Ht/2}$ .

Concerning  $A_z$ , it has an oscillating evolution with frequency  $|c_z H|$  suppressed by  $e^{-Ht/2}$  for  $24\omega_\lambda + 6\sigma_\lambda > 1$  and it evolves as  $e^{(c_z-1/2)Ht}$  for  $24\omega_\lambda + 6\sigma_\lambda < 1$ . Finally, for  $24\omega_\lambda + 6\sigma_\lambda = 1$  we have that  $c_z = 0$  and the field evolve as  $A_z = (C_1^z + C_2^z t)e^{-3Ht/2}$ .

When we insert solutions (3.18) into (3.17) we obtain the energy density evolution, which can be written as:

$$\rho_{A_0} = \rho_{A_0^+} a^{2c_0-3} + \rho_{A_0^-} a^{-2c_0-3} \quad (3.21)$$

$$\rho_{A_z} = \rho_{A_z^+} a^{2c_z-3} + \rho_{A_z^-} a^{-2c_z-3} \quad (3.22)$$

where we have defined:

$$\begin{aligned} \rho_{A_0^\pm} = & \lambda [3(3 + 2\omega_\lambda + 2\sigma_\lambda) + 6(1 + 2\omega_\lambda + \sigma_\lambda)(\pm c_0 - 3/2) \\ & + (\pm c_0 - 3/2)^2] (HA_0^\pm)^2 \end{aligned}$$

$$\begin{aligned} \rho_{A_z^\pm} = & -2\epsilon [-(3\omega_\epsilon + \sigma_\epsilon) + (6\omega_\epsilon + \sigma_\epsilon)(\pm c_z - 1/2) \\ & + (\pm c_z - 1/2)^2] (HA_z^\pm)^2. \end{aligned}$$

In these expressions we see that the temporal component is suppressed during inflation in models with  $2c_0 < 3 \Rightarrow 4\omega_\lambda + \sigma_\lambda > 0$  whereas an inflationary epoch amplifies  $A_0$  for those models with  $4\omega_\lambda + \sigma_\lambda < 0$ . For  $4\omega_\lambda + \sigma_\lambda = 0$ , the temporal component has constant energy density. Moreover, for the aforementioned special case with  $c_0 = 0$  the energy density is given by:

$$\rho_{A_0}|_{c_0=0} = \frac{\lambda}{2} C_2^0 \left[ 3(5 - 8\omega_\lambda)HC_2^0 t - (24\omega_\lambda - 15)HC_1^0 + 2C_2^0 \right] a^{-3} \quad (3.23)$$

so it decays as  $\sim ta^{-3}$  (unless  $5 - 8\omega_\lambda = 0$ ).

Analogously, we find that the spatial component is amplified during inflation in models with  $12\omega_\epsilon + 3\sigma_\epsilon < -4$ , it is suppressed for those models with  $12\omega_\epsilon + 3\sigma_\epsilon > -4$  and it has constant energy density if the condition  $12\omega_\epsilon + 3\sigma_\epsilon = -4$  is satisfied. Again, for the special case with  $c_z = 0$  we have a different evolution given by:

$$\rho_{A_z}|_{c_z=0} = \frac{\epsilon}{3} C_2^z [(5 - 12\omega_\epsilon) HC_2^z t - (12\omega_\epsilon - 5) HC_1^z + 2C_2^z] a^{-3} \quad (3.24)$$

so it decays as  $\sim ta^{-3}$  (unless  $5 - 12\omega_\epsilon = 0$ ).

Finally, notice that the oscillating behavior of the field will translate into an oscillating evolution of the energy density so that in those cases in which the field oscillates the energy density for the corresponding component is suppressed by a factor  $a^{-3}$ . In fact, if the inflationary era lasts  $N$  e-folds, i.e., the scale factor increases as  $a_{end}/a_{in} = e^N$ , we can calculate the amplification or suppression of the field at the end of inflation which is given by:

$$\ln \left[ \frac{A_0(t_{end})}{A_0(t_{in})} \right] = \left[ \text{Re}(c_0) - \frac{3}{2} \right] N, \quad (3.25)$$

$$\ln \left[ \frac{A_z(t_{end})}{A_z(t_{in})} \right] = \left[ \text{Re}(c_z) - \frac{1}{2} \right] N. \quad (3.26)$$

For the energy densities of each component we can proceed similarly to obtain:

$$\ln \left[ \frac{\rho_{A_0}(t_{end})}{\rho_{A_0}(t_{in})} \right] = [2\text{Re}(c_0) - 3] N, \quad (3.27)$$

$$\ln \left[ \frac{\rho_{A_z}(t_{end})}{\rho_{A_z}(t_{in})} \right] = [2\text{Re}(c_z) - 3] N. \quad (3.28)$$

In the special cases with  $c_{0,z} = 0$  we have to add a term  $\ln \frac{t_{end}}{t_{in}}$  on the right hand sides of the above expressions, although such a term is usually much smaller than  $N$  and can be safely neglected.

### 3.3.2 Barotropic fluid domination

In a universe dominated by a barotropic perfect fluid with constant equation of state  $w = p/\rho$ , the scale factor evolves according to a power law

of the form  $a \propto t^p$  with  $p = \frac{2}{3(1+w)}$  so that  $H = p/t$ . In such a case, the field equations (3.16) have the following solutions:

$$\begin{aligned} A_0(t) &= A_0^+ t^{\alpha_+} + A_0^- t^{\alpha_-} \\ A_z(t) &= A_z^+ t^{\beta_+} + A_z^- t^{\beta_-} \end{aligned} \quad (3.29)$$

with

$$\begin{aligned} \alpha_{\pm} &= \frac{1}{2} \left[ 1 - 3p \pm \sqrt{1 + 6(1 + 4\omega_\lambda + 2\sigma_\lambda)p + 3(3 - 16\omega_\lambda - 4\sigma_\lambda)p^2} \right], \\ \beta_{\pm} &= \frac{1}{2} \left[ 1 - p \pm \sqrt{1 + 2(6\omega_\epsilon + \sigma_\epsilon - 1)p - (24\omega_\epsilon + 6\sigma_\epsilon - 1)p^2} \right]. \end{aligned} \quad (3.30)$$

As in the inflationary epoch, we see that the components of the vector field have different evolutions depending on whether  $\alpha_{\pm}$  and  $\beta_{\pm}$  are real or complex. Thus, if the term inside the root is positive, the corresponding component of the field will evolve as a power law essentially given by the growing mode whereas if the term inside the root is negative, the field will oscillate with an amplitude proportional to  $t^{(1-3p)/2}$  for  $A_0$  or  $t^{(1-p)/2}$  for  $A_z$ . In fact, for  $\alpha, \beta \in \mathbb{C}$ , the solutions of the vector field can be expressed as:

$$\begin{aligned} A_0(t) &= t^{\text{Re}(\alpha)} \left[ C_1^0 \cos(\text{Im}(\alpha) \ln t) + C_2^0 \sin(\text{Im}(\alpha) \ln t) \right] \\ A_z(t) &= t^{\text{Re}(\beta)} \left[ C_1^z \cos(\text{Im}(\beta) \ln t) + C_2^z \sin(\text{Im}(\beta) \ln t) \right] \end{aligned} \quad (3.31)$$

where we see that the vector field actually oscillates harmonically in  $\ln t$  and not in the proper time  $t$ . There is still another special case when we have degeneration in the solutions, i.e., when  $\alpha_+ = \alpha_-$  or  $\beta_+ = \beta_-$ . If any of these relations takes place, the corresponding component of the vector field has a logarithmic solution in addition to the potential solution, being the complete solution as follows:

$$\begin{aligned} A_0 &= (C_1^0 + C_2^0 \ln t) t^{(1-3p)/2} \\ A_z &= (C_1^z + C_2^z \ln t) t^{(1-p)/2} \end{aligned} \quad (3.32)$$

The evolutions of the energy densities are achieved by inserting solutions (3.29) into (3.17) and, for  $\alpha, \beta \in \mathbb{R}$ , are given by:

$$\rho_{A_0} = \rho_{A_0^+} a^{\kappa_0^+} + \rho_{A_0^-} a^{\kappa_0^-}, \quad (3.33)$$

$$\rho_{A_z} = \rho_{A_z^+} a^{\kappa_z^+} + \rho_{A_z^-} a^{\kappa_z^-} \quad (3.34)$$

where:

$$\begin{aligned}\rho_{A_0^\pm} &= \lambda \left[ 3(3 + 2\omega_\lambda + 2\sigma_\lambda)p^2 + 6(1 + 2\omega_\lambda + \sigma_\lambda)p \alpha_\pm + \alpha_\pm^2 \right] (A_0^\pm)^2, \\ \rho_{A_z^\pm} &= -2\epsilon \left[ -(3\omega_\epsilon + \sigma_\epsilon)p^2 + (6\omega_\epsilon + \sigma_\epsilon)p \beta_\pm + \beta_\pm^2 \right] (A_z^\pm)^2\end{aligned}$$

and

$$\begin{aligned}\kappa_0^\pm &= 2 \frac{\alpha_\pm - 1}{p}, \\ \kappa_z^\pm &= 2 \frac{\beta_\pm - 1 - p}{p}.\end{aligned}\tag{3.35}$$

Again, given that  $\kappa_{0,z}^+ \geq \kappa_{0,z}^-$ , the energy densities will evolve proportionally to  $a^{\kappa_{0,z}^+}$  so that the vector field behaves as the superposition of two perfect fluids with equations of state  $w_{0,z} = -\frac{1}{3}(1 + \kappa_{0,z}^+)$ . However, in some cases, it might happen that  $\rho_{A_{0,z}^+}$  vanishes and, as a consequence, the corresponding energy density will evolve as  $a^{\kappa_{0,z}^-}$  rather than  $a^{\kappa_{0,z}^+}$ .

When  $\alpha_\pm$  and  $\beta_\pm$  are complex, the energy densities still evolve as  $\rho_{A_{0,z}} = \rho_{A_{0,z}^+} a^{\kappa_{0,z}^+}$  although we must replace  $\alpha_+ \rightarrow \text{Re}(\alpha_+)$  and  $\beta_+ \rightarrow \text{Re}(\beta_+)$  in (3.35) and  $\rho_{A_{0,z}^+}$  are oscillating functions instead of constants.

For the degenerate case with a logarithmic solution, the energy densities are given by:

$$\begin{aligned}\rho_{A_0}|_{\alpha_+=\alpha_-} &= \lambda (C_2^0)^2 \left[ \frac{1 - 2p + (24\omega_\lambda - 15)p^2}{2(1-p)} \left( \frac{C_1^0}{C_2^0} + \ln t \right) + 1 \right] a^{\kappa_0} \\ \rho_{A_z}|_{\beta_+=\beta_-} &= 2\epsilon (C_2^z)^2 \left[ \frac{-1 + 6p + (12\omega_\epsilon - 5)p^2}{2(1-3p)} \left( \frac{C_1^z}{C_2^z} + \ln t \right) - 1 \right] a^{\kappa_z}\end{aligned}\tag{3.36}$$

Therefore, the evolution is the same as in the non-degenerate case modified by a logarithmic variation.

In any case, we can carry out a classification of the models according to whether the energy density of each component grows, decays or remains constant. Finally, we can also identify scaling behaviors or whether the energy density of the vector field grows or decays with respect to that of the dominant component. In Fig. 3.1 and Fig. 3.2 we show the evolution in the different regions in the parameter space for temporal and spatial components respectively

### Radiation dominated epoch

In the radiation dominated epoch we have that  $p = 1/2$  and the evolution of the vector field, according to (3.30), is given by:

$$\alpha_{\pm}^R = -\frac{1}{4} \left[ 1 \mp \sqrt{25 + 12\sigma_{\lambda}} \right] \quad (3.37)$$

$$\beta_{\pm}^R = \frac{1}{4} \left[ 1 \pm \sqrt{1 - 2\sigma_{\epsilon}} \right] \quad (3.38)$$

These expressions allow to obtain that the temporal component evolves as a power law for  $\sigma_{\lambda} > -\frac{25}{12}$  whereas it oscillates with an amplitude decaying as  $t^{-1/4}$  for  $\sigma_{\lambda} < -\frac{25}{12}$ . The degenerate case happens for  $\sigma_{\lambda} = -\frac{25}{12}$ . For the spatial component of the vector field, we have power law behavior for  $\sigma_{\epsilon} < \frac{1}{2}$  and it oscillates with an amplitude growing as  $t^{1/4}$  for  $\sigma_{\epsilon} > \frac{1}{2}$ , whereas the logarithmic solution appears for  $\sigma_{\epsilon} = \frac{1}{2}$ . Notice that the evolution of the vector field does not depend on the parameter  $\omega$  of the action, which is due to the fact that the Ricci scalar  $R$  vanishes in a universe dominated by radiation.

Concerning the evolution of the energy densities, according to (3.35), we have that:

$$\kappa_{0\pm}^R = -5 \pm \sqrt{25 + 12\sigma_{\lambda}} \quad (3.39)$$

$$\kappa_{z\pm}^R = -5 \pm \sqrt{1 - 2\sigma_{\epsilon}} \quad (3.40)$$

If we want the vector field to be dominated by its temporal component we must impose the condition  $\kappa_{0+} > \kappa_{z+}$ , which leads to the constraint  $6\sigma_{\lambda} + \sigma_{\epsilon} > -12$ . That way we prevent the generation of large scale anisotropy that would be in conflict with observations.

The temporal component of the vector field will have constant energy density in this epoch for  $\kappa_{0+}^R = 0$  which is satisfied by the model with  $\sigma_{\lambda} = 0$  and it has scaling evolution if  $\kappa_{0+}^R = -4$  which happens for  $\sigma_{\lambda} = -2$ . From this last condition we also obtain that, in models with  $\sigma_{\lambda} > -2$ , the energy density associated to the temporal component grows with respect to that of the radiation fluid  $\rho_R$  whereas in those models with  $\sigma_{\lambda} < -2$ , the ratio  $\rho_{A_0}/\rho_R$  decays as the universe expands. See Fig. 3.1 for a summary of these behaviors.

Concerning the spatial component, the condition of constant energy density is satisfied for models with  $\sigma_{\epsilon} = -12$  whereas it scales as radiation in models with  $\sigma_{\epsilon} = 0$ . Finally, the energy density associated to the

Property	Inflation	Radiation	Matter
Oscillating	$4\omega_\lambda + \sigma_\lambda > \frac{3}{4}$	$\sigma_\lambda < -\frac{25}{12}$	$2\omega_\lambda - \sigma_\lambda > \frac{27}{8}$
Decaying	$0 < 4\omega_\lambda + \sigma_\lambda < \frac{3}{4}$	$-\frac{25}{12} < \sigma_\lambda < -2$	$3 < 2\omega_\lambda - \sigma_\lambda < \frac{27}{8}$
Scaling	$4\omega_\lambda + \sigma_\lambda = 0$	$\sigma_\lambda = -2$	$2\omega_\lambda - \sigma_\lambda = 3$
Growing	$4\omega_\lambda + \sigma_\lambda < 0$	$\sigma_\lambda > -2$	$2\omega_\lambda - \sigma_\lambda < 3$
Constant	$4\omega_\lambda + \sigma_\lambda = 0$	$\sigma_\lambda = 0$	$2\omega_\lambda - \sigma_\lambda = 0$

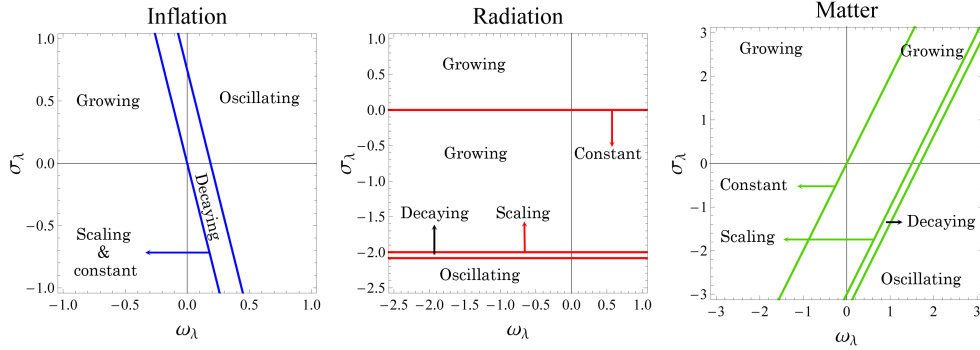


Figure 3.1: Behavior of the temporal component of the vector field in the different phases of the universe history according to the values of the parameters of the model. The labels Decaying and Growing refers to the behavior with respect to the dominant component, whereas Scaling means that it evolves in the same way as the background.

spatial component of the vector field grows (decays) with respect to  $\rho_R$  in models with  $\sigma_\epsilon < 0$  ( $\sigma_\epsilon > 0$ ). This classification is shown in Fig. 3.2.

### Matter dominated epoch

In a universe dominated by a pressureless fluid the scale factor evolves as  $a \propto t^{2/3}$  so that

$$\alpha_{\pm}^M = -\frac{1}{6} \left[ 3 \mp \sqrt{81 - 48\omega_{\lambda} + 24\sigma_{\lambda}} \right] \quad (3.41)$$

$$\beta_{\pm}^M = \frac{1}{6} \left[ 1 \pm \sqrt{1 - 24\omega_{\epsilon} - 12\sigma_{\epsilon}} \right] \quad (3.42)$$

In this case, the temporal component oscillates with amplitude proportional to  $t^{-1/2}$  for  $16\omega_{\lambda} - 8\sigma_{\lambda} > 27$ , it evolves with a power law for  $16\omega_{\lambda} - 8\sigma_{\lambda} < 27$  and the degenerate case corresponds to  $16\omega_{\lambda} - 8\sigma_{\lambda} = 27$ . On the other hand,  $A_z$  follows a power law evolution for  $24\omega_{\epsilon} + 12\sigma_{\epsilon} < 1$ , it oscillates with amplitude proportional to  $t^{1/6}$  for  $24\omega_{\epsilon} + 12\sigma_{\epsilon} > 1$  and the degenerate case happens for  $24\omega_{\epsilon} + 12\sigma_{\epsilon} = 1$ .

Moreover,  $\kappa_{0\pm}^R$  and  $\kappa_{z\pm}^R$  become:

$$\kappa_{0\pm}^M = \frac{1}{2} \left[ -9 \pm \sqrt{81 - 48\omega_{\lambda} + 24\sigma_{\lambda}} \right], \quad (3.43)$$

$$\kappa_{z\pm}^M = \frac{1}{2} \left[ -9 \pm \sqrt{1 - 24\omega_{\epsilon} - 12\sigma_{\epsilon}} \right]. \quad (3.44)$$

In this epoch, the condition for the temporal contribution to dominate over the spatial one reads  $6(\omega_{\epsilon} - 2\omega_{\lambda}) + 3(\sigma_{\epsilon} - 2\sigma_{\lambda}) > -80$ .

The scaling behavior for the energy density associated to the temporal component in this epoch is obtained from the condition  $\kappa_{0+}^M = -3$ , whose solution is  $2\omega_{\lambda} - \sigma_{\lambda} = 3$ . Moreover, for  $2\omega_{\lambda} - \sigma_{\lambda} < 3$  the energy density of the vector field grows with respect to that of matter and, as a consequence, the universe is eventually dominated by it. Notice that this is a necessary condition to have a dark energy model, i.e., those models with  $2\omega_{\lambda} - \sigma_{\lambda} > 3$  will never dominate the energy content of the universe if there is a matter component and, as a consequence, it cannot be the responsible for the present acceleration. Fig. 3.1 shows this classification.

For the spatial component we obtain constant energy density in models with  $2\omega_{\epsilon} + \sigma_{\epsilon} = -20/3$  and scaling evolution for  $2\omega_{\epsilon} + \sigma_{\epsilon} = -2/3$ . Finally, the energy density of  $A_z$  grows (decays) with respect to  $\rho_M$  in models with  $2\omega_{\epsilon} + \sigma_{\epsilon} < -2/3$  ( $2\omega_{\epsilon} + \sigma_{\epsilon} > -2/3$ ). See Fig. 3.2.

Property	Inflation	Radiation	Matter
Oscillating	$4\omega_\epsilon + \sigma_\epsilon > \frac{1}{6}$	$\sigma_\epsilon > \frac{1}{2}$	$2\omega_\epsilon + \sigma_\epsilon > \frac{1}{12}$
Decaying	$-\frac{4}{3} < 4\omega_\epsilon + \sigma_\epsilon < \frac{1}{6}$	$0 < \sigma_\epsilon < 1$	$-\frac{2}{3} < 2\omega_\epsilon + \sigma_\epsilon < \frac{1}{12}$
Scaling	$4\omega_\epsilon + \sigma_\epsilon = -\frac{4}{3}$	$\sigma_\epsilon = 0$	$2\omega_\epsilon + \sigma_\epsilon = -\frac{2}{3}$
Growing	$4\omega_\epsilon + \sigma_\epsilon < -\frac{4}{3}$	$\sigma_\epsilon < 0$	$2\omega_\epsilon + \sigma_\epsilon < -\frac{2}{3}$
Constant	$4\omega_\epsilon + \sigma_\epsilon = -\frac{4}{3}$	$\sigma_\epsilon = -12$	$2\omega_\epsilon + \sigma_\epsilon = -\frac{20}{3}$

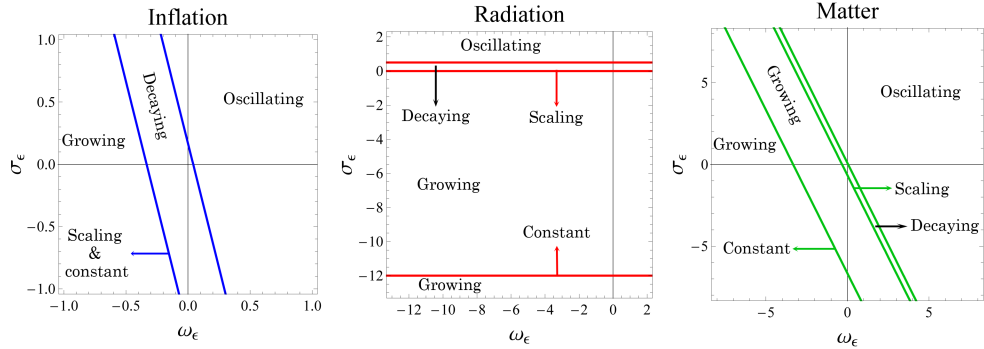


Figure 3.2: Behavior of the spatial component of the vector field in the different phases of the universe history according to the values of the parameters of the model. The labels Decaying and Growing refers to the behavior with respect to the dominant component, whereas Scaling means that it evolves in the same way as the background.

### 3.4 Vector dominance

In this section we shall study the case in which the universe becomes dominated by the temporal component of the vector field so that the anisotropy is small and we can use the isotropic equations. Thus, we have

the field equation for  $A_0$  given in (3.16) and the two Einstein equations:

$$3H^2 = 8\pi G\rho_{A_0}, \quad (3.45)$$

$$3H^2 + 2\dot{H} = -8\pi Gp_{A_0}. \quad (3.46)$$

Although, of course, only two of the three equations are independent, it will be useful to work with all of them.

For the subsequent analysis, it will be convenient to introduce the field variable  $x \equiv \frac{d \ln A_0}{d \ln a}$  so that we can obtain the following autonomous system:

$$\begin{aligned} \frac{dH}{dN} &= 3 \frac{(2\omega_\lambda + \sigma_\lambda)x^2 - 2(4\omega_\lambda + \sigma_\lambda)x - 3(4\omega_\lambda + \sigma_\lambda)(2\omega_\lambda + \sigma_\lambda + 1)}{[x + 3(2\omega_\lambda + \sigma_\lambda + 1)]^2} H \\ \frac{dx}{dN} &= - \frac{x^2 + 6(2\omega_\lambda + \sigma_\lambda + 1)x + 3(2\omega_\lambda + 2\sigma_\lambda + 3)}{x + 3(2\omega_\lambda + \sigma_\lambda + 1)} x \end{aligned} \quad (3.47)$$

with  $N = \ln a$ . These two equations can be combined to give the following equation for the trajectories in the phase map:

$$\frac{d \ln H}{d \ln x} = \frac{-3(2\omega_\lambda + \sigma_\lambda)x^2 + 6(4\omega_\lambda + \sigma_\lambda)x + 9(4\omega_\lambda + \sigma_\lambda)(2\omega_\lambda + \sigma_\lambda + 1)}{[x^2 + 6(2\omega_\lambda + \sigma_\lambda + 1)x + 3(2\omega_\lambda + 2\sigma_\lambda + 3)] [x + 3(2\omega_\lambda + \sigma_\lambda + 1)]}. \quad (3.48)$$

This equation can be readily integrated for given values of the parameters, although we shall not do it, but we shall study the phase map and, from its features, we shall obtain the relevant information.

In addition to the equations given above, we have the following constraint provided by the Friedman equation:

$$\frac{1}{3} \lambda A_0^2 \left[ x^2 + 6(2\omega_\lambda + \sigma_\lambda + 1)x + 3(2\omega_\lambda + 2\sigma_\lambda + 3) \right] = 1 \quad (3.49)$$

This relation constrains the possible values of  $x$  because the condition

$$\lambda \left[ x^2 + 6(1 + \sigma_\lambda + 2\omega_\lambda)x + 3(3 + 2\sigma_\lambda + 2\omega_\lambda) \right] \geq 0 \quad (3.50)$$

must hold. This condition restricts the physically admissible trajectories as those for which the vector field carries positive energy density and can always be achieved by means of a suitable choice of the sign of  $\lambda$ . Notice that all the dependency of the problem on the parameter  $\lambda$  is indeed contained in this condition.

In (3.47) we see that the equation  $\frac{dH}{dN} = 0$  has two solutions:  $H = 0$  and  $x = x_l^\pm$ , with:

$$x_l^\pm = \frac{4\omega_\lambda + \sigma_\lambda \pm \sqrt{(4\omega_\lambda + \sigma_\lambda) [2(5\omega_\lambda + 2\sigma_\lambda) + 3(2\omega_\lambda + \sigma_\lambda)^2]}}{2\omega_\lambda + \sigma_\lambda}. \quad (3.51)$$

whereas the solutions of  $\frac{dx}{dN} = 0$  are  $x = 0$  and  $x = x_c^\pm$ , with:

$$x_c^\pm = -3(2\omega_\lambda + \sigma_\lambda + 1) \pm \sqrt{6(5\omega_\lambda + 2\sigma_\lambda) + 9(2\omega_\lambda + \sigma_\lambda)^2}. \quad (3.52)$$

Therefore, the autonomous system has generally three critical points:  $P_0 = (0, 0)$  and  $P_\pm = (x_c^\pm, 0)$ . Moreover, when the equality  $x_c^\pm = x_l^\pm$  takes place, we have a critical line instead of a critical point because both  $\frac{dH}{dN}$  and  $\frac{dx}{dN}$  vanish regardless the value of  $H$ . Notice that the critical points  $P_\pm$  only exist when the constraint  $6(5\omega_\lambda + 2\sigma_\lambda) + 9(2\omega_\lambda + \sigma_\lambda)^2 \geq 0$  is satisfied, which corresponds to the white region shown in Fig. 3.3. Moreover, the trajectories in the phase map have vertical tangents in the lines  $x = 0$  and  $x = x_c^\pm$  so that, apart from being critical points, they are vertical separatrices (see Fig. 3.4). However, these are not the only separatrices in the phase map, but we have another vertical one in  $x_s = -3(2\omega_\lambda + \sigma_\lambda + 1)$  and an horizontal one in the axis  $H = 0$ . One interesting feature of the phase map is that  $x_s = (x_c^+ + x_c^-)/2$ , i.e., the separatrix at  $x_s$  is always located in the middle of the two critical points. Notice that the critical points  $x_c^\pm$  also separate the region with physically admissible trajectories according to (3.50) which imposes the energy density of the vector field to be positive, although to identify each of these regions we need to specify the sign of  $\lambda$ . According to the previous discussion, the phase map will be divided into several rectangular regions parallel to the axis which, indeed, are disconnected from each other, i.e., the trajectories will not be able to cross from one to another. However, the particular picture will depend on the particular values of the parameters, being possible to distinguish the following cases (see Fig. 3.4):

- Case I: The critical points  $x_c^\pm$  exist and are different from each other, which imposes the condition  $9(2\omega_\lambda + \sigma_\lambda + 1)^2 - 3(2\omega_\lambda + 2\sigma_\lambda + 3) > 0$  and corresponds to the grey region in Fig. 3.3. Moreover, in this case we still have three different possibilities:
  - Case Ia: Both critical points are different from zero and they do not coincide with  $x_s$ . In this case we have 4 vertical separatrices and the phase map is divided into 10 disconnected regions.

- Case Ib: One of the two critical points is zero. This case happens when  $2\omega_\lambda + 2\sigma_\lambda + 3 = 0$  but  $2\omega_\lambda + \sigma_\lambda + 1 \neq 0$  so that they are not zero simultaneously. In fact, if  $2\omega_\lambda + \sigma_\lambda + 1$  is positive (negative), then  $x_c^+$  ( $x_c^-$ ) is at the origin. Notice that this simply says that, given that the separatrix located at  $x_s$  is in the middle of  $x_-$  and  $x_+$ , the critical point that is at the origin depends on the sign of  $x_s$ . In this case we only have 3 vertical asymptotes and, as a consequence, the phase map contains 8 regions. This case corresponds to the dashed line in Fig. 3.3, which represents the equation  $2\omega_\lambda + 2\sigma_\lambda + 3 = 0$
- Case Ic: The vertical separatrix satisfies  $x_s = 0$  so that the two critical points are symmetric with respect to the origin. The condition  $x_s = 0$  reads in terms of the parameters  $2\omega_\lambda + \sigma_\lambda + 1 = 0$  and, as a consequence, the critical point  $P_0$  is absent. In this case we also have 3 vertical asymptotes and 8 regions in the phase map and it corresponds to the dotted line inside the grey region in Fig. 3.3.
- Case II: Neither of the two critical points  $x_c^\pm$  exists. This case satisfies  $9(2\omega_\lambda + \sigma_\lambda + 1)^2 - 3(2\omega_\lambda + 2\sigma_\lambda + 3) > 0$  and corresponds to the white region in Fig. 3.3. Again, we have several subcases:
  - Case IIa: The separatrix  $x_s$  is different from zero. Then, we have two different vertical asymptotes and the phase map contains 6 regions.
  - Case IIb: The separatrix is located at the origin,  $x_s = 0$  so that  $2\omega_\lambda + \sigma_\lambda + 1 = 0$  ( $P_0$  is not a critical point) and we are left with just one vertical asymptote that divides the phase map in 4 regions. This case corresponds to the dotted line inside the white region in Fig. 3.3.
- Case III: The two critical points become equal so we only have one critical point which, indeed, coincides with  $x_s$ , i.e.,  $x_c^+ = x_c^- = x_s = -3(2\omega_\lambda + \sigma_\lambda + 1)$ . This case is represented by the solid line in Fig. 3.3. The two possibilities we have in this case are:
  - Case IIIa: The critical point is different from zero so that we have two vertical asymptotes and the phase map contains 6 regions.
  - Case IIIb: The critical point is zero. Then, we only have one vertical separatrix and four regions. This case corresponds to

the particular model ( $\sigma_\lambda = -2, \omega_\lambda = 1/2$ ) and is represented by the orange dot in Fig. 3.3.

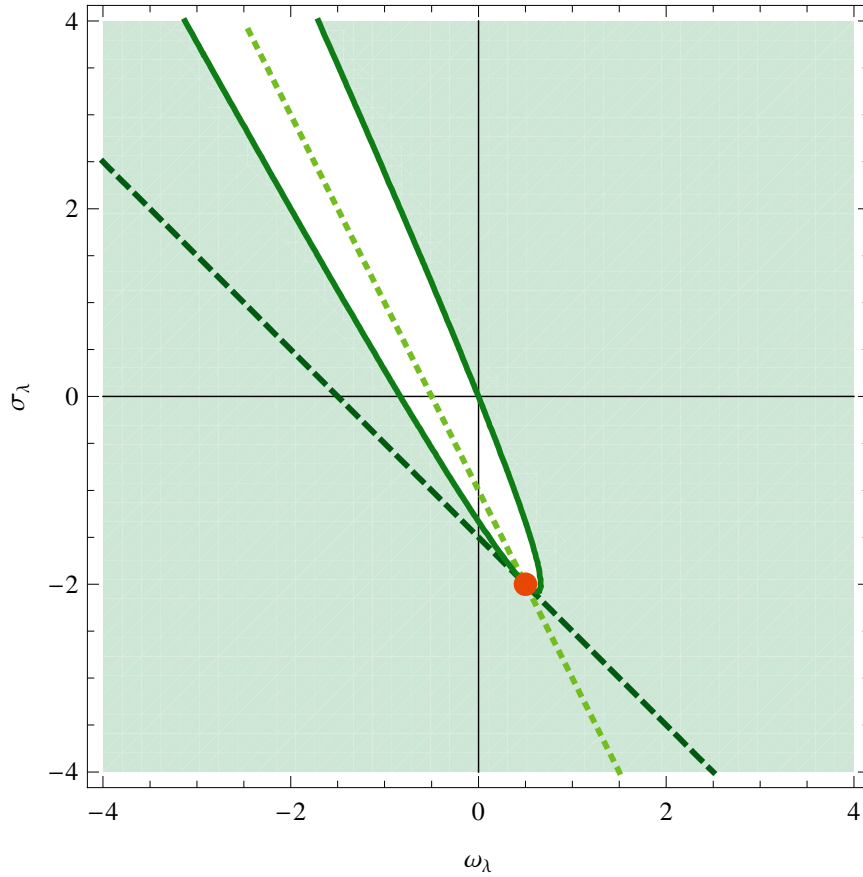


Figure 3.3: This plot shows the different cases explained in the main text in the parameter space. The green region corresponds to models in which both  $x_\pm$  exist (Case I) whereas in the white region neither of them is present (Case II). The solid line identifies the models for which  $x_+ = x_-$  corresponding to Case III. The dashed line (whose equation is  $2\omega_\lambda + 2\sigma_\lambda + 3 = 0$ ) represents those models that have either  $x_-$  or  $x_+$  at the origin (Case Ib) and the models whose parameters lie on the dotted line (with equation  $2\omega_\lambda + \sigma_\lambda + 1 = 0$ ) have the separatrix  $x_s$  at the origin. Thus, in the region above (below) that line  $x_s$  is negative (positive). Case Ic corresponds to the piece of the dotted line inside the white region whereas the piece of the dotted line inside the grey region corresponds to Case IIb. Finally, the orange dot with parameters  $\omega_\lambda = 1/2, \sigma_\lambda = -2$  gives the Case IIIb in which  $x_\pm = x_s = 0$ .

Now that we know the arrangement of the phase map for the different models according to the existence and location of the critical points, we shall study the particular features of each critical point according to the values of the parameters:

- $P_0 = (0,0)$ . The eigenvalues for this critical point are:

$$\mu_H = -\frac{4\omega_\lambda + \sigma_\lambda}{2\omega_\lambda + \sigma_\lambda + 1}, \quad \mu_x = -\frac{2\omega_\lambda + 2\sigma_\lambda + 3}{2\omega_\lambda + \sigma_\lambda + 1}. \quad (3.53)$$

Thus, we have that the critical point is a saddle point for models whose parameters are between the lines  $4\omega_\lambda + \sigma_\lambda = 0$  and  $2\omega_\lambda + 2\sigma_\lambda + 3 = 0$  whereas it is an attractor node if the parameters are in the external region. Notice that this critical point does not exist when  $2\omega_\lambda + \sigma_\lambda + 1 = 0$ , that corresponds to Case Ic in which the separatrix  $x_s$  is placed at the origin. When  $4\omega_\lambda + \sigma_\lambda = 0$  we have that  $\mu_H = 0$  and the critical point becomes a critical line because  $x = 0$  is a singular point irrespectively of the value of  $H$ .

- $P_\pm = (x_c^\pm, 0)$ . For these critical points the eigenvalues can be expressed as  $\mu_H = -(2x_c^\pm + 3)$  and  $\mu_x = -2x_c^\pm$ . Then, if the critical

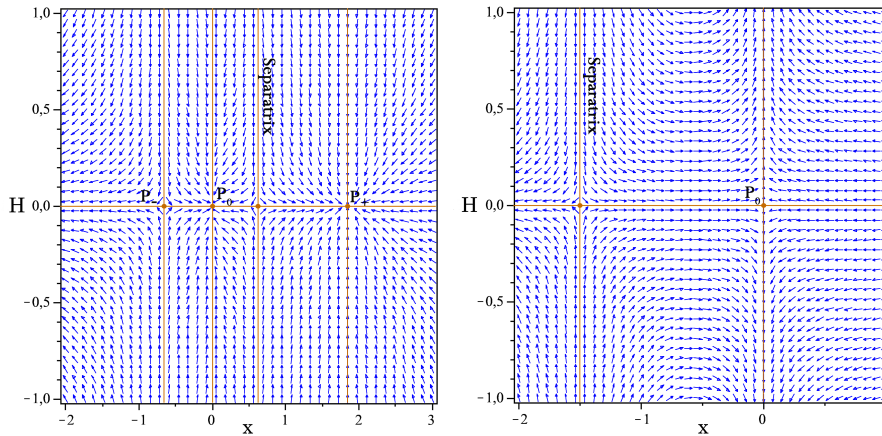


Figure 3.4: These plots show two examples of phase maps for the autonomous system describing a universe dominated by the vector field. The left panel corresponds to a model lying in the grey region in Fig. 3.3 in which the two critical points  $P_\pm$  are present whereas the right panel shows the phase map for a model in which these two critical points do not exist. We can see that all the critical points as well as the separatrix are vertical tangents and the  $x$ -axis is a horizontal separatrix, as explained in the main text.

point is positive we have an attractor node whereas it behaves as a repelling node if  $x_c^\pm < -3/2$ . Finally, in the range  $-3/2 < x_c^\pm < 0$  we get a saddle point. These ranges correspond to the regions in the parameter space showed in Fig. 3.5. The eigenvalues  $\mu_x^\pm$  vanish when the corresponding critical point is located at the origin, i.e.,  $2\sigma_\lambda + 2\omega_\lambda + 3 = 0$ . Then, we can have three different cases depending on the sign of  $2\omega_\lambda + \sigma_\lambda + 1$ , namely:

- i)  $2\omega_\lambda + \sigma_\lambda + 1 > 0$ . In this case  $\mu_x^+ = 0$  and  $\mu_x^- = -6(2\omega_\lambda + \sigma_\lambda + 1) < 0$ .
- ii)  $2\omega_\lambda + \sigma_\lambda + 1 = 0$ . This is the case IIIb described above in which both critical points are located at the origin and, as a consequence,  $\mu_x^+ = \mu_x^- = 0$ .
- iii)  $2\omega_\lambda + \sigma_\lambda + 1 < 0$ . This case is the opposite to i), i.e.,  $\mu_x^- = 0$  and  $\mu_x^+ = -6(2\omega_\lambda + \sigma_\lambda + 1) > 0$ .

On the other hand, the eigenvalues  $\mu_H^\pm$  vanish in the case that the critical points are such that  $x_c^\pm = -3/2$  which is satisfied for models with  $\sigma_\lambda + 4\omega_\lambda = 3/4$ . In this case we also obtain three possibilities in terms of the sign of  $12\omega_\lambda - 15/2$  as follows:

- i)  $12\omega_\lambda - 15/2 > 0$ . In this case we have  $\mu_H^- = 0$  and  $\mu_H^+ = 24\omega_\lambda - 15 > 0$ .
- ii)  $12\omega_\lambda - 15/2 = 0$ . In this case we have  $\mu_H^- = \mu_H^+ = 0$ .
- iii)  $12\omega_\lambda - 15/2 < 0$ . In this case we have  $\mu_H^+ = 0$  and  $\mu_H^- = 24\omega_\lambda - 15 < 0$ .

- Separatrix  $x = x_s$ . For values of  $x$  close to  $x_s$ , i.e.,  $x = x_s + \delta$  with  $\delta \rightarrow 0$  the equations become:

$$\frac{dH}{dN} \simeq \mu_s \frac{H}{\delta^2} \quad (3.54)$$

$$\frac{dx}{dN} \simeq -\mu_s \frac{1}{\delta} \quad (3.55)$$

with

$$\mu_s = 9(2\omega_\lambda + \sigma_\lambda + 1) \left[ 12\omega_\lambda^2 + \sigma_\lambda(4 + 3\sigma_\lambda) + 2\omega_\lambda(5 + 6\sigma_\lambda) \right]. \quad (3.56)$$

Then, the separatrix will attract the trajectories of the phase map for models in which  $\mu_s > 0$  whereas for models with  $\mu_s < 0$  the trajectories will go away from  $x_s$ . Note that this is true for both sides of the separatrix.

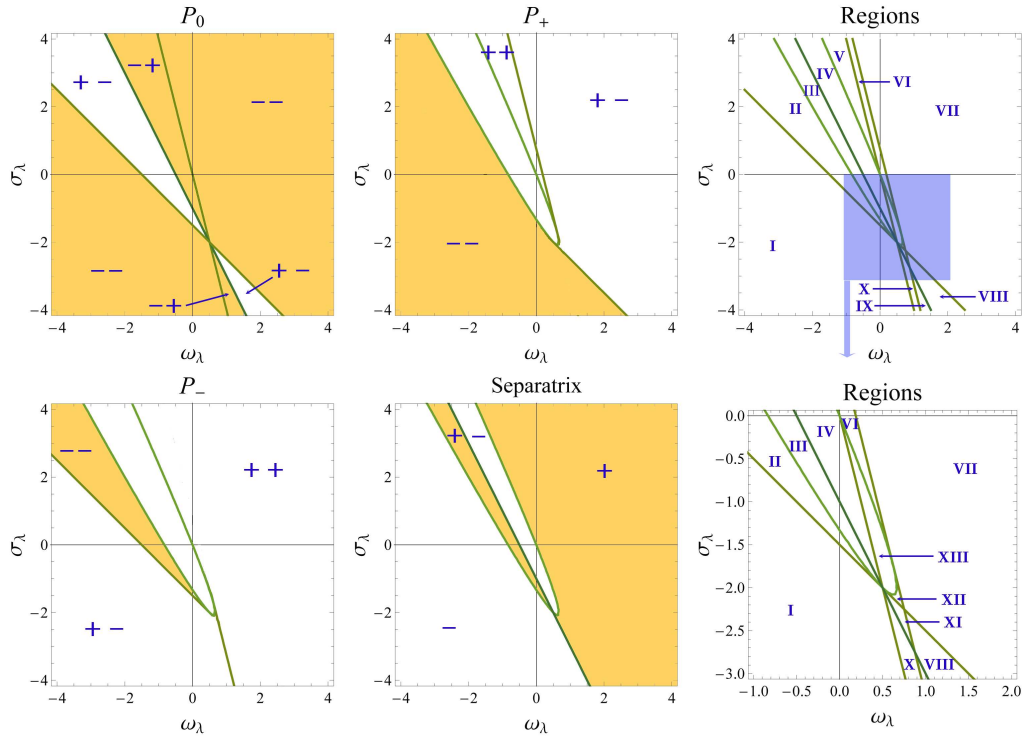


Figure 3.5: In this plot we show the different regions obtained in the parameter space according to the features of the critical points. We have shaded (in orange) the regions where the eigenvalue of  $x$  is negative so that the trajectories in the phase map approach the corresponding point. We have also indicated the sign of each eigenvalue in the form  $(\mu_x, \mu_H)$ . For the separatrix we indicate the regions where the trajectories approach the separatrix. Finally, the two plots on the right show the 13 regions explained in the text (and summarized in table 1). The last plot corresponds to a zoom of the blue-shaded region in the third panel.

- $x \rightarrow \pm\infty$ . In this case we have that  $\frac{dx}{dN} \sim -x^2$  so that the trajectories will always approach from  $+\infty$  and will move away to  $-\infty$ , i.e., the region with large values of  $x$  repels the trajectories of the phase map whereas the trajectories become attracted by the region with  $x \rightarrow -\infty$  irrespectively of the values of the parameters in the action. This means that the region with large positive values of  $x$  is always unstable for any choice of  $\omega_\lambda$  and  $\sigma_\lambda$  and, on the contrary, the region with negative large values of  $x$  is always stable.

Region	$P_0$	$P_-$	Separatrix	$P_+$
I	Attractor node	Saddle point $\mu_x > 0$	Repelling	Attractor node
II	Saddle point $\mu_x > 0$	Attractor node	Repelling	Attractor node
III	Saddle point $\mu_x > 0$	-	Attractor	-
IV	Saddle point $\mu_x < 0$	-	Repelling	-
V	Saddle point $\mu_x < 0$	Repelling node	Attractor	Repelling node
VI	Attractor node	Repelling node	Attractor	Repelling node
VII	Attractor node	Repelling node	Attractor	Saddle point $\mu_x > 0$
VIII	Saddle point $\mu_x > 0$	Repelling node	Attracting	Attractor node
IX	Saddle point $\mu_x < 0$	Repelling node	Repelling	Attractor node
X	Saddle point $\mu_x < 0$	Saddle point $\mu_x > 0$	Repelling	Attractor node
XI	Saddle point $\mu_x > 0$	Saddle point $\mu_x > 0$	Attractor	Attractor node
XII	Attractor node	Saddle point $\mu_x > 0$	Attractor	Saddle point $\mu_x > 0$
XIII	Attractor node	-	Repelling	-

Table 3.1: In this table we summarize the features of the phase map for the different regions shown in Fig. 3.5. When a given critical point is a saddle point we give the sign of the eigenvalue corresponding to  $x$  so that we can know whether the trajectories approach the critical point (negative eigenvalue) or move away from it (positive eigenvalue) along the  $x$ -direction.

### 3.4.1 Accelerating solutions

In this section we shall enumerate the necessary conditions for a vector-tensor model to lead to accelerating solutions. To that end we shall express the equation of state in terms of the field variable  $x$ :

$$w = \frac{-(4\omega_\lambda + 2\sigma_\lambda + 1)x^2 + (2\omega_\lambda - \sigma_\lambda - 3)[2x + 3(2\omega_\lambda + \sigma_\lambda + 1)]}{[x + 3(2\omega_\lambda + \sigma_\lambda + 1)]^2}. \quad (3.57)$$

Notice that this equation of state only depends on  $x$  and not on the Hubble parameter  $H$ . The models with accelerating solutions will be those in which  $w$  evolves towards  $w < -1/3$ . Moreover, as, in this Chapter, we are interested in finding models in which the vector field could play the role of dark energy, we shall demand that the accelerated phase is an attractor. To that end, we shall look at the equation of state for all the possible attracting places in the phase map as well as in the repelling ones. Notice that, as the equation of state does not depend on  $H$  but only on  $x$  we only need to require attractor or repelling properties with respect to  $x$ . For instance, if a critical point is a saddle point but with the trajectories going towards  $x \rightarrow x_{crit}$  ( $\mu_x < 0$ ) it will be considered as an attractor and the opposite for a repelling point. Now, we shall study the existence of accelerating regimes in the phase map:

- $P_0$ . As we pointed out above, this critical point will be an attractor in models with  $\mu_x < 0$ . On the other hand, the equation of state for this critical point is

$$w_{P_0} = \frac{2\omega_\lambda - \sigma_\lambda - 3}{3(2\omega_\lambda + \sigma_\lambda + 1)}. \quad (3.58)$$

From this expression we see that  $P_0$  corresponds to an accelerated phase ( $w_{P_0} < -1/3$ ) if the following condition holds:

$$\frac{2\omega_\lambda - 1}{2\omega_\lambda + \sigma_\lambda + 1} < 0, \quad (3.59)$$

which is satisfied for models in which either  $1 < 2\omega_\lambda < -(1 + \sigma_\lambda)$  or  $-(1 + \sigma_\lambda) < 2\omega_\lambda < 1$ . The corresponding region is shown in Fig. 3.6 and, in that figure, we see that there exists a region in which  $P_0$  is an attractor and gives rise to accelerated expansion simultaneously.

- $P_{\pm}$ . For these critical points, the equation of state becomes:

$$w_{P_{\pm}} = -(8\omega_{\lambda} + 4\sigma_{\lambda} + 3) \pm \frac{4}{3} \sqrt{6(5\omega_{\lambda} + 2\sigma_{\lambda}) + 9(2\omega_{\lambda} + \sigma_{\lambda})^2}. \quad (3.60)$$

Notice that if the condition of accelerated expansion is satisfied for  $P_+$ , then, it is also satisfied for  $P_-$  since  $w_{P_+} \geq w_{P_-}$ . The models that lead to accelerated expansion are shown in Fig. 3.6. However, in the same figure, we see that neither of the critical points  $P_{\pm}$  behaves as an attractor in the region where we get accelerated expansion.

- Separatrix  $x = x_s$ . In this case the equation of state will evolve either to  $+\infty$  or to  $-\infty$  as the trajectory approaches the separatrix. The interesting case here is when  $w \rightarrow -\infty$  so that we get acceleration. For  $x = x_s + \delta$  with  $\delta \rightarrow 0$ , the equation of state becomes:

$$w_s \simeq -\frac{2\mu_s}{3\delta^2}. \quad (3.61)$$

In Fig. 3.6 we show the region in which the equation of state goes to  $-\infty$ , corresponding to the condition  $\mu_s > 0$ . Notice that this condition also guarantees that the separatrix behaves as an attractor so all the cases in which the separatrix is an attractor give rise to accelerated expansion.

- $x \rightarrow \pm\infty$ . As we showed above,  $x = -\infty$  is always an attractor whereas  $x = +\infty$  is always a repelling point. Moreover, as  $x$  approaches  $\pm\infty$  the equation of state is given by:

$$w(x \rightarrow \pm\infty) = -(4\omega_{\lambda} + 2\sigma_{\lambda} + 1), \quad (3.62)$$

so that it gives rise to accelerated expansion in models with  $2\omega_{\lambda} + \sigma_{\lambda} > -1/3$ . This case is interesting for the vector field to drive an inflationary era because it could start with a large value of  $x$  and, as  $x = \infty$  repels the trajectories, it would be forced to evolve towards smaller values of  $x$  until it reaches either  $P_+$  or  $P_0$ . Moreover, such an evolution can lead to accelerated expansion as long as the condition  $2\omega_{\lambda} + \sigma_{\lambda} > -1/3$  holds.

After having obtained the general conditions necessary to have accelerated expansion, we shall study the particular solutions in which the scale factor evolves as a power of the cosmic time, i.e.,  $a \propto t^p$  and we shall get some analytical solutions. For this expansion law, the vector field evolves

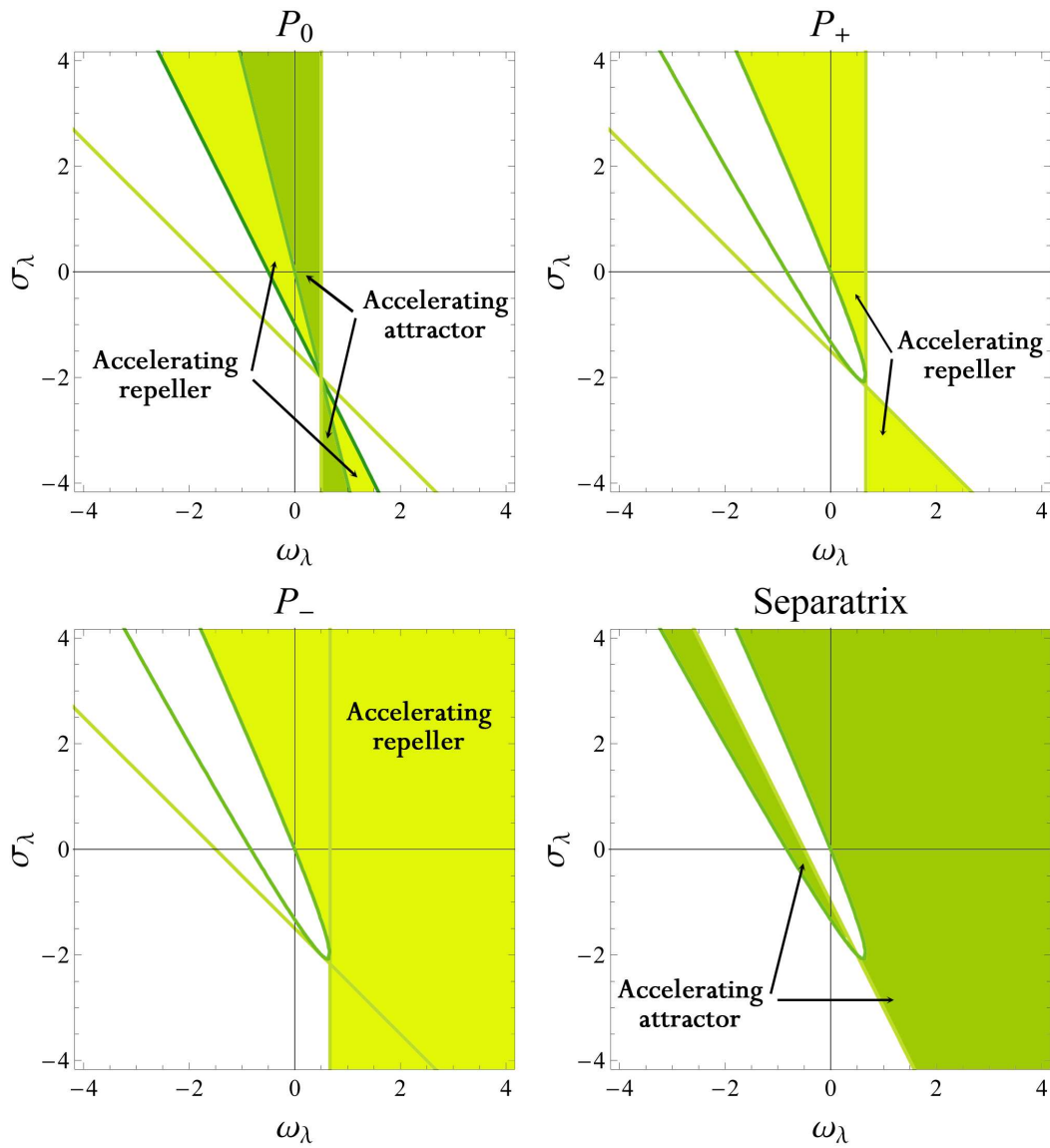


Figure 3.6: In this plot we show the regions in which we get accelerated solutions in a universe dominated by the vector field for each critical point. The darkest shaded regions are those in which the accelerated solutions are attractors. We can see that neither for  $P_+$  nor for  $P_-$  we can obtain attracting accelerated solutions.

according to (3.29), although, in this case, the parameter  $p$  must be determined from Einstein equations. When we introduce (3.29) in (3.45) we obtain that the vector field must take a constant value given by:

$$A_0^\infty = \frac{\pm 1}{\sqrt{8\pi G\lambda(3 + 2\omega_\lambda + 2\sigma_\lambda)}}. \quad (3.63)$$

Notice that this value only makes sense for  $\lambda(3 + 2\omega_\lambda + 2\sigma_\lambda) > 0$ , which can always be fulfilled by a suitable choice of the parameter  $\lambda$ . Moreover, we also obtain that  $p$  is given by:

$$p = \frac{1 + 2\omega_\lambda + \sigma_\lambda}{4\omega_\lambda + \sigma_\lambda}. \quad (3.64)$$

With this expression we can calculate the deceleration parameter:

$$q_\infty \equiv -\frac{\ddot{a}a}{\dot{a}^2} = \frac{2\omega_\lambda - 1}{2\omega_\lambda + \sigma_\lambda + 1}. \quad (3.65)$$

This deceleration parameter must be negative in order to have an accelerated expansion, but this is indeed the same condition that we found above in (3.59) when studying the critical point  $P_0$ . This was expected because the Hubble expansion rate goes to zero for a power law expansion and this imposes that  $A_0$  has to be constant which means that  $x = 0$ . Thus, we have just obtained nothing but the analytical solutions for the trajectories approaching  $P_0$  along the  $H$ -axis. Notice that this is, indeed, the only critical point attracting trajectories with accelerated expansion and having a finite value for the vector field equation of state.

### 3.5 Late-time accelerated solutions with matter

In previous sections we have studied a universe completely dominated by the vector field and obtained the necessary conditions to have accelerated solutions. In this section, however, we shall consider the case in which the universe contains matter in addition to the vector field and study the circumstances under which we can get a transition from a matter dominated universe to an accelerated phase provided by the vector field so that the vector field can play the role of dark energy. To do so, we shall proceed as in previous sections, i.e., we shall obtain the corresponding autonomous system and identify attracting solutions in which the vector

field eventually dominates the energy content of the universe and has equation of state smaller than  $-1/3$ .

Before going on with the study of the autonomous system, we remind that a necessary condition to have a candidate to dark energy is that the energy density associated to the vector field decays slower than that of a pressureless fluid in the matter dominated epoch. This requirement guarantees the dominance of the vector field at late times so that it can drive the expansion of the universe. According to Table 1, such models are those whose parameters satisfy the condition

$$2\omega_\lambda - \sigma_\lambda < 3. \quad (3.66)$$

We shall take this condition as a necessary requirement for the model to be able to play the role of dark energy.

The system of equations must be modified by introducing the matter contribution to the Friedman equation so that:

$$3H^2 = 8\pi G(\rho_{A_0} + \rho_M). \quad (3.67)$$

Moreover, we have a new equation provided by the energy conservation of the matter fluid:

$$\dot{\rho}_M + 3H\rho_M = 0 \quad (3.68)$$

As we did in the previous sections, we shall introduce the field variable  $x \equiv \frac{d \ln A_0}{d \ln a}$  and the matter energy density will be described by the density parameter  $\Omega_M \equiv \frac{\rho_M}{3H^2}$ . In terms of these variables, we can obtain the following autonomous system:

$$\begin{aligned} \frac{dH}{dN} &= \frac{F_H^1(x) + F_H^2(x)\Omega_M}{F_s(x)} H \\ \frac{dx}{dN} &= \frac{F_x^1(x) + F_x^2(x)\Omega_M}{F_s(x)} \\ \frac{d\Omega_M}{dN} &= \frac{F_{\Omega_M}(x)(1 - \Omega_M)\Omega_M}{F_s(x)} \end{aligned} \quad (3.69)$$

where we have defined:

$$\begin{aligned}
F_H^1(x) &= 3(2\omega_\lambda + \sigma_\lambda)x^2 - 6(4\omega_\lambda + \sigma_\lambda)x - 9(4\omega_\lambda + \sigma_\lambda)(2\omega_\lambda + \sigma_\lambda + 1), \\
F_H^2(x) &= -\frac{3}{2} \left[ (4\omega_\lambda + 2\sigma_\lambda + 1)x^2 - 2(2\omega_\lambda - \sigma_\lambda - 3)x \right. \\
&\quad \left. + 6(4\omega_\lambda + \sigma_\lambda)(2\omega_\lambda + \sigma_\lambda) + 9(2\omega_\lambda - 1) \right], \\
F_x^1(x) &= - \left[ x^2 + 6(2\omega_\lambda + \sigma_\lambda + 1)x + 3(2\omega_\lambda + 2\sigma_\lambda + 3) \right] \\
&\quad \times [x + 3(2\omega_\lambda + \sigma_\lambda + 1)] x, \\
F_x^2(x) &= \frac{3}{2} \left[ x^2 + 6(2\omega_\lambda + \sigma_\lambda + 1)x + 3(2\omega_\lambda + 2\sigma_\lambda + 3) \right] \\
&\quad [(4\omega_\lambda + 2\sigma_\lambda + 1)x - 2\omega_\lambda + \sigma_\lambda + 3], \\
F_{\Omega_M}(x) &= 3 \left[ (4\omega_\lambda + 2\sigma_\lambda + 1)x^2 - 2(2\omega_\lambda - \sigma_\lambda - 3)x \right. \\
&\quad \left. - 3(2\omega_\lambda + \sigma_\lambda + 1)(2\omega_\lambda - \sigma_\lambda - 3) \right], \\
F_s(x) &= [x + 3(2\omega_\lambda + \sigma_\lambda + 1)]^2 - \left[ 9(2\omega_\lambda + \sigma_\lambda)^2 + 6(5\omega_\lambda + 2\sigma_\lambda) \right] \Omega_M.
\end{aligned} \tag{3.70}$$

These equations are supplemented by the following constraint provided by the Friedman equation:

$$\frac{1}{3} \lambda A_0^2 \left[ x^2 + 6(2\omega_\lambda + \sigma_\lambda + 1)x + 3(2\omega_\lambda + 2\sigma_\lambda + 3) \right] + \Omega_M = 1. \tag{3.71}$$

As before, this relation will determine the sign of the parameter  $\lambda$  in order to fulfill the condition  $\lambda [x^2 + 6(2\omega_\lambda + \sigma_\lambda + 1)x + 3(2\omega_\lambda + 2\sigma_\lambda + 3)] > 0$ .

The equation of state for the vector field is given in this case by:

$$w = -\frac{1}{3} \frac{F_{\Omega_M}(x)}{F_s(x)}. \tag{3.72}$$

The sections  $\{x, \Omega_M\}$  of the phase map do not depend on  $H$ . Notice that, as expected, the equations for  $\frac{dH}{dN}$  and  $\frac{dx}{dN}$  reduce to (3.47) when  $\Omega_M = 0$  so that all the critical points analyzed in the previous sections are also critical points of (3.69) with  $\Omega_M = 0$ , which is the interesting

case here because this means that the vector fields eventually dominates the energy of the universe. Apart from these critical points with  $\Omega_M = 0$  we also have critical points with  $\Omega_M = 1$  which correspond to situations where matter drives the universe expansion. As we are interested in obtaining solutions leading to late-time accelerated expansion driven by the vector field, we shall study just the critical points with  $\Omega_M = 0$  so that the critical values of  $x$  and  $H$  are the same as those studied in the vector dominance case. However, the features of the critical points may change because of the presence of matter. Therefore, for each critical point, we shall identify the necessary conditions for the corresponding critical point to be an attractor with respect to  $\Omega_M$  and  $x$  and, then, compute the equation of state in the critical point. This is possible because the equations for  $\Omega_M$  and  $x$  does not depend on  $H$ . Notice that the condition for  $\Omega_M = 0$  to be an attractor will, in general, differ from the condition given in (3.66) obtained by imposing that the energy density of the vector field grows with respect to that of matter. This is so because to achieve that condition we assumed that the amount of matter was initially dominant with respect to that of the vector field and, however, for  $\Omega_M = 0$  to be an attractor, such a condition does not need to be satisfied. Finally, it is interesting to remark that the region with  $\Omega_M > 0$  is disconnected from that with  $\Omega_M < 0$  because the trajectories are always tangent to the plane  $\Omega_M = 0$  which ensures that the energy density of matter remains positive as long as it is initially positive. See Fig. 3.7 to have an idea of how the phase maps look like.

Let us analyze then each critical point for this case:

- $P_0 = (0,0)$ . For this critical point, the linearized system becomes:

$$\begin{aligned} \frac{dH}{dN} &\simeq -\frac{4\omega_\lambda + \sigma_\lambda}{2\omega_\lambda + \sigma_\lambda + 1}H \\ \frac{dx}{dN} &\simeq -\frac{2\omega_\lambda + 2\sigma_\lambda + 3}{2\omega_\lambda + \sigma_\lambda + 1} \left[ x + \frac{2\omega_\lambda - \sigma_\lambda - 3}{2(2\omega_\lambda + \sigma_\lambda + 1)}\Omega_M \right] \\ \frac{d\Omega_M}{dN} &\simeq \frac{2\omega_\lambda - \sigma_\lambda - 3}{2\omega_\lambda + \sigma_\lambda + 1}\Omega_M \end{aligned}$$

The eigenvalues for this system are the same as those of the vector dominance case plus  $\mu_{\Omega_M} = (2\omega_\lambda - \sigma_\lambda - 3)/(2\omega_\lambda + \sigma_\lambda + 1)$ , which determines the stability of the solutions with  $\Omega_M \rightarrow 0$ . Therefore, the analysis proceeds exactly the same as before with the supplementary condition  $\mu_{\Omega_M} < 0$  ensuring the late-time domination of

the vector field. Notice that, as commented above, this condition is not the same as that given in (3.66). Indeed, this supplementary condition happens not to reduce the region of the parameter space in which we get attracting solutions with accelerated expansion, i.e., all the models indicated in Fig. 3.6 corresponding to this type of solutions have indeed  $\Omega_M = 0$  as an attractor.

- $P_{\pm} = (x_{\pm}, 0)$ . In this case the linearized system becomes diagonal with the same eigenvalues for  $x$  and  $H$  as in the vector dominance case, i.e.,  $\mu_H = -(2x_c^{\pm} + 3)$  and  $\mu_x = -2x_c^{\pm}$ . Moreover, the eigenvalue for  $\Omega_M$  is given by  $\mu_{\Omega_M} = 4x_c^{\pm} + 3$ . Hence, as in the case of  $P_0$  the stability analysis is the same as that already performed above, although we must impose the condition  $4x_c^{\pm} + 3 < 0$  so that the vector field eventually dominates. However, when we impose the latter condition we find that these critical points happen not to be attractors for any value of the parameters.

So far, we have seen that the presence of a matter fluid only affects the solutions in the sense that the parameter space is restricted to that region in which  $\Omega_M = 0$  is an attractor, otherwise the vector field would never dominate and we cannot produce late-time acceleration. In other words,

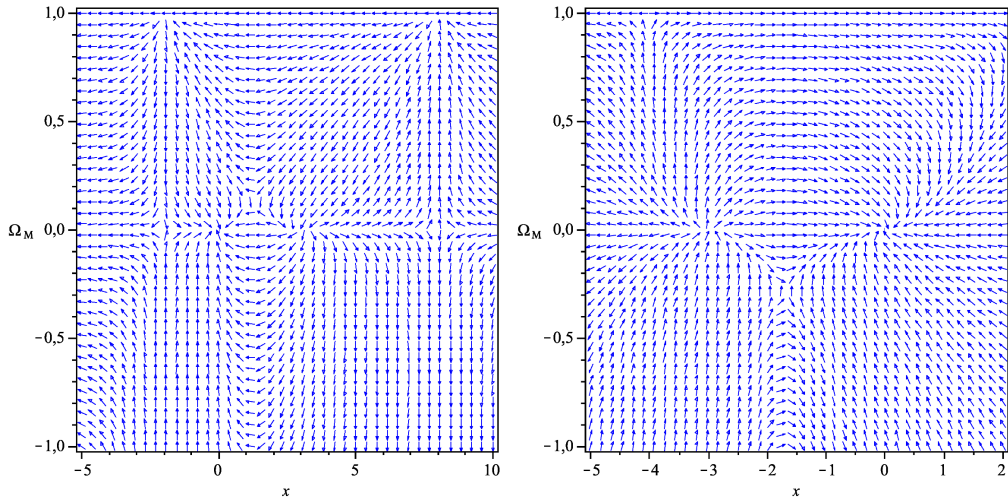


Figure 3.7: In these two plots we show two examples of phase maps corresponding to the cases when the two critical points are present (left) and when they are not (right), or, equivalently, when the separatrix is open from above or from below.

the features of the critical points remain the same as those studied in the vector domination case, although only the cases in the allowed region are admissible. The novelties appear when studying the separatrix:

- Separatrix. In this case the separatrix is no longer given by  $x = x_s$ , but by the parabola:

$$\Omega_M = \frac{[x + 3(2\omega_\lambda + \sigma_\lambda + 1)]^2}{[9(2\omega_\lambda + \sigma_\lambda)^2 + 6(5\omega_\lambda + 2\sigma_\lambda)]} \quad (3.73)$$

Notice that the vertex of this parabola always lies on the  $x$ -axis, i.e., in the vertex we always get  $\Omega_M = 0$  so that it will be interesting to have solutions attracted by it. Whether this parabola is open from above or below in the  $(x, \Omega_M)$  plane depends on the sign of  $9(2\omega_\lambda + \sigma_\lambda)^2 + 6(5\omega_\lambda + 2\sigma_\lambda)$  which also determines the existence of  $x_c^\pm$  so that if the critical points  $x_c^\pm$  exist the parabola goes up and if they do not exist the parabola goes down. Since negative values of  $\Omega_M$  are physically unreasonable, an open from below parabola does not represent a proper separatrix for the physically admissible region of the phase map.

Close to the vertex of the separatrix, i.e., for:

$$\Omega_M = \frac{[x + 3(2\omega_\lambda + \sigma_\lambda + 1)]^2}{[9(2\omega_\lambda + \sigma_\lambda)^2 + 6(5\omega_\lambda + 2\sigma_\lambda)]} + \delta_{\Omega_M} \quad (3.74)$$

$$x = -3(2\omega_\lambda + \sigma_\lambda + 1) + \delta_x \quad (3.75)$$

with  $\delta_{\Omega_M}, \delta_x \ll 1$  the autonomous system becomes:

$$\begin{aligned} \frac{dH}{dN} &\simeq 3 \frac{2\omega_\lambda + \sigma_\lambda + 1}{\delta_{\Omega_M}} H \\ \frac{dx}{dN} &\simeq 3(2\omega_\lambda + \sigma_\lambda + 1) \frac{\delta_x}{\delta_{\Omega_M}} \\ \frac{d\Omega_M}{dN} &\simeq 2 \frac{2\omega_\lambda + \sigma_\lambda + 1}{3(2\omega_\lambda + \sigma_\lambda)^2 + 2(5\omega_\lambda + 2\sigma_\lambda)} \frac{\delta_x^2}{\delta_{\Omega_M}} \end{aligned}$$

In the previous expressions,  $\delta_{\Omega_M}$  parametrizes the separation to the separatrix and is positive (negative) for points above (below) it, whereas  $\delta_x$  gives the separation on the right ( $\delta_x > 0$ ) or on the left ( $\delta_x < 0$ ) from the vertex of the parabola. From the equation for  $dH/dx$  we see that the trajectories will not be able to cross the vertex

because  $dH/dN$  becomes singular at that point. On the other hand, it is easy to see from the equations for  $dx/dN$  and  $d\Omega_M/dN$  that the vertex will always act as an attractor for the trajectories approaching from one side of the parabola so that, in the cases in which the parabola is open from above, there always exist trajectories that are attracted by the vertex of the separatrix. Whether the trajectories approaching the vertex are those going from above or below the parabola is determined by the sign of  $2\omega_\lambda + \sigma_\lambda + 1$  as follows:

- i)  $2\omega_\lambda + \sigma_\lambda + 1 > 0$ . In this case the trajectories approaching from below are attracted towards the vertex whereas those solution contained in the region above the separatrix are repelled by the vertex.
- ii)  $2\omega_\lambda + \sigma_\lambda + 1 < 0$ . In this case, the solutions in the region above the separatrix are attracted towards the vertex whereas the trajectories below the parabola go away from the vertex.

To study the cases when the parabola is open from below we shall analyze the autonomous systems for  $x + 3(2\omega_\lambda + \sigma_\lambda + 1) = \delta_x \ll 1$  and  $\Omega_M \ll 1$ . In that case we obtain

$$\begin{aligned}\frac{dx}{dN} &\simeq 3(2\omega_\lambda + \sigma_\lambda + 1)\frac{\delta_x}{\Omega_M} \\ \frac{d\Omega_M}{dN} &\simeq 6(2\omega_\lambda + \sigma_\lambda + 1)\end{aligned}\quad (3.76)$$

Thus, only if  $(2\omega_\lambda + \sigma_\lambda + 1) < 0$  the vertex of the separatrix is an attractor when the separatrix is contained in the region with  $\Omega_M < 0$ .

Finally, it remains to study the behavior of the equation of state as the trajectory approaches the vertex of the separatrix. If we use the parametrization given in (3.75) again, we obtain that the equation of state becomes:

$$w \simeq 2\frac{2\omega_\lambda + \sigma_\lambda + 1}{\delta_{\Omega_M}} \quad (3.77)$$

Therefore, if the trajectory approaches the vertex from above the separatrix, the equation of state will evolve towards  $+\infty$  ( $-\infty$ ) as long as  $2\omega_\lambda + \sigma_\lambda + 1$  is positive (negative). On the contrary, when the trajectory goes to the vertex from below the separatrix the equation of state of the vector field goes to  $+\infty$  ( $-\infty$ ) as long as  $2\omega_\lambda + \sigma_\lambda + 1$  is negative (positive).

Then, if the parabola is open from above ( $3(2\omega_\lambda + \sigma_\lambda)^2 + 2(5\omega_\lambda + 2\sigma_\lambda) > 0$ ), irrespective of the sign of  $2\omega_\lambda + \sigma_\lambda + 1$  we have that the vertex acts as an attractor for some trajectories with solutions whose equation of state goes to  $-\infty$ . On the other hand, when the parabola is open from below ( $3(2\omega_\lambda + \sigma_\lambda)^2 + 2(5\omega_\lambda + 2\sigma_\lambda) < 0$ ), only when  $2\omega_\lambda + \sigma_\lambda + 1$  is negative the vertex acts as an attractor and, in that

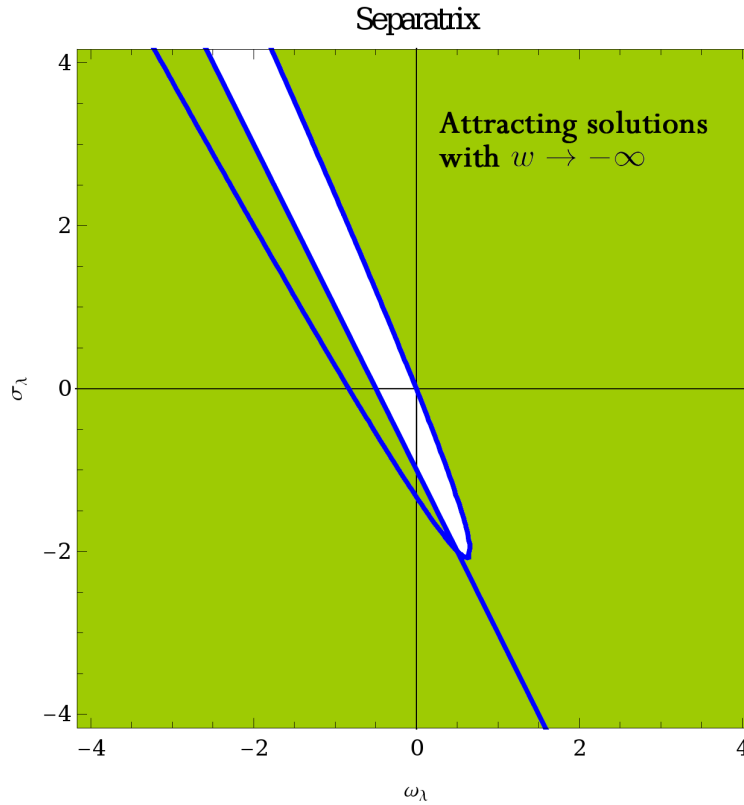


Figure 3.8: In this plot we show the regions where we have the vertex of the separatrix attracting trajectories with accelerated expansion (green shaded region) and where there are not solutions attracted by the vertex in which the expansion is accelerated (white region). We see that, in most of the parameter space, we have that the vertex attracts some trajectories in which the equation of state of the vector field diverges evolving towards  $-\infty$ . The curve plotted in the graph separates those models in which the separatrix is open from above (outer region) and those in which the separatrix is open from below (inner region). Notice that these regions coincide with those in which the critical points  $P_{\pm}$  exist (separatrix open from above) and they do not (separatrix open from below), as explained in the main text.

case, the equation of state in the vertex goes to  $-\infty$ .

Finally, we would like to comment on the existence of certain models in which we can have critical points with  $\Omega_M \neq 0, 1$ . Those critical points can be found from (3.69) by solving  $\frac{d\Omega_M}{dN} = 0$  with respect to  $x$  and for arbitrary values of  $\Omega_M$  and, then, obtain the corresponding critical value for  $\Omega_M$  from the equation  $\frac{dx}{dN} = 0$ . In these critical points, one generally gets  $H = 0$ . The explicit expressions for these critical points are:

$$\begin{aligned} x_{\Omega_M}^{\pm} &= \frac{2\omega_\lambda - \sigma_\lambda - 3 \pm \sqrt{2(2\omega_\lambda - \sigma_\lambda - 3) [2(5\omega_\lambda + 2\sigma_\lambda) + 3(2\omega_\lambda + \sigma_\lambda)^2]}}{4\omega_\lambda + 2\sigma_\lambda + 1} \\ \Omega_M^{\pm} &= -\frac{x_{\Omega_M}^{\pm} [x_{\Omega_M}^{\pm} + 3(2\omega_\lambda + \sigma_\lambda + 1)]}{F_x(x_{\Omega_M}^{\pm})} \end{aligned} \quad (3.78)$$

Therefore, only models in which

$$(2\omega_\lambda - \sigma_\lambda - 3) [2(5\omega_\lambda + 2\sigma_\lambda) + 3(2\omega_\lambda + \sigma_\lambda)^2] > 0 \quad (3.79)$$

can contain this type of critical points. Moreover, this condition does not guarantee the existence of physically admissible values for  $\Omega_M$  because one could, in principle, obtain both positive and negative values for  $\Omega_M$ . However, these critical points cannot lead to accelerated solutions because the equation of state for the vector field in such points is identically zero, i.e., it behaves as a dust fluid.

To summarize the results of this section, we have shown that the features of the critical points for the case when we have matter in addition to the vector field remain unaffected, but the behavior of the separatrix presents novelties and, generally, in all the models we shall have attracting solutions with future singularities. Finally, we have shown that solutions in which  $\Omega_M$  goes to some values different from 0 and 1 are such that the equation of state of the vector field goes to zero, i.e., it asymptotically behaves as a matter fluid.

## 3.6 Conclusions and discussion

In this Chapter we have developed a general study of the cosmological evolution of a vector field non-minimally coupled to gravity and without potential terms. We have given the evolution of this vector field in terms of the parameters of the theory for the different epochs of the expansion history of the universe, namely: inflation, radiation dominated era and matter dominated era. We have shown that it is possible to obtain a wide variety of behaviors for the evolution of the vector field by suitable choices of the parameters. In particular, we have obtained conditions for the parameters so that the vector field energy density grows or decays with respect to that of the dominant component. Moreover, conditions to have scaling evolution have also been calculated. The case of a universe dominated by the temporal component of the vector field has been studied in detail. We have obtained an autonomous system describing the evolution of the Hubble expansion rate and the vector field. The general features of the phase map have been given and all the critical points have been appropriately characterized. For those points that act as attractors we have obtained the general conditions under which the vector field gives rise to accelerated expansion.

To study the viability of these theories as dark energy candidates we have performed an analysis of the field equations together with Einstein's equations when the universe contains matter in addition to the vector field. Then, we have identified solutions which allow a transition from matter-domination to vector-domination with accelerated expansion. We have also shown that these models generally contain future singularities in which the equation of state diverges and that most of the models can give rise to periods of accelerated expansion.

In addition to the general results commented above, we have also found a wide variety of particular model examples with interesting properties, thus: models with late-time attractors with  $\Omega_M \neq 0, 1$  all of them with equation of state for the vector field resembling that of non-relativistic matter. This type of models could provide vector dark matter candidates. We have also found models with early time accelerated solutions which are unstable thus giving rise to possible finite inflationary periods. Two particular models as candidates to play the role of dark energy are of special interest. On one hand, the model with  $\sigma_\lambda = -2$  which has a scaling behavior during the radiation dominated era. The importance of this fact

is that it could avoid the need of unnatural initial conditions in the same way as those quintessence models with scaling evolution. On the other hand, the model with  $\omega = \sigma = 0$  behaves like a cosmological constant because its temporal component gives rise to a constant energy density throughout the expansion history of the universe. These two models will receive the deserved attention in the last Chapters of this thesis.

We would like to remark that, throughout this Chapter, we have focused on the viability of vector-tensor theories as candidates for dark energy just for the first stage, i.e., we have given the general conditions under which the homogeneous part of a vector-tensor theory can lead to late-time acceleration. However, to propose a serious candidate one should also study the perturbations of the corresponding model and check the presence of instabilities both at classical and quantum levels. The absence of classical instabilities is required in order not to have exponentially growing modes that could spoil the predictions of the model for the zero-mode. The issue of quantum instabilities has to do with the existence of modes with negative energy (ghosts) so that non-linear interactions of the field might produce an unlimited number of such particles. The existence of such instabilities for those vector-tensor theories which are indistinguishable from GR at small scales will be the goal of next Chapter by considering perturbations in both the vector field and the metric.

As a final comment, although we have focused on vector fields as candidates for dark energy, we would like to mention that, because of their generality, the results that we have obtained can also be used in other cosmological contexts in which vector fields could play a relevant role.

# Viability of vector-tensor theories of gravity

---

## 4.1 Introduction

The thorough classification of the cosmological evolution in general vector-tensor theories performed in the precedent Chapter has shown the existence of accelerated solutions for a wide range of the model parameters. However, the fact that the model contains solutions leading to an accelerated universe is only the first step when we want to construct a viable candidate for dark energy. After confirming the presence of accelerated solutions in the homogeneous regime, one has to face two sets of additional conditions which are compulsory in order to consider the model as a serious candidate, namely consistency with local gravity tests and absence of instabilities.

The viability of any alternative theory of gravity is subject to its agreement with Solar System experiments, which provide very tight constraints on the so-called Parameterized-Post Newtonian (PPN) parameters. These parameters are a set of quantities that characterize most of gravity theories at small scales and are extremely useful to measure deviations from GR. They have been measured with high precision by different experiments performed in the Solar System and the results are in excellent agreement with GR so that any alternative theory of gravity should lead to the same small scales limit as GR, or very tiny differences. In particular, the optimal case would be that the alternative theory had the same limit, i.e., the same set of PPN parameters as GR since, although theories with different PPN parameters could still satisfy the Solar System test, fine

tuning of the model parameter would likely be needed in those cases.

On the other hand, the presence of instabilities is a highly undesirable feature in any physical theory. The nature of such instabilities can be twofold [118, 119]:

- **Classical instabilities.** This sort of instabilities are caused by the existence of exponentially growing modes for the inhomogeneous part or the fields or, in other words, modes whose propagation speed is imaginary. A dark energy model having these modes is risky because the inhomogeneous perturbations of the model will be out of control and could eventually spoil all the nice properties obtained for the zero mode so that all the predictions obtained for the homogeneous case lack reliability.
- **Quantum instabilities.** These instabilities appear when we want to quantize the corresponding theory and are induced by the presence of modes with negative energy, which are usually called ghosts. The existence of these ghosts in the theory is very dangerous because it would allow the creation of an unlimited number of positive energy particles by emitting ghosts so that the vacuum of theory would be unstable [24]. Even though this problem arises mostly at the quantum level (which may be out of the scope of the dark energy model), it is important to note that it also poses a problem at the classical level because, in a theory containing ghosts, one might produce gravitational waves carrying positive energy by emitting dark energy waves with negative energy.

In addition to the problems raised in the previous paragraphs, we should also mention that some authors consider that the existence of superluminal modes could induce causality inconsistencies [120, 121], although this conclusion is far from clear [122] and even some authors claim that consistency requires the presence of such modes [119]. For this reason we shall omit this as a consistency condition, although it could be easily implemented at some point.

In order to continue with our program of studying general vector-tensor theories started in Chapter 3 for the homogeneous case, we shall study the small scales limit and the presence of stabilities in this Chapter. We shall present the PPN parameters for an arbitrary vector-tensor theory and use the current Solar System limits to obtain constraints on the amplitude of the vector field at Solar System scales. We should remark here

that such a value does not need to be the same as the cosmological one, as we shall explain. We have already said above that the optimal case for an alternative theory of gravity is such that the PPN parameters resemble those of GR. For this reason we shall obtain the particular vector-tensor theories which are indistinguishable from GR at small scales (having that way the same PPN parameters). After that, we shall study the existence of instabilities in such models, both classical and quantum. We should remark here that the study of the instabilities will be performed by looking at both metric and vector field perturbations around a Minkowski spacetime.

This Chapter comprises the results presented in the paper:

- *Viability of vector-tensor theories of gravity.* Jose Beltrán Jiménez and Antonio L. Maroto. JCAP **0902**:025 (2009).

## 4.2 Local gravity constraints

We shall start by reminding here the general action for a vector-tensor theory given in the previous Chapter:

$$S[g_{\mu\nu}, A_\mu] = \int d^4x \sqrt{-g} \left[ -\frac{1}{16\pi G} R + \omega R A_\mu A^\mu + \sigma R_{\mu\nu} A^\mu A^\nu + \lambda (\nabla_\mu A^\mu)^2 + \epsilon F_{\mu\nu} F^{\mu\nu} \right] \quad (4.1)$$

with  $\omega, \sigma, \lambda, \epsilon$  dimensionless parameters and  $F_{\mu\nu} = \partial_\mu A_\nu - \partial_\nu A_\mu$ . Notice that the term including the Ricci tensor can be rewritten as  $\nabla_\mu A^\mu \nabla_\nu A^\nu - \nabla_\mu A^\nu \nabla_\nu A^\mu$  and that these two terms do not appear independently in the most general action because they can be recasted in the terms written in (4.1) so that we obtain the alternative equivalent action given in (3.1). Moreover, the relations given in (3.3) will allow to translate very straightforwardly the results given in this Chapter to the alternative form of the action.

For the general vector-tensor theory described by the action (4.1), the PPN parameters are given by [116]:

$$\begin{aligned}
\gamma &= \frac{1 + 4\omega A^2 \left(1 + \frac{2\omega + \sigma}{\epsilon}\right)}{1 - 4\omega A^2 \left(1 - \frac{4\omega}{\epsilon}\right)} \\
\beta &= \frac{1}{4}(3 + \gamma) + \frac{1}{2}\Theta \left[1 + \frac{\gamma(\gamma - 2)}{G}\right] \\
\alpha_1 &= 4(1 - \gamma) [1 + 2\epsilon\Delta] + 16\omega A^2 \Delta a \\
\alpha_2 &= 3(1 - \gamma) \left[1 + \frac{4}{3}\epsilon\Delta\right] + 8\omega A^2 \Delta a - 2\frac{bA^2}{G} \\
\alpha_3 &= \xi = \zeta_1 = \zeta_2 = \zeta_3 = \zeta_4 = 0
\end{aligned} \tag{4.2}$$

with:

$$\begin{aligned}
\Theta &= \frac{(1 - 4\omega A^2)(2\epsilon + \sigma - 2\omega)}{(1 - 4\omega A^2)2\epsilon + 32\omega^2 A^2} \\
\Delta &= \frac{1}{2A^2\sigma^2 - 2\epsilon [1 - 4A^2(\omega + \sigma)]} \\
a &= 2\epsilon(1 - 3\gamma) + 2\sigma(1 - 2\gamma) \\
b &= \begin{cases} (2\omega + \sigma) [(2\gamma - 1)(\gamma + 1) + \Theta(\gamma - 2)] \\ - (2\gamma - 1)^2(2\omega + \sigma + \lambda) \left(1 - \frac{2\omega + \sigma + \lambda}{\lambda}\right) & \lambda \neq 0 \\ 0 & \lambda = 0 \end{cases}
\end{aligned}$$

Moreover, the effective Newton constant is defined as:

$$G_{eff} \equiv G \left[ \frac{1}{2}(\gamma + 1) + 6\omega A^2(\gamma - 1) - 2A^2\sigma(1 + \Theta) \right]^{-1}. \tag{4.3}$$

In the above expressions we have assumed  $G_{eff} = 1$  and  $A$  is the value of the vector field at Solar System scales (in units of  $1/\sqrt{4\pi G}$ ). The parameters  $(\gamma, \beta)$  are usually called the static PPN parameters and measure the space-curvature produced by a unit mass and the degree of nonlinearity relative to GR respectively. The parameter  $\xi$  measures effects of preferred location whereas  $\alpha_i$  have to do with preferred frame effects. Finally,  $\alpha_3$  and  $\zeta_i$  are non-vanishing for theories in which the conservation of total momentum is violated. In GR, the PPN parameters are such that  $\gamma - 1 = \beta - 1 = \alpha_1 = \alpha_2 = \alpha_3 = \xi = \zeta_1 = \zeta_2 = \zeta_3 = \zeta_4 = 0$ . On the other hand, for a general vector-tensor theory we see that there

are neither preferred location effects nor violation of the total momentum conservations. However, these theories typically lead to preferred frame effects (as expected because of the presence of a vector field) as well as deviations from GR for the static PPN parameters. Current observational limits on the PPN parameters impose very stringent limits on modified gravity theories because they do not allow much deviation from GR, i.e., GR agrees with local gravity tests with very good precision [116]:

$$\begin{aligned}
 \gamma - 1 &\lesssim 2.3 \times 10^{-5} \\
 \beta - 1 &\lesssim 2.3 \times 10^{-4} \\
 \alpha_1 &\lesssim 10^{-4} \\
 \alpha_2 &\lesssim 10^{-4} (10^{-7})
 \end{aligned} \tag{4.4}$$

In order to obtain constraints on the vector field from these limits we linearize the PPN parameters given in (4.2) as follows:

$$\begin{aligned}
 \gamma - 1 &\simeq \frac{4\omega}{\epsilon} [2(\epsilon - \omega) + \sigma] A^2 \\
 \beta - 1 &\simeq \frac{(2\omega - \sigma)(2\epsilon - 2\omega + \sigma)(4\epsilon - 2\omega + \sigma)}{4\epsilon^2} A^2 \\
 \alpha_1 &\simeq \frac{16\omega(2\epsilon + \sigma)}{\epsilon} A^2 \\
 \alpha_2 &\simeq \begin{cases} \left[ (2\omega + \sigma)^2 \left( \frac{1}{\epsilon} - \frac{2}{\lambda} \right) - 4\sigma \right] A^2 & \lambda \neq 0 \\ \frac{4\omega}{\epsilon} [2(\epsilon + \omega) + \sigma] A^2 & \lambda = 0 \end{cases}
 \end{aligned} \tag{4.5}$$

Therefore, we can set that, typically, the vector field at the Solar System scale will be constrained to be  $A \lesssim 10^{-2}$ , for models in which all the parameters are order unity. Let's remark that this value of the vector field does not need to coincide with its cosmological value.

On the other hand, the linearized Newton's constant is given by:

$$G \simeq 1 - \left[ \frac{(2\omega - \sigma)^2}{\epsilon} + 4(\sigma - \omega) \right] A^2 \tag{4.6}$$

Then, if we use the existing limits on its time-variation  $\dot{G}/G \lesssim 10^{-13} \text{yr}^{-1}$  [116] together with the constraints on the vector field obtained above, we can also set bounds on the cosmological time variation of the vector.

As commented before, since GR agrees with Solar System experiments with high precision, we shall obtain those vector-tensor theories with the

same set of PPN parameters as GR, i.e.  $\gamma = \beta = 1$  and  $\alpha_1 = \alpha_2 = 0$ . Notice that the rest of PPN parameters vanishes identically for models described by (4.1). When we impose that such parameters exactly agree with those of GR for any value of  $A$ , we obtain two sets of compatible models, according to their behavior in flat space-time, both with  $\omega = 0$ :

- Gauge non-invariant models. These models have  $\lambda \neq 0$  and the corresponding gauge-fixing term  $(\nabla_\mu A^\mu)^2$  breaks the  $U(1)$  general gauge invariance (although it preserves a residual gauge invariance) in Minkowski spacetime. The three possibilities we obtain in this case are: *i*)  $\sigma = -4\lambda = -4\epsilon$ , *ii*)  $\sigma = -3\lambda = -2\epsilon$ , *iii*)  $\sigma = 0$ .
- Gauge invariant models. In this case we have  $\lambda = 0$  and the only term remaining in Minkowski space-time is the gauge invariant one. The possibilities in this case are  $\sigma = m\epsilon$  with  $m = 0, -2, -4$ .

Notice that except for the  $\sigma = \lambda = 0$  case (which is nothing but GR plus Maxwell electromagnetism), all the considered cases break gauge invariance in general space-times. Therefore, there are six different classes of models which are indistinguishable from GR by means of Solar System experiments and, therefore, do not spoil the current bounds on the PPN parameters. To our knowledge best, none of these models (apart from Maxwell's theory) had been considered previously in the literature.

### 4.3 Classical and quantum stability

To study the existence of unstable classical modes and ghosts we shall perform perturbations around a Minkowski background. In addition, we will also consider perturbations around the constant background vector field  $A_\mu = (A, 0, 0, 0)$ . This is possible because Minkowski space-time is an admissible solution of the theory in the case in which the vector field takes a constant value, as that introduced above. For this constant background, the vector field breaks Lorentz invariance and we have a preferred frame defined as that in which the vector field has only temporal component. In this background we decompose the perturbations in Fourier modes and solve the equations for the corresponding amplitudes. That way, we obtain the dispersion relation, which provides us with the propagation speed of the modes, that is required to be real in order not to have exponentially growing perturbations. As we explained above, here

we shall not care about superluminal propagation of the modes, although it could be easily imposed at some point. Notice that although we are assuming constant background, in practice, this background could evolve on cosmological timescales.

On the other hand, we define the energy density for the modes as [104]:

$$\rho = \left\langle T_{00}^{(2)} - \frac{1}{8\pi G} G_{00}^{(2)} \right\rangle \quad (4.7)$$

where  $T_{\mu\nu}^{(2)}$  and  $G_{\mu\nu}^{(2)}$  are the energy-momentum tensor of the vector field and the Einstein tensor calculated up to quadratic terms in the perturbations and  $\langle \dots \rangle$  denotes an average over spatial regions. Then, we insert the solutions obtained for the perturbations into this expression and study under which conditions they are positive.

Notice also that the preferred frame respects the invariance under spatial rotations and therefore, in order to simplify the analysis we can perform the usual split of the perturbations into spin-0 (scalar), spin-1 (vector) and spin-2 (tensor). For simplicity, the longitudinal gauge has been chosen in the calculations below, although we have checked that the final results for the mode frequencies and energy densities defined in (4.7) do not depend on the gauge choice.

The scalar perturbations of the vector field can be written as  $S_\mu = (S_0, \vec{\nabla} S)$  and the perturbed metric in the longitudinal gauge is:

$$ds^2 = (1 + 2\phi)dt^2 - (1 - 2\psi)\delta_{ij}dx^i dx^j \quad (4.8)$$

For vector perturbations we have  $V_\mu = (0, \vec{v})$  and the metric is as follows:

$$ds^2 = dt^2 + 2\vec{F} \cdot d\vec{x}dt - \delta_{ij}dx^i dx^j \quad (4.9)$$

with  $\nabla \cdot \vec{v} = \nabla \cdot \vec{F} = 0$ . Although the vector field does not generate tensor perturbations, we still can have effects on the gravitational waves propagation by the presence of the background vector field as we shall see later. Let us first consider the scalar and vector perturbations.

### 4.3.1 Gauge non-invariant models

**Model I:**  $\sigma = -4\lambda = -4\epsilon$

In this model, the Fourier components of the gravitational potentials relate to those of the vector field as follows<sup>1</sup>:

$$\phi_k = \frac{2\epsilon A}{1 + 4\epsilon A^2} [S_{0k} - 3\dot{S}_k], \quad (4.10)$$

$$\psi_k = \frac{2\epsilon A}{1 + 4\epsilon A^2} [(1 - 16\epsilon A^2)\dot{S}_k + S_{0k}], \quad (4.11)$$

whereas  $S_{0k}$  and  $S_k$  are related to each other by means of:

$$S_{0k} = -\frac{1}{k^2(1 - 4\epsilon A^2)} \left[ 24\epsilon A^2 k^2 \frac{dS_k}{dt} + (1 + 4\epsilon A^2)(1 + 8\epsilon A^2)(1 + 32\epsilon A^2) \frac{d^3 S_k}{dt^3} \right]. \quad (4.12)$$

Thus, the problem is solved once we know the solution of  $S_k$ , which happens to satisfy the following fourth order equation:

$$\frac{d^4 S_k}{dt^4} + \frac{k^2}{(1 + 8\epsilon A^2)(1 + 32\epsilon A^2)} \left[ 2(1 + 20\epsilon A^2) \frac{d^2 S_k}{dt^2} + k^2 S_k \right] = 0. \quad (4.13)$$

This equation yields two independent modes:

$$S_k = C_1 e^{-i\omega_1 t} + C_2 e^{-i\omega_2 t}, \quad (4.14)$$

with their respective dispersion relations:

$$\omega_1^2 = \frac{k^2}{1 + 32\epsilon A^2}, \quad (4.15)$$

$$\omega_2^2 = \frac{k^2}{1 + 8\epsilon A^2}. \quad (4.16)$$

Then, in order to have stable solutions we need to satisfy the following condition:

$$-32\epsilon A^2 < 1 \quad (4.17)$$

because, in that case, both modes have real propagation speeds.

<sup>1</sup>Hereafter we will measure the field in units of  $1/\sqrt{4\pi G}$  as in the PPN parameters expressions.

On the other hand, the energy density evaluated over the solutions for each mode is given by:

$$\rho_{\omega_1}^{(s)} = -96\epsilon^2 A^2 k^4 \frac{(1 + 64\epsilon A^2)}{(1 - 32\epsilon A^2)^2} |C_1|^2 \quad (4.18)$$

$$\rho_{\omega_2}^{(s)} = 96\epsilon^2 A^2 k^4 \frac{(1 + 16\epsilon A^2)}{(1 + 4\epsilon A^2)^2} |C_2|^2. \quad (4.19)$$

These energies are both positive under the following constraint:

$$1 < -64\epsilon A^2 < 4. \quad (4.20)$$

Now, by combining (4.17) and (4.20) we find the following viability condition for the scalar modes:

$$1 < -64\epsilon A^2 < 2. \quad (4.21)$$

Concerning vector perturbations, we obtain the following relation between the amplitudes:

$$\vec{F}_k = \frac{8\epsilon A^2}{1 + 8\epsilon A^2} \vec{v}_k \quad (4.22)$$

and both evolve as plane waves with the following dispersion relation:

$$\omega^2 = \frac{k^2}{1 + 8\epsilon A^2} \quad (4.23)$$

which leads to the stability condition:

$$-8\epsilon A^2 < 1. \quad (4.24)$$

Finally, the energy density associated to the vector perturbations is given by:

$$\rho^{(v)} = -4\epsilon \frac{1 + 16\epsilon A^2}{(1 + 8\epsilon A^2)^2} k^2 |\vec{v}_{0k}|^2. \quad (4.25)$$

From this expression we see that  $\epsilon$  must be negative and we have to satisfy:

$$-16\epsilon A^2 < 1 \quad (4.26)$$

in order not to have vector modes with negative energy.

In this model, according to the definition given in (4.3),  $G = 1$  and the constraints on the variation of  $G$  do not set any limit on the possible variation of  $A$ .

**Model II:**  $\sigma = -3\lambda = -2\epsilon$

In this case,  $\phi$  and  $\psi$  are given in terms of the perturbation of the vector field as follows:

$$\phi_k = -\frac{3\lambda A}{1 + 3\lambda A^2} \dot{S}_k, \quad (4.27)$$

$$\psi_k = 3\lambda A \frac{1 + 6\lambda A}{1 + 3\lambda A^2} \dot{S}_k. \quad (4.28)$$

On the other hand, the perturbation  $S_{0k}$  can be expressed as:

$$S_{0k} = -\frac{1}{2k^2(1 + 3\lambda A^2)} \left[ (1 + 6\lambda A^2)(1 + 15\lambda A^2) \frac{d^3 S_k}{dt^3} - k^2(1 - 3\lambda A^2) \frac{dS_k}{dt} \right]. \quad (4.29)$$

Then, all the perturbations are given in terms of  $S_k$ , for which we can obtain the following fourth-order differential equation:

$$\frac{d^4 S_k}{dt^4} + 2k^2 \frac{1 + 3\lambda A^2}{(1 + 6\lambda A^2)(1 + 15\lambda A^2)} \left[ 2(1 + 9\lambda A^2) \frac{d^2 S_k}{dt^2} + k^2 S_k \right] = 0. \quad (4.30)$$

The solution of this equation is a superposition of two independent modes:

$$S_k = C_+ e^{-i\omega_+ t} + C_- e^{-i\omega_- t}, \quad (4.31)$$

with their respective dispersion relations:

$$\omega_{\pm}^2 = \frac{k^2}{(1 + 6\lambda A^2)(1 + 15\lambda A^2)} \left[ 1 + 12\lambda A^2 - 27\lambda^2 A^4 \pm 3|\lambda| A^2 \sqrt{(1 + 3\lambda A^2)(5 + 27\lambda A^2)} \right]. \quad (4.32)$$

Then, we have two modes with two different speeds of propagation which depend on  $\lambda A^2$  as it is shown in Fig. 4.1. The  $\omega_-$ -mode has real propagation speed for  $\lambda A^2 > -\frac{1}{6}$ , whereas for the  $\omega_+$ -mode to have real propagation speed we need to satisfy either  $\lambda A^2 > -\frac{1}{15}$  or  $\lambda A^2 < -\frac{1}{3}$ . Therefore, the necessary condition in order not to have instabilities is  $\lambda A^2 > -\frac{1}{15}$ . Finally, the degeneracy disappears for  $\lambda A^2 = 0$  when both propagation speeds are 1, recovering thus the usual result.

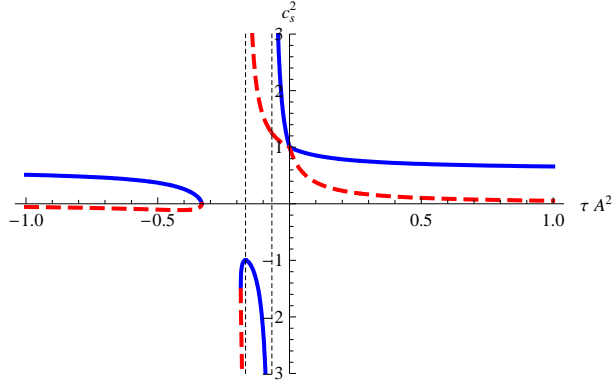


Figure 4.1: This plot shows the dependence of both modes propagation speeds on  $\lambda A^2$  for the model II: blue for  $\omega_+$  and dashed-red for  $\omega_-$ .

The energy density corresponding to each mode can be expressed as:

$$\rho_{\pm}^{(s)} = \lambda f_{\pm}(\lambda A^2) k^4 |C_{\pm}|^2, \quad (4.33)$$

where  $f_{\pm}(\lambda A^2)$  are the functions plotted in Fig. 4.2. Notice that  $f$  and  $\lambda$  must have the same sign for the energy density to be positive. We find the following condition in order to have positive energy density for both modes:

$$\lambda A^2 \in (-0.5, -0.383) \cup (-0.105, -0.033). \quad (4.34)$$

For this model, the vector perturbation on the metric relates to that of the vector field by means of:

$$\vec{F}_k = \frac{6\lambda A}{1 + 6\lambda A^2} \vec{v}_k, \quad (4.35)$$

which evolve as:

$$\vec{v}_k = \vec{v}_{0k} e^{-i\omega_v t}, \quad (4.36)$$

where  $\vec{v}_{0k} \cdot \vec{k} = 0$  and

$$\omega_v^2 = \frac{1 + 3\lambda A^2}{1 + 6\lambda A^2} k^2. \quad (4.37)$$

From this expression we obtain that for  $\lambda A^2 > -\frac{1}{6}$  the propagation speed is real.

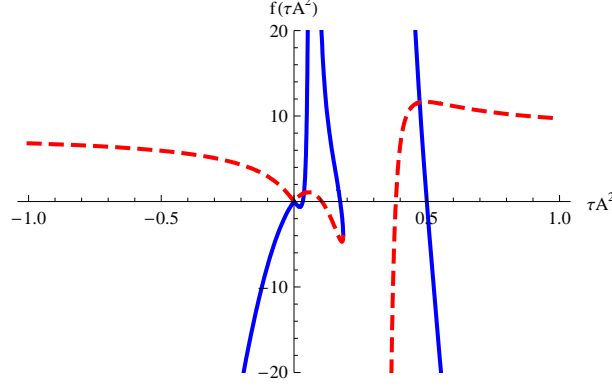


Figure 4.2: This plot shows the functions  $f_{\pm}(\lambda A^2)$  which determine the sign of the energy density for the scalar modes in the model II: blue for  $f_+$  and dashed-red for  $f_-$

The energy density corresponding to the vector perturbations is:

$$\rho^{(v)} = -6\lambda k^2 \frac{1 + 12\lambda A^2 + 18\lambda^2 A^4}{(1 + 6\lambda A^2)^2} |\vec{v}_{0k}|^2. \quad (4.38)$$

One can easily verify that this expression is positive if:

$$\lambda A^2 \in (-\infty, c_-] \cup [c_+, 0), \quad (4.39)$$

with  $c_{\pm} = -\frac{1}{3}(1 \mp \frac{1}{\sqrt{2}})$ . Note that  $\lambda < 0$  is a necessary condition and that the singular value  $\lambda A^2 = -\frac{1}{6}$  is not contained in the interval.

In this case,  $G = 1 - 6\lambda A^2$ . The present constraints on the variation of the Newton's constant will translate into a limit on the possible variation of  $A$  which will depend on the present cosmological value of  $A$ .

### Model III: $\sigma = 0$

The perturbations of this model propagate at the speed of light so there are no classically unstable modes. However, the scalar perturbations are not just plane waves, but they have also a growing mode:

$$\begin{aligned} S_{0k} &= [-ik\mu(D_0 + ikD)t + D_0] e^{-ikt}, \\ S_k &= [\mu(D_0 + ikD)t + D] e^{-ikt}, \end{aligned} \quad (4.40)$$

with

$$\mu = \frac{2\epsilon - \lambda - 8\lambda\epsilon A^2}{2\epsilon - 8\lambda\epsilon A^2}$$

In principle, this solution can give rise to both positive or negative energies depending on the value of the amplitudes. However, there exists a way to get this difficulty around which is motivated by the fact that the action corresponding to this model can be rewritten as that of Maxwell's electromagnetism in the Gupta-Bleuler formalism, that is:

$$S = \int d^4x \sqrt{-g} \left[ -\frac{1}{16\pi G} R - \frac{1}{4} F_{\mu\nu} F^{\mu\nu} + \frac{\xi}{2} (\nabla_\mu A^\mu)^2 \right]. \quad (4.41)$$

Notice that this action is the physically relevant action in the covariant formalism, since the energy of the modes and all the observables are calculated from (4.41) (see for instance [123]). In order to get rid of the negative energy modes, it is necessary to restrict the Hilbert space of the theory, by imposing the (Lorentz) condition  $\langle \phi | \partial_\mu A^\mu | \phi \rangle = 0$ , which determines the physical states  $|\phi\rangle$ . Indeed, this is equivalent to remove the growing mode i.e.  $D_0 = -ikD$  so that perturbations of the vector field propagate as pure plane waves. Then, using this condition we obtain that, as in the electromagnetic case, in the restricted Hilbert space, the energy of the scalar modes is identically zero. A detailed treatment of the quantization for this model will be performed in Chapter 6.

The solution of the vector perturbation of the vector field is:

$$\vec{v}_k = \vec{v}_{0k} e^{-ikt} \quad (4.42)$$

Moreover, the vector perturbation of the metric vanishes.

The energy density associated to the vector perturbations is:

$$\rho^{(v)} = -2\epsilon k^2 |\vec{v}_{0k}|^2 \quad (4.43)$$

which is positive if  $\epsilon < 0$ .

In this model we have again  $G = 1$  and no constraints on the variation of  $A$  can be established.

### 4.3.2 Gauge invariant models

Since the case  $m = 0$  is nothing but Einstein's gravity plus electromagnetism (which can be easily seen to satisfy all the viability conditions), we

shall focus just on the cases  $m = -2, -4$ . In such cases, we can obtain the following relations between the perturbations:

$$\begin{aligned}\dot{S}_k &= -\frac{1 - (m+3)m\epsilon A^2}{m\epsilon A(1 - 2m\epsilon A^2)}\psi_k, \\ S_{0k} &= -\frac{1 + m\epsilon A^2(3 + 2m^2\epsilon A^2)}{m\epsilon A(1 - 2m\epsilon A^2)}\psi_k, \\ \phi_k &= \psi_k + 2m\epsilon A\dot{S}_k.\end{aligned}\quad (4.44)$$

Therefore, all the perturbations can be immediately obtained once we know the solution of  $\psi_k$  which happens to evolve as:

$$\psi_k = C_k e^{-i\omega_s t}, \quad (4.45)$$

with:

$$\omega_s^2 = \frac{1}{3} \frac{3 - 2(4+m)m\epsilon A^2}{1 - 2m\epsilon A^2} k^2. \quad (4.46)$$

Then, the classical stability of these modes is guaranteed in the range:

$$\epsilon A^2 \in \left(-\infty, \frac{3}{2(4+m)m}\right) \cup \left(\frac{1}{2m}, \infty\right).$$

Notice that the first interval vanishes for the model with  $m = -4$ .

When we insert the corresponding solutions into the energy density we obtain:

$$\rho^{(s)} = \frac{3 - 4m\epsilon A^2(3 - (4+m)m\epsilon A^2)}{2\pi G(1 - 2m\epsilon A^2)} k^2 |C_k|^2. \quad (4.47)$$

This energy density is positive for:

$$\epsilon A^2 \in \left(a_-, \frac{1}{2m}\right) \cup \left(a_+, \infty\right), \quad (4.48)$$

with:

$$a_{\pm} = \frac{1}{2m \left(1 \pm \sqrt{-\frac{1+m}{3}}\right)}. \quad (4.49)$$

Notice that  $a_-$  is  $-\infty$  for the model  $m = -4$ .

On the other hand, the vector perturbations of the field evolve as plane waves  $\vec{v}_k = \vec{v}_{0k} e^{-i\omega_v t}$  with the following dispersion relation:

$$\omega_v^2 = \frac{1 - (2 + \frac{1}{2}m)m\epsilon A^2}{1 - 2m\epsilon A^2} k^2, \quad (4.50)$$

which imposes the condition:

$$\epsilon A^2 \in \left( -\infty, \frac{1}{(2 + \frac{1}{2}m)m} \right) \cup \left( \frac{1}{2m}, \infty \right)$$

in order to have real propagation speed. Notice that for  $m = -4$  the first interval vanishes.

Besides, the vector perturbation of the metric relates to  $\vec{v}$  by means of:

$$\vec{F}_k = -\frac{2m\epsilon A}{1 - 2m\epsilon A^2} \vec{v}_k. \quad (4.51)$$

These solutions for the vector perturbations lead to the following expression for the energy density:

$$\rho^{(v)} = -\epsilon \frac{1 - 4m\epsilon A^2 \left( 1 - (1 + \frac{1}{4}m)m\epsilon A^2 \right)}{(1 - 2m\epsilon A^2)} k^2 |\vec{v}_{0k}|^2 \quad (4.52)$$

The requirement for this energy to be positive is:

$$\epsilon A^2 \in \left( b_-, \frac{1}{2m} \right) \cup (b_+, 0), \quad (4.53)$$

where

$$b_{\pm} = \frac{1}{m(2 \pm \sqrt{-m})} \quad (4.54)$$

Note also that for  $m = -4$ ,  $b_-$  becomes  $-\infty$ .

In this case we get:  $G = 1 + \epsilon m(4 + m)A^2$ , so the only model with  $G \neq 1$  is that with  $m = -2$ .

## 4.4 Gravitational Waves

At first glance, one may think that as the vector field does not generate tensor modes at first order, gravitational waves will not be affected. However, the presence of a constant value of the vector field in the background can modify the speed of propagation of tensor perturbations. For the general vector-tensor action (4.1) with  $\omega = 0$  we have the following dispersion relation:

$$\omega_t^2 = \frac{k^2}{\sqrt{1 - 2\sigma A^2}} \quad (4.55)$$

	Model I	Model II	Model III	Gauge invariant models $m = -2, -4$
Classical stability	$-32\epsilon A^2 < 1$	$-15\lambda A^2 < 1$	Always	$\epsilon A^2 \notin \left[ \frac{1}{(2+\frac{1}{2}m)m}, \frac{1}{2m} \right]$
Gravitational waves	$-16\epsilon A^2 < 1$	$-12\lambda A^2 < 1$	Unaffected	$4m\epsilon A^2 < 1$
Quantum stability	$1 < -64\epsilon A^2 < 4$	$\lambda A^2 \in (-0.098, -0.033)$	$\partial_\mu A^\mu = 0$ and $\epsilon < 0$	$\epsilon A^2 \in (a_-, \frac{1}{2m}) \cup (b_+, 0)$
Viability condition	$1 < -64\epsilon A^2 < 2$	$\lambda A^2 \in (-\frac{1}{15}, -0.033)$	$\partial_\mu A^\mu = 0$ and $\epsilon < 0$	$\epsilon A^2 \in (b_+, \frac{1}{4m})$

Table 4.1: In this table we summarize the conditions obtained in order to have both classical and quantum stability for the models with the same set of PPN parameters as GR studied in this Chapter. The  $m = 0$  gauge invariant model satisfies all the viability conditions.

for both  $\oplus$  and  $\otimes$  polarizations. Therefore, the speed of gravitational waves is modified in the presence of the vector field, recovering the usual value for  $A = 0$ . Thus, if  $2\sigma A^2 < 1$  we do not have unstable modes. In particular, the constraint  $\sigma \leq 0$  is a sufficient condition (although not necessary) which is independent of the background vector field.

On the other hand, the energy density associated to the tensor perturbations is also modified by the presence of the background vector field:

$$\rho^{(t)} = \frac{k^2}{32\pi G} \frac{1 - 4\sigma A^2}{1 - 2\sigma A^2} (|C_\oplus|^2 + |C_\otimes|^2) \quad (4.56)$$

where  $C_\oplus, C_\otimes$  are the amplitudes of the corresponding graviton polarizations.

Then, in order not to have modes with negative energy density we need either  $2\sigma A^2 > 1$  or  $4\sigma A^2 < 1$ . These conditions combined with the classical stability condition lead to the constraint  $4\sigma A^2 < 1$ . For models I and II this condition reads  $-16\epsilon A^2 < 1$  and  $-12\lambda A^2 < 1$  respectively. On the other hand, Model III has  $\sigma = 0$  so gravitational waves are unaffected. Finally, for the gauge invariant models we obtain  $\epsilon A^2 < \frac{1}{4m}$ .

## 4.5 Conclusions and discussion

In this Chapter we have given the PPN parameters for a general vector-tensor theory and used the current limits from Solar System experiments to obtain constraints on the model parameters value of the vector field at small scales. However, the small scales amplitude obtained for the vector field from Solar System tests does not apply for the corresponding cosmological value. In fact, to relate both values one should give the physical mechanism that originated the vector field so that one can calculate the primordial power spectrum that would yield the amplitude for the vector field at any scale and, thus, one could compare the predictions coming from the theory and the amplitude given by the Solar System tests. On the other hand, we have obtained those vector-tensor theories whose PPN parameters are exactly the same as those of GR for any value of the background vector field  $A$  so that one cannot distinguish between both theories just by small scales experiments. We have found that there are only six models satisfying this condition that can be classified in two groups attending to its symmetries in flat spacetime.

For those models with the same set of PPN parameters as GR we have analyzed the presence of both classical and quantum instabilities by considering perturbations in both the metric and the vector field. Then, we have split the perturbations into scalar, vector and tensor parts and the conditions for the stability of each sector have been given and summarized in Table 4.4. We have found that only two models satisfy all the consistency conditions, namely Maxwell theory and Maxwell theory supplemented with a gauge-fixing term. The former was already known to be a viable theory, whereas the latter is especially interesting in a cosmological context because, as commented in Chapter 3, this theory gives rise to a cosmological constant-like contribution to Friedmann equation so that it can play the role of dark energy. For this reason, this particular model will be exhaustively studied in the last Chapter of this thesis. Here, we will only remark the fact that such a theory looks exactly like the starting action in the quantization of the electromagnetic field in the covariant formalism. Indeed, this will motivate us to identify this field with the electromagnetic field as a dark energy candidate.

To end this Chapter we will comment on the fact that we have focused on the stability of the those models with the same set of PPN parameters as GR, but this does not exclude the possibility of having other stable

vector-tensor theories. However, these theories will be subject to the constraints (4.4) for the amplitude of the vector field on Solar System scales, although this is not an extremely serious problem if the primordial power spectrum is red-tilted or the sub-Hubble modes are suppressed for some reason.

# Cosmic Vector for dark energy

---

## 5.1 Introduction

In this Chapter we shall present a particular vector-tensor model in which the vector field can play the role of dark energy. However, our aim is not merely to propose a new dark energy candidate to add to the already existing plethora of possible explanations for the accelerated expansion of the Universe, but to go a step further and contributing a possible solution to the coincidence problem affecting most of the dark energy models proposed to date. For this purpose, the detailed treatment of the cosmological evolution carried out in Chapter 3 for a general vector-tensor theory turns out to be extremely useful because we only need to specify the desired properties for the behavior of the vector field and then choose the action parameters accordingly. Naturally, we will be left with, at least, one free parameter related to the normalization of the field so that we shall be able to fix it by means of a normalization choice. Since we are concerned about solving the coincidence problem, we shall require the model to have scaling properties during the radiation dominated epoch so that (hopefully) we do not need to introduce unnatural initial conditions in the same fashion as in the usual scaling quintessence models explained in the first Chapter. To that end, we only need to look at Fig. 3.1 to realize that such a model corresponds to  $\sigma_\lambda = -2$ . The parameter  $\omega$  remains undetermined by the scaling behavior requirement because the scalar curvature  $R$  vanishes in a radiation-dominated universe so that the  $\omega$ -term in the action, being proportional to  $R$ , cannot affect the scaling property of the vector field in such an epoch. However, we can appeal to the small scales behavior of the theory in order to fix  $\omega$  because, as we can see from the PPN parameters given in (4.2), the condition  $\omega = 0$

guarantees that the static PPN parameters  $\gamma$  and  $\beta$  are the same as those of GR. Naturally, this model will have preferred frame effects, encoded in a non-vanishing value of  $\alpha_2$ , so that the amplitude of the vector field at small scales will be constrained by Solar System experiments.

The fact that the vector field behaves as a radiation fluid at early times is a desired property for the model not to be sensitive to the initial conditions. However, this does not guarantee the absence of either fine-tunings or unnatural initial conditions for the vector field. Moreover, after the equality time when the Universe starts being dominated by the matter fluid, the energy density of the vector field will change its evolution and the new evolution should enable the vector field to be able to dominate the Universe at late times, i.e its energy density should grow with respect to the matter contribution. We shall show that this is indeed the case for the parameters choice (in particular for  $\omega = 0$ ) so that the vector field can actually play the role of dark energy.

Although we shall be mostly focused on the study of the homogeneous cosmology of the model, we cannot forget the viability requirements concerning both the small scales behavior and the presence of instabilities that we have discussed in the previous Chapter. Notice that, since the PPN parameters of this model differ from those of GR, it does not fit in the analysis performed in Chapter 3 and a particular investigation is required. From the very construction of the model we already know that it will lead to some preferred frame effects that will be constrained by Solar System experiments. However, this could pose a problem in the case in which the field amplitude on Solar System scales turns out to be too large.

Finally, we shall eventually confront the model to observations to check how well it works in explaining the cosmological observations. This is what we shall be doing in the last part of the Chapter by using geometrical tests to constrain the cosmological parameters of the model. It is interesting to note that the model will have the same number of parameters as the standard  $\Lambda$ CDM model because we have fixed all the parameters in the action so that there is no much room to play, at least not more than in  $\Lambda$ CDM.

This Chapter is based on the following works:

- *Cosmic vector for dark energy: constraints from supernovae, cosmic microwave background and baryon acoustic oscillations.*  
Jose Beltrán Jiménez, Ruth Lazkoz and Antonio L. Maroto.  
*Physical Review D* **D80**, 023004 (2009).
- *Cosmic vector for dark energy.*  
Jose Beltrán Jiménez and Antonio L. Maroto.  
*Physical Review D* **D78**, 063005 (2008).

## 5.2 Vector Dark energy

As we have already explained in the Introduction, the vector-tensor theory giving rise to a scaling behavior during the radiation dominated era reads:

$$S = \int d^4x \sqrt{-g} \left[ -\frac{R}{16\pi G} - \frac{1}{4} F_{\mu\nu} F^{\mu\nu} - \frac{1}{2} (\nabla_\mu A^\mu)^2 + R_{\mu\nu} A^\mu A^\nu \right]. \quad (5.1)$$

Notice that the theory contains no free parameters, the only dimensional scale being Newton constant and the numerical factors in front of the vector kinetic terms can be fixed by the field normalization. It is interesting to note that a modification in the factor in front of the Maxwell-like  $F_{\mu\nu} F^{\mu\nu}$  term does not modify the homogeneous evolution of the temporal component so that one could, in principle, modify it without spoiling the predictions for the homogeneous evolution. Moreover, we can see that the vector sector of the theory corresponds to a vector field supplemented with a gauge-fixing term in the Feynman gauge and a direct coupling to the Ricci tensor which acts as an effective matrix mass term for the vector field. The alternative way of writing the action is as follows:

$$S = \int d^4x \sqrt{-g} \left[ -\frac{R}{16\pi G} - \frac{1}{2} \nabla_\mu A_\nu \nabla^\mu A^\nu + \frac{1}{2} R_{\mu\nu} A^\mu A^\nu \right], \quad (5.2)$$

where, as we said above, we can safely add a Maxwell term  $F^2$  without modifying the homogeneous cosmology of the model. Indeed, this freedom could be helpful at some point when going through the inhomogeneous perturbations.

The classical equations of motion derived from the action in (5.1) are

the Einstein and vector field equations given by:

$$R_{\mu\nu} - \frac{1}{2}Rg_{\mu\nu} = 8\pi G(T_{\mu\nu} + T_{\mu\nu}^A), \quad (5.3)$$

$$\square A_\mu + R_{\mu\nu}A^\nu = 0, \quad (5.4)$$

where  $T_{\mu\nu}$  is the conserved energy-momentum tensor for matter and radiation (or other possible components present in the Universe) and  $T_{\mu\nu}^A$  is the energy-momentum tensor coming from the vector field sector and whose expression can be found in (3.5). Since we want the vector field to play the role of dark energy, we shall proceed to study the homogeneous cosmology of the model. Moreover, the highly isotropic CMB that we observe today with anisotropies only at  $10^{-5}$  level<sup>1</sup> motivates us to neglect possible contributions from the spatial components of the vector field. Naturally, we should (and shall) eventually check the consistency of such an assumption. With the mentioned requirements, the vector field takes the form  $A_\mu = (A_0(t), 0, 0, 0)$  so that, even though it is a vector field, we are left with only one degree of freedom (at the background level). Finally and for simplicity we shall consider the spatially flat case and leave the non-flat case for a later study. For the FLRW metric (5.4) reads:

$$\ddot{A}_0 + 3H\dot{A}_0 - 3 \left[ 2H^2 + \dot{H} \right] A_0 = 0, \quad (5.5)$$

where, as always,  $H = \dot{a}/a$  is the Hubble parameter. Assuming that the Universe has gone through radiation and matter phases in which the contribution from dark energy was negligible, we can easily solve these equations in those periods just taking  $H = p/t$ , with  $p = 1/2$  for radiation and  $p = 2/3$  for matter eras respectively, which is equivalent to assume that  $a \propto t^p$ . In that case, the general solution of the above equation has a growing and a decaying mode:

$$A_0(t) = A_0^+ t^{\alpha_+} + A_0^- t^{\alpha_-}, \quad (5.6)$$

with  $A_0^\pm$  constants of integration and  $\alpha_\pm = -(1 \pm 1)/4$  in the radiation era, and  $\alpha_\pm = (-3 \pm \sqrt{33})/6$  in the matter era.

On the other hand, the Friedmann equation reads:

$$H^2 = \frac{8\pi G}{3} \left[ \sum_\alpha \rho_\alpha + \rho_A \right], \quad (5.7)$$

<sup>1</sup>Leaving aside the  $10^{-3}$  dipole contribution which is usually ascribed to our relative motion with respect to the CMB photons and that has been thoroughly discussed in Chapter 2.

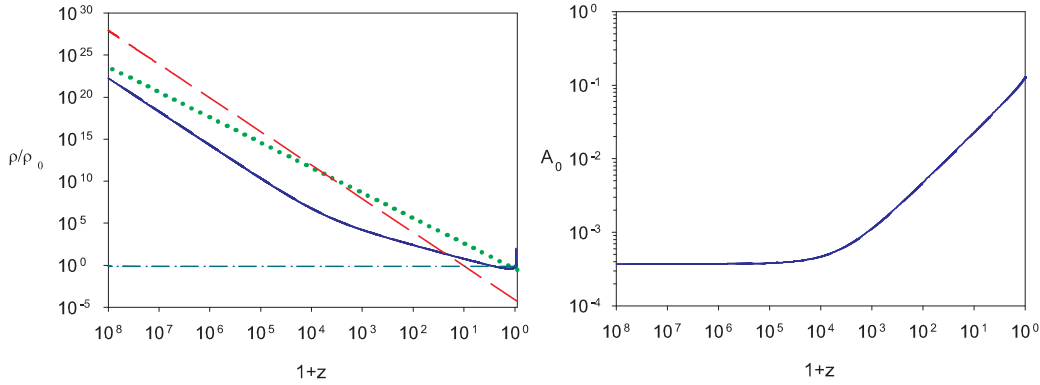


Figure 5.1: Left panel: evolution of energy densities. Dashed (red) for radiation, dotted (green) for matter and solid (blue) for vector dark energy. We also show for comparison the cosmological constant energy density in dashed-dotted line. We see the rapid growth of dark energy contribution at late times approaching the final singularity. Right panel: cosmological evolution of the vector field. In these two plots we see the unimportance of the time at which we set the initial conditions due to the fact that both the vector field and the fraction of dark energy density are constant in the early Universe.

with  $\alpha = M, R$  and:

$$\rho_A = \frac{3}{2}H^2 A_0^2 + 3HA_0\dot{A}_0 - \frac{1}{2}\dot{A}_0^2 \quad (5.8)$$

the energy density associated to the vector field. Using the growing mode solution in (5.6) we obtain:

$$\rho_A = \rho_{A0} a^\kappa, \quad (5.9)$$

with  $\kappa = -4$  in the radiation era and  $\kappa = (\sqrt{33} - 9)/2 \simeq -1.63$  in the matter era. Thus, the energy density of the vector field starts scaling as radiation at early times (as we had required), so that  $\rho_A/\rho_R = \text{const}$ . However, when the Universe enters its matter era,  $\rho_A$  starts growing relative to  $\rho_M$  eventually overcoming it at some point, in which the dark energy vector field would become the dominant component. From that point on, we cannot obtain analytic solutions to the field equations. In Fig. 5.1 we show the numerical solution to the exact equations, which confirms our analytical estimates in the radiation and matter eras. Notice that, since  $A_0$  is essentially constant during radiation era, the solutions

do not depend on the precise time at which we specify the initial conditions as long as we set them well inside the radiation epoch. Thus, once the present value of the Hubble parameter  $H_0$  and the constant  $A_0$  during radiation (which fixes the total matter density  $\Omega_M$ ) are specified, the model is completely determined. In other words, this model contains the same number of parameters as  $\Lambda$ CDM, i.e. the minimum number of parameters of any cosmological model with dark energy. On the other hand, as seen from Fig. 5.1 the evolution of the Universe ends at a finite time  $t_{end}$  with a singularity in which  $a \rightarrow a_{end}$  with  $a_{end}$  finite,  $\rho_{DE} \rightarrow \infty$  and  $p_{DE} \rightarrow -\infty$ . This corresponds to a Type III (Big Freeze) singularity according to the classification in [124].

We can also calculate the effective equation of state for dark energy as:

$$w_{DE} = \frac{p_A}{\rho_A} = \frac{-3 \left( \frac{5}{2} H^2 + \frac{4}{3} \dot{H} \right) A_0^2 + H A_0 \dot{A}_0 - \frac{3}{2} \dot{A}_0^2}{\frac{3}{2} H^2 A_0^2 + 3 H A_0 \dot{A}_0 - \frac{1}{2} \dot{A}_0^2}. \quad (5.10)$$

Again, using the approximate solutions in (5.6), we obtain;

$$w_{DE} = \begin{cases} \frac{1}{3} & \text{radiation era} \\ \frac{3\sqrt{33}-13}{\sqrt{33}-15} \simeq -0.457 & \text{matter era} \end{cases} \quad (5.11)$$

After dark energy starts dominating, the equation of state abruptly falls towards  $w_{DE} \rightarrow -\infty$  as the Universe approaches  $t_{end}$ . As shown in Fig. 5.2 the equation of state can cross the so-called phantom divide line, so that we can have  $w_{DE}(z=0) < -1$ .

Our next step will be to confront the predictions of the model with observations of high-redshift type Ia supernovae. At this moment we only want to check the consistency of the model with the cosmological observations<sup>2</sup> and compute the scale for the constant value of the field during the radiation era as well as the required initial fraction of dark energy inferred from observations. These findings will enable us to discuss whether the model actually suffers from either fine-tunings or naturalness problems. In order to do that, we shall calculate the distance modulus  $\mu(z)$  as a function of redshift. Then, comparing  $\mu_{th}(z)$  with its observational value in a given data set will enable us to carry out a  $\chi^2$  statistical analysis. For this purpose, we have considered two sets of supernovae: the Gold set [125], containing 157 points with  $z < 1.7$ , and the

<sup>2</sup>A more detailed analysis by considering spatial curvature and a more extended data set comprising observations from SNIa, CMB and BAO will be performed in Section

independent SNLS data set [126], comprising 115 supernovae but with lower redshifts ( $z < 1$ ).

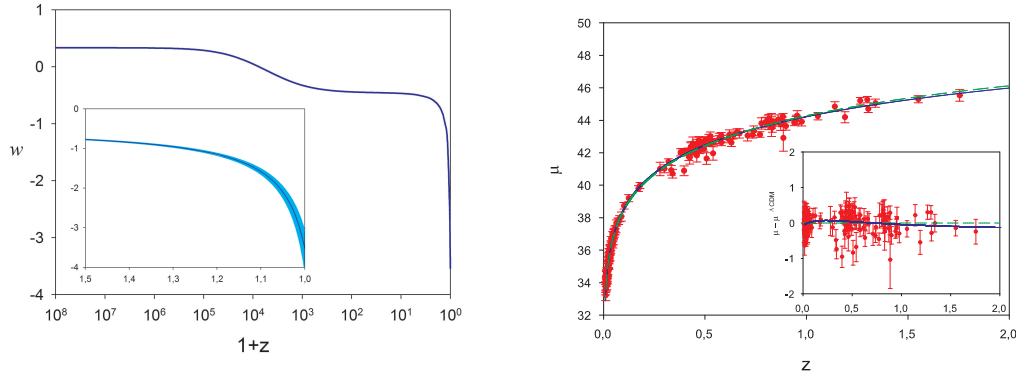


Figure 5.2: Left Panel: Evolution of dark energy equation of state for the best fit model. The lower panel shows the  $1\sigma$  confidence interval. Right panel: Distance modulus vs. redshift. The experimental data corresponds to the Gold data set. The continuous (blue) line corresponds to the best fit for the vector model. The dashed (green) line is the prediction for the  $\Lambda$ CDM model. The inner panel shows the difference in distance modulus from the pure cosmological constant case.

In Table 5.1 we show the results for the best fit together with its corresponding  $1\sigma$  intervals for the two data sets. We also show for comparison the results for a standard  $\Lambda$ CDM model. We see that the vector model (VCDM) fits the data considerably better than  $\Lambda$ CDM (at more than  $2\sigma$ ) in the Gold set, whereas the situation is reversed in the SNLS set. This is just a reflection of the well-known  $2\sigma$  tension [127] between the two data sets. The best fit parameters for the VCDM model are identical for the two data sets with small differences in the confidence intervals. Compared with  $\Lambda$ CDM, we see that VCDM favors a younger Universe (in  $H_0^{-1}$  units) with larger matter density. In addition, the deceleration-acceleration transition takes place at a lower redshift in the VCDM case. Another important difference arises in the present value of the equation of state with  $w_0 = -3.53^{+0.46}_{-0.57}$  which clearly excludes the cosmological constant value  $-1$ .

We have also compared with other parameterizations for the dark energy equation of state. Thus, for instance, taking  $w_{DE}(z) = w_0 + w_1 z(1+z)^{-1}$  [128, 129], we find  $\chi^2 = 173.5$  for the Gold set. Since this is a three-parameter fit, in order to compare with the one-parameter fits of VCDM or  $\Lambda$ CDM, we use the reduced chi-squared:  $\chi^2/d.o.f = 1.108$  for VCDM,

	VCDM Gold	$\Lambda$ CDM Gold	VCDM SNLS	$\Lambda$ CDM SNLS
$\Omega_M$	$0.388^{+0.023}_{-0.024}$	$0.309^{+0.039}_{-0.037}$	$0.388^{+0.022}_{-0.020}$	$0.263^{+0.038}_{-0.036}$
$w_0$	$-3.53^{+0.46}_{-0.57}$	-1	$-3.53^{+0.44}_{-0.48}$	-1
$A_0$ ( $10^{-4} M_P$ )	$3.71^{+0.022}_{-0.026}$	—	$3.71^{+0.020}_{-0.024}$	—
$z_T$	$0.265^{+0.011}_{-0.012}$	$0.648^{+0.101}_{-0.095}$	$0.265^{+0.010}_{-0.012}$	$0.776^{+0.120}_{-0.108}$
$t_0$ ( $H_0^{-1}$ )	$0.926^{+0.026}_{-0.023}$	$0.956^{+0.035}_{-0.032}$	$0.926^{+0.022}_{-0.022}$	$1.000^{+0.041}_{-0.037}$
$t_{end}$ ( $H_0^{-1}$ )	$0.976^{+0.018}_{-0.014}$	—	$0.976^{+0.015}_{-0.013}$	—
$\chi^2_{min}$	172.9	177.1	115.8	111.0

Table 5.1: Best fit parameters with  $1\sigma$  intervals for the vector model (VCDM) and the cosmological constant model ( $\Lambda$ CDM) for the Gold (157 SNe) and SNLS (115 SNe) data sets.  $w_0$  denotes the present equation of state of dark energy.  $A_0$  is the constant value of the vector field component during radiation.  $z_T$  is the deceleration-acceleration transition redshift.  $t_0$  is the age of the Universe in units of the present Hubble time.  $t_{end}$  is the duration of the Universe in the same units.

$\chi^2/d.o.f = 1.127$  for the  $(w_0, w_1)$  parametrization and  $\chi^2/d.o.f = 1.135$  for  $\Lambda$ CDM. As a matter of fact, to our knowledge best, VCDM provides the best fit to date for the Gold data set, since the oscillatory four-parameter model previously reported in [130] still has  $\chi^2/d.o.f = 1.115$ .

The evolution of dark energy for the best-fit model is plotted in Fig. 5.1. We see that unlike the cosmological constant case, throughout the radiation era  $\rho_{DE}/\rho_R \sim 10^{-6}$ . Notice that although the onset of cosmic acceleration depends on the value of  $A_0$  during that era, for the best-fit we have  $A_0 = 3.71 \times 10^{-4} M_P$ , which is relatively close to the Planck scale and could arise naturally in the early Universe without the need of introducing extremely small parameters. Hence, we see that this model can actually help alleviating the coincidence problem present in most dark energy models because it does not require the introduction of unnatural scales. We should remind here that this was not guaranteed from the very beginning, even though we *designed* the model to have scaling properties during the early Universe, because the required initial condition for the vector field in order to fit the observations could have happened to be unnaturally small.

### 5.3 Phase Map

We can gain some understanding on the properties of the model by looking at the corresponding phase map, which is nothing but a particular case of the general study performed in Chapter 3. The associated autonomous system for this model is given by:

$$\begin{aligned} \frac{dH}{dN} &= -\frac{34(x^2 - 2x + 3) - (3x^2 - 2x + 15)\Omega_M}{2(x-3)^2 - 12\Omega_M} \\ \frac{dx}{dH} &= -\frac{1(x^2 - 6x - 3)[2x^2 - 6x + 3(3x - 1)\Omega_M]}{2(x-3)^2 - 12\Omega_M} \\ \frac{d\Omega_M}{dN} &= 3\frac{3x^2 - 2x + 3}{(x-3)^2 - 12\Omega_M}\Omega_M(1 - \Omega_M) \end{aligned} \quad (5.12)$$

with  $x \equiv \frac{A_0}{HA_0}$  and  $N \equiv \ln a$ . We can see that this model, having  $\sigma_\lambda = -2$  and  $\omega_\lambda = 0$ , lies in the shaded region of Fig. 3.3 so that its phase map has the two critical points  $x_c^\pm$  and they are different. By looking at Fig. 3.5 we realize that this model corresponds to the class I according to the classification of Table 3.1 so that  $P_0$  and  $P_+$  are attractor nodes,  $P_-$  is

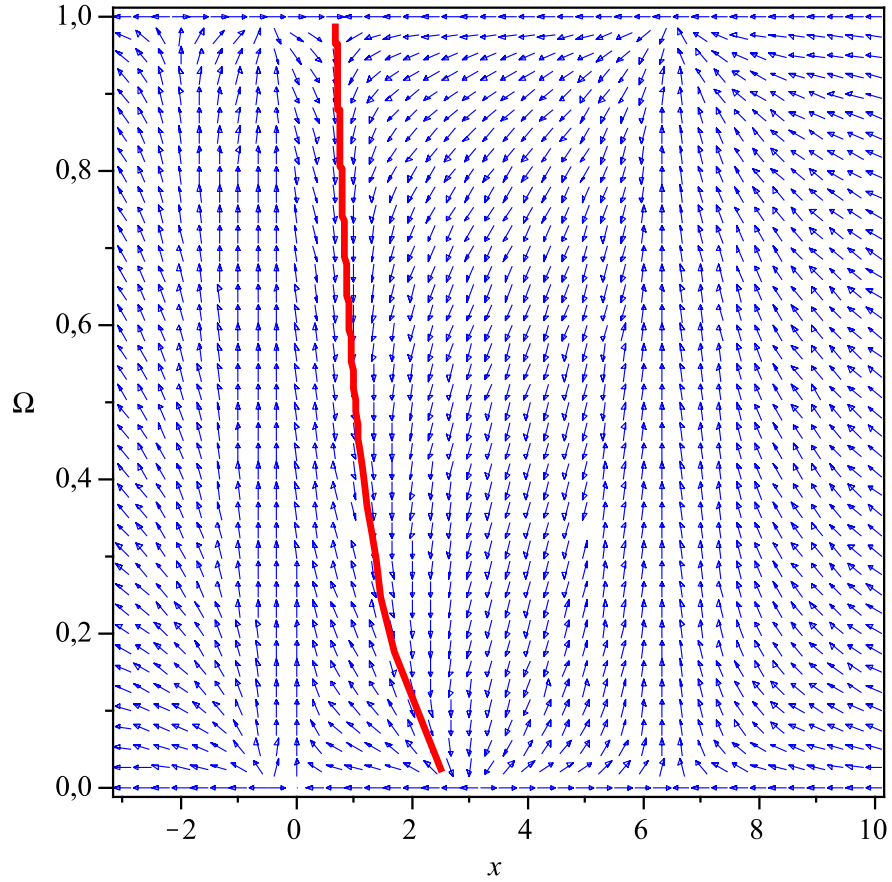


Figure 5.3: In this plot we show the phase map of the autonomous system associated to this model. The red line represents the realistic trajectory with  $x = 3$  and  $\Omega_M \simeq 1$  explained in the main text. We can see that such a solution evolves towards the vertex of the separatrix.

a saddle point with  $\mu_x > 0$  and the separatrix has repelling properties. This latter circumstance seems to contradict our findings of the previous Section because we have seen that the cosmological evolution leads to a future singularity corresponding to a solution approaching the separatrix, but this repels the trajectories. However, we have to remember that the mentioned classification was performed in the case of vector dominance and we need to consider the effects of introducing a matter component in which case, as we showed in Chapter 3, most of the models lead to future singularities with  $w \rightarrow -\infty$  as the one that we have found for the present model (see Fig. 3.8). However, although we know that there are

trajectories attracted by the vertex of the separatrix we need to ensure that our initial conditions are such that the corresponding trajectory gets attracted by the separatrix. To see this, we first have to note that the separatrix is given by the equation  $\Omega_M = \frac{1}{12}(x-3)^2$  and, in particular, the vertex corresponds to  $x = 3$  and  $\Omega_M = 0$ . Since the vector field evolves in the matter dominated era as  $A_0 \propto t^{\alpha_+}$  as shown in (5.6) we have that  $x = 3/2\alpha_+ \simeq 0.67$  in such an epoch. However, for  $x \simeq 0.67$  we have that the separatrix goes by  $\Omega_M \simeq 0.45$  so that the points corresponding to realistic initial condition with  $x \simeq 0.67$  and  $\Omega_M \simeq 1$  belong to the region above the separatrix whose trajectories, as we can see from Fig. 5.3, are attracted towards the vertex, in agreement with our previous result.

On the other hand, we can calculate the value that the vector field takes in the singularity by considering the Friedmann equation (5.7), which can be written close to the singularity (where we can safely neglect the matter contribution) and in terms of the variable  $x$  as:

$$1 = \frac{8\pi G}{3} A_0^2 \left( \frac{3}{2} + 3x - \frac{1}{2}x^2 \right). \quad (5.13)$$

Hence, since  $x = 3$  in the singularity we have that  $(1 - 16\pi G A_{0,end}^2) = 0$ , i.e.,  $A_{0,end}^2 = (16\pi G)^{-1}$ . We shall see later that this is indeed the value of the background vector field for which the inhomogeneous perturbations become unstable.

## 5.4 Anisotropic evolution

So far we have only considered the temporal component of the vector field to analyze the homogeneous cosmology of the model. However, the presence of spatial components could, in principle, have adverse effects because it could give rise to extremely large anisotropies that could be in conflict with CMB data. For this reason, in the following we shall study the evolution of the spatial components. Without loss of generality we shall take the spatial component lying along the  $z$ -axis. Then, the equation of motion for such a component is:

$$\ddot{A}_z + H\dot{A}_z - 2(\dot{H} + 3H^2)A_z = 0 \quad (5.14)$$

whose general solution for a power law expansion with  $H = p/t$  is:

$$A_z(t) = A_z^+ t^{2p} + A_z^- t^{1-3p}. \quad (5.15)$$

Therefore, in a radiation dominated Universe ( $p=1/2$ ) we have that  $A_z$  grows proportionally to the cosmic time, whereas in the matter era ( $p=2/3$ ) it grows as  $t^{4/3}$ . On the other hand, the energy density corresponding to the spatial component is given by:

$$\rho_{A_z} = \frac{1}{2a^2} \left( 4H^2 A_z^2 - 4HA_z \dot{A}_z + \dot{A}_z^2 \right). \quad (5.16)$$

When we insert the full solution (5.15) into the expression for the energy density we find:

$$\rho_{A_z} = \frac{(A_z^-)^2}{2a^8} \left( 25p^2 - 10p + 1 \right). \quad (5.17)$$

The remarkable result is that the energy density of the spatial component depends only on the decaying mode and, in addition, it decays as  $a^{-8}$  irrespectively of the particular expansion rate. Hence, even though the spatial component grows faster than the temporal component, the physically relevant quantity, i.e., the energy density, is dominated by the contribution coming from the temporal component since  $\rho_{A_z}/\rho_{A_0} \propto a^{-(\kappa+8)}$ . In particular, we have that  $\rho_{A_z}/\rho_{A_0} \propto a^{-4}$  in the radiation era and  $\rho_{A_z}/\rho_{A_0} \propto a^{-6.37}$ , so the contribution of the spatial components to the energy density can be safely neglected.

Another effect that can arise from the spatial components of the vector field is the generation of anisotropies. Such effect is originated by the presence of stresses in the energy-momentum tensor so we shall study the corresponding evolution of such stresses in order to quantify their importance. One can naively estimate whether they will be important by studying the evolution of the quantity  $(p_{\parallel} - p_{\perp})/\rho_{A_0}$ , with  $p_{\parallel}$  the pressure along the direction of the spatial component ( $z$ -axis) and  $p_{\perp}$  is the pressure along the perpendicular direction ( $xy$ -plane). The difference of pressures is given by:

$$p_{\parallel} - p_{\perp} = \frac{3}{a^2} \left( 4H^2 A_z^2 - 4HA_z \dot{A}_z + \dot{A}_z^2 \right) \quad (5.18)$$

and we see that  $p_{\parallel} - p_{\perp} = 6\rho_{A_z}$  so, according to the discussion concerning the energy density of the spatial components, this difference of pressures will be strongly suppressed as well. This fact can also be seen from the expression given in the general analysis of Chapter 3 for the degree of anisotropy. Indeed, if we calculate the degree of anisotropy given by (3.14) we find that  $h \propto t^{2-8p}$  so that it decays as  $t^{-2}$  and  $t^{-10/3}$  in the radiation

and matter eras respectively, what confirms our previous estimate. This is again a consequence of the fact that the growing mode of  $A_z$  does not contribute to the energy-momentum components.

To summarize, we have found that the potential problems that may arise when considering spatial components of the vector field are not such because the total energy density is essentially given by the contribution coming from the temporal component, being  $\rho_{A_z}$  negligible, and the possible anisotropies related to the presence of those spatial components decay as the Universe expands. Therefore, the results given in the previous Sections by considering only temporal components of the vector field are perfectly reliable.

## 5.5 Stability and consistency

In order to study the model stability we have to consider the evolution of metric and vector field perturbations and follow the procedure described in Chapter 4. That way, we shall consider a Minkowski background for the metric and a constant temporal component for the vector field  $A^3$  and study the evolution of inhomogeneous perturbations in this background.

For the scalar modes of the perturbations we can find the following relation between the gravitational potentials and the vector field perturbations from Einstein equations:

$$\begin{aligned}\psi &= \phi - 16\pi G A S_0, \\ \phi &= 4\pi G A \frac{3\dot{S} - S_0}{1 - 8\pi G A^2}.\end{aligned}\tag{5.19}$$

On the other hand, by inserting these relations in the vector field equations of motion we obtain the evolution equations for the Fourier modes of the vector field perturbations.

$$\begin{aligned}\ddot{S}_{0k} + \frac{k^2}{1 - 16\pi G A^2} S_{0k} &= 0, \\ \ddot{S}_k + \frac{k^2}{1 - 16\pi G A^2} S_k &= 0.\end{aligned}\tag{5.20}$$

---

<sup>3</sup>This background value could indeed evolve on cosmological timescales as we already said in Chapter 4.

Then, we have two independent propagating scalar modes sharing the same dispersion relation given by:

$$\omega_s^2 = \frac{1}{1 - 16\pi GA^2} k^2, \quad (5.21)$$

which guarantees the classical stability of the scalar modes as long as  $1 - 16\pi GA^2 > 0$ .

Concerning the vector modes, we find the following expression for the metric perturbations in terms of the vector field perturbation:

$$\vec{F} = -\frac{16\pi GA}{1 - 16\pi GA^2} \vec{v}. \quad (5.22)$$

When we insert these relations into the vector field equation for the Fourier modes we obtain:

$$\ddot{\vec{v}}_k + \frac{k^2}{1 - 16\pi GA^2} \vec{v}_k = 0. \quad (5.23)$$

We see that the dispersion relation is exactly the same as that found for the scalar modes, i.e.

$$\omega_v^2 = \frac{1}{1 - 16\pi GA^2} k^2. \quad (5.24)$$

so the vector modes are also stable until the singularity is reached.

Finally, the gravitational waves becomes modified only through the coupling of the spin-2 perturbations to the background vector field. Moreover, we can directly use the result found in Chapter 4 because it was valid for any vector-tensor theory. According to that result, we obtain the following dispersion relation for the gravitational modes:

$$\omega_t^2 = \frac{1}{1 - 16\pi GA^2} k^2, \quad (5.25)$$

so that, once again, the stability breakdowns only in the final singularity.

By combining the classical stability analysis for all the modes we find that, as we had already anticipated in the study of the phase map of the model, all the perturbations remain stable right until the final singularity of the homogeneous evolutions. This, indeed, establish a link between singularities appearing in the homogeneous cosmological evolution of the model and instabilities showing up in the inhomogeneous case.

The quantum stability of the model is more difficult to accomplish. For the scalar modes, one may try to take advantage of the presence of two independent modes in order to get rid of the ghosts by a suitable definition of the physical Hilbert space. However, for the vector perturbations, we have that the energy density of such modes is given by:

$$\rho_v = \frac{1 - 32\pi GA^2}{(1 - 16\pi GA^2)^2} k^2 |\vec{v}_{0k}|^2. \quad (5.26)$$

This energy becomes negative when the vector field takes a value half of its value at the final singularity so that the quantum stability breakdowns before the classical stability does. Although, in principle, this would presumably mean a serious flaw that the model should face, we should remind here that this model is intended as a dark energy candidate and, as such, only the classical evolution on very large scales is really relevant. A fully consistent quantization of this model as well as an extension to comprise smaller scales could need an UV completion that may cure this problems. However, we have not found such a completion yet.

Now we will study the evolution of the scalar perturbations of the vector field during radiation and matter dominated eras. The perturbation of the metric in the longitudinal gauge can be written in conformal time as follows:

$$ds^2 = a^2(\eta) \left[ (1 + 2\phi(\eta, \mathbf{x})) d\eta - (1 - 2\psi(\eta, \mathbf{x})) d\mathbf{x}^2 \right] \quad (5.27)$$

Besides, when the Universe is radiation or matter-dominated both scalar metric perturbations are the same, i.e.  $\phi = \psi$ . As we are considering only the temporal component of the vector field the background will be given by  $\mathcal{A}_\mu = (\mathcal{A}_0(\eta), 0, 0, 0)$  with  $\mathcal{A}_0 = aA_0$ . Moreover, the perturbed field can be written as  $\delta\mathcal{A}_\mu = (\delta\mathcal{A}_0(\eta, \mathbf{x}), \nabla\delta\mathcal{A}(\eta, \mathbf{x}))$ . Thus, the equations of the perturbations read:

$$\begin{aligned} \delta\mathcal{A}_0'' - \nabla^2\delta\mathcal{A}_0 - 4 \left( \mathcal{H}^2 + \mathcal{H}' \right) \delta\mathcal{A}_0 &= -2\mathcal{H}\nabla^2\delta\mathcal{A} + 6\mathcal{A}_0'\phi' \\ &\quad - 2 \left[ \phi'' + \nabla^2\phi + 8\mathcal{H}\phi' \right] \mathcal{A}_0, \\ \delta\mathcal{A}'' - \nabla^2\delta\mathcal{A} - 2 \left( 2\mathcal{H}^2 + \mathcal{H}' \right) \delta\mathcal{A} &= -2\mathcal{H}\delta\mathcal{A}_0 + 2\phi\mathcal{A}_0'. \end{aligned} \quad (5.28)$$

On the other hand, the perturbation on the energy density of the vector

field is given by:

$$\begin{aligned}
8\pi G\delta\rho_A = & -32\pi G\phi\rho_A - \frac{1}{a^4} \left[ 2 \left( 2\mathcal{H}\phi' - \nabla^2\phi \right) \mathcal{A}_0^2 \right. \\
& + \left( 2\mathcal{A}_0\phi' - 4\mathcal{H}\delta\mathcal{A}_0 - \nabla^2\delta\mathcal{A} + \delta\mathcal{A}'_0 \right) \mathcal{A}'_0 \\
& \left. + \left( 4\mathcal{H}^2\delta\mathcal{A}_0 - 4\mathcal{H}\delta\mathcal{A}'_0 + \nabla^2\delta\mathcal{A}' + \nabla^2\delta\mathcal{A}_0 + 2\mathcal{H}\nabla^2\delta\mathcal{A} \right) \mathcal{A}_0 \right]. \quad (5.29)
\end{aligned}$$

Since we know that the metric perturbation in the radiation era is given by[131]:

$$\phi_k = \frac{C_{1k}[\omega\eta \cos(\omega\eta) - \sin(\omega\eta)] + C_{2k}[\omega\eta \sin(\omega\eta) + \cos(\omega\eta)]}{\eta^3} \quad (5.30)$$

with  $\omega = k/\sqrt{3}$  and it is constant in the matter era, we can compute the perturbations on the vector field generated during such epochs. Then, we can introduce the solutions into (5.29) and obtain the evolution of the energy density contrast for the vector field  $\delta_A = \frac{\delta\rho_A}{\rho_A}$ . By solving numerically the equations of the perturbations with the corresponding expressions for the metric perturbations we obtain the results shown in Fig. 5.4. In that figure, we see that the super-Hubble modes of the density contrast remain constant, whereas the sub-Hubble modes oscillate with an amplitude growing as  $a^2$  in the radiation era and as  $a^{0.3}$  in the matter era. Therefore again, we do not find exponentially growing modes throughout the expansion history of the Universe. Moreover, the growing behavior of the vector field perturbations on sub-Hubble scales may enhance the growth of matter perturbations.

To end this Section we shall comment on the fact that, even though the proposed model can be considered only as an effective description of dark energy on cosmological scales, extending the applicability range to smaller scales requires consistency with local gravity tests. From the general expressions given in Chapter 4 for the PPN parameters, we can see that, in the present case, the static PPN parameters agree with those of General Relativity, i.e.  $\gamma = \beta = 1$ . This was already known since we constructed our model for this to happen. For the parameters associated to preferred frame effects we get:  $\alpha_1 = 0$  and  $\alpha_2 = 8\pi A_\odot^2/M_p^2$  where  $A_\odot^2$  is the norm of the vector field at the Solar System scale. Therefore, current limits  $\alpha_2 \lesssim 10^{-4}$  (or  $\alpha_2 \lesssim 10^{-7}$  for static vector fields during Solar System formation) then impose a bound  $A_\odot^2 \lesssim 10^{-5}(10^{-8})M_p^2$ ,

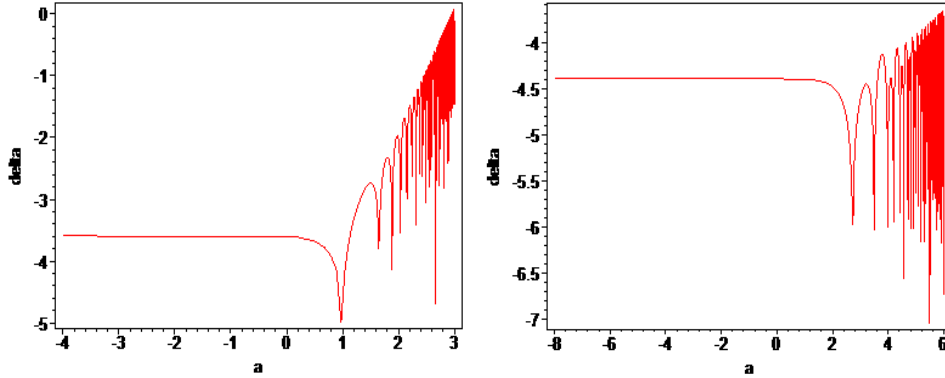


Figure 5.4: In this figure we show the evolution of  $\delta_A$  for modes reentering the horizon in the radiation era (right panel) and in the matter era (left panel). We see that it is constant on super-Hubble scales and it oscillates with growing amplitude on sub-Hubble scales.

which could conflict with the model predictions, since the present (Solar system formation) values on cosmological scales are:  $1.3 \times 10^{-1} M_p$  ( $7.5 \times 10^{-2} M_p$ ). However, notice that, as we have already commented several times, the cosmological values do not need to agree with those at lower scales. The latter will be determined by the mechanism that generated this field in the early Universe characterized by its primordial spectrum of perturbations, and the subsequent evolution in the formation of the galaxy and Solar System.

## 5.6 Constraints from SN, CMB and BAO

In this Section we shall obtain constraints for the cosmological parameters of the model from observations of SN, CMB and BAO. However, unlike in the previous Sections, here we shall give up the flatness assumption to include the effects of the spatial curvature so that the metric is now given by (1.5). In this case, the field equation given in (5.31) remains the same, although for the purposes of this Section it will be convenient to write it in terms of the redshift variable as follows:

$$\frac{d^2 A_0}{dz^2} + \frac{1}{(1+z)H(z)} \frac{d}{dz} \left[ \frac{H(z)}{(1+z)^2} \right] \frac{d}{dz} \left[ (1+z)^3 A_0 \right] = 0 \quad (5.31)$$

and, therefore, the solutions (5.6) adopt the following form:

$$A_0(z) = \tilde{A}_0^+(1+z)^{\tilde{\alpha}^+} + \tilde{A}_0^-(1+z)^{\tilde{\alpha}^-} \quad (5.32)$$

with  $\tilde{A}_0^\pm$  constants of integration and  $\tilde{\alpha}_\pm = (1 \pm 1)/2$  in the radiation era, and  $\tilde{\alpha}_\pm = (3 \pm \sqrt{33})/4$  in the matter era.

The novelties when we include the curvature effects appear in the Einstein equations. On one hand, the  $({}^0_0)$  component of these equations becomes:

$$\frac{H^2}{H_0^2} = \Omega_m(1+z)^3 + \Omega_r(1+z)^4 + \Omega_k(1+z)^2 + \rho_A(z) \quad (5.33)$$

where  $H_0$  is the present value of the Hubble parameter, which is usually expressed as<sup>4</sup>  $H_0 = 100 h \text{ km s}^{-1} \text{ Mpc}^{-1}$ ,  $\Omega_m$  and  $\Omega_r$  are the density parameters corresponding to matter and radiation respectively,  $\Omega_k = -\frac{k}{H_0^2}$  and  $\rho_A$  is the energy density of the vector field, whose expression in terms of redshift is:

$$\rho_A = \frac{H^2}{H_0^2} \left[ \frac{1}{2} A_0^2 - (1+z) A_0 \frac{dA_0}{dz} - \frac{1}{6} (1+z)^2 \left( \frac{dA_0}{dz} \right)^2 \right]. \quad (5.34)$$

Notice that we are measuring the vector field in units of the reduced Planck mass  $\tilde{M}_P = 1/\sqrt{8\pi G}$ . Moreover, the energy density evolves in terms of redshift as:

$$\rho_A = \rho_{A0}(1+z)^{-\kappa}. \quad (5.35)$$

Finally, it is worth mentioning that the inclusion of spatial curvature does not eliminate the future Type III singularity of the models when the vector field dominates the energy density of the Universe.

On the other hand, the  $({}^i_i)$  component of Einstein equations becomes:

$$\frac{H^2}{H_0^2} \left[ 3 - \frac{1+z}{H} \frac{dH}{dz} \right] = \Omega_r(1+z)^4 + \Omega_k(1+z)^2 - p_A(z) \quad (5.36)$$

where we have used that  $p_r = \frac{1}{3}\rho_r$  and  $p_m = 0$  and the pressure of the

---

<sup>4</sup>The parameter  $h$  in the definition of  $H_0$  must not be confused with the degree of anisotropy defined in Chapter 2. However, we shall not refer to the degree of anisotropy throughout this Section, so no confusion will be possible.

vector field in terms of the redshift is given by:

$$p_A(z) = -\frac{H^2}{H_0^2} \left\{ 3 \left[ \frac{5}{2} - \frac{4}{3}(1+z) \frac{1}{H} \frac{dH}{dz} \right] A_0^2 + (1+z) A_0 \frac{dA_0}{dz} + \frac{3}{2} (1+z)^2 \left( \frac{dA_0}{dz} \right)^2 \right\}. \quad (5.37)$$

In order to perform the analysis in next sections it will be convenient to write equations (6.43) and (5.36) in terms of  $\{\Omega_r h^2, \Omega_m h^2, \Omega_k h^2\}$  as follows:

$$\hat{H}^2 = \Omega_m h^2 (1+z)^3 + \Omega_r h^2 (1+z)^4 + \Omega_k h^2 (1+z)^2 + \rho_A(z) \quad (5.38)$$

$$\hat{H} \left[ 3 - \frac{1+z}{\hat{H}} \frac{d\hat{H}}{dz} \right] = \Omega_r h^2 (1+z)^4 + \Omega_k h^2 (1+z)^2 - p_A(z) \quad (5.39)$$

where  $\hat{H} \equiv H/(100 \text{ km s}^{-1} \text{ Mpc}^{-1})$ , i.e.,  $\hat{H}(z=0) = h$ . Note that neither  $\rho_A$  nor  $p_A$  depend on the normalization of the Hubble parameter. Moreover,  $\Omega_r h^2$  contains the contribution of photons as well as relativistic neutrinos,

$$\Omega_r h^2 = \Omega_\gamma h^2 (1 + 0.2271 N_{eff}) \quad (5.40)$$

with  $N_{eff} = 3.04$  the effective number of neutrino species and  $\Omega_\gamma h^2 = 2.469 \times 10^{-5}$  for  $T_{CMB} = 2.725 \text{ K}$ .

The model is completely determined once we fix the set of parameters  $\{\Omega_m, \Omega_k, A_{rad}\}$ , being  $A_{rad}$  the constant value of the vector field during the radiation dominated era (see Fig. 5.1), so that the model has three free parameters. To confront the model to SN and BAO datasets we only need to integrate the system of equations below redshift  $\sim 2$  whereas CMB dataset requires to obtain the solution up to the last scattering surface so that the method to solve the equations will be different for each case. The present value of the Hubble expansion rate is no longer a free parameter in this model because it can be obtained in terms of the previous parameters after integrating the equations. In fact, we could take  $\{\Omega_m, \Omega_k, h\}$  as independent parameters and, therefore,  $A_{rad}$  would already be determined, although this approach is more difficult to implement numerically. Notice that, as commented before, this model contains exactly the same number of parameters as  $\Lambda$ CDM.

### 5.6.1 Likelihood calculations

In this Section we shall explain the procedure followed to confront the vector dark energy model to the different distance indicators.

#### SN

The apparent magnitude of a supernova placed at a given redshift  $z$  is related to the expansion history of the Universe through the distance modulus:

$$\mu \equiv m - M = 5 \log D_L - 5 \log h + \mu_0 \quad (5.41)$$

where  $m$  and  $M$  are the apparent and absolute magnitudes respectively,  $\mu_0 = 42.38$  and  $D_L = H_0 d_L$  with  $d_L$  the luminosity distance  $d_L = (1 + z)r(z)$ , being  $r(z)$  the comoving distance, given for the FLRW metric with curvature (1.5) by:

$$r(z) = \frac{1}{H_0 \sqrt{|\Omega_k|}} S_k \left[ \sqrt{|\Omega_k|} \int_0^z \frac{H_0}{H(z')} dz' \right] \quad (5.42)$$

with  $S_k[x] = \sin x, x, \sinh x$  for  $\Omega_k < 0, \Omega_k = 0, \Omega_k > 0$  respectively.

Then, to confront the model to each supernovae data set we construct the corresponding  $\chi^2$  estimator:

$$\chi_{SN}^2 = \sum_{i=1}^N \frac{(\mu(z_i; \Omega_m, \Omega_k, h) - \mu_i)^2}{\sigma_i^2} \quad (5.43)$$

which must be marginalized over  $h$  in order to obtain the constraints on the parameters  $\Omega_m$  and  $\Omega_k$ .

In order to calculate  $\chi_{SN}^2$ , we use the fact that the SNIa dataset corresponds to redshifts below 2 so that we can neglect the contribution from radiation in Einstein's equations. With this in mind, we solve numerically the system of equations (5.31) and (5.36) for  $H/H_0$  and  $A_0$ . As this system is of second order with respect to  $A_0$  and first order with respect to  $H/H_0$  we need to set the initial values of  $A_0$ ,  $dA_0/dz$  and  $H/H_0$ . However, these three initial values are related by means of Friedmann equation (6.43) so that we can obtain the initial value for  $H/H_0$  in terms of the initial values of  $A_0$  and its derivative. On the other hand, as we know the analytic solution of the vector field in the matter dominated era as that given in (5.6)

, we can relate the initial value of the derivative of the vector field to the initial value of the vector field (neglecting the decaying mode). Therefore, we only need to give the initial value for  $A_0$  in order to set the initial conditions and we are left with  $A_0^{ini}$ ,  $\Omega_m$  and  $\Omega_k$  as free parameters in terms of which we obtain the corresponding  $\chi_{SN}^2$  estimator. Therefore, we shall use:

$$\chi_{SN}^2 = \sum_{i=1}^N \frac{(\mu(z_i; \Omega_m, \Omega_k, A_{ini}) - \mu_i)^2}{\sigma_i^2} \quad (5.44)$$

instead of (5.43) and marginalize over  $A_{ini}$ .

The results that we shall show have been obtained from the following two sets of supernovae: the Gold set [125] and the more recent Union set [8].

## BAO

BAO measurements provide the following distance ratios [10]:

$$\mathbf{V}_{BAO} \equiv \begin{pmatrix} \frac{r_s(z_d)}{D_V(0.2)} \\ \frac{r_s(z_d)}{D_V(0.35)} \end{pmatrix} = \begin{pmatrix} 0.1980 \pm 0.0058 \\ 0.1094 \pm 0.0033 \end{pmatrix}, \quad (5.45)$$

where  $r_s(z)$  is the sound horizon size given by:

$$r_s(z) = \frac{1}{\sqrt{3}} \int_0^{\frac{1}{1+z}} \frac{da}{a^2 H(a) \sqrt{\left(1 + \frac{3\Omega_b h^2}{4\Omega_\gamma h^2} a\right)}} \quad (5.46)$$

and

$$D_V(z) = \left[ r^2(z) \frac{z}{H} \right]^{1/3} \quad (5.47)$$

is the dilation scale. Finally,  $z_d$  is redshift of the drag epoch at which baryons were released from photons and which can be calculated by using the fitting formula [132]:

$$z_d = \frac{1291(\Omega_m h^2)^{0.251}}{1 + 0.659(\Omega_m h^2)^{0.828}} \left[ 1 + b_1(\Omega_b h^2)^{b_2} \right] \quad (5.48)$$

with

$$b_1 = 0.313(\Omega_m h^2)^{-0.419} \left[ 1 + 0.607(\Omega_m h^2)^{0.674} \right] \quad (5.49)$$

$$b_2 = 0.238(\Omega_m h^2)^{0.223}. \quad (5.50)$$

Then, we define the BAO array:

$$\mathbf{X}_{BAO} \equiv \begin{pmatrix} \frac{r_s(z_d)}{D_V(0.2)} - 1.980 \\ \frac{r_s(z_d)}{D_V(0.35)} - 0.1094 \end{pmatrix}, \quad (5.51)$$

so that:

$$\chi_{BAO}^2 = \mathbf{X}_{BAO}^T \mathbf{C}_{BAO}^{-1} \mathbf{X}_{BAO}. \quad (5.52)$$

In this expression, the inverse covariance matrix is

$$\mathbf{C}_{BAO}^{-1} = \begin{pmatrix} 35059 & -24031 \\ -24031 & 108300 \end{pmatrix}. \quad (5.53)$$

The procedure we follow in this case is analogous to that used for the SNIa analysis, although, as  $\chi_{BAO}^2$  depends on the amount of baryons  $\Omega_b$ , we also need to marginalize over this parameter.

## CMB

Following [133], we use the distance priors method to confront dark energy models to CMB data [134, 135]. This method uses two distance ratios measured by means of the CMB temperature power spectrum:

- The "acoustic scale", which measures the ratio of the angular diameter distance to the decoupling epoch and the comoving sound horizon size at decoupling epoch. This first distance ratio can be expressed as:

$$l_A \equiv \frac{\pi r(z_*)}{r_s(z_*)} \quad (5.54)$$

where  $z_*$  the redshift corresponding to the decoupling time and for which we shall use the fitting formula proposed in [136]:

$$z_* = 1048 \left[ 1 + 0.00124(\Omega_b h^2)^{-0.738} \right] \left[ 1 + g_1(\Omega_m h^2)^{g_2} \right] \quad (5.55)$$

with

$$g_1 = \frac{0.0783(\Omega_b h^2)^{-0.238}}{1 + 39.5(\Omega_b h^2)^{0.763}}, \quad (5.56)$$

$$g_2 = \frac{0.560}{1 + 21.1(\Omega_b h^2)^{1.81}}. \quad (5.57)$$

- The second distance ratio measures the ratio of the angular diameter distance and the Hubble radius at the decoupling time. It is usually called the "shift parameter" and can be expressed as

$$R = \sqrt{\Omega_m H_0^2 r(z_*)} \quad (5.58)$$

The values reported in [133] for these distance priors are:

$$\mathbf{V}_{CMB} \equiv \begin{pmatrix} l_A(z_*) \\ R(z_*) \\ z_* \end{pmatrix} = \begin{pmatrix} 302.10 \pm 0.86 \\ 1.710 \pm 0.019 \\ 1090.04 \pm 0.93 \end{pmatrix} \quad (5.59)$$

with the following inverse of the covariance matrix

$$\mathbf{C}_{CMB}^{-1} = \begin{pmatrix} 1.800 & 27.968 & -1.103 \\ 27.968 & 5667.577 & -92.263 \\ -1.103 & -92.263 & 2.923 \end{pmatrix}. \quad (5.60)$$

Then, we define the CMB array as

$$\mathbf{X}_{CMB} = \begin{pmatrix} l_A - 302.10 \\ R - 1.710 \\ z_* - 1090.04 \end{pmatrix}, \quad (5.61)$$

so that  $\chi_{CMB}^2 = \mathbf{X}_{CMB}^T \mathbf{C}_{CMB}^{-1} \mathbf{X}_{CMB}$ .

The procedure we follow in this case is somewhat different to that used in the previous sections. The main difference comes from the fact that CMB distance priors are evaluated at a time when radiation is important so that we cannot neglect its contribution in Einstein's equations anymore. To simplify numerical calculations we use equations (5.31), (5.38) and (5.39). Notice that, unlike the SN and BAO approach, from these equations we obtain the Hubble expansion rate normalized to 100 km s<sup>-1</sup>Mpc<sup>-1</sup> so that  $\hat{H}(z=0) = h$ . Thus, for given  $\{\Omega_m h^2, \Omega_k h^2\}$  we use (5.38) to relate the initial condition for the Hubble expansion rate to the initial condition of the vector field (that we shall name  $A_{rad}$ ) and, then, solve numerically (5.31) and (5.39). Since the initial conditions are set in the radiation-dominated era when, according to (5.6), the vector field is constant, the initial condition for the derivative of the vector field is set to zero. Moreover, the constancy of the vector field during that epoch eliminates the dependency on the time at which we place the initial conditions, i.e.,  $A_{rad}$  does not depend on  $z_{ini}$ . That way, we obtain the

expansion rate  $\hat{H}(z)$  that will allow us to compute the distance indicators described above in terms of  $\{\Omega_m h^2, \Omega_k h^2, A_{rad}\}$  (notice that such indicators do not depend on the normalization of the Hubble expansion rate). Hence, we can compute the corresponding  $\chi_{CMB}^2$  which will depend on  $\{\Omega_m h^2, \Omega_k h^2, \Omega_b h^2, A_{rad}\}$  and, following the prescription given in [133], we marginalize over  $\Omega_b h^2$  and  $A_{rad}$  (which is equivalent to marginalize over  $h$ ) and use the resulting marginalized likelihood to obtain the corresponding contours.

Since CMB distance priors were derived in [133] assuming that dark energy was not important at decoupling time ( $z_* \simeq 1090$ ) and given that the vector field model does not produce a significant amount of dark energy at high redshifts, these priors are, in principle, applicable in this case.

## 5.6.2 Results

In this section we present the results obtained after confronting the model with the tests explained above. We have also performed the analysis for a  $\Lambda$ CDM model for comparison.

Using the Gold data set we obtain a best fit for  $\Omega_m = 0.385$  and  $\Omega_A = 0.611$  with  $\chi_{min}^2 = 172.92$ , which is the same value found in previous Sections, where we imposed spatially flat sections. This is understandable because, from the above values of  $\Omega_m$  and  $\Omega_A$  we obtain  $\Omega_k = 0.0043$  so that the best fit is very close to the flat case. However the  $1\sigma$  contour allows both open and close Universes and, unlike our previous analysis, a wide range of values for  $\Omega_m$  and  $\Omega_A$  is within the  $1\sigma$  region, as we can see in Fig. 5.5. For a  $\Lambda$ CDM model with non-vanishing curvature we obtain the best fit for  $\Omega_m = 0.46$  and  $\Omega_\Lambda = 0.98$  with  $\chi_{min}^2 = 175.04$  so we still obtain a better fit to the Gold data set than  $\Lambda$ CDM. On the other hand, the best fit obtained for the vector dark energy model from the Union data set corresponds to  $\Omega_m = 0.260$  and  $\Omega_A = 0.503$  with  $\chi_{min}^2 = 311.96$ . From Fig. 5.5 we see that this data set favors an open Universe for this model, being the flat case at more than  $2\sigma$ . For  $\Lambda$ CDM the best fit happens for  $\Omega_m = 0.41$  and  $\Omega_\Lambda = 0.93$ , being  $\chi_{min}^2 = 310.23$ , which is lower than that obtained for the vector field. This effect is probably due to the SNLS points contained in the Union data set which, as it was shown in our previous analysis, favor  $\Lambda$ CDM over the vector field model at more than  $2\sigma$  in the flat case. However, when the flatness assumption is dropped,

$\Lambda$ CDM fits the Union data set better than the vector field model at the level of less than  $1\sigma$ , thus, without statistical significance.

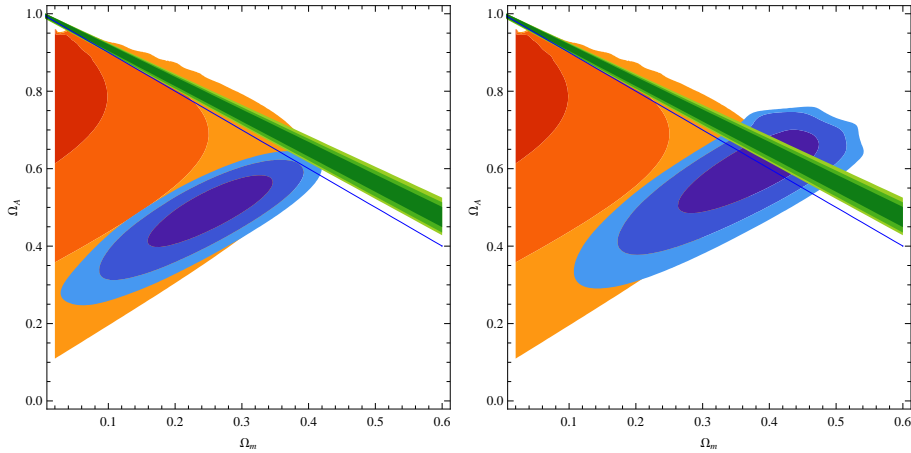


Figure 5.5: In this plots we show the 68%, 95% and 99% C.L. regions for BAO (orange), CMB (green) and SNIa (blue). We show the contours obtained for both the Union data set (left) and the Gold data set (right). The blue line corresponds to a flat Universe.

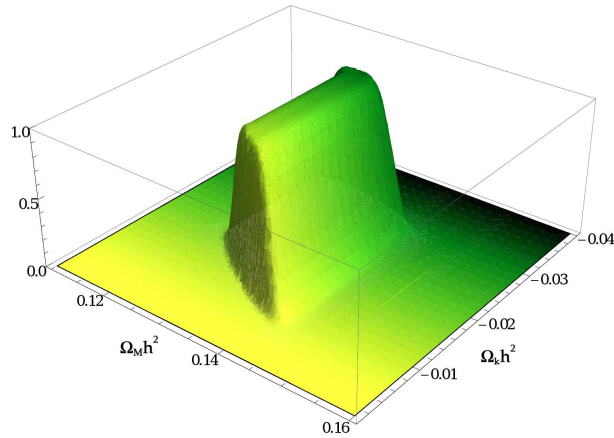


Figure 5.6: In this plot we show the likelihood obtained from the CMB dataset for the vector field model. We can see that a flat Universe is clearly ruled out and a closed geometry for the spatial sections is strongly favored.

Concerning BAO dataset, it favors an open Universe with a small amount of matter for the vector field model, as we see in Fig. 5.5. Moreover, the compatibility of these data with SNIa data is only at the  $3\sigma$  level.

However, it is worth mentioning that these distance indicators are obtained after analyzing the actual observational data with  $\Lambda$ CDM as fiducial model so that its applicability to test dark energy models is justified as long as such models do not differ much from a cosmological constant. Nevertheless, this is not the case for the vector dark energy model whose equation of state varies very rapidly and, indeed, has a future singularity so that the obtained  $3\sigma$  tension could be due to the dependence of BAO data on the fiducial model. In any case, this is the less confident dataset to constraint the vector model and, in general, any dark energy model, since it may give shifted parameters due to a biased determination of the sound horizon scale due to the presence of additional relativistic degrees of freedom, early dark energy or a non-standard recombination scheme [137, 138].

Finally, CMB data is totally incompatible with flat spatial sections and, in fact, it predicts a closed Universe with a wide range of  $\Omega_m$  allowed. These results show that, contrary to common belief, CMB data do not necessarily favors a flat Universe. In Fig. 5.6, the corresponding likelihood for the CMB dataset is plotted and we can see how the flat case is ruled out for the vector model.

In Fig. 5.5 we see that CMB contours are compatible with BAO at  $2\sigma$  level for small values of  $\Omega_m$  and  $\Omega_k$  close to zero. Concerning SNIa contours, CMB is in conflict with the Union data set contours at more than  $3\sigma$  whereas it is compatible at  $1\sigma$  level with the Gold data set.

## 5.7 Conclusions and discussion

In this Chapter we have proposed a particular vector-tensor theory as possible candidate to explain the current phase of accelerated expansion. Such a model has been built so that it presents scaling properties during the early Universe as well as the same set of static PPN parameters as GR. We have shown the ability of the model in order to account for the accelerated expansion without the need of introducing any unnatural scale. Thus, the required initial fraction of dark energy required during the early Universe is  $\sim 10^{-6}$  and the value of the vector field must be  $10^{-4}M_p$ , values that can arise naturally as fluctuations in the early Universe. Moreover, the comoving component of the vector field turns out to be constant in the early Universe so that the solutions are completely

insensitive to the time at which we set the initial conditions. An interesting feature of the model is that it leads to a future Type III singularity in which the vector field equation of state approaches  $-\infty$ , crossing the phantom divide line as suggested by cosmological observations.

The cosmological evolution obtained by considering only temporal components of the vector field has been shown to be robust against the potential presence of spatial components. Indeed, the contribution to the vector field total energy density coming from the spatial components are strongly suppressed with respect to the contribution corresponding to the temporal component. On the other hand, the anisotropy generated by the model is expected to be small because the difference of transverse and longitudinal pressures, which is the source of the vector field stress, decays as the Universe expands. Moreover, the degree of anisotropy generated in this model happens to be a decaying quantity, which confirms that this model is not able to produce large scale anisotropies.

The classical stability of the model is completely guaranteed until the end of the Universe because the propagation speed of the inhomogeneous modes remains real until the future singularity found in the homogeneous evolution. Moreover, at that moment the propagation speed also blows up what may suggest a link between singularities in homogeneous solutions and instabilities for the inhomogeneous modes. The quantum stability poses an important problem because the vector modes become ghost-like before the future singularity is reached. However, this could be cured by the completion of the model when extended to smaller scales. In addition, we have seen that this model leads to preferred frame effects and that the amplitude of the vector field at small scales must be smaller than the cosmological value. Finally, we have performed a detailed analysis of the constraints imposed by SNIa, CMB and BAO data on the vector dark energy model. In order to get such constraints we have given up the spatial flatness assumption and obtained confidence regions in the  $(\Omega_m, \Omega_A)$  plane. We have found that for the SNIa Gold dataset, the vector model fit is better than that of  $\Lambda$ CDM and, in fact, provides the best fit to date for this dataset, but for the Union dataset the situation is reversed. We find that contrary to standard cosmology, CMB data *excludes* a flat Universe for this model and, in fact, predicts a closed spatial geometry. On the other hand, CMB and SNIa Gold data are perfectly compatible at the 1-sigma level, however SNIa Union dataset exhibits a 3-sigma tension with CMB. The same level of tension is also found between SNIa and BAO measurements, although this may be due to the dependency of BAO measurements on the fiducial model.



# Electromagnetic dark energy

---

## 6.1 Introduction

The particular model studied in the previous Chapter shows that vector fields can be compelling candidates to drive the current accelerated expansion of the Universe avoiding naturalness problems. In this Chapter, we shall go a step further and show that this can indeed be achieved not by resorting to new physics with the introduction of an unknown field, but by means of the very familiar electromagnetic interaction. This in principle seems to be difficult to realize since Maxwell electromagnetism is conformally coupled to gravity in four dimensions so that it cannot be excited in the early Universe by gravitational fields. Moreover, the high conductivity of the Universe after reheating together with its electrical neutrality makes the electromagnetic field to decay as the Universe expands and, as a consequence, we would have negligible electromagnetic fields on large scales today. Previous proposals have suggested the breaking of conformal invariance but preserving the  $U(1)$  gauge symmetry, as in [107] where non-linear terms are introduced to produce accelerated expansion, or by breaking that symmetry, as in [139] where couplings to the curvature are introduced to generate large-scale magnetic fields. However, in this Chapter we show that the very same theory that is used to covariantly quantize the electromagnetic interaction allows us to explain the presence of electromagnetic fields over cosmological scales. The energy density of such fields are shown to behave as an effective cosmological constant. This possibility requires a fundamental change in the interpretation of the covariant action. As is well known, this action includes a gauge breaking term which appears as a mathematical artifact in the gauge fixing procedure. Here we propose that such a term should

be considered as a truly physical term on equal footing to the Maxwell term and therefore that the fundamental electromagnetic theory is not invariant under arbitrary gauge transformations.

In order to modify the electromagnetic interaction, one should be aware that quantum electrodynamics is probably the most successful physical theory and has received an extraordinary experimental support. However, as any other fundamental physical theory, the success of the electromagnetic theory as currently established is subject to a determined range of applicability. Indeed, its infrared experimental limit is given by the constraints on the photon mass  $m_\gamma \lesssim 10^{-17}$  eV (see for instance [140]), corresponding to frequencies  $\nu \simeq 1\text{mHz}$  or wavelengths  $\lambda \simeq 1.3\text{AU}$ <sup>1</sup>. Therefore, any alternative to (or extended version of) standard electromagnetism whose differences only appear beyond that infrared limit are, in principle, not excluded. The situation is analogous to the case of the gravitational interaction for which we have GR as a very successful theory of gravitation at the Solar System scales, where it has been extensively tested. However, modifications beyond those scales are allowed and, indeed, some attempts to accommodate the dark matter and dark energy within extended versions of GR have been made. These modifications are quite natural because gravity is a long range interaction so that one might expect it to become modified when considering very large scales, i.e. in the infrared regime of GR. We can apply the same reasoning to the electromagnetic case because it is also a long range interaction with an infrared limit (given by  $\nu \simeq 1\text{mHz}$ ) beyond which it remains unknown. However, since the standard electromagnetism has been extensively tested in its range of applicability with great accuracy, one has to ensure that, in that range, the modified electromagnetic theory reproduces the behavior of the standard theory.

Interestingly, although Maxwell electromagnetism is a well-established theory whose results are in excellent agreement with the experiments, it shows some troubles when we try to quantize it. In particular, in the canonical formalism, the fact that the temporal component has vanishing conjugate momentum makes difficult to impose canonical commutation relations for the field. One solution to this problem is to add a gauge-fixing term in the starting action to provide the temporal component with a non-vanishing conjugate momentum so that we can write canoni-

---

<sup>1</sup>Notice that this limit corresponds to the wavelength of the photon, not to the distance along which the photon has travelled. In fact, we can see photons coming from the last scattering surface in the CMB that lie in the microwave range.

cal commutation relations. However, we obtain a theory with four states instead of the two usual states corresponding to a massless spin 1 particle, so that we need to restrict our Hilbert space for the two additional degrees of freedom not to contribute to physical quantities. We shall start this Chapter by reviewing these difficulties in the different quantization procedures in flat spacetime and we shall see how the Lorenz condition is essential to consistently quantize the theory. Then, we shall consider quantization in an expanding universe and show how such a condition cannot be consistently imposed. In order to avoid this problem, we shall propose a quantization procedure such that the gauge-fixing term is considered as a fully physical term of the fundamental theory that introduces an extra scalar degree of freedom. In that approach, we shall show that the theory can be consistently quantized without the need of imposing the Lorenz condition, although we have to consider three physical states. One interesting example of electromagnetic theories with three physical states also arises when we consider massive photons and take the massless limit. In that case, an additional state which is only gravitationally coupled remains [139].

In the framework described in the previous paragraph, we shall compute the initial power spectrum generated during an inflationary era in the early Universe for the new electromagnetic mode and study the subsequent cosmological evolution. We shall see that the gauge-fixing term gives rise to an effective cosmological constant whose value is related to the scale of inflation. Also, the evolution of the perturbations will be analyzed and confronted to CMB and LSS observations to check the experimental viability of the theory.

Finally, it is worth mentioning that the extension for electromagnetism that we shall study with the gauge-fixing term has the same form as the vector-tensor theory that behaves like a cosmological constant obtained in Chapter 3. Moreover, in Chapter 4, we showed that such a particular vector-tensor theory has the same PPN parameters as GR, so it passes all the Solar System tests, and it is free of both classical and quantum instabilities. Therefore, even though we will be dealing with the electromagnetic field, most of the results that we shall obtain in this Chapter will be applicable to any vector-tensor theory with the same set of parameters.

This Chapter is based on the results presented in the following works:

- *Cosmological electromagnetic fields and dark energy.*  
Jose Beltrán Jiménez and Antonio L. Maroto.  
JCAP **0903**:016 (2009).

- *Perturbations in electromagnetic dark energy.*  
Jose Beltrán Jiménez, Tomi S. Koivisto, Antonio L. Maroto and David F. Mota.  
JCAP **0910**:029 (2009).
- *The electromagnetic dark sector.*  
Jose Beltrán Jiménez and Antonio L. Maroto.  
arXiv:0903.4672 [astro-ph.CO]

## 6.2 Quantization in Minkowski spacetime

Electromagnetic interaction is considered as a paradigm of a well-behaved quantum field theory in Minkowski space-time. Standard Maxwell electromagnetism is the theory describing a pure spin one massless particle. Nevertheless, the presence of the local  $U(1)$  symmetry in the kinematical term for the photon leads to some difficulties when we want to quantize the theory. The underlying reason for the appearance of these difficulties is the redundancy in the description of the theory due to the  $U(1)$  invariance so that we can be wrongly trying to quantize superfluous degrees of freedom corresponding to pure gauge modes. Let us briefly review these difficulties, since it will be useful for our approach.

The usual electromagnetic field is described by Maxwell action:

$$S = \int d^4x \left( -\frac{1}{4} F_{\mu\nu} F^{\mu\nu} + A_\mu J^\mu \right) \quad (6.1)$$

where  $F_{\mu\nu} = \partial_\mu A_\nu - \partial_\nu A_\mu$  and  $J_\mu$  is a conserved current. This action is invariant under gauge transformations  $A_\mu \rightarrow A_\mu + \partial_\mu \chi$  with  $\chi$  an arbitrary function of space-time coordinates. At the classical level, this action gives rise to the well-known Maxwell equations, that is:

$$\partial_\nu F^{\mu\nu} = J^\mu. \quad (6.2)$$

However, when we try to quantize the theory, several problems arise because of the impossibility of constructing a propagator for the  $A_\mu$  field. Two different approaches are usually followed in order to avoid these difficulties. In the first one, which is the basis of the Coulomb gauge quantization, the gauge invariance of the action (6.1) is used to eliminate the *unphysical* degrees of freedom. With that purpose the (Lorenz) condition  $\partial_\mu A^\mu = 0$  is imposed by means of a suitable gauge transformation.

Thus, the equations of motion reduce to:

$$\square A_\mu = J_\mu. \quad (6.3)$$

The Lorenz condition does not fix completely the gauge freedom, still it is possible to perform residual gauge transformations  $A_\mu \rightarrow A_\mu + \partial_\mu \theta$ , provided  $\square \theta = 0$ . Using this residual symmetry and taking into account the form of equations (6.3), it is possible to eliminate one additional component of the  $A_\mu$  field in the asymptotically free regions (typically  $A_0$ ) which means  $\vec{\nabla} \cdot \vec{A} = 0$ , so that finally the temporal and longitudinal photons are removed and we are left with the two transverse polarizations of the massless free photon, which are the only modes (with positive energies) which are quantized in this formalism.

The second approach is the basis of the covariant (Gupta-Bleuler) and path-integral formalisms. The starting point is a modification of the action in (6.1), namely:

$$S = \int d^4x \left( -\frac{1}{4} F_{\mu\nu} F^{\mu\nu} + \frac{\xi}{2} (\partial_\mu A^\mu)^2 + A_\mu J^\mu \right). \quad (6.4)$$

This action is no longer invariant under general gauge transformations, but only under residual ones. The equations of motion obtained from this action now read:

$$\partial_\nu F^{\mu\nu} + \xi \partial^\mu (\partial_\nu A^\nu) = J^\mu. \quad (6.5)$$

In order to recover Maxwell equation, the Lorenz condition must be imposed so that the  $\xi$  term disappears. At the classical level this can be achieved by means of appropriate boundary conditions on the field. Indeed, taking the four-divergence of the above equation, we find:

$$\square (\partial_\nu A^\nu) = 0 \quad (6.6)$$

where we have made use of current conservation. This means that the field  $\partial_\nu A^\nu$  evolves as a free scalar field, so that if it vanishes for large  $|t|$ , it will vanish for all time. At the quantum level, the Lorenz condition cannot be imposed as an operator identity, but only in the weak sense  $\partial_\nu A^{\nu(+)} |\phi\rangle = 0$ , where  $(+)$  denotes the positive frequency part of the operator and  $|\phi\rangle$  stands for a physical state. This condition is equivalent to imposing  $[\mathbf{a}_0(\vec{k}) + \mathbf{a}_\parallel(\vec{k})] |\phi\rangle = 0$ , with  $\mathbf{a}_0$  and  $\mathbf{a}_\parallel$  the annihilation operators corresponding to temporal and longitudinal electromagnetic states. Thus, in the covariant formalism, the physical states contain the same number

of temporal and longitudinal photons, so that their energy densities, having opposite signs, cancel each other. Thus we see that also in this case, the Lorenz condition seems to be essential in order to recover standard Maxwell equations and get rid of the negative energy states. Now let us see what happens when moving on to an expanding universe.

### 6.3 Quantization in an expanding universe

So far we have only considered Maxwell theory in flat spacetime. However when we move to a curved background and, in particular, to an expanding universe, then consistently imposing the Lorenz condition in the covariant formalism turns out to be difficult to realize [141]. Indeed, let us consider the curved space-time version of action (6.4):

$$S = \int d^4x \sqrt{g} \left[ -\frac{1}{4} F_{\mu\nu} F^{\mu\nu} + \frac{\xi}{2} (\nabla_\mu A^\mu)^2 + A_\mu J^\mu \right] \quad (6.7)$$

Now the modified Maxwell equations read:

$$\nabla_\nu F^{\mu\nu} + \xi \nabla^\mu (\nabla_\nu A^\nu) = J^\mu \quad (6.8)$$

and taking again the four divergence, we get:

$$\square(\nabla_\nu A^\nu) = 0 \quad (6.9)$$

We see that once again  $\nabla_\nu A^\nu$  behaves as a scalar field which is decoupled from the conserved electromagnetic currents, but it is non-conformally coupled to gravity. This means that, unlike the flat space-time case, this field can be excited from quantum vacuum fluctuations by the expanding background in a completely analogous way to the inflaton fluctuations during inflation. Thus this poses the question of the validity of the Lorenz condition at all times.

In order to illustrate this effect, we will present a toy example. Let us consider quantization in the absence of currents, in a spatially flat expanding background, whose metric is written in conformal time as  $ds^2 = a(\eta)^2(d\eta^2 - d\vec{x}^2)$  with  $a(\eta) = 2 + \tanh(\eta/\eta_0)$  where  $\eta_0$  is constant. This metric has two asymptotically Minkowskian regions in the remote past and far future. We solve the coupled system of equations (6.8) for the corresponding Fourier modes, which are defined as<sup>2</sup>  $\mathcal{A}_\mu(\eta, \vec{x}) =$

<sup>2</sup>Here we follow the notation followed in the previous Chapters denoting by  $\mathcal{A}_\mu$  the components of the vector field in conformal time.

$\int d^3k \mathcal{A}_{\mu\vec{k}}(\eta) e^{i\vec{k}\vec{x}}$ . Thus, for a given mode  $\vec{k}$ , the  $\mathcal{A}_\mu$  field is decomposed into temporal, longitudinal and transverse components. The corresponding equations read:

$$\begin{aligned} \mathcal{A}''_{0k} - \left[ \frac{k^2}{\xi} - 2\mathcal{H}' + 4\mathcal{H}^2 \right] \mathcal{A}_{0k} - 2ik \left[ \frac{1+\xi}{2\xi} \mathcal{A}'_{\parallel k} - \mathcal{H} \mathcal{A}_{\parallel k} \right] &= 0 \\ \mathcal{A}''_{\parallel k} - k^2 \xi \mathcal{A}_{\parallel k} - 2ik\xi \left[ \frac{1+\xi}{2\xi} \mathcal{A}'_{0k} + \mathcal{H} \mathcal{A}_{0k} \right] &= 0 \\ \vec{\mathcal{A}}''_{\perp k} + k^2 \vec{\mathcal{A}}_{\perp k} &= 0 \end{aligned} \quad (6.10)$$

with  $\mathcal{H} = a'/a$  and  $k = |\vec{k}|$ . We see that the transverse modes are decoupled from the background, whereas the temporal and longitudinal ones are non-trivially coupled to each other and to gravity. Let us prepare our system in an initial state  $|\phi\rangle$  belonging to the physical Hilbert space, i.e. satisfying  $\partial_\nu \mathcal{A}_{in}^{v(+)} |\phi\rangle = 0$  in the initial flat region. Because of the expansion of the universe, the positive frequency modes in the *in* region with a given temporal or longitudinal polarization  $\lambda$  will become a linear superposition of positive and negative frequency modes in the *out* region and with different polarizations  $\lambda'$  (we will work in the Feynman gauge  $\xi = -1$ ), thus we have:

$$\mathcal{A}_{\mu\vec{k}}^{\lambda(in)} = \sum_{\lambda'=0,\parallel} \left[ \alpha_{\lambda\lambda'}(\vec{k}) \mathcal{A}_{\mu\vec{k}}^{\lambda'(out)} + \beta_{\lambda\lambda'}(\vec{k}) \overline{\mathcal{A}_{\mu-\vec{k}}^{\lambda'(out)}} \right] \quad (6.11)$$

or in terms of creation and annihilation operators:

$$\mathbf{a}_{\lambda}^{(out)}(\vec{k}) = \sum_{\lambda'=0,\parallel} \left[ \alpha_{\lambda\lambda'}(\vec{k}) \mathbf{a}_{\lambda'}^{(in)}(\vec{k}) + \overline{\beta_{\lambda\lambda'}(\vec{k})} \mathbf{a}_{\lambda'}^{(in)\dagger}(-\vec{k}) \right] \quad (6.12)$$

with  $\lambda, \lambda' = 0, \parallel$  and where  $\alpha_{\lambda\lambda'}$  and  $\beta_{\lambda\lambda'}$  are the so-called Bogolyubov coefficients (see [142] for a detailed discussion), which are normalized in our case according to:

$$\sum_{\rho, \rho'=0,\parallel} (\alpha_{\lambda\rho} \overline{\alpha_{\lambda'\rho'}} \eta_{\rho\rho'} - \beta_{\lambda\rho} \overline{\beta_{\lambda'\rho'}} \eta_{\rho\rho'}) = \eta_{\lambda\lambda'} \quad (6.13)$$

with  $\eta_{\lambda\lambda'} = \text{diag}(-1, 1)$  with  $\lambda, \lambda' = 0, \parallel$ . Notice that the normalization is different from the standard one [142], because of the presence of negative norm states.

Thus, the system will end up in a final state which no longer satisfies the weak Lorenz condition i.e. in the *out* region  $\partial_\nu \mathcal{A}_{out}^{v(+)} |\phi\rangle \neq 0$ . This is

shown in Fig. 6.1, where we have computed the final number of temporal and longitudinal photons  $n_\lambda^{out}(k) = \sum_{\lambda'} |\beta_{\lambda\lambda'}(\vec{k})|^2$ , starting from an initial vacuum state with  $n_0^{in}(k) = n_{||}^{in}(k) = 0$ . We see that, as commented above, in the final region  $n_0^{out}(k) \neq n_{||}^{out}(k)$  and the state no longer satisfies the Lorenz condition. Notice that the failure comes essentially from large scales ( $k\eta_0 \ll 1$ ), since on small scales ( $k\eta_0 \gg 1$ ), the Lorenz condition can be restored. This can be easily interpreted from the fact that on small scales the geometry can be considered as essentially Minkowskian.

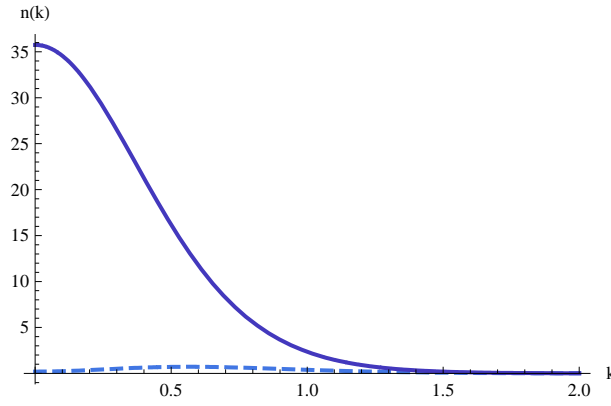


Figure 6.1: Occupation numbers for temporal (continuous line) and longitudinal (dashed line) photons in the *out* region vs.  $k$  in  $\eta_0^{-1}$  units.

In order to overcome this problem, it is possible to impose a more stringent gauge-fixing condition. Indeed, we have shown above that in a space-time configuration with asymptotic flat regions, an initial state satisfying the weak Lorenz condition does not necessarily satisfy it at a later time. However, it would be possible (see [143]) to define the physical states  $|\phi\rangle$  as those such that  $\nabla_\mu A^{\mu(+)}|\phi\rangle = 0, \forall\eta$ . Although this is a perfectly consistent solution, notice that the separation in positive and negative frequency parts depends on the space-time geometry and therefore, the determination of the physical states requires a previous knowledge of the geometry of the universe at all times.

Another possible way out would be to modify the standard Gupta-Bleuler formalism by including ghosts fields as done in non-abelian gauge theories [144]. With that purpose, the action of the theory (6.7) can be modified by including the ghost term (see [145, 146]):

$$S_g = \int d^4x \sqrt{g} g^{\mu\nu} \partial_\mu \bar{c} \partial_\nu c \quad (6.14)$$

where  $c$  are the complex scalar ghost fields. It is a well-known result [145, 146, 147] that by choosing appropriate boundary conditions for the electromagnetic and ghosts Green's functions, it is possible to get  $\langle \phi | T_{\mu\nu}^{\zeta} + T_{\mu\nu}^g | \phi \rangle = 0$ , where  $T_{\mu\nu}^{\zeta}$  and  $T_{\mu\nu}^g$  denote the contribution to the energy-momentum tensor from the  $\zeta$  term in (6.7) and from the ghost term (6.14) respectively. Notice that a choice of boundary conditions in the Green's functions corresponds to a choice of vacuum state. Therefore, also in this case an a priori knowledge of the future behavior of the universe geometry is required in order to determine the physical states.

In the following, we shall follow a different approach in order to deal with the difficulties found in the Gupta-Bleuler formalism and we shall explore the possibility of quantizing electromagnetism in an expanding universe without imposing any subsidiary condition.

## 6.4 Quantization without the Lorenz condition

In the previous Section it has been shown that although the Lorenz gauge-fixing conditions can be formally imposed in the covariant formalism, this cannot be done in a straightforward way. These difficulties could be suggesting some more fundamental obstacle in the formulation of an electromagnetic gauge invariant theory in an expanding universe. As a matter of fact, electromagnetic models which break gauge invariance on cosmological scales have been widely considered in the context of generation of primordial magnetic fields (see, for instance, [139]).

Let us then explore the possibility that the fundamental theory of electromagnetism is not given by the gauge invariant action (6.1), but by the gauge non-invariant action:

$$S = \int d^4x \sqrt{g} \left[ -\frac{1}{4} F_{\mu\nu} F^{\mu\nu} + \frac{\zeta}{2} (\nabla_{\mu} A^{\mu})^2 + A_{\mu} J^{\mu} \right]. \quad (6.15)$$

Notice that although this action is not invariant under general gauge transformations, it respects the invariance under residual ones and, as shown below, in Minkowski space-time, the theory is completely equivalent to standard QED. Let us emphasize that we are assuming that the inclusion of the gauge-fixing term is not a mathematical trick in order to quantize an otherwise gauge-invariant theory, but that such a term is an essential part of a gauge non-invariant electromagnetic theory. Since the

fundamental electromagnetic theory is assumed non-invariant under arbitrary gauge transformations, then there is no need to impose the Lorenz constraint in the quantization procedure. Therefore, having removed one constraint, the theory contains one additional degree of freedom. Naturally, the proposed modification of standard electromagnetism might have potential problems such as charge non-conservation, modification of usual Maxwell equations, introduction of unobserved extra polarizations or modification of interactions with charged fields. However, as we shall show later, none of these problems are actually present.

The general solution for the modified equations (6.8) can be written as:

$$\mathcal{A}_\mu = \mathcal{A}_\mu^{(1)} + \mathcal{A}_\mu^{(2)} + \mathcal{A}_\mu^{(s)} + \partial_\mu \theta \quad (6.16)$$

where  $\mathcal{A}_\mu^{(i)}$  with  $i = 1, 2$  are the two transverse modes of the massless photon,  $\mathcal{A}_\mu^{(s)}$  is a new scalar state that represents the mode that would have been eliminated if we had imposed the Lorenz condition and, finally,  $\partial_\mu \theta$  is a purely residual gauge mode, which can be eliminated by means of a residual gauge transformation in the asymptotically free regions, in a completely analogous way to the elimination of the  $A_0$  component in the Coulomb gauge.

In order to quantize the free theory, we perform the mode expansion of the field with the corresponding creation and annihilation operators for the *three* physical states:

$$\mathcal{A}_\mu = \int d^3\vec{k} \sum_{\lambda=1,2,s} \left[ \mathbf{a}_\lambda(k) \mathcal{A}_{\mu k}^{(\lambda)} + \mathbf{a}_\lambda^\dagger(k) \overline{\mathcal{A}_{\mu k}^{(\lambda)}} \right] \quad (6.17)$$

where the modes are required to be orthonormal with respect to the scalar product (see for instance [143]):

$$\begin{aligned} \left( \mathcal{A}_k^{(\lambda)}, \mathcal{A}_{k'}^{(\lambda')} \right) &= i \int_\Sigma d\Sigma_\mu \left[ \overline{\mathcal{A}_{\nu k}^{(\lambda)}} \Pi_{k'}^{(\lambda')\mu\nu} - \overline{\Pi_k^{(\lambda)\mu\nu}} \mathcal{A}_{\nu k'}^{(\lambda')} \right] \\ &= \delta_{\lambda\lambda'} \delta^{(3)}(\vec{k} - \vec{k}'), \quad \lambda, \lambda' = 1, 2, s \end{aligned} \quad (6.18)$$

where  $d\Sigma_\mu$  is the three-volume element of the Cauchy hypersurfaces. In a Robertson-Walker metric in conformal time, it reads  $d\Sigma_\mu = a^4(\eta)(d^3x, 0, 0, 0)$ . The generalized conjugate momenta are defined as:

$$\Pi^{\mu\nu} = -(F^{\mu\nu} - \zeta g^{\mu\nu} \nabla_\rho A^\rho) \quad (6.19)$$

Notice that the three modes can be chosen to have positive normalization. The equal-time commutation relations:

$$[\mathcal{A}_\mu(\eta, \vec{x}), \mathcal{A}_\nu(\eta, \vec{x}')] = [\Pi^{0\mu}(\eta, \vec{x}), \Pi^{0\nu}(\eta, \vec{x}')] = 0 \quad (6.20)$$

and

$$[\mathcal{A}_\mu(\eta, \vec{x}), \Pi^{0\nu}(\eta, \vec{x}')] = i \frac{\delta_\mu^\nu}{\sqrt{g}} \delta^{(3)}(\vec{x} - \vec{x}') \quad (6.21)$$

can be seen to imply the canonical commutation relations

$$[\mathbf{a}_\lambda(\vec{k}), \mathbf{a}_{\lambda'}^\dagger(\vec{k}')] = \delta_{\lambda\lambda'} \delta^{(3)}(\vec{k} - \vec{k}'), \quad \lambda, \lambda' = 1, 2, s \quad (6.22)$$

by means of the normalization condition in (6.18). Notice that the sign of the commutators is positive for the three physical states, i.e. there are no negative norm states in the theory, which in turn guarantees that there are no negative energy states as we will see below in an explicit example.

Since  $\nabla_\mu \mathcal{A}^\mu$  evolves as a minimally coupled scalar field, as shown in (6.9), on sub-Hubble scales ( $|k\eta| \gg 1$ ), we find that for arbitrary background evolution,  $|\nabla_\mu \mathcal{A}_k^{(s)\mu}| \propto a^{-1}$ , i.e. the field is suppressed by the universe expansion, thus effectively recovering the Lorenz condition on small scales. Notice that this is a consequence of the cosmological evolution, not being imposed as a boundary condition as in the flat space-time case.

On the other hand, on super-Hubble scales ( $|k\eta| \ll 1$ ),  $|\nabla_\mu \mathcal{A}_k^{(s)\mu}| = \text{const.}$  which implies that the field contributes as a cosmological constant in (6.7). Indeed, the energy-momentum tensor derived from (6.7) reads:

$$\begin{aligned} T_{\mu\nu} &= -F_{\mu\alpha} F_\nu^\alpha + \frac{1}{4} g_{\mu\nu} F_{\alpha\beta} F^{\alpha\beta} \\ &+ \frac{\xi}{2} \left[ g_{\mu\nu} \left[ (\nabla_\alpha A^\alpha)^2 + 2A^\alpha \nabla_\alpha (\nabla_\beta A^\beta) \right] - 4A_{(\mu} \nabla_{\nu)} (\nabla_\alpha A^\alpha) \right] \end{aligned} \quad (6.23)$$

Notice that for the scalar electromagnetic mode in the super-Hubble limit, the contributions involving  $F_{\mu\nu}$  vanish and only the piece proportional to  $\xi$  is relevant. Thus, it can be easily seen that, since in this case  $\nabla_\alpha A^\alpha = \text{constant}$ , the energy-momentum tensor is just given by:

$$T_{\mu\nu} = \frac{\xi}{2} g_{\mu\nu} (\nabla_\alpha A^\alpha)^2 \quad (6.24)$$

which is the energy-momentum tensor of a cosmological constant and whose value is given by the four-divergence of the electromagnetic field. Notice that, as seen in (6.9), the new scalar mode is a massless free field. This is one of the most relevant aspects of the present model in which, unlike existing dark energy theories based on scalar fields, dark energy can be generated without including any potential term or dimensional constant.

Since, as shown above, the field amplitude remains frozen on super-Hubble scales and starts decaying once the mode enters the horizon in the radiation or matter eras, the effect of the  $\zeta$  term in (6.8) is completely negligible on sub-Hubble scales, since the initial amplitude generated during inflation is very small as we will show below. Thus, below 1.3 AU, which is the largest distance scale at which electromagnetism has been tested [140], the modified Maxwell's equations (6.8) are physically indistinguishable from the flat space-time ones (6.2).

Notice that in Minkowski space-time, the theory (6.7) is completely equivalent to standard QED. This is so because, although non-gauge invariant, the corresponding effective action is equivalent to the standard BRS invariant effective action of QED. Thus, the effective action for QED obtained from (6.2) by the standard gauge-fixing procedure reads:

$$e^{iW} = \int [dA][dc][d\bar{c}][d\psi][d\bar{\psi}] e^{i \int d^4x \left( -\frac{1}{4} F_{\mu\nu} F^{\mu\nu} + \frac{\zeta}{2} (\partial_\mu A^\mu)^2 + \eta^{\mu\nu} \partial_\mu \bar{c} \partial_\nu c + \mathcal{L}_F \right)} \quad (6.25)$$

where  $\mathcal{L}_F$  is the Lagrangian density of charged fermions. The  $\zeta$  term and the ghosts field appear in the Faddeev-Popov procedure when selecting an element of each gauge orbit. However, ghosts being decoupled from the electromagnetic currents can be integrated out in flat space-time, so that up to an irrelevant normalization constant we find:

$$e^{iW} = \int [dA][d\psi][d\bar{\psi}] e^{i \int d^4x \left( -\frac{1}{4} F_{\mu\nu} F^{\mu\nu} + \frac{\zeta}{2} (\partial_\mu A^\mu)^2 + \mathcal{L}_F \right)} \quad (6.26)$$

which is nothing but the effective action coming from the gauge non-invariant theory (6.7) in flat space-time, in which no gauge-fixing procedure is required. Hence, the aforementioned potential problems related to charge conservation and charged fermions interactions are evaded because the effective actions are exactly the same in both cases. To summarize:

- Ordinary Maxwell's equations are recovered on those small scales in which electromagnetism has been tested.

- Electric charge is conserved since only the gauge electromagnetic sector is modified but not the sector of charged particles which preserves its gauge symmetry.
- The new state only couples gravitationally and evades laboratory detection.
- The new state has positive norm (energy).
- The effective action is completely equivalent to standard QED in the flat space-time limit. This guarantees, not only that the standard phenomenology is recovered, but also that no new interaction terms will appear in the renormalization procedure.

## 6.5 Quantum fluctuations during inflation

Let us consider an explicit example which is given by the quantization in an inflationary de Sitter spacetime with  $a(\eta) = -1/(H_I\eta)$ , with  $H_I$  the constant Hubble parameter during inflation. The explicit solution in the case  $\xi = 1/3$  for the normalized scalar state is:

$$\mathcal{A}_{0k}^{(s)} = \frac{-1}{(2\pi)^{3/2}} \frac{i}{\sqrt{2k}} \left\{ k\eta e^{-ik\eta} + \frac{1}{k\eta} \left[ \frac{1}{2}(1 + ik\eta)e^{-ik\eta} - k^2\eta^2 e^{ik\eta} E_1(2ik\eta) \right] \right\} e^{i\vec{k}\vec{x}}$$

$$\mathcal{A}_{\parallel k}^{(s)} = \frac{1}{(2\pi)^{3/2}} \frac{1}{\sqrt{2k}} \left\{ (1 + ik\eta)e^{-ik\eta} - \left[ \frac{3}{2}e^{-ik\eta} + (1 - ik\eta)e^{ik\eta} E_1(2ik\eta) \right] \right\} e^{i\vec{k}\vec{x}}$$
(6.27)

where  $E_1(x) = \int_1^\infty e^{-tx}/tdt$  is the exponential integral function. Using this solution, we find:

$$\nabla_\mu \mathcal{A}_k^{(s)\mu} = -\frac{a^{-2}(\eta)}{(2\pi)^{3/2}} \frac{ik}{\sqrt{2k}} \frac{3}{2} \frac{(1 + ik\eta)}{k^2\eta^2} e^{-ik\eta + i\vec{k}\vec{x}} \quad (6.28)$$

so that the field is suppressed in the sub-Hubble limit as  $\nabla_\mu \mathcal{A}_k^{(s)\mu} \sim \mathcal{O}((k\eta)^{-2})$  and the Maxwell equations are recovered on small scales, as commented before.

On the other hand, from the energy density given by  $\rho_A = T^0_0$ , we obtain in the sub-Hubble limit the corresponding Hamiltonian, which is

given by:

$$H = \frac{1}{2} \int \frac{d^3\vec{k}}{a^4(\eta)} k \sum_{\lambda=1,2,s} \left[ \mathbf{a}_\lambda^\dagger(\vec{k}) \mathbf{a}_\lambda(\vec{k}) + \mathbf{a}_\lambda(\vec{k}) \mathbf{a}_\lambda^\dagger(\vec{k}) \right]. \quad (6.29)$$

We see that the theory does not contain negative energy states (ghosts). In fact, as shown in Chapter 4, the theory does not exhibit either local gravity inconsistencies or classical instabilities.

Also, from (6.27) it is possible to obtain the dispersion of the effective cosmological constant during inflation:

$$\langle 0 | (\nabla_\mu \mathcal{A}^\mu)^2 | 0 \rangle = \int \frac{dk}{k} P_A(k) \quad (6.30)$$

with  $P_A(k) = 4\pi k^3 |\nabla_\mu \mathcal{A}_k^{(s)\mu}|^2$ . In the super-Hubble limit, we obtain for the power-spectrum:

$$P_A(k) = \frac{9H_I^4}{16\pi^2}. \quad (6.31)$$

Notice that this result implies that  $\rho_A \sim (H_I)^4$ . The measured value of the cosmological constant then requires  $H_I \sim 10^{-3}$  eV, which corresponds to an inflationary scale of  $M_I \sim 1$  TeV. Thus we see that the cosmological constant scale can be naturally explained in terms of physics at the electroweak scale.

In the case of quasi-de Sitter slow-roll inflation, the Hubble parameter reads  $\mathcal{H} = -1/((1-\varepsilon)\eta)$ , where the slow-roll parameter is defined as  $\varepsilon = 1/(16\pi G)(V'/V)^2 \ll 1$ , with  $V$  the inflaton potential. Following the same steps as before, we obtain the power spectrum for the comoving field  $A_0 = a\mathcal{A}_0$  on super-Hubble scales:

$$\mathcal{P}_{A_0}(k) \equiv \frac{k^3}{2\pi^2} \langle |A_{0k}|^2 \rangle = \frac{H_I^2}{16\pi^2} \left[ \frac{k}{aH_I} \right]^{n_{A_0}} \quad (6.32)$$

which is almost scale-invariant (as in the scalar field case) since for the electromagnetic spectral index we obtain  $n_{A_0} = -4\varepsilon$ . In a similar way it is possible to obtain the primordial power spectrum of longitudinal modes on super-Hubble scales:

$$\mathcal{P}_{A_\parallel}(k) = \frac{k^2}{16\pi^2\varepsilon^2} \left[ \frac{k}{aH_I} \right]^{-4\varepsilon} \quad (6.33)$$

If we now compare the power spectra for the conformal fields  $\mathcal{A}_0$  and  $\mathcal{A}_\parallel$  we find that:

$$\frac{\mathcal{P}_{\mathcal{A}_\parallel}(k)}{\mathcal{P}_{\mathcal{A}_0}(k)} = \frac{1}{\varepsilon^2} \left( \frac{k}{aH_I} \right)^2 \quad (6.34)$$

which is negligible on super-Hubble scales, and allows us to safely ignore the longitudinal modes on such scales after inflation. This also indicates that the effective cosmological constant will be essentially given by the temporal component of the scalar mode.

Notice that since  $\varepsilon > 0$ ,  $\mathcal{P}_{\mathcal{A}_0}(k)$  is a red-tilted spectrum which means that the contribution to  $\langle A_0^2 \rangle$  from long wavelengths dominates over small scales. In particular, provided inflation lasted for a sufficiently large number of e-folds, this allows to decompose the fluctuations field at any given time into a large homogeneous contribution (with scales  $k < \mathcal{H}$ ) and a small inhomogeneous perturbation ( $k > \mathcal{H}$ ), and therefore we can use standard perturbation theory around the homogeneous background. Thus, for the homogeneous part we get:

$$\langle A_0^2 \rangle_{hom} = \int_{k_{min}}^{k_*} \frac{dk}{k} \mathcal{P}_{\mathcal{A}_0}(k) \simeq H_I^2 \frac{e^{-n_{A_0} \tilde{N}}}{16\pi^2 |n_{A_0}|} \quad (6.35)$$

where  $k_* \lesssim H_0$ ,  $\tilde{N} = N_{tot} - N_0$  and  $k_{min} = e^{-\tilde{N}} H_0$  is set by the Hubble horizon at the beginning of inflation [148]. Here  $N_{tot}$  is the total number of e-folds of inflation which should not be confused with  $N_0$  which is the number of e-folds since the time when the scale  $H_0^{-1}$  left the horizon. Typical values for  $N_0$  are around 50, whereas generically there is no upper limit to  $N_{tot}$ . Thus as expected, up to tilt corrections,  $H_I$  sets the scale for the field dispersion.

## 6.6 Cosmological evolution

In this Section we shall study the cosmological evolution of the homogeneous part (zero mode) for the proposed theory of electromagnetism which will be nothing but the application of the results obtained in Chapter 3 to the present case. In order to do that, we need to consider the Einstein equations in addition to the equations of motion for the vector

field so that we have the set of equations

$$R_{\mu\nu} - \frac{1}{2}Rg_{\mu\nu} = 8\pi G (T_{\mu\nu} + T_{\mu\nu}^A) \quad (6.36)$$

$$\nabla_\nu F^{\mu\nu} + \zeta \nabla^\mu \nabla_\nu A^\nu = 0 \quad (6.37)$$

where  $T_{\mu\nu}$  is the energy-momentum tensor for matter and radiation and  $T_{\mu\nu}^A$  is the energy-momentum tensor of the electromagnetic field. Now, we shall consider a spatially flat FLRW universe whose metric is given by (1.5) with  $k = 0$ . In this Section we will be using cosmic time instead of conformal time, being the corresponding components of the vector field related by  $\mathcal{A}_0 = aA_0$  and  $\vec{\mathcal{A}} = \vec{A}$ . In this spacetime, equations (6.37) read:

$$\ddot{A}_0 + 3H\dot{A}_0 + 3\dot{H}A_0 = 0 \quad (6.38)$$

$$\ddot{\vec{A}} + H\dot{\vec{A}} = 0. \quad (6.39)$$

Notice that (6.38) implies that the gauge-fixing term exactly behaves as a cosmological constant throughout the history of the universe irrespective of the background evolution. Indeed, for homogeneous fields we have:

$$\frac{d}{dt}(\nabla_\mu A^\mu) = \frac{d}{dt}(\dot{A}_0 + 3HA_0) = 0 \quad (6.40)$$

confirming that the gauge-fixing term acts as an effective cosmological constant on super-Hubble scales in a FLRW universe, as we had already deduced from the fact  $\nabla_\mu A^\mu$  behaves as a scalar field and, hence, it is constant on such scales.

We can solve (6.38) and (6.39) during the radiation and matter dominated epochs when the Hubble parameter is given by  $H = p/t$  with  $p = 1/2$  for radiation and  $p = 2/3$  for matter. In such a case the solutions for (6.39) are:

$$A_0(t) = A_0^+ t + A_0^- t^{-3p} \quad (6.41)$$

$$\vec{A}(t) = \vec{A}^+ t^{1-p} + \vec{A}^- \quad (6.42)$$

where  $A_0^\pm$  and  $\vec{A}^\pm$  are constants of integration. Hence, the growing mode of the temporal component does not depend on the epoch being always proportional to the cosmic time  $t$ , whereas the growing mode of the spatial component evolves as  $t^{1/2}$  during radiation and as  $t^{1/3}$  during matter, i.e. at late times the temporal component will dominate over the spatial ones.

On the other hand, the Friedmann equation adopts the following form:

$$H^2 = \frac{8\pi G}{3} \left[ \sum_{\alpha=R,M} \rho_\alpha + \rho_{A_0} + \rho_{\vec{A}} \right] \quad (6.43)$$

where  $R, M$  stands for radiation and matter respectively and the energy densities of the temporal and spatial parts of the electromagnetic field are given by:

$$\rho_{A_0} = \xi \left( \frac{9}{2} H^2 A_0^2 + 3 H A_0 \dot{A}_0 + \frac{1}{2} \dot{A}_0^2 \right) \quad (6.44)$$

$$\rho_{\vec{A}} = \frac{1}{2a^2} (\dot{\vec{A}})^2 \quad (6.45)$$

Notice that we need  $\xi > 0$  in order to have positive energy density for  $A_0$ . Besides, when inserting the solutions (6.41) and (6.42) into these expressions we obtain that  $\rho_{A_0} = \rho_{A_0}^0$ ,  $\rho_{\vec{A}} = \rho_{\vec{A}}^0 a^{-4}$ , as we expected from our previous results. Thus, once again we have that the electromagnetic field behaves as a cosmological constant throughout the evolution of the universe since its temporal component gives rise to a constant energy density whereas the energy density corresponding to  $\vec{A}$  always decays as radiation. Moreover, this fact together with our result that the initial amplitude of the longitudinal component generated during inflation is strongly suppressed with respect to the temporal one, as shown in (6.34), prevents the generation of too large anisotropies which could be in conflict with CMB measurements. Finally, when the universe is dominated by the effective cosmological constant arising from the gauge-fixing term, both the Hubble parameter and  $A_0$  become constant leading therefore to a future de Sitter universe.

Finally, it is straightforward to show that the value of  $\nabla_\mu A^\mu$  giving rise to the effective cosmological constant on large scales is not affected by the high conductivity of the universe. The effects of conductivity can be taken into account by introducing the corresponding conserved current on the r.h.s. of Maxwell equations. However as shown in (6.9), the field  $\nabla_\mu A^\mu$  behaves as a free scalar field so that it is constant on super-Hubbles scales independently of the presence of external conserved currents.

## 6.7 Perturbations

In this Section we shall derive the equations for the perturbations and solve them analytically for some simple cases. We shall do the calculations in the conformal Newtonian gauge, although we shall also give the corresponding expressions for the synchronous gauge which will be necessary in order to modify the publicly available numerical CAMB code [149]. Moreover, it will be convenient to introduce a redefinition of the vector field as  $\hat{\mathcal{A}}_0 = a^2 \mathcal{A}_0$  so that the field equation and the energy density look much simpler:

$$\left(a^{-4} \hat{\mathcal{A}}_0'\right)' = 0 \quad (6.46)$$

$$\rho_{A_0} = \frac{1}{6a^8} (\hat{\mathcal{A}}_0')^2 \quad (6.47)$$

and we clearly see that the energy density is constant.

We only consider the case of scalar perturbations because we have checked that the vector perturbations evolve in the same way as in standard Maxwell theory and the tensor perturbations remain unaffected by the presence of the gauge fixing term as well. One might expect this because the gauge fixing term only affects the new scalar mode which, being scalar, can contribute to the scalar perturbations, but not to the pure transverse vector perturbations (i.e., the usual photons). We shall do the calculations of this Section in the conformal Newtonian gauge, although we shall give the corresponding expressions for the synchronous gauge as well because we will need them later on.

In principle, as commented above, the effect of the high-electric conductivity of the universe should be taken into account including the corresponding electromagnetic current in the r.h.s of Maxwell equations. The reason why we can neglect such effects also in the presence of perturbations is the following. The electromagnetic current should satisfy the conservation equation:

$$\nabla_\mu J^\mu = 0 \quad (6.48)$$

and also the condition of electric neutrality, i.e.

$$u^\mu J_\mu = 0 \quad (6.49)$$

with  $u_\mu$  the four-velocity of the comoving observers. Let us expand also the current up to first order as:

$$J_\mu = J_\mu^0 + \delta J_\mu \quad (6.50)$$

but  $J_\mu^0 = 0$  for the homogeneous and isotropic electrically neutral background (this is the reason why we did not consider the current term in the background equations). If we now assume that the universe remains neutral at first order in the perturbations we have that  $\delta J_0 = 0$  and, finally, from current conservation, we get:  $\vec{\nabla} \cdot \vec{\delta J} = 0$ , i.e. the perturbed current is transverse. In other words, when computing scalar perturbations, we can ignore the effect of electric conductivity by assuming that the electric charge vanishes at first order as well.

In the newtonian gauge, the perturbed line element is given by:

$$ds^2 = a(\eta)^2 \left[ (1 + 2\psi)d\eta^2 - (1 - 2\phi)\delta_{ij}dx^i dx^j \right] \quad (6.51)$$

In the absence of any anisotropic stress sources we have  $\phi = \psi$ . In order to simplify the expressions we will use latter, we define the scalar perturbation of the vector field in an analogous manner to that of the background field with a factor  $a^2$ :

$$\delta \mathcal{A}_\mu = a^{-2}(\delta \hat{\mathcal{A}}_0, \nabla \hat{\mathcal{A}}) \quad (6.52)$$

As usual, we shall introduce the Fourier components of the perturbations and solve the corresponding equations for them. Then, from the modified Maxwell equations we can obtain the following equations for the Fourier modes of the vector field perturbations:

$$\begin{aligned} \delta \hat{\mathcal{A}}''_{0k} - 4\mathcal{H}\delta \hat{\mathcal{A}}'_{0k} - 3k^2\delta \hat{\mathcal{A}}_{0k} = \\ 2k^2 (5\mathcal{H}\delta \hat{\mathcal{A}}_k - 2\delta \hat{\mathcal{A}}'_k) + [(\psi''_k - 4\mathcal{H}\psi'_k + 3\phi''_k - 12\mathcal{H}\phi'_k) \hat{\mathcal{A}}_0 + 3(\psi'_k + \phi'_k)\hat{\mathcal{A}}'_0], \end{aligned} \quad (6.53)$$

$$\begin{aligned} \delta \hat{\mathcal{A}}''_k - 4\mathcal{H}\delta \hat{\mathcal{A}}'_k + \left(4\mathcal{H}^2 - 2\mathcal{H}' - \frac{1}{3}k^2\right) \delta \hat{\mathcal{A}}_k = \\ 2 \left( \frac{2}{3}\delta \hat{\mathcal{A}}'_{0k} - \mathcal{H}\delta \hat{\mathcal{A}}_{0k} \right) - \left[ \left( \frac{1}{3}\psi'_k + \phi'_k \right) \hat{\mathcal{A}}_0 + \frac{2}{3}\psi_k \hat{\mathcal{A}}'_0 \right]. \end{aligned} \quad (6.54)$$

In these equations we can see that the two perturbations of the vector field are coupled to each other and that the metric perturbations act as a source of them. Then, even in the case that the initial perturbations vanish

the gravitational potentials will generate perturbations of the vector field that, eventually, may also be source of the metric perturbations.

On the other hand, the corresponding perturbed energy-momentum tensor components are given by:

$$\begin{aligned}\delta T^0_0 &= \frac{1}{3a^8} \left\{ [-2\psi_k \hat{\mathcal{A}}'_0 + \delta \hat{\mathcal{A}}'_{0k} - (3\phi'_k + \psi'_k) \hat{\mathcal{A}}_0] \hat{\mathcal{A}}'_0 \right. \\ &\quad \left. + k^2 [(3\delta \hat{\mathcal{A}}'_k - 6\mathcal{H}\delta \hat{\mathcal{A}}_k - 3\delta \hat{\mathcal{A}}_{0k}) \hat{\mathcal{A}}_0 + \delta \hat{\mathcal{A}}_k \hat{\mathcal{A}}'_0] \right\}, \\ \delta T^i_j &= \frac{1}{3a^8} \left\{ [-2\psi_k \hat{\mathcal{A}}'_0 + \delta \hat{\mathcal{A}}'_{0k} - (3\phi'_k + \psi'_k) \hat{\mathcal{A}}_0] \hat{\mathcal{A}}'_0 \right. \\ &\quad \left. + k^2 [(-3\delta \hat{\mathcal{A}}'_k + 6\mathcal{H}\delta \hat{\mathcal{A}}_k + 3\delta \hat{\mathcal{A}}_{0k}) \hat{\mathcal{A}}_0 + \delta \hat{\mathcal{A}}_k \hat{\mathcal{A}}'_0] \right\} \delta^i_j, \\ \delta T^0_i &= -\frac{ik_i}{3a^8} \hat{\mathcal{A}}_0 \left[ -(3\phi'_k + \psi'_k) \hat{\mathcal{A}}_0 - 2\psi_k \hat{\mathcal{A}}'_0 + \delta \hat{\mathcal{A}}'_{0k} + k^2 \delta \hat{\mathcal{A}}_k \right].\end{aligned}\quad (6.55)$$

It is interesting to note that this model has vanishing shear, i.e.,  $\delta T^i_j = -\delta p_k \delta^i_j$ . This is due to there being only one physical scalar mode present. Moreover, from expressions (6.55) one can find the following relation between the perturbed energy density and pressure of the field:

$$\delta(\rho_k + p_k) = -\frac{2\hat{\mathcal{A}}_0 k^2}{a^8} (\delta \hat{\mathcal{A}}_{0k} - \delta \hat{\mathcal{A}}'_k + 2\mathcal{H}\delta \hat{\mathcal{A}}_k). \quad (6.56)$$

This relation is important because for a gauge mode satisfying  $\delta \mathcal{A}_\mu = a^{-2} \delta \hat{\mathcal{A}}_\mu = \partial_\mu \chi$  (remember here the definition of the perturbations given in (6.52)) one has that  $\delta \hat{\mathcal{A}}_0 = \delta \hat{\mathcal{A}}' + 2\mathcal{H}\delta \hat{\mathcal{A}}$  and, as a consequence,  $\delta(\rho_k + p_k) = 0$ .

In the following we shall derive the equations of the perturbations and all the other expressions in the synchronous gauge, for which the perturbed line element is:

$$ds^2 = a(\eta)^2 \left[ d\eta^2 - (\delta_{ij} + h_{ij}) dx^i dx^j \right]. \quad (6.57)$$

The scalar modes of the perturbation are usually expressed in terms of the scalar functions  $h_k$  and  $\eta_k$ <sup>3</sup> defined by means of [150]:

$$h_{ij}^{(s)} = \int d^3k \left[ \frac{k_i k_j}{k^2} h_k(\eta) + \left( \frac{k_i k_j}{k^2} - \frac{1}{3} \delta_{ij} \right) 6\eta_k(\eta) \right] e^{i\vec{k}\cdot\vec{x}}. \quad (6.58)$$

<sup>3</sup>The metric perturbation  $\eta_k$  should not be confused with conformal time  $\eta$

To go from one gauge to another we perform a coordinate transformation given by:

$$\hat{x}^\mu = x^\mu + \zeta^\mu. \quad (6.59)$$

Since we are considering only scalar perturbations we can set  $\zeta^\mu = (\alpha, \vec{\nabla}\beta)$ . The relation between the scalar metric perturbations in both gauges is as follows [150]:

$$\psi_k = \frac{1}{2k^2} [h_k'' + 6\eta_k'' + \mathcal{H}(h_k' + 6\eta_k')] \quad (6.60)$$

$$\phi_k = \eta_k - \frac{1}{2k^2} \mathcal{H}(h_k' + 6\eta_k') \quad (6.61)$$

with  $\alpha_k = \beta_k'$  and

$$\beta_k = -\frac{1}{2k^2} (h_k + 6\eta_k). \quad (6.62)$$

The transformation for the vector field  $\mathcal{A}_\mu$  and its energy-momentum tensor are given in terms of the Lie derivative  $\mathcal{L}$  by  $\delta_\zeta \mathcal{A}_\mu = -\mathcal{L}_\zeta \mathcal{A}_\mu$  and  $\delta_\zeta T^\mu_\nu = -\mathcal{L}_\zeta T^\mu_\nu$  respectively. From these transformation laws we obtain for the vector field

$$\delta_\zeta \mathcal{A}_0 = -(\alpha \mathcal{A}_0)' \quad (6.63)$$

$$\delta_\zeta \mathcal{A}_i = -\partial_i \alpha \mathcal{A}_0 \quad (6.64)$$

so that the perturbations  $\delta \hat{\mathcal{A}}_0$  and  $\delta \hat{\mathcal{A}}$  in both gauges relate as:

$$\begin{aligned} \delta \hat{\mathcal{A}}_0^{conf} &= \delta \hat{\mathcal{A}}_0^{syn} + (\alpha \hat{\mathcal{A}}_0)' - 2\mathcal{H}\alpha \hat{\mathcal{A}}_0, \\ \mathcal{A}^{conf} &= \mathcal{A}^{syn} + \alpha \hat{\mathcal{A}}_0. \end{aligned} \quad (6.65)$$

These relations show that the combination  $\delta \hat{\mathcal{A}}_0 - \mathcal{A} + 2\mathcal{H}\mathcal{A}_0$  is gauge-invariant (in the sense of cosmological perturbations).

On the other hand, for the energy-momentum tensor we obtain:

$$\delta_\zeta T^0_0 = -\alpha T^0_{0,0} \quad (6.66)$$

$$\delta_\zeta T^i_j = -\alpha T^i_{j,0} \quad (6.67)$$

$$\delta_\zeta T^0_i = -\left(T^0_0 - \frac{1}{3} T^j_j\right) \partial_i \alpha \quad (6.68)$$

It is very interesting to note that, given that the background evolution of the vector field is the same as that of a cosmological constant we have that both the unperturbed energy density and pressure are constant and they

satisfy  $\rho + p = 0$  so that the energy momentum tensor remains invariant after the gauge transformation. In fact, this is what one would expect from Stewart-Walker lemma [151]. Notice also that due to the gauge invariance of the energy momentum tensor the results obtained in the conformal gauge are also valid for the synchronous gauge.

The perturbed equations for the vector field in the synchronous gauge are:

$$\begin{aligned} \delta \hat{\mathcal{A}}''_{0k} - 4\mathcal{H}\delta \hat{\mathcal{A}}'_{0k} - 3k^2\delta \hat{\mathcal{A}}_{0k} = \\ - 2k^2(2\delta \hat{\mathcal{A}}'_k - 5\mathcal{H}\delta \hat{\mathcal{A}}_k) - \frac{1}{2}[(h''_k - 4\mathcal{H}h'_k)\hat{\mathcal{A}}_0 + h'_k\hat{\mathcal{A}}'_0] \end{aligned} \quad (6.69)$$

$$\delta \hat{\mathcal{A}}''_k - 4\mathcal{H}\delta \hat{\mathcal{A}}'_k + \left(4\mathcal{H}^2 - 2\mathcal{H}' - \frac{1}{3}k^2\right)\delta \hat{\mathcal{A}}_k = 2\left(\frac{2}{3}\delta \hat{\mathcal{A}}'_{0k} - \mathcal{H}\delta \hat{\mathcal{A}}_{0k}\right) + \frac{1}{6}h'_k\hat{\mathcal{A}}_0 \quad (6.70)$$

and the perturbed energy-momentum components in the synchronous gauge are:

$$\begin{aligned} \delta T^0_0 &= \frac{1}{6a^8} \left\{ (2\delta \hat{\mathcal{A}}'_{0k} + \hat{\mathcal{A}}_0 h'_k) \hat{\mathcal{A}}'_0 \right. \\ &\quad \left. + 2k^2 [(-3\delta \hat{\mathcal{A}}_{0k} + 3\delta \hat{\mathcal{A}}'_k - 6\mathcal{H}\delta \hat{\mathcal{A}}_k)\hat{\mathcal{A}}_0 + \hat{\mathcal{A}}'_0\delta \hat{\mathcal{A}}_k] \right\}, \\ \delta T^i_j &= \frac{1}{6a^8} \left\{ (2\delta \hat{\mathcal{A}}'_{0k} + \hat{\mathcal{A}}_0 h'_k) \hat{\mathcal{A}}'_0 \right. \\ &\quad \left. + 2k^2 [3\delta \hat{\mathcal{A}}_{0k} - 3\delta \hat{\mathcal{A}}'_k + 6\mathcal{H}\delta \hat{\mathcal{A}}_k)\hat{\mathcal{A}}_0 + \hat{\mathcal{A}}'_0\delta \hat{\mathcal{A}}_k] \right\} \delta^i_j, \\ \delta T^0_i &= -\frac{ik_i}{6a^8} \hat{\mathcal{A}}_0 [h'_k\hat{\mathcal{A}}_0 + 2\delta \hat{\mathcal{A}}'_{0k} + 2k^2\delta \hat{\mathcal{A}}_k]. \end{aligned} \quad (6.71)$$

Condition (6.56) remains the same in this case:

$$\delta(\rho_k + p_k) = -\frac{2\hat{\mathcal{A}}_0 k^2}{a^8} (\delta \hat{\mathcal{A}}_{0k} - \delta \hat{\mathcal{A}}'_k + 2\mathcal{H}\delta \hat{\mathcal{A}}_k) \quad (6.72)$$

which is just a consequence of the aforementioned fact that the combination  $\delta \hat{\mathcal{A}}_0 - \delta \hat{\mathcal{A}}' + 2\mathcal{H}\delta \hat{\mathcal{A}}$  does not depend on the gauge choice.

### 6.7.1 Evolution during radiation and matter dominated eras

In order to obtain some analytical results, in the following we shall consider that the metric perturbations are generated by some dominating fluid and study the evolution of the electromagnetic perturbations in such a scenario. In other words, we shall assume that the perturbations of the electromagnetic field will not affect the metric perturbations evolution. This assumption is justified as long as the electromagnetic energy density is clearly subdominant as it happens in most of the universe evolution when the energy density associated to the electromagnetic field is many orders of magnitude below that of the dominant component. However, such a condition will eventually breakdown at low redshift when dark energy becomes dominant and the results obtained here lack validity, being necessary to resort to a numerical treatment. In the early universe when radiation represents the dominant contribution to the energy density of the universe and neglecting neutrinos shear (which implies that  $\psi = \phi$ ) the metric perturbation evolves as [131]:

$$\phi_k = \frac{C_{1k}[\omega\eta \cos(\omega\eta) - \sin(\omega\eta)] + C_{2k}[\omega\eta \sin(\omega\eta) + \cos(\omega\eta)]}{\eta^3} \quad (6.73)$$

with  $\omega = k/\sqrt{3}$ . On the other hand, in a matter dominated universe, the gravitational potential becomes constant in time, i.e.,  $\phi_k = \text{const}$ . Then, we can solve the equations (6.54) in the presence of the gravitational perturbations produced by a radiation or matter fluid and obtain the evolution of the vector field perturbations in those epochs. The results are shown in Fig. 6.2. We can see that, on super-Hubble scales, the perturbation  $\delta\hat{A}_0$  evolves in the same way as the background vector field so that  $\delta\hat{A}_0/A_0 = \text{const}$  as one would expect. This also implies that the perturbed energy density is constant on large-scales as we can see in the figure. Moreover, this feature does not depend on the dominating fluid, i.e., it happens for both the radiation and matter eras. On small scales, the perturbed energy density evolves with constant amplitude when the universe is dominated by radiation whereas the amplitude decays as  $1/\eta$  in the matter era. Notice that this behavior on small scales is a common feature for all the perturbed components of the energy-momentum tensor, i.e., the energy, the pressure and the scalar component of the momentum.

We shall obtain the explicit evolution for the electromagnetic perturbations during the matter-dominated era, when most of the cosmologically relevant scales reenter the horizon. In that epoch, the gravitational potential is constant as we said above so that  $\phi_k = \psi_k = \phi_0$  and the Hubble parameter satisfies  $\mathcal{H}' = -\frac{1}{2}\mathcal{H}^2$ . With these conditions, we can obtain the following expression for  $\delta\hat{\mathcal{A}}$  in terms of  $\delta\hat{\mathcal{A}}_0$  and  $\phi_0$ :

$$\delta\hat{\mathcal{A}}_k = \frac{-3}{4k^2} \left[ \delta\hat{\mathcal{A}}_{0k}''' - \frac{11}{2}\mathcal{H}\delta\hat{\mathcal{A}}_{0k}'' + \left( \frac{7}{3}k^2 - 8\mathcal{H}^2 \right) \delta\hat{\mathcal{A}}_{0k}' - \frac{7}{2}\mathcal{H}k^2\delta\hat{\mathcal{A}}_{0k} - \frac{8}{3}\hat{\mathcal{A}}_0'\phi_0 \right]. \quad (6.74)$$

This relation allows to find the following fourth-order differential equation for  $\delta\hat{\mathcal{A}}_{0k}$ :

$$\delta\hat{\mathcal{A}}_{0k}^{\text{iv}} - 8\mathcal{H}\delta\hat{\mathcal{A}}_{0k}''' + 2 \left( k^2 - \frac{49}{4}\mathcal{H}^2 \right) \delta\hat{\mathcal{A}}_{0k}'' - 8\mathcal{H}^2 \left( k + \frac{7}{2}\mathcal{H} \right) \delta\hat{\mathcal{A}}_{0k}' + k^2 \left( k^2 + \frac{21}{2}\mathcal{H}^2 \right) \delta\hat{\mathcal{A}}_{0k} = 4k^2\mathcal{H}\hat{\mathcal{A}}_0'\phi_0. \quad (6.75)$$

This equation together with the relation (6.74) determine the evolution of the electromagnetic perturbations in a matter dominated universe. It is convenient to remind here the assumptions under which such equations remain valid. In order to obtain those equations we have assumed that the metric perturbations act as an external source for the electromagnetic perturbations and that this external source is uniquely determined by the matter fluid. This means that the contribution of the electromagnetic field to the perturbed Einstein equations are negligible with respect to that of the matter component, which is a good approximation as long as the electromagnetic field energy density is well below the matter energy density. However, this condition eventually breakdowns because the electromagnetic field becomes dominant and it contributes in a non-negligible way to the Einstein equations so that the metric perturbations becomes affected by the electromagnetic field perturbations and the full system of coupled equations must be solved.

In order to solve eq. (6.75), we shall take advantage of the residual gauge symmetry of the theory, namely,  $A_\mu \rightarrow A_\mu + \partial_\mu\theta$  with  $\square\theta = 0$ . From this symmetry, we know that  $\delta\hat{\mathcal{A}}_0 = a^2\theta'$  will be solution of (6.75) so that we can factorize it as  $\mathcal{F}[\mathcal{G}(\delta\hat{\mathcal{A}}_0)] = 4k^2\mathcal{H}\hat{\mathcal{A}}_0'\phi_0$ , where  $\mathcal{F}$  is a second order differential operator and  $\mathcal{G}$  is the operator determining the evolution of  $a^2\theta'$  which can be deduced from the equation satisfied for  $\theta$  and turns out to be  $\mathcal{G} = \frac{d^2}{d\eta^2} - 2\mathcal{H}\frac{d}{d\eta} + k^2$ . Therefore, the equation (6.75)

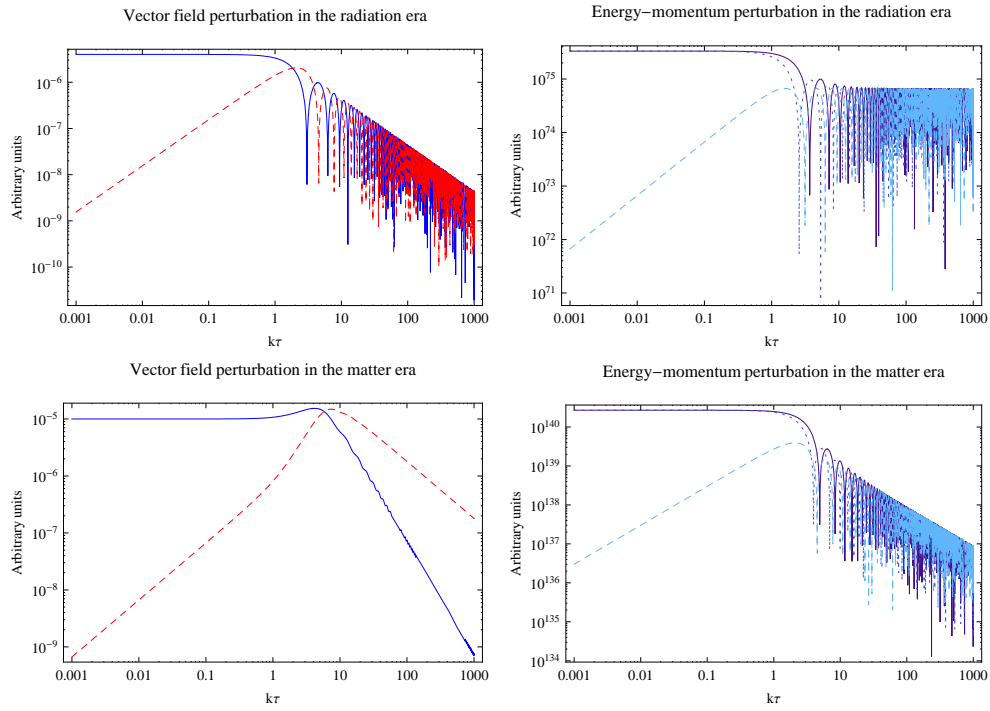


Figure 6.2: In these figures we show the evolution of the vector field perturbations in the Newtonian gauge for radiation (upper panel) and matter (lower panel) dominated universes. In the left panels we show the evolution of the vector field perturbations  $\delta\hat{\mathcal{A}}_0/\hat{\mathcal{A}}_0$  (solid-blue) and  $k\delta\hat{\mathcal{A}}/\hat{\mathcal{A}}_0$  (dashed-red). The right panels show the perturbed energy density  $\delta T_0^0$  (solid), pressure  $-\frac{1}{3}\delta T_i^i$  (dotted) and momentum  $-\frac{1}{ik^2}k_i\delta T_i^0$  (dashed).

can be expressed as:

$$\left[ \frac{d^2}{d\eta^2} - 6\mathcal{H} \frac{d}{d\eta} + \left( k^2 + \frac{21}{2} \mathcal{H}^2 \right) \right] \left[ \frac{d^2}{d\eta^2} - 2\mathcal{H} \frac{d}{d\eta} + k^2 \right] \delta \hat{\mathcal{A}}_{0k} = 4k^2 \mathcal{H} \hat{\mathcal{A}}'_0 \phi_0. \quad (6.76)$$

Thus, the solution for  $\delta \hat{\mathcal{A}}_0$  will be determined by the equation  $\mathcal{G}(\delta \hat{\mathcal{A}}_0) = S$  with  $S$  the solution of the equation  $\mathcal{F}(S) = 4k^2 \mathcal{H} \hat{\mathcal{A}}'_0 \phi_0$ . Since  $\mathcal{H} = \frac{2}{\eta}$  in the matter era, we can obtain the explicit form of the kernel of  $\mathcal{F}$  (solutions of the homogeneous equation) and is given by:

$$S_{hom}(\eta) = \eta^6 \left( C_{S1} e^{-ik\eta} + C_{S2} e^{ik\eta} \right) \quad (6.77)$$

whereas a particular solution can be obtained by:

$$S_{part} = S_1 \int \frac{S_2}{\det W_S} 4k^2 \mathcal{H} \hat{\mathcal{A}}'_0 \phi_0 d\eta - S_2 \int \frac{S_1}{\det W_S} 4k^2 \mathcal{H} \hat{\mathcal{A}}'_0 \phi_0 d\eta \quad (6.78)$$

where  $S_1$  and  $S_2$  are the two independent solutions given above and  $\det W_S = S'_1 S_2 - S'_2 S_1 = 2ik\eta^{12} C_{S1} C_{S2}$  is the determinant of the Wronskian. Following the same procedure, we obtain the kernel of  $\mathcal{G}$

$$\delta \hat{\mathcal{A}}_0^{hom}(\eta) = C_1 \left( k^2 \eta^2 - 3ik\eta - 3 \right) e^{-ik\eta} + C_2 \left( k^2 \eta^2 + 3ik\eta - 3 \right) e^{ik\eta} \quad (6.79)$$

whereas the particular solution is

$$\delta \hat{\mathcal{A}}_0^{part} = \delta \hat{\mathcal{A}}_{0,C1} \int \frac{\delta \hat{\mathcal{A}}_{0,C2}}{\det W_C} S(\eta) d\eta - \delta \hat{\mathcal{A}}_{0,C2} \int \frac{\delta \hat{\mathcal{A}}_{0,C1}}{\det W_C} S(\eta) d\eta \quad (6.80)$$

with  $\det W_C = 2ik^5 \eta^4 C_1 C_2$ . The homogeneous solution corresponds to the pure gauge degree of freedom and it does not contribute to the perturbed energy density, whereas the particular solution gives rise to the oscillating behavior with an amplitude decaying as  $\eta^{-1}$  for small scales shown in Fig. 6.2.

We would like to remark that the procedure followed in order to solve the equations for a matter dominated universe is completely general and can be applied in any other situation where the metric perturbations is originated by some other component.

### 6.7.2 Evolution of the perturbations

In this Section we shall present the results we obtain by modifying the publicly available CAMB code [149] to compute the CMB power spectrum

when electromagnetic perturbations are taken into account. Since the background of the electromagnetic model is the same as that of  $\Lambda$ CDM, we do not need to modify the background equations of the code, although we do have to add the evolution equation for  $\hat{\mathcal{A}}_0$ . We use the first order equation (6.47) so that we can relate the background electromagnetic field directly to the present value of its density parameter. The initial condition for this equation is unimportant for the background evolution, although it becomes relevant for the perturbations and it is set by assuming a power law behavior for  $\hat{\mathcal{A}}_0$ . For the perturbation equations, we add the two evolution equations for the electromagnetic perturbations given by (6.70) and modify the corresponding terms involving dark energy perturbations. With these modifications, the code is ready to compute the evolution of the perturbations in the cosmology corresponding to the electromagnetic model and, thus, obtain the CMB power spectrum as well as the matter power spectrum.

Before proceeding to show the obtained results, we shall discuss what the initial conditions for the electromagnetic field perturbations should be. A natural origin for the presence of the new mode of the electromagnetic field on cosmological scales has been proved to be the quantum fluctuations of such a mode during an inflationary epoch. In such a scenario, only the new scalar mode can be excited because of the conformal invariance of the usual transverse modes. The "homogeneous part" of this scalar mode, defined as the sum of all the modes which remain super-Hubble today, gives rise to the effective cosmological constant whereas the modes which have already reentered into the horizon constitute the origin of the electromagnetic perturbations discussed in the present Section. In other words, we can split the primordial quantum fluctuations of the scalar mode generated during inflation in a homogeneous part comprising all the modes with  $k < k_0$  (being  $k_0$  the scale that is entering into the horizon today, i.e., the present Hubble radius) and an inhomogeneous part formed by those modes with  $k > k_0$ . Notice that such a split can be performed because the primordial power spectrum for the scalar mode is red-tilted, as shown in the previous Sections, so that the homogeneous part is large as compared to the inhomogeneous one and this enable us to treat the latter as a perturbation. For the mentioned scalar mode, one can see that the longitudinal component decays with respect to the temporal component on super-Hubble scales for a de-Sitter inflationary epoch (in an analogous manner to that shown for the background evolution) so that, at the end of inflation, the amplitude of the longitudinal component would be expected to be much smaller than the temporal one. Moreover,

we have already shown that the longitudinal components also decay with respect to the temporal one in the radiation dominated epoch so that the super-Hubble modes would be expected to be strongly suppressed at the time when the initial conditions are given, which justifies setting the initial condition for  $\delta\hat{\mathcal{A}}_k$  to zero. On the other hand, the power spectrum of the quantum fluctuations generated during a de Sitter inflation for the temporal component happens to be scale-invariant<sup>4</sup> so that we can set the initial condition for  $\delta\hat{\mathcal{A}}_{0k}$  as  $\delta\hat{\mathcal{A}}_{0k}(\tau_{ini}) = A k^{-3/2}$  with  $A$  a constant depending on the details of the inflationary epoch such as the initial amplitude of the power spectrum after inflation or the duration of inflation. For our purposes in this Section, this constant  $A$  will play the role of a free parameter to be constrained by comparing the CMB power spectrum produced by the model to the WMAP data. In the same way as for the background vector field, we shall give the initial condition for the derivative of  $\delta\hat{\mathcal{A}}_{0k}$  by assuming a power-law behavior. This is justified because we know that this is the type of evolution for the perturbations on super-Hubble scales, where the initial conditions are given.

In Fig. 6.3 and Fig. 6.4 we show the results obtained from the modified version of the CAMB code. The modifications in both the CMB and matter power spectrum is originated thanks to the fact that, unlike in the cosmological constant case, the electromagnetic dark energy model produces fluctuations that might modify the evolution of the gravitational potential. In that figure, we can see that the small scales behavior is unaffected with respect to the standard  $\Lambda$ CDM case. The reason for this is that the electromagnetic perturbations decay very rapidly once they enter into the horizon as we have shown in the previous section so that only those electromagnetic modes whose scales have become sub-Hubble very recently (corresponding to the low multipoles part of the spectrum) can contribute in a non-negligible way to the metric perturbation evolution through Einstein equations. Moreover, since dark energy density is negligible during decoupling, the contribution of electromagnetic perturbations to the ordinary Sachs-Wolfe effect is also negligible. The main effect will appear in the late-time Integrated Sachs-Wolfe (ISW) effect as due to the evolution of the metric perturbation. The analytical estimate of such an effect is difficult to obtain since it requires to know the time

---

<sup>4</sup>We should remind here that, in a more realistic quasi-de-Sitter inflationary epoch, the power spectrum of the temporal component becomes slightly red-tilted with a spectral index  $n_{A_0} = \mathcal{O}(\varepsilon)$  with  $\varepsilon$  the slow-roll parameter, as shown in (6.32). However, we shall neglect this small spectral index in order to set the initial conditions, being the expected effect small.

evolution of the metric perturbation when the electromagnetic perturbations contribute in a non-negligible way to the Einstein equations, so that the approximated solutions obtained in the previous section are no longer valid. However, we can easily understand how the ISW effect will be modified by noticing that those modes that have become sub-Hubble very recently can still have an appreciable amplitude and, therefore, modify the late-time evolution of the gravitational potentials, which gives rise to a modification of the ISW, but only for low redshift so that the early ISW remains unaffected. Moreover, if the corresponding mode crosses the horizon with a too large amplitude, the modification in the gravitational potentials evolutions might be excessively large and, thus, conflict with observations. This is the reason why on large scales we obtain some distinctive signatures for large enough values of the primordial amplitude  $A$ . Notice that such signatures are more apparent in the matter power spectrum.

Instead of giving the constraints in terms of the parameter  $A$  we shall give the results in terms of the more physical quantity  $\delta_A$  defined as:

$$\delta_A \equiv \frac{\mathcal{P}_k^{1/2}}{\rho_{A_0}} . \quad (6.81)$$

with  $\mathcal{P}_k = \frac{k^3}{2\pi^2} |\delta\rho_k|^2$  the power spectrum of the electromagnetic energy density perturbations. Hence, the magnitude  $\delta_A$  gives the amplitude of the energy density fluctuations of the electromagnetic field at a given scale  $k$  relative to the homogeneous contribution. Since  $\delta\rho_k$  and  $\rho_{A_0}$  evolve in the same way on super-Hubble scales, the quantity  $\delta_A$  does not depend on time as long as the corresponding mode remains super-Hubble. Notice also that  $\delta\rho_k$  contains two types of contributions, namely: one proportional to the metric perturbation and other proportional to the electromagnetic perturbation. Thus, in the case when the component proportional to the electromagnetic perturbation becomes dominant, the quantity  $\delta_A$  becomes scale-invariant on super-Hubble scales because  $\delta\rho_k \propto \delta\hat{A}_{0k}$  and  $\delta\hat{A}_{0k}$  is proportional to  $k^{-3/2}$  due to the flatness of its primordial power spectrum. However, if the metric perturbation contribution is dominant  $\delta_A$  will depend on the wave-number of the considered mode. In any case, the upper bound that we shall obtain for  $\delta_A$  will show how large the primordial electromagnetic perturbations are allowed to be in order to be compatible with CMB measurements. In particular, we obtain that  $\delta_A$  must satisfy the constraint  $\delta_A \lesssim 10^{-7}$  in order not to be in conflict with the CMB quadrupole. In fact, the overall effect on the CMB

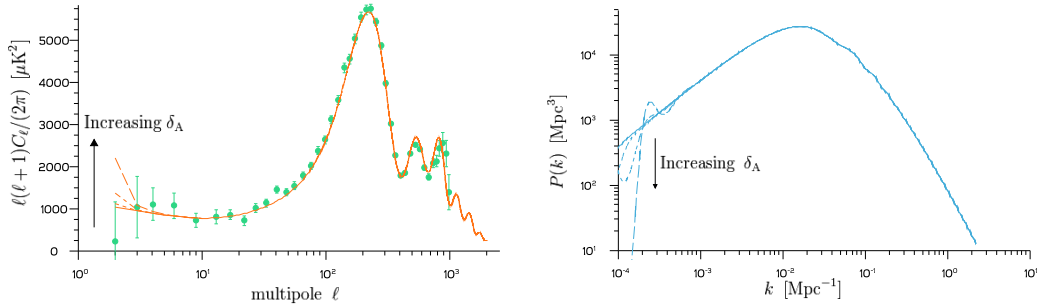


Figure 6.3: In this figure we show the CMB power spectrum (left panel) and the matter power spectrum (right panel) for both the electromagnetic dark energy model (dotted lines) and the standard  $\Lambda$ CDM model (solid lines). We have plotted several cases with increasing values of the initial amplitude for the electromagnetic perturbations and we see that the only modifications appear for large scales. In particular, the CMB quadrupole becomes excessive large, being incompatible with WMAP data (green dots) for  $\delta_A > 10^{-7}$  and the small  $k$  region of the matter power spectrum becomes very different from that of  $\Lambda$ CDM.

power spectrum would be that the higher value of  $\delta_A$  is, the more tilted the lower multipoles part of the spectrum becomes. In fact, since the  $\delta\rho_k$  modes decay rapidly once they reenter into the horizon (as we already commented above) the only important effect appears for the quadrupole and, as a consequence, the bound on  $\delta_A$  is actually a bound on such a quantity at the quadrupole scale.

On the other hand, the upper bound obtained for  $\delta_A$  can be linked to a variation of the Hubble parameter in a quasi-de-Sitter inflationary epoch where the Hubble parameter is not exactly constant but varies slightly. To show such a link, we first have to notice that, as commented before, the background energy density of the electromagnetic field is given by all the modes whose scales are larger than the Hubble radius today, whereas the perturbations correspond to modes whose scales are smaller than the present Hubble radius. In other words, the background is given by the modes that remain super-Hubble at the present epoch and the perturbations correspond to those modes which have already entered into the horizon. In the previous sections we have shown that the amplitude of the electromagnetic field fluctuations (for the temporal component) at a scale  $k$  is given by  $H_{k'}$ , with  $H_k$  the Hubble parameter at the time when

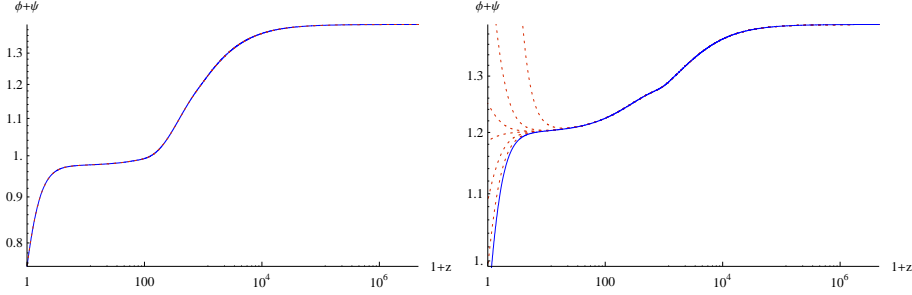


Figure 6.4: In this figure we show the evolution of the gravitational potentials for large ( $k = 1.1 \times 10^{-5} \text{ Mpc}^{-1}$ ) and small ( $k = 5.8 \times 10^{-3} \text{ Mpc}^{-1}$ ) scales in the left and right panels respectively. We also show the evolution in a  $\Lambda$ CDM model (solid blue lines) for comparison. As commented in the main text, the evolution for the small scales is exactly the same as in the case of a cosmological constant. In the large scales case we see how the evolution can be very different for large enough initial amplitudes of the electromagnetic perturbations. We plot the electromagnetic model in dotted (red) lines and we see that the larger the electromagnetic perturbations are, the more distinctive the evolution of the gravitational potential is.

the scale  $k$  leaves the horizon. Now, let us notice that

$$\delta_A \sim \frac{H_k^2 A_0 \delta \hat{\mathcal{A}}_{0k}}{H_I^2 A_0^2} \sim \left( \frac{H_k}{H_I} \right)^3 \quad (6.82)$$

where  $H_I$  is the Hubble parameter at the beginning of inflation. Then, the constraint  $\delta_A \lesssim 10^{-7}$  implies that the Hubble parameter must have reduced (at least) by a factor  $\sim 200$  since the beginning of inflation until the time when the scale of the present Hubble radius (quadrupole scale) left the horizon, i.e.,  $H_{k_0} \lesssim H_I/200$ . Since the Hubble parameter is proportional to the square of the inflation scale we also obtain that the scale of inflation must reduce in a factor  $\sim 15$ . Notice also that this fact requires a red-tilted spectrum for inflation, i.e., the Hubble parameter must decay throughout the inflationary epoch. Moreover, since  $\delta \hat{\mathcal{A}}_{0k} \sim H_k$  (as we have already said) we have that the fluctuations of the temporal component must satisfy:

$$\frac{\delta \hat{\mathcal{A}}_{0k}}{A_0} \lesssim 5 \times 10^{-3}. \quad (6.83)$$

Then, we conclude that the electromagnetic dark energy model is compatible with current CMB and LSS unless very large electromagnetic initial perturbations are generated during inflation.

## 6.8 Conclusions and discussion

In the quantization of the electromagnetic field, either in the covariant or in the path-integral formalism, one has to introduce a gauge-fixing term in the action in order to be able to define a propagator for the photon. The form of the gauge fixing term is unique in the sense that it is the only one that does not require the introduction of additional scales in the action and leads to linear equations of motion, although one may even consider nonlinear terms. However, in order to recover Maxwell theory one needs to impose some subsidiary (Lorenz) condition so that we end up with the usual electromagnetic theory describing the two transverse polarizations of the photon. This procedure is perfectly valid in a flat spacetime, but when we try to apply it to an expanding universe we have found that it becomes inconsistent because such a condition is violated by the superhorizon modes in the evolution of the system, although it remains valid for small scales. For this reason, we have proposed a quantization of the electromagnetic field without introducing the Lorenz condition and assuming that the action with the gauge fixing term is the fundamental action of electromagnetism and not just a mathematical trick in order to be able to quantize the theory. In other words, we promote the gauge-fixing term into a physical term which is included in the fundamental action and not introduced during the quantization procedure as usually. This means that the electromagnetic theory contains a new scalar mode in addition to the two transverse components of the photon. In flat space, the usual predictions of electromagnetism are retained, whereas a gravitational field may excite the new scalar degree of freedom of the electromagnetic field, which now is not a gauge mode but has physical consequences.

It is very remarkably the fact that the proposed action has exactly the same form as the only vector-tensor theory with the same PPN parameters as GR and that is free from instabilities, as we shown in Chapter 4. Moreover, according to the results of Chapter 3, the cosmological evolution of such an action leads to the presence of an effective cosmological constant, so that the new scalar mode introduced in the electromagnetic theory could play the role of dark energy. We have computed the initial power spectrum for the electromagnetic scalar mode generated from quantum fluctuations during an inflationary era and obtained that the observed value of the cosmological constant can be achieved if inflation occurred at the electroweak scales, which seems a quite physically mean-

ingful scale. This result enables us to avoid naturalness problems and to *explain* the value of the cosmological constant.

Although the homogeneous part of the gauge-fixing term behaves as an effective cosmological constant, its internal dynamics implies that there will be fluctuations, unlike in  $\Lambda$ CDM where the cosmological constant is a true constant. We analyzed these fluctuations both analytically and numerically. At superhorizon scales, the perturbations tend to freeze to constant value, while after entering horizon, they decay exhibiting oscillations. As the cosmological constant begins to contribute more significantly to the energy density, the fluctuations of the field begin to affect the gravitational potentials. Since this happens at recent times, the effects to the matter power spectrum is confined to large scales, and to the CMB at low multipoles. However, depending on the initial amplitude of the perturbations, which in turn depends on the details of inflation, these effects might be detectable. In terms of the parameter (6.81) we find  $\delta_A \lesssim 10^{-7}$  in order to avoid conflicts with observations. This implies that the amplitude of fluctuations generated for the electromagnetic field should be  $\lesssim 5 \times 10^{-3}$ . Moreover, this fact requires a reduction of the scale of inflation in a factor (at least)  $\sim 15$  since the beginning of inflation until the scale of the quadrupole crossed the horizon.

To sum up the results of this last Chapter, we have presented a modification of electromagnetism in which the observed value of the cosmological constant arises naturally in an inflationary epoch at the electroweak scale, linking that way two physically relevant scales. The resulting theory passes all the Solar System tests because it has the same PPN parameters as GR and is free of both classical and quantum instabilities. Finally, the evolution of the perturbations is in agreement with CMB and LSS measurements, being the corresponding fits as good as those of  $\Lambda$ CDM. Hence, we have shown that the true nature of dark energy can be established without resorting to new physics by means of the electromagnetic field.



# Final conclusions and prospects

---

Throughout this thesis we have studied possible vector properties of dark energy from both phenomenological and theoretical points of view and confronted our theoretical proposals to existing data.

The first approach to dark energy that we have adopted has been intended to study the potential observational consequences of having a coherent dark energy flow on very large scales. The existence of such a flow at decoupling time enables matter and radiation to acquire a relative motion that, indeed, might explain the anomalously high peculiar velocities of galaxies on scales up to  $300h^{-1} \text{ Mpc}^{-1}$ . Actually, we might look at this argument the other way around and consider that the large peculiar velocities could be signaling the existence of a coherent motion of dark energy. Moreover, we have shown that these relative velocities among all the components in the Universe generate a certain degree of anisotropy so that the expansion of the Universe becomes axisymmetric and a new contribution to the CMB anisotropies appears, mainly to the CMB quadrupole. In fact, for some models (scaling and null dark energy) this new contribution could help lowering the standard quadrupole contribution generated during inflation to make it compatible with the observed one. Also, allowing a relative motion for dark energy has shown the non-viability of some models with a stiff phase, which had previously been proposed as good candidates, because they are unstable against velocity perturbations.

Even though the existence of a dark energy relative motion with respect to the primordial plasma in the early Universe seems to be a real possibility as long as dark energy interacted very weakly with the rest of components of the Universe by that time, the actual situation is that the origin of dark energy remains unspecified in most of the models. For that reason, it would be interesting to study the constraints on the primordial

dark energy flow from current observations. This might be done on phenomenological grounds by considering general parameterizations for the origin of such a primordial flow. Then, it seems worthwhile to pursue further investigations of this fact and it could be the goal of future work.

Another interesting possibility arising in these moving dark energy models is the generation of large scale magnetic fields. Such a generation follows from the fact that the dark energy flow at decoupling time allows the presence of relative velocities between matter and radiation. Thus, at reionization time, electrons and protons, having different masses, can acquire relative velocities between them because of being differently dragged by photons so that an effective net electric current might arise from the relative motion of the charges and a magnetic field on large scales could be generated.

The second approach considered in this thesis to deal with the dark energy problem has been in the context of vector-tensor theories of gravity. We have shown that one can easily achieve accelerated solutions for a wide region of the parameter space and, in fact, these accelerated solutions can be useful for realizing both an inflationary era and a dark energy model. This is so because of the existence of attractors and repellers in the phase map in which the expansion becomes accelerated. Moreover, an interesting feature found for these models when we have a matter component in addition to the vector field is that most of them contain a transition from a matter dominated epoch to a phantom era. This phantom era leads to a future Type III singularity in which the scale factor takes a constant value, but  $H$ , the energy density and the pressure diverge with  $w \rightarrow -\infty$ . For the discussed vector-tensor theories, we have found that there are 6 particular models whose PPN parameters are identical to those of GR so that they give the same small scales behavior. For such models, we have analyzed the existence of instabilities at the classical and quantum levels and found that both Maxwell and Maxwell supplemented with a gauge-fixing term theories are free from instabilities.

These vector-tensor theories can help to alleviate or even solve some of the fundamental problems in Modern Cosmology like the cosmological constant problem or the coincidence problem. In fact, we have presented a vector-tensor model in which an initial fraction of dark energy density of order  $\sim 10^{-6}$  in the early Universe, where it remains constant because of having scaling properties, can give rise to a late-time accelerated phase with a future Type III singularity. However, this model has to face some problems related to the presence of instabilities which require some fur-

ther work to be solved (if possible).

Finally, we have proposed a modified version of Maxwell electromagnetism in which the gauge fixing term is promoted into a physical one rather than being merely a mathematical trick to quantize the theory. In fact, we have shown that the covariant approach for quantizing the Maxwell action turns out to be inconsistent when considering curved backgrounds. Our approach, however, introduces a new scalar degree of freedom whose quantum fluctuations during an inflationary era occurring at the electroweak scale give rise to an effective cosmological constant with the correct value. Moreover, the perturbations of the model accomplish the CMB anisotropies and large scale structures observations as long as the primordial amplitude of the field is not excessively large. A new mechanism for generating large scale magnetic fields might arise from the modified version of electromagnetism on large scale that deserves further investigations in order to calculate their actual amplitude.

To conclude, the results contained in this thesis have shown that cosmological vector fields are compelling candidates for dark energy. Unlike many of the existing proposals, they allow to explain the cosmic acceleration without introducing new dimensional scales and avoiding naturalness or fine-tuning problems. Moreover, the study of cosmological electromagnetic fields has shown that, contrary to usual claims, the true nature of dark energy could be established without resorting to new physics. Next generations of satellites and experiments, which will provide extraordinarily accurate cosmological observations, will determine the potential vector properties of dark energy.



# Bibliography

---

- [1] **WMAP Collaboration**, M. R. Nolta *et. al.*, *Five-Year Wilkinson Microwave Anisotropy Probe (WMAP) Observations: Angular Power Spectra*, *Astrophys. J. Suppl.* **180** (2009) 296–305, [arXiv:0803.0593].
- [2] **SDSS Collaboration**, M. Tegmark *et. al.*, *Cosmological Constraints from the SDSS Luminous Red Galaxies*, *Phys. Rev.* **D74** (2006) 123507, [astro-ph/0608632].
- [3] **Supernova Search Team Collaboration**, A. G. Riess *et. al.*, *Observational Evidence from Supernovae for an Accelerating Universe and a Cosmological Constant*, *Astron. J.* **116** (1998) 1009–1038, [astro-ph/9805201].
- [4] **Supernova Cosmology Project Collaboration**, S. Perlmutter *et. al.*, *Measurements of Omega and Lambda from 42 High-Redshift Supernovae*, *Astrophys. J.* **517** (1999) 565–586, [astro-ph/9812133].
- [5] A. N. Aguirre, *Dust Versus Cosmic Acceleration*, *Astrophys. J.* **512** (1999) L19, [astro-ph/9811316].
- [6] P. S. Drell, T. J. Loredo, and I. Wasserman, *Type Ia supernovae, evolution, and the cosmological constant*, *Astrophys. J.* **530** (2000) 593, [astro-ph/9905027].
- [7] **Supernova Search Team Collaboration**, A. G. Riess *et. al.*, *The Farthest Known Supernova: Support for an Accelerating Universe and a Glimpse of the Epoch of Deceleration*, *Astrophys. J.* **560** (2001) 49–71, [astro-ph/0104455].
- [8] **Supernova Cosmology Project Collaboration**, M. Kowalski *et. al.*, *Improved Cosmological Constraints from New, Old and Combined Supernova Datasets*, *Astrophys. J.* **686** (2008) 749–778, [arXiv:0804.4142].

- [9] S. Weinberg, *Curvature dependence of peaks in the cosmic microwave background distribution*, *Phys. Rev.* **D62** (2000) 127302, [astro-ph/0006276].
- [10] W. J. Percival *et al.*, *Measuring the Baryon Acoustic Oscillation scale using the SDSS and 2dFGRS*, *Mon. Not. Roy. Astron. Soc.* **381** (2007) 1053–1066, [arXiv:0705.3323].
- [11] W. J. Percival *et al.*, *Baryon Acoustic Oscillations in the Sloan Digital Sky Survey Data Release 7 Galaxy Sample*, arXiv:0907.1660.
- [12] E. Gaztanaga, A. Cabre, and L. Hui, *Clustering of Luminous Red Galaxies IV: Baryon Acoustic Peak in the Line-of-Sight Direction and a Direct Measurement of  $H(z)$* , arXiv:0807.3551.
- [13] E. Gaztanaga, R. Miquel, and E. Sanchez, *First Cosmological Constraints on Dark Energy from the Radial Baryon Acoustic Scale*, *Phys. Rev. Lett.* **103** (2009) 091302, [arXiv:0808.1921].
- [14] H. B. Richer *et al.*, *The Lower Main Sequence and Mass Function of the Globular Cluster Messier 4*, *Astrophys. J.* **574** (2002) L151–L154, [astro-ph/0205086].
- [15] L. M. Krauss and B. Chaboyer, *Age Estimates of Globular Clusters in the Milky Way: Constraints on Cosmology*, *Science* **299** (2003) 65–70.
- [16] A. G. Riess *et al.*, *A Redetermination of the Hubble Constant with the Hubble Space Telescope from a Differential Distance Ladder*, *Astrophys. J.* **699** (2009) 539–563, [arXiv:0905.0695].
- [17] E. I. Guendelman and A. B. Kaganovich, *Dynamical measure and field theory models free of the cosmological constant problem*, *Phys. Rev.* **D60** (1999) 065004, [gr-qc/9905029].
- [18] A. Davidson and S. Rubin, *Zero Cosmological Constant from Normalized General Relativity*, *Class. Quant. Grav.* **26** (2009) 235019, [arXiv:0905.0661].
- [19] E. J. Copeland, M. Sami, and S. Tsujikawa, *Dynamics of dark energy*, *Int. J. Mod. Phys.* **D15** (2006) 1753–1936, [hep-th/0603057].
- [20] J. Frieman, M. Turner, and D. Huterer, *Dark Energy and the Accelerating Universe*, *Ann. Rev. Astron. Astrophys.* **46** (2008) 385–432, [arXiv:0803.0982].

- [21] A. Silvestri and M. Trodden, *Approaches to Understanding Cosmic Acceleration*, *Rept. Prog. Phys.* **72** (2009) 096901, [arXiv:0904.0024].
- [22] R. R. Caldwell, *A Phantom Menace?*, *Phys. Lett.* **B545** (2002) 23–29, [astro-ph/9908168].
- [23] S. M. Carroll, M. Hoffman, and M. Trodden, *Can the dark energy equation-of-state parameter  $w$  be less than  $-1$ ?*, *Phys. Rev.* **D68** (2003) 023509, [astro-ph/0301273].
- [24] J. M. Cline, S. Jeon, and G. D. Moore, *The phantom menaced: Constraints on low-energy effective ghosts*, *Phys. Rev.* **D70** (2004) 043543, [hep-ph/0311312].
- [25] C. Armendariz-Picon, T. Damour, and V. F. Mukhanov, *k-Inflation*, *Phys. Lett.* **B458** (1999) 209–218, [hep-th/9904075].
- [26] T. Chiba, T. Okabe, and M. Yamaguchi, *Kinetically driven quintessence*, *Phys. Rev.* **D62** (2000) 023511, [astro-ph/9912463].
- [27] C. Armendariz-Picon, V. F. Mukhanov, and P. J. Steinhardt, *Essentials of k-essence*, *Phys. Rev.* **D63** (2001) 103510, [astro-ph/0006373].
- [28] C. Armendariz-Picon, V. F. Mukhanov, and P. J. Steinhardt, *A dynamical solution to the problem of a small cosmological constant and late-time cosmic acceleration*, *Phys. Rev. Lett.* **85** (2000) 4438–4441, [astro-ph/0004134].
- [29] A. A. Starobinsky, *A new type of isotropic cosmological models without singularity*, *Phys. Lett.* **B91** (1980) 99–102.
- [30] S. Capozziello, S. Carloni, and A. Troisi, *Quintessence without scalar fields*, *Recent Res. Dev. Astron. Astrophys.* **1** (2003) 625, [astro-ph/0303041].
- [31] S. Capozziello, V. F. Cardone, S. Carloni, and A. Troisi, *Curvature quintessence matched with observational data*, *Int. J. Mod. Phys.* **D12** (2003) 1969–1982, [astro-ph/0307018].
- [32] S. M. Carroll, V. Duvvuri, M. Trodden, and M. S. Turner, *Is cosmic speed-up due to new gravitational physics?*, *Phys. Rev.* **D70** (2004) 043528, [astro-ph/0306438].

- [33] A. de la Cruz-Dombriz and A. Dobado, *A  $f(R)$  gravity without cosmological constant*, *Phys. Rev.* **D74** (2006) 087501, [gr-qc/0607118].
- [34] A. D. Dolgov and M. Kawasaki, *Can modified gravity explain accelerated cosmic expansion?*, *Phys. Lett.* **B573** (2003) 1–4, [astro-ph/0307285].
- [35] M. E. Soussa and R. P. Woodard, *The Force of Gravity from a Lagrangian containing Inverse Powers of the Ricci Scalar*, *Gen. Rel. Grav.* **36** (2004) 855–862, [astro-ph/0308114].
- [36] T. Chiba,  *$1/R$  gravity and scalar-tensor gravity*, *Phys. Lett.* **B575** (2003) 1–3, [astro-ph/0307338].
- [37] S. Nojiri and S. D. Odintsov, *Modified gravity with negative and positive powers of the curvature: Unification of the inflation and of the cosmic acceleration*, *Phys. Rev.* **D68** (2003) 123512, [hep-th/0307288].
- [38] S. Fay, R. Tavakol, and S. Tsujikawa,  *$f(R)$  gravity theories in Palatini formalism: cosmological dynamics and observational constraints*, *Phys. Rev.* **D75** (2007) 063509, [astro-ph/0701479].
- [39] D. N. Vollick, *Curvature Corrections as the Source of the Cosmological Acceleration*, *Phys. Rev.* **D68** (2003) 063510, [astro-ph/0306630].
- [40] X. Meng and P. Wang, *Modified Friedmann Equations in  $R^{-1}$ -Modified Gravity*, *Class. Quant. Grav.* **20** (2003) 4949–4962, [astro-ph/0307354].
- [41] G. R. Dvali, G. Gabadadze, and M. Porrati, *4D gravity on a brane in 5D Minkowski space*, *Phys. Lett.* **B485** (2000) 208–214, [hep-th/0005016].
- [42] C. de Rham *et. al.*, *Cascading gravity: Extending the Dvali-Gabadadze-Porrati model to higher dimension*, *Phys. Rev. Lett.* **100** (2008) 251603, [arXiv:0711.2072].
- [43] A. Y. Kamenshchik, U. Moschella, and V. Pasquier, *An alternative to quintessence*, *Phys. Lett.* **B511** (2001) 265–268, [gr-qc/0103004].
- [44] I. L. Shapiro and J. Sola, *On the scaling behavior of the cosmological constant and the possible existence of new forces and new light degrees of freedom*, *Phys. Lett.* **B475** (2000) 236–246, [hep-ph/9910462].

- [45] I. L. Shapiro and J. Sola, *Scaling behavior of the cosmological constant: Interface between quantum field theory and cosmology*, *JHEP* **02** (2002) 006, [hep-th/0012227].
- [46] J. Grande, J. Sola, and H. Stefancic, *LXCDM: a cosmological model solution to the cosmological coincidence problem?*, *JCAP* **0608** (2006) 011, [gr-qc/0604057].
- [47] S. Rasanen, *Dark energy from backreaction*, *JCAP* **0402** (2004) 003, [astro-ph/0311257].
- [48] E. W. Kolb, S. Matarrese, A. Notari, and A. Riotto, *The effect of inhomogeneities on the expansion rate of the universe*, *Phys. Rev.* **D71** (2005) 023524, [hep-ph/0409038].
- [49] E. Barausse, S. Matarrese, and A. Riotto, *The Effect of Inhomogeneities on the Luminosity Distance- Redshift Relation: is Dark Energy Necessary in a Perturbed Universe?*, *Phys. Rev.* **D71** (2005) 063537, [astro-ph/0501152].
- [50] K. Tomita, *A Local Void and the Accelerating Universe*, *Mon. Not. Roy. Astron. Soc.* **326** (2001) 287, [astro-ph/0011484].
- [51] M. Tanimoto, Y. Nambu, and K. Iwata, *The Role of Anisotropy in the Void Models without Dark Energy*, arXiv:0906.4857.
- [52] N. R. Tanvir *et al.*, *A glimpse of the end of the dark ages: the gamma-ray burst of 23 April 2009 at redshift 8.3*, arXiv:0906.1577.
- [53] J. D. Barrow, *Cosmological limits on slightly skew stresses*, *Phys. Rev.* **D55** (1997) 7451–7460, [gr-qc/9701038].
- [54] D. C. Rodrigues, *Anisotropic Cosmological Constant and the CMB Quadrupole Anomaly*, *Phys. Rev.* **D77** (2008) 023534, [arXiv:0708.1168].
- [55] L. Campanelli, P. Cea, and L. Tedesco, *Ellipsoidal Universe Can Solve The CMB Quadrupole Problem*, *Phys. Rev. Lett.* **97** (2006) 131302, [astro-ph/0606266].
- [56] T. Koivisto and D. F. Mota, *Accelerating Cosmologies with an Anisotropic Equation of State*, *Astrophys. J.* **679** (2008) 1, [arXiv:0707.0279].

- [57] D. F. Mota, J. R. Kristiansen, T. Koivisto, and N. E. Groeneboom, *Constraining Dark Energy Anisotropic Stress*, *Mon. Not. Roy. Astron. Soc.* **382** (2007) 793–800, [arXiv:0708.0830].
- [58] T. Koivisto and D. F. Mota, *Anisotropic Dark Energy: Dynamics of Background and Perturbations*, *JCAP* **0806** (2008) 018, [arXiv:0801.3676].
- [59] D. Langlois and T. Piran, *Dipole anisotropy from an entropy gradient*, *Phys. Rev.* **D53** (1996) 2908–2919, [astro-ph/9507094].
- [60] M. S. Turner, *A Tilted universe (and other remnants of the preinflationary universe)*, *Phys. Rev.* **D44** (1991) 3737–3748.
- [61] A. L. Maroto, *Moving dark energy and the CMB dipole*, *JCAP* **0605** (2006) 015, [astro-ph/0512464].
- [62] A. L. Maroto, *Dark energy in motion*, *Int. J. Mod. Phys.* **D15** (2006) 2165–2170, [astro-ph/0605381].
- [63] P. Peebles, *Principles of physical cosmology*. Princeton University Press, 1993.
- [64] A. Dressler *et al.*, *Spectroscopy and photometry of elliptical galaxies. 1. A New distance estimator*, *Astrophys. J.* **313** (1987) 42–58.
- [65] D. S. Mathewson, V. L. Ford, and M. Buchhorn, *A Southern sky survey of the peculiar velocities of 1355 spiral galaxies*, *Astrophys. J. Suppl.* **81** (1992) 413.
- [66] D. S. Mathewson, V. L. Ford, and M. Buchhorn, *The Las Campanas observatory/Palomar 10,000 kilometer per second cluster survey. II. Constraints on large-scale streaming*, *Astrophys. J.* **522** (1999) 647.
- [67] S. Courteau, J. A. Willick, M. A. Strauss, D. Schlegel, and M. Postman, *Shellflow. I. The Convergence of the Velocity Field at 6000 km/s*, *Astrophys. J.* **544** (2000) 636, [astro-ph/0002420].
- [68] T. R. Lauer and M. Postman, *The motion of the local group with respect to the 15,000 kilometer per second Abell cluster inertial frame*, *Astrophys. J.* **425** (1994) 418.
- [69] M. J. Hudson, R. J. Smith, J. R. Lucey, D. J. Schlegel, and R. L. Davies, *A Large-Scale Bulk Flow of Galaxy Clusters*, *Astrophys. J.* **512** (1999) L79, [astro-ph/9901001].

- [70] M. J. Hudson and H. Ebeling, *The Environmental Dependence of Brightest Cluster Galaxies: Implications for Large-Scale Flows*, *Astrophys. J.* **479** (1997) 621.
- [71] A. G. Riess, M. Davis, J. Baker, and R. P. Kirshner, *The Velocity field from type Ia supernovae matches the gravity field from galaxy surveys*, *Astrophys. J.* **488** (1997) L1, [astro-ph/9707261].
- [72] R. Juszkiewicz, P. G. Ferreira, H. A. Feldman, A. H. Jaffe, and M. Davis, *Evidence for a low-density Universe from the relative velocities of galaxies*, astro-ph/0001041.
- [73] H. A. Feldman, R. Watkins, A. L. Melott, and S. W. Chambers, *Optimal Moments for the Analysis of Peculiar Velocity Surveys II: Testing*, *Astrophys. J.* **599** (2003) 820–828, [astro-ph/0304316].
- [74] R. W. Pike and M. J. Hudson, *Cosmological Parameters from the Comparison of the 2MASS Gravity Field with Peculiar Velocity Surveys*, *Astrophys. J.* **635** (2005) 11–21, [astro-ph/0511012].
- [75] D. Sarkar, H. A. Feldman, and R. Watkins, *Current Status Of Velocity Field Surveys: A Consistency Check*, *Mon. Not. Roy. Astron. Soc.* **375** (2007) 691–697, [astro-ph/0607426].
- [76] R. Watkins and H. A. Feldman, *Power Spectrum Shape from Peculiar Velocity Data*, *Mon. Not. Roy. Astron. Soc.* **379** (2007) 343–348, [astro-ph/0702751].
- [77] H. A. Feldman and R. Watkins, *Bulk Flow and Shear Moments of the SFI++ Survey*, *Mon. Not. Roy. Astron. Soc.* **387** (2008) 825–829, [arXiv:0802.2961].
- [78] A. Kashlinsky and F. Atrio-Barandela, *Measuring cosmological bulk flows via the kinematic Sunyaev-Zeldovich effect in the upcoming cosmic microwave background maps*, *Astrophys. J.* **536** (2000) L67, [astro-ph/0005197].
- [79] A. Kashlinsky, F. Atrio-Barandela, D. Kocevski, and H. Ebeling, *A measurement of large-scale peculiar velocities of clusters of galaxies: technical details*, *Astrophys. J.* **691** (2009) 1479–1493, [arXiv:0809.3733].
- [80] A. Kashlinsky, F. Atrio-Barandela, D. Kocevski, and H. Ebeling, *A measurement of large-scale peculiar velocities of clusters of galaxies: results and cosmological implications*, arXiv:0809.3734.

- [81] R. Watkins, H. A. Feldman, and M. J. Hudson, *Consistently Large Cosmic Flows on Scales of 100 Mpc/h: a Challenge for the Standard LCDM Cosmology*, arXiv:0809.4041.
- [82] D. Lynden-Bell *et. al.*, *Spectroscopy and photometry of elliptical galaxies. V - Galaxy streaming toward the new supergalactic center*, *Astrophys. J.* **326** (1988) 19.
- [83] A. Dresler, *The supergalactic plane redshift survey - a candidate for the great attractor*, *Astrophys. J.* **329** (1988) 519.
- [84] S. Dodelson, *Modern Cosmology*. Academic Press, 2003.
- [85] M. Giovannini, *Theoretical tools for the physics of CMB anisotropies*, *Int. J. Mod. Phys. D***14** (2005) 363–510, [astro-ph/0412601].
- [86] E. F. Bunn, P. Ferreira, and J. Silk, *How Anisotropic is our Universe?*, *Phys. Rev. Lett.* **77** (1996) 2883–2886, [astro-ph/9605123].
- [87] **WMAP** Collaboration, D. N. Spergel *et. al.*, *Wilkinson Microwave Anisotropy Probe (WMAP) three year results: Implications for cosmology*, *Astrophys. J. Suppl.* **170** (2007) 377, [astro-ph/0603449].
- [88] **WMAP** Collaboration, G. Hinshaw *et. al.*, *Three-year Wilkinson Microwave Anisotropy Probe (WMAP) observations: Temperature analysis*, *Astrophys. J. Suppl.* **170** (2007) 288, [astro-ph/0603451].
- [89] K. Land and J. Magueijo, *The axis of evil*, *Phys. Rev. Lett.* **95** (2005) 071301, [astro-ph/0502237].
- [90] K. Land and J. Magueijo, *The Axis of Evil revisited*, *Mon. Not. Roy. Astron. Soc.* **378** (2007) 153–158, [astro-ph/0611518].
- [91] D. J. Schwarz, G. D. Starkman, D. Huterer, and C. J. Copi, *Is the low- $l$  microwave background cosmic?*, *Phys. Rev. Lett.* **93** (2004) 221301, [astro-ph/0403353].
- [92] C. Copi, D. Huterer, D. Schwarz, and G. Starkman, *The Uncorrelated Universe: Statistical Anisotropy and the Vanishing Angular Correlation Function in WMAP Years 1-3*, *Phys. Rev. D***75** (2007) 023507, [astro-ph/0605135].
- [93] E. Kolb and M. Turner, *The early universe*. Addison-Wesley, 1990.

- [94] P. J. Steinhardt, L.-M. Wang, and I. Zlatev, *Cosmological tracking solutions*, *Phys. Rev.* **D59** (1999) 123504, [astro-ph/9812313].
- [95] C. M. Will and J. Nordtvedt, Kenneth, *Conservation Laws and Preferred Frames in Relativistic Gravity. I. Preferred-Frame Theories and an Extended PPN Formalism*, *Astrophys. J.* **177** (1972) 757.
- [96] J. Nordtvedt, Kenneth and C. M. Will, , *Astrophys. J.* **177** (1972) 775.
- [97] R. W. Hellings and K. Nordtvedt, *Vector-Metric Theory of Gravity*, *Phys. Rev.* **D7** (1973) 3593–3602.
- [98] V. A. Kostelecky and S. Samuel, *Gravitational Phenomenology in Higher Dimensional Theories and Strings*, *Phys. Rev.* **D40** (1989) 1886–1903.
- [99] C. Eling, T. Jacobson, and D. Mattingly, *Einstein-aether theory*, gr-qc/0410001.
- [100] R. Bluhm and V. A. Kostelecky, *Spontaneous Lorentz violation, Nambu-Goldstone modes, and gravity*, *Phys. Rev.* **D71** (2005) 065008, [hep-th/0412320].
- [101] Q. G. Bailey and V. A. Kostelecky, *Signals for Lorentz violation in post-Newtonian gravity*, *Phys. Rev.* **D74** (2006) 045001, [gr-qc/0603030].
- [102] R. Bluhm, S.-H. Fung, and V. A. Kostelecky, *Spontaneous Lorentz and Diffeomorphism Violation, Massive Modes, and Gravity*, *Phys. Rev.* **D77** (2008) 065020, [arXiv:0712.4119].
- [103] R. Bluhm, N. L. Gagne, R. Potting, and A. Vrublevskis, *Constraints and Stability in Vector Theories with Spontaneous Lorentz Violation*, *Phys. Rev.* **D77** (2008) 125007, [arXiv:0802.4071].
- [104] C. Eling, *Energy in the Einstein-aether theory*, *Phys. Rev.* **D73** (2006) 084026, [gr-qc/0507059].
- [105] S. M. Carroll, T. R. Dulaney, M. I. Gresham, and H. Tam, *Instabilities in the Aether*, *Phys. Rev.* **D79** (2009) 065011, [arXiv:0812.1049].
- [106] S. M. Carroll, T. R. Dulaney, M. I. Gresham, and H. Tam, *Sigma-Model Aether*, *Phys. Rev.* **D79** (2009) 065012, [arXiv:0812.1050].

- [107] M. Novello, S. E. Perez Bergliaffa, and J. Salim, *Nonlinear electrodynamics and the acceleration of the Universe*, *Phys. Rev.* **D69** (2004) 127301, [astro-ph/0312093].
- [108] V. V. Kiselev, *Vector field as a quintessence partner*, *Class. Quant. Grav.* **21** (2004) 3323–3336, [gr-qc/0402095].
- [109] C. Armendariz-Picon, *Could dark energy be vector-like?*, *JCAP* **0407** (2004) 007, [astro-ph/0405267].
- [110] B. Himmetoglu, C. R. Contaldi, and M. Peloso, *Instability of anisotropic cosmological solutions supported by vector fields*, *Phys. Rev. Lett.* **102** (2009) 111301, [arXiv:0809.2779].
- [111] C. G. Boehmer and T. Harko, *Dark energy as a massive vector field*, *Eur. Phys. J.* **C50** (2007) 423–429, [gr-qc/0701029].
- [112] T. S. Koivisto and D. F. Mota, *Vector Field Models of Inflation and Dark Energy*, *JCAP* **0808** (2008) 021, [arXiv:0805.4229].
- [113] L. H. Ford, *Inflation driven by a vector field*, *Phys. Rev.* **D40** (1989) 967.
- [114] J. D. Bekenstein, *Relativistic gravitation theory for the MOND paradigm*, *Phys. Rev.* **D70** (2004) 083509, [astro-ph/0403694].
- [115] T. G. Zlosnik, P. G. Ferreira, and G. D. Starkman, *Modifying gravity with the Aether: an alternative to Dark Matter*, *Phys. Rev.* **D75** (2007) 044017, [astro-ph/0607411].
- [116] C. M. Will, *Theory and experiment in gravitational physics*. Cambridge University Press, 1993.
- [117] J. D. Barrow and R. Maartens, *Anisotropic stresses in inhomogeneous universes*, *Phys. Rev.* **D59** (1999) 043502, [astro-ph/9808268].
- [118] B. Z. Foster and T. Jacobson, *Post-Newtonian parameters and constraints on Einstein- aether theory*, *Phys. Rev.* **D73** (2006) 064015, [gr-qc/0509083].
- [119] J. W. Elliott, G. D. Moore, and H. Stoica, *Constraining the new aether: Gravitational Cherenkov radiation*, *JHEP* **08** (2005) 066, [hep-ph/0505211].

- [120] S. M. Carroll and E. A. Lim, *Lorentz-violating vector fields slow the universe down*, *Phys. Rev.* **D70** (2004) 123525, [hep-th/0407149].
- [121] E. A. Lim, *Can we see Lorentz-violating vector fields in the CMB?*, *Phys. Rev.* **D71** (2005) 063504, [astro-ph/0407437].
- [122] E. Babichev, V. Mukhanov, and A. Vikman, *k-Essence, superluminal propagation, causality and emergent geometry*, *JHEP* **02** (2008) 101, [arXiv:0708.0561].
- [123] C. Itzikson and J.-B. Zuber, *Quantum field theory*. Dover Publications, INC., 1980.
- [124] S. Nojiri, S. D. Odintsov, and S. Tsujikawa, *Properties of singularities in (phantom) dark energy universe*, *Phys. Rev.* **D71** (2005) 063004, [hep-th/0501025].
- [125] **Supernova Search Team** Collaboration, A. G. Riess *et. al.*, *Type Ia Supernova Discoveries at  $z>1$  From the Hubble Space Telescope: Evidence for Past Deceleration and Constraints on Dark Energy Evolution*, *Astrophys. J.* **607** (2004) 665–687, [astro-ph/0402512].
- [126] **The SNLS** Collaboration, P. Astier *et. al.*, *The Supernova Legacy Survey: Measurement of  $\Omega_M$ ,  $\Omega_{\Lambda}$  and  $w$  from the First Year Data Set*, *Astron. Astrophys.* **447** (2006) 31–48, [astro-ph/0510447].
- [127] S. Nesseris and L. Perivolaropoulos, *Tension and Systematics in the Gold06 SnIa Dataset*, *JCAP* **0702** (2007) 025, [astro-ph/0612653].
- [128] M. Chevallier and D. Polarski, *Accelerating universes with scaling dark matter*, *Int. J. Mod. Phys.* **D10** (2001) 213–224, [gr-qc/0009008].
- [129] E. V. Linder, *Exploring the expansion history of the universe*, *Phys. Rev. Lett.* **90** (2003) 091301, [astro-ph/0208512].
- [130] R. Lazkoz, S. Nesseris, and L. Perivolaropoulos, *Exploring Cosmological Expansion Parametrizations with the Gold SnIa Dataset*, *JCAP* **0511** (2005) 010, [astro-ph/0503230].
- [131] V. F. Mukhanov, H. A. Feldman, and R. H. Brandenberger, *Theory of cosmological perturbations. Part 1. Classical perturbations. Part 2. Quantum theory of perturbations. Part 3. Extensions*, *Phys. Rept.* **215** (1992) 203–333.

- [132] D. J. Eisenstein and W. Hu, *Baryonic Features in the Matter Transfer Function*, *Astrophys. J.* **496** (1998) 605, [astro-ph/9709112].
- [133] **WMAP** Collaboration, E. Komatsu *et. al.*, *Five-Year Wilkinson Microwave Anisotropy Probe (WMAP) Observations: Cosmological Interpretation*, *Astrophys. J. Suppl.* **180** (2009) 330–376, [arXiv:0803.0547].
- [134] Y. Wang and P. Mukherjee, *Observational Constraints on Dark Energy and Cosmic Curvature*, *Phys. Rev.* **D76** (2007) 103533, [astro-ph/0703780].
- [135] E. L. Wright, *Constraints on Dark Energy from Supernovae, Gamma Ray Bursts, Acoustic Oscillations, Nucleosynthesis and Large Scale Structure and the Hubble constant*, *Astrophys. J.* **664** (2007) 633–639, [astro-ph/0701584].
- [136] W. Hu and N. Sugiyama, *Small scale cosmological perturbations: An Analytic approach*, *Astrophys. J.* **471** (1996) 542–570, [astro-ph/9510117].
- [137] E. V. Linder and G. Robbers, *Shifting the Universe: Early Dark Energy and Standard Rulers*, *JCAP* **0806** (2008) 004, [arXiv:0803.2877].
- [138] F. De Bernardis *et. al.*, *Delayed Recombination and Standard Rulers*, *Phys. Rev.* **D79** (2009) 043503, [arXiv:0812.3557].
- [139] M. S. Turner and L. M. Widrow, *Inflation Produced, Large Scale Magnetic Fields*, *Phys. Rev.* **D37** (1988) 2743.
- [140] A. S. Goldhaber and M. M. Nieto, *Photon and Graviton Mass Limits*, arXiv:0809.1003.
- [141] A. Higuchi, L. Parker, and Y. Wang, *Consistency of Faddeev-Popov ghost statistics with gravitationally induced pair creation*, *Phys. Rev.* **D42** (1990) 4078–4081.
- [142] N. Birrell and P. Davies, *Quantum fields in curved space*. Cambridge University Press, 1982.
- [143] M. J. Pfenning, *Quantum inequalities for the electromagnetic field*, *Phys. Rev.* **D65** (2002) 024009, [gr-qc/0107075].

- [144] T. Kugo and I. Ojima, *Manifestly Covariant Canonical Formulation of Yang-Mills Field Theories: Physical State Subsidiary Conditions and Physical S Matrix Unitarity*, *Phys. Lett.* **B73** (1978) 459.
- [145] S. L. Adler, J. Lieberman, and Y. J. Ng, *Regularization of the Stress Energy Tensor for Vector and Scalar Particles Propagating in a General Background Metric*, *Ann. Phys.* **106** (1977) 279.
- [146] B. S. DeWitt and R. W. Brehme, *Radiation damping in a gravitational field*, *Ann. Phys.* **9** (1960) 220–259.
- [147] M. R. Brown and A. C. Ottewill, *Photon propagators and the definition and approximation of renormalized stress tensors in curved space-time*, *Phys. Rev.* **D34** (1986) 1776–1786.
- [148] A. R. Liddle and D. L. Lyth, *Cosmological inflation and large-scale structure*. Cambridge University Press, 2000.
- [149] A. Lewis, A. Challinor, and A. Lasenby, *Efficient Computation of CMB anisotropies in closed FRW models*, *Astrophys. J.* **538** (2000) 473–476, [astro-ph/9911177].
- [150] C.-P. Ma and E. Bertschinger, *Cosmological perturbation theory in the synchronous and conformal Newtonian gauges*, *Astrophys. J.* **455** (1995) 7–25, [astro-ph/9506072].
- [151] J. M. Stewart and M. Walker, *Perturbations of spacetimes in general relativity*, *Proc. Roy. Soc. Lond.* **A341** (1974) 49–74.